THE UNIVERSITY *of* EDINBURGH

Influenza Virus Infection in a Compromised Immune System

Gillian Mhairi Campbell

Doctor of Philosophy
The University of Edinburgh

2011

Declaration

I declare that all work included in this thesis is my own, except where otherwise stated. No part of this work has been, or will be, submitted for any other degree or professional qualification.

Gillian Mhairi Campbell
2011

The Roslin Institute and
Royal (Dick) School of Veterinary Studies
University of Edinburgh
Midlothian
EH25 9RG

Abstract

Severe influenza virus infection, including human infection with highly pathogenic H5N1 viruses is characterised by massive pulmonary inflammation, immunopathology and excessive cytokine production, a process in which macrophages may play a vital role. The aim of this project was to investigate the hypothesis that inhibition of inflammatory responses from infected macrophages, using either alternatively activated bone marrow derived macrophages (BMDMϕ), or IFNγ receptor deficient (IFNγR$^{-/-}$) mice may ameliorate the devastating immunopathology and inflammation routinely observed in highly pathogenic influenza virus infections.

Infection of alternatively activated BMDMϕ resulted in enhanced positivity for viral proteins, compared with classically activated, inflammatory BMDMϕ. However, neither subset propagated the infection indicating that while infection is abortive in both classical and alternatively activated BMDMϕ, the latter may prove more efficient at removing infectious virus from the site of infection due to enhanced infectivity. However, influenza virus was capable of driving expression of proinflammatory mediators such as iNOS and TNFα from classical and alternatively activated BMDMϕ even in the absence of IFNγ signalling. IFNγR$^{-/-}$ BMDMϕ demonstrated a reduced inflammatory response to infection compared to Sv129 counterparts, suggesting a potentially impaired inflammatory response in vivo.

This was investigated by infection of IFNγR$^{-/-}$ mice, which resulted in ameliorated disease, lower viral titres and mild immunopathology, demonstrating that inhibition of IFNγ signalling limits the severity of disease. Additionally, mRNA expression for key inflammatory mediators was reduced, demonstrating that inhibition of the overwhelming inflammatory response to influenza virus infection is beneficial to the host, resulting in protection from immunopathology and improved prognosis, without impairing viral clearance.

Acknowledgements

I would like to thank my supervisors Bernadette Dutia, Tony Nash and Ian Dransfield for their continued support over the last few years. Their comments, criticisms and novel points of view have been invaluable in reminding me where I am going when I get bogged down in the detail. But especially to Bernadette, my heartfelt gratitude for the support, encouragement and advice you have given me throughout the duration of this PhD. Everything that could be hoped for in a supervisor and mentor, you are. Thank you.

The blood sweat and tears that went into this PhD were shared in no small part by my fellow post grads Pete Wasson and Claire Levy. Thank you both for listening to the rants, keeping me sane and for many enjoyable lunches. I'm glad we have all resisted the temptation to grow thesis beards.

A huge debt of thanks is owed to Yvonne Ligertwood, without whom our lab would undoubtedly fall apart. The font of all technical knowledge and my many time partner in the mouse house, thank you for everything! Thanks also to Marlynne Quigg-Nicol for her support and sense of humour, to Darren Shaw for guiding me on my statistical journey and his many words of wisdom, and to Frances Fowler. I am grateful to Ian Bennet (cloning guru), Anton Gossner (qPCR guru), Dave Sester (macrophage guru), Dave Jackson (WSN guru and provider), Trudi Gillespie (confocal guru), Shonna Johnston (FACS guru) and Chris Palgrave (pathology guru) for their help and advice over the last four years.

It goes without saying that my family have been wonderful during the course of this PhD, the love and support that they have given me has made this possible. However, above all others my undying gratitude and love go to my long suffering husband Iain, who has been through every failed PCR and every beautiful confocal image with me. He has picked me up after 1am timepoints and joined me in cursing Microsoft Word. His patience, understanding and love have been boundless. In the immortal words of the Beach Boys, 'God only knows what I'd be without you.' Thank you.

Contents

List of Figures

List of Tables

List of Abbreviations

-	Negative
+	Positive
↔	No change
↓	Downregulation
↑	Upregulation
A	Adenine
Abs	Absorbance
AEC	Airway epithelial cells
AHR	Airway hyperresponsiveness
Amp	Ampicillin
ANOVA	Analysis of variance
APC	Antigen presenting cell
ARDS	Acute respiratory distress syndrome
Arg-1	Arginase 1
BMDMϕ	Bone marrow derived macrophage
C	Cysteine
CCL	Chemokine (C-C motif) ligand
CCR	Chemokine (C-C motif) receptor
CD	Cluster of differentiation
cDNA	Complementary deoxyribonucleic acid
Ck	Cytokine
CNX	Calnexin
cRNA	Complementary ribonucleic acid
CR	Complement receptor
CRM1	Exportin 1
CSF-1R	Macrophage colony stimulating factor receptor
CTL	Cytotoxic T lymphocyte
D	Aspartic acid
DAB	3,3'-Diaminobenzidine
DAPI	4',6-diamidino-2-phenylindole
DC-SIGN	Dendritic cell-specific intercellular adhesion molecule-3-grabbing non-integrin
delNS1	Mutant influenza virus with deleted NS1
DF	Degrees of freedom
DMEM	Dulbecco's Modified Eagle's Medium
DNA	Deoxyribonbucleic acid
dNTP	Deoxyribonucleotide
D-PBS	Dulbecco's phosphate buffered saline
DTT	Dithiothreitol
E	Glutamic acid
ELISA	Enzyme-linked immunosorbent assay
ER	Endoplasmic reticulum

FACS	Fluorescence activated cell sorting
FasL	Fas ligand
FcR	Fragment crystallisable receptor
FIZZ	Found in inflammatory zone
G	Guanadine
GAS	Gamma activated sequence
GM-CSF	Granulocyte/macrophage colony stimulating factor
H; HA	Haemagglutinin
Hr	Hour
IFN	Interferon
Ig	Immunoglobulin
IL	Interleukin
Inf	Infected
iNKT	Invariant natural killer T cells
iNOS	Inducible nitric oxide synthetase
IPS	Interferon-beta promoter stimulator
IRF	Interferon regulatory factor
ISG	Interferon stimulated gene
ISGF	Interferon stimulated gene factor
ISRE	Interferon stimulated response element
Jak	Janus kinase
Kan	Kanamycin
LB	Lysogeny broth
LCMV	Lymphochoriomeningitis virus
L. major	*Leishmania major*
LPS	Lipopolysaccharide
Ly	Lymphocyte antigen
M	Matrix
MCP	Monocyte chemotactic protein
M-CSF	Macrophage colony stimulating factor (CSF-1)
MDCK	Madine-Darby canine kidney cells
MHC	Major histocompatibility complex
MIP	Macrophage inflammatory protein
MOI	Multiplicity of infection
mRNA	Messenger ribonucleic acid
MyD88	Myeloid differentiation primary response gene 88
n	Number
N; NA	Neuraminidase
NFκB	Nuclear factor kappa-light-chain-enhancer of activated B cells
NP	Nuclear protein
NS	Non-structural
OAS	2'-5'-oligoadenylatesynthetase
OCT	Optimal cutting temperature compound
OVA	Ovalbumin
PA	Polymerase acid
PB	Polymerase basic

PB1-F2	Polymerase basic gene 1 open reading frame 2
PBS	Phosphate buffered saline
PBSA	5% Bovine serum albumin in phosphate buffered saline
PCR	Polymerase chain reaction
PFA	Paraformaldehyde
pfu	Plaque forming units
PFU	*Pyrococcus furiosus* DNA polymerase
PI3K	Phosphoinositide 3-kinase
PKR	Protein kinase, RNA activated
PR8	A/PR/8/34 influenza virus
qPCR	Quantitative polymerase chain reaction
r	Recombinant
R	Receptor
$R^{-/-}$	Receptor deficiency
RANTES	Regulated upon activation, normal T-cell expressed, and secreted (CCL5)
RBC	Red blood cells
RIG-I	Retinoic acid-inducible gene 1
RNA	Ribonucleic acid
RNAseL	Ribonuclease L
RNP	Ribonucleic protein
RPMI	Rosewell Park Memorial Institute 1640 medium
RT	Reverse transcription
s	Soluble
SA	Sialic acid
SDHA	Succinate dehydrogenase A
S. mansoni	*Schistosoma mansoni*
SOC	Super optimal broth with catabolite repression
SOCS	Suppressor of cytokine signalling
SR	Scavenger receptor#
Stat	Signal transducers and activators of transcription
Sv129	129Sv/Ev
T	Thymidine
TBS	Tris buffered saline
TGF	Transforming growth factor
T_H	T helper
TLR	Toll-like receptor
TMB	3,3',5,5'-tetramethylbenzidine
TNFα	Tumour necrosis factor α
TRAIL	TNF-related apoptosis-inducing ligand
TRIF	Toll/interleukin-1 receptor domain-containing adapter-inducing interferon-β
U	Uracil
v	Volume
vRNA	Viral ribonucleic acid
WSN	A/WSN/33 influenza virus

1 Introduction

1.1 Influenza A Virus

A member of the Orthomyxoviridae family, influenza A virus is a negative sense RNA virus with an eight segmented genome. This family comprises three different genera of influenza viruses; A, B and C, as well as thogotovirus and isavirus (Palese & Shaw, 2006). While the generally mild symptoms of influenza A virus infection in humans include sneezing, headaches, coughing, fever and general aches and pains, infection in high risk groups such as the elderly, the immunocompromised or individuals with underlying medical conditions, can prove fatal particularly with the onset of secondary bacterial infections and pneumonia. Several strains of virus can be circulating in a population at any one time.

Each segment of the genome encodes at least one viral protein including the surface antigens haemagglutinin (H, HA) and neuraminadase (N, NA). These are responsible for attachment, entry and exit of the virus to and from the cell, and also allow identification and differentiation between viral strains. The segmented genome allows genetic reassortment between viral strains within a single genus, known as genetic shift (Palese & Shaw, 2006).

Influenza A virus can infect birds and various mammalian hosts, including humans, in a strain dependent manner. However, co-infection of a host can occur, leading to genetic shift and emergence of new viral strains. This in turn can lead to pandemics as entire populations are naïve to the new virus.

Of the sixteen HA and nine NA subtypes identified, viruses comprising subtype combinations H1N1, H2N2 and H3N2 have caused pandemic infections in humans, while others have been restricted to avian hosts. This species restriction is facilitated by the preference of viral HA to bind to sialic acid (SA)

on the cell surface via different linkages in birds and humans (Connor *et al.*, 1994). Despite this apparent incompatibility, avian influenza strains H5N1, H7N7 and H9N2 have been known to successfully infect humans causing disease (Butt *et al.*, 2005; CDC, 1997; Fouchier *et al.*, 2004; Koopmans *et al.*, 2004).

1.2 Biology of Influenza A Virus

1.2.1 Attachment and Entry

Interactions between SA on the host cell surface and the viral HA protein result in viral attachment. As mentioned above, avian and human viruses recognise and bind SA differently. This is due to different amino acids present at the binding site for SA altering the shape of the binding pocket and therefore dictating interactions with different configurations of N-acetylneuraminic acid-bound galactose (Connor *et al.*, 1994). Glaser and colleagues found that in two isolates of the 1918 H1N1 virus, a single differing amino acid at position 190 of HA enabled one isolate to bind both mammalian α2,6 linked and avian α2,3 linked SA. An isolate with sequence 190D, 225G successfully bound both forms of SA, while reversion of 190D to the avian consensus sequence 190E abrogated binding to α2,6 linked SA. A further point mutation in the double binding virus resulting in the sequence 190D 225D, rendered it specific for the mammalian configuration of SA (Glaser *et al.*, 2005). This demonstrates the ability of the HA protein to undergo small rapid mutations, a process known as genetic drift, which can contribute to virus adaptation to mammalian hosts.

Once attached to the host cell membrane, the virus utilises an as yet unidentified sialylated surface receptor(s) to become internalised in an endosome (Figure 1.1). The matrix 2 (M2) protein forms a pore in the endosome membrane, allowing entry of H^+ ions (Pinto *et al.*, 1992). This lowers

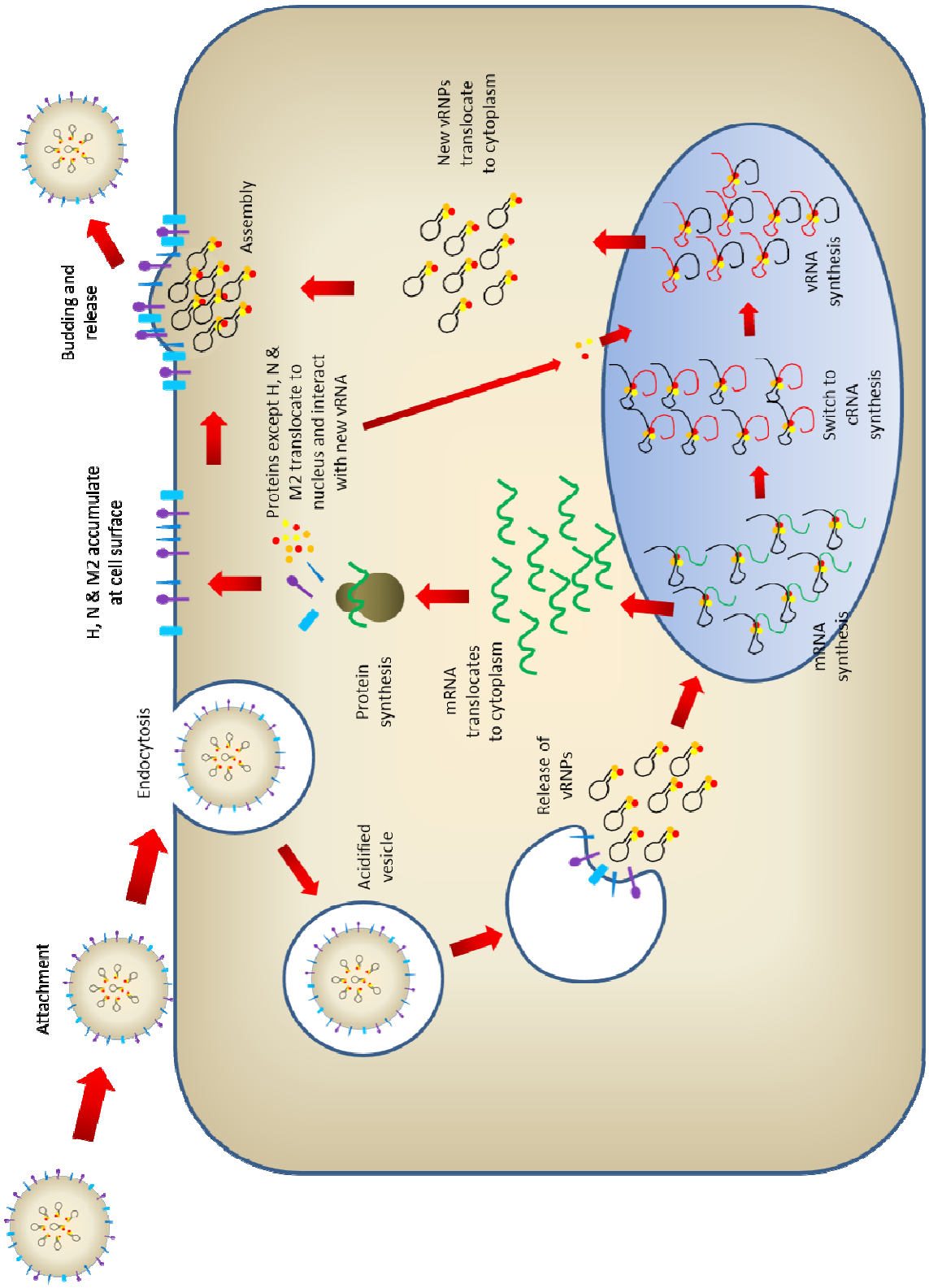
Attachment
Endocytosis
Acidified vesicle
Release of vRNPs
mRNA translocates to cytoplasm
Protein synthesis
H, N & M2 accumulate at cell surface
Budding and release
Assembly
Proteins except H, N & M2 translocate to nucleus and interact with new vRNA
New vRNPs translocate to cytoplasm
mRNA synthesis
Switch to cRNA synthesis
vRNA synthesis

Figure 1.1 Replication cycle of influenza A virus
Influenza virus attaches to the cell surface via sialylated receptor(s) and becomes internalised in an endosome. Uncoating occurs as M2 forms a pore and allows influx of ions resulting in a conformational change in the HA protein which fuses the viral and endosomal membranes. Viral ribonucleic proteins are released into the cytoplasm and translocate to the nucleus for replication. Viral mRNA, cRNA and genomic RNA are synthesised in the nucleus, viral proteins are synthesised in the cytoplasm and virion assembly takes place at regions of accumulation of viral glycoproteins at the plasma membrane, resulting in budding and release of progeny virus.

the internal pH, allowing a conformational change in the HA protein. It is cleaved into HA1 and HA2 proteins by cellular proteases, a process that is essential for viral infection (Klenk *et al.*, 1975; Lazarowitz & Choppin, 1975). HA2 facilitates fusion of the viral membrane with that of the endosome, and several HA molecules come together to form a pore releasing the viral ribonucleic proteins (RNPs) into the cytoplasm (Palese & Shaw, 2006).

1.2.2 Transcription and Replication

As previously described, influenza A is a negative sense RNA virus comprised of eight gene segments, which have been found to code for up to 12 viral proteins. These are the viral surface antigens HA, NA and the M2 protein, the M1 protein, which lies just below the viral membrane, three viral polymerase complex proteins polymerase basic (PB) 1, PB2 and polymerase acid (PA), non-structural (NS) proteins 1 and 2, the nuclear protein (NP). In some strains, an eleventh protein encoded by an alternative open reading frame on the PB1 gene, PB1-F2 is expressed (Chen *et al.*, 2001). A further twelfth peptide encoded by the PB1 gene segment, N40, has recently been identified but the function of this protein is yet to be determined (Wise *et al.*, 2009). These proteins and their functions are summarised in Table 1.1.

The RNA segments are coated by NP to form RNPs. The viral polymerase proteins are also involved in formation of RNPs, imposing a panhandle structure on the RNA (Gonzalez & Ortin, 1999a; Hsu *et al.*, 1987). Upon release from the virion into the cytoplasm, the RNPs are transported to the nucleus via localisation signals in NP (Cros *et al.*, 2005; O'Neill *et al.*, 1995). Once localised in the nucleus, the RNPs undergo transcription, producing viral mRNA. To do this, PB2 binds the 5' caps of cellular pre-mRNAs, which PB1 then cleaves (Blaas *et al.*, 1982). After cleavage, a G residue is added to the 3' end of the cap, allowing it to base pair with a C at the 3' end of the viral mRNA held by the polymerase in its panhandle shape. PB1 then elongates the capped molecule as the viral RNA is spooled through the polymerase complex

Gene Segment	Proteins Encoded	Function
Haemagglutinin	H spike	Attachment to host cell
	H1	Contains receptor binding site
	H2	Facilitates fusion of endosome and viral membranes for uncoating
Neuraminidase	N	Destruction of cellular sialic acid to complete release from host cell
Non Structural	NS1	IFN antagonist; role in immune dysregulation
	NS2	Nuclear export of genome Regulation of RNA species
Polymerase Basic 1	PB1	Polymerase complex; binds and elongates vRNA; role in pathogenesis
	PB1-F2	Virulence factor; induction of inflammation; induces apoptosis in some strains
	N40	N terminally truncated PB1-related protein; function unkown
Polymerase Basic 2	PB2	Polymerase complex; cap binding protein
Polymerase Acid	PA	Polymerase complex protein
Matrix 1	M1	Assembly and budding of new virions from host cell
	M2	Forms ion pore to allow pH mediated uncoating
Nuclear Protein	NP	Binds ribonucleic proteins, involved in nuclear export of genome

Table 1.1 Influenza virus gene segments and proteins.
Influenza A virus encodes up to 12 proteins from its 8 gene segments

(reviewed by Palese & Shaw, 2006). The 5' end remains bound, however, preventing further transcription and causing the polymerase to stutter at a polyU sequence, creating a polyA tail on the new viral mRNA (Luo *et al.*, 1991). Once these viral mRNAs have been synthesised the virus then commandeers the cellular splicing machinery to produce templates for the spliced transcripts NS1, NS2 (Lamb *et al.*, 1980), M1 and M2 (Lamb *et al.*, 1981). After transcription of the viral mRNAs, a full length cRNA must be synthesised to provide a template for viral genomic RNA (vRNA). This template is neither capped or polyadenylated (Hay *et al.*, 1977). The mechanism by which the polymerase complex switches between transcription of mRNA and cRNA is largely unknown, although differing binding sites for vRNA and cRNA have been identified (Gonzalez & Ortin, 1999b). The process is also dependent on newly synthesised NP, which is responsible for coating cRNA and protecting it from degradation. It is hypothesised that the polymerase complex can transcribe both mRNA and cRNA (Vreede & Brownlee, 2007), but until NP and the polymerase complex have been translated, cRNA undergoes degradation and so is not readily detectable early in infection indicating that RNA stability may facilitate the switch to viral replication over mRNA transcription (Vreede *et al.*, 2004). The nuclear export protein NS2 has also been implicated in regulating the ratios of mRNA to cRNA, favouring accumulation of cRNA intermediates for replication over mRNA production (Robb *et al.*, 2009). Recently, however, small viral RNAs (svRNA) have been discovered, the expression of which temporally correlates with accumulation of genomic vRNA. These svRNAs appear to be segment specific and interact with the polymerase complex. Inhibition of svRNA results in reduced replication of the corresponding vRNA, implicating this newly discovered influenza RNA species in regulation of replication versus transcription (Perez *et al.*, 2010).

Once vRNAs are synthesised and assembled into RNPs in association with NP and the polymerase complex, they then interact with M1 (Martin & Helenius, 1991) and NS2 (O'Neill *et al.*, 1998), allowing nuclear export of the RNPs into

the cytoplasm for virion assembly. It has also been suggested that NP may interact directly with the cellular CRM1 nuclear export pathway to facilitate this process (Elton *et al.*, 2001).

1.2.3 Assembly and Exit

Once the mRNAs have been transcribed, viral proteins are synthesised on cellular ribosomes, passaged through the ER and golgi apparatus, from which they are transported to the cell membrane. At the membrane, HA and NA are found to preferentially accumulate at areas rich in cholesterol and sphingolipids, with M2 accumulating at the edges of these regions. This results in viral budding from these domains, known as lipid rafts (Scheiffele *et al.*, 1999; Takeda *et al.*, 2003). Little is known of how the remaining viral components locate to these lipid rafts and assemble. The ability of M1 to bind to HA may lead to it and associated RNPs being transported to the cell surface along with the HA protein (Ali *et al.*, 2000). It has also been suggested that M1 and NP interact with the host cytoskeleton and are transported to the site of budding in this manner (Avalos *et al.*, 1997).

Packaging of the full complement of eight RNPs into each virion is also poorly understood. It has been proposed that RNPs are packaged at random into virions to ensure a full complement (Enami *et al.*, 1991), but more recently it has been suggested that individual packaging signals on the 5' and 3' end of the RNPs allow selective uptake of eight different RNPs into the virion (Fujii *et al.*, 2003; Muramoto *et al.*, 2006). The virus buds through the plasma membrane, encapsulating the virion in the cell's lipid bilayer with HA, NA and M2 protruding through. This process has previously been shown to require only the M1 protein (Gomez-Puertas *et al.*, 2000), although this is somewhat controversial. Although M1 appears capable of forming virion-like particles, this may be dependent on targeting of M1 to the plasma membrane either by the VLP system being used (Gomez-Puertas *et al.*, 2000), foreign targeting signals (Wang *et al.*, 2010), or by M1 interactions with the cytpolasmic tail of

HA during translocation to the cell surface (Ali *et al.*, 2000). HA alone has also been demonstrated to form VLPs in a virus-free transfection system (Chen *et al.*, 2007), implying that M1 is not essential for VLP formation. However, efficiency of particle formation was greatest in the presence of HA, NA, M1 and M2 indicating roles for multiple viral proteins in virus release. Further to this, Rossman et al showed that M2 is required for release of budding particles from the cell membrane by facilitating membrane scission (Rossman *et al.*, 2010). NA functions to remove SA from the cell surface and the surface of the viral membrane preventing aggregation of virus (Palese *et al.*, 1974) and releasing the virus to infect neighbouring cells and new hosts.

1.3 Influenza Pandemics

1.3.1 1918 – H1N1

Otherwise known as 'Spanish Flu', the H1N1 virus that swept the globe in 1918 was the most pathogenic strain of influenza A virus on record to infect humans. The death toll rises with every reassessment, with the current figure conservatively around 50 million deaths worldwide (Kobasa *et al.*, 2007).

The 1918 pandemic arose in the USA, with soldiers falling ill in military camps when they reported for training. However, the war prevented much of this early outbreak being publicised and it was not until the infection spread to Spain, more neutral in its wartime involvement, that this virus was publicly reported. At this point, the infection was highly contagious but caused relatively few fatalities. Later in the year, a highly virulent form of this H1N1 virus emerged and spread rapidly around the world, causing extremely high mortality rates. In the US, it thought that between 3 and 10 deaths occurred per 1,000 population, while Asian and African countries may have seen such high rates as high as 50 deaths per 1,000 (Wright *et al.*, 2006).

Onset of symptoms of the 1918 H1N1 virus was sudden, characterised by high fever, severe headache, aches and pains with pathology mostly limited to the respiratory tract. Although secondary bacterial pneumonia was the most common cause of death, some patients showed massive pulmonary oedema and haemorrhage (Wright *et al.*, 2006). This was studied in a macaque model using the 1918 virus, generated by reverse genetics. The infected macaques became moribund within days of infection, ultimately leading to euthanasia at day 8 post infection. These animals displayed elevated cytokine levels and dysregulated immune responses, thought to lead to the dramatic pulmonary pathology observed (Kobasa *et al.*, 2007). Indeed the ability of this virus to induce elevated cytokine production from macrophages, leading to influx of proinflammatory cells has been attributed to the 1918 HA gene (Kobasa *et al.*, 2004; Tumpey *et al.*, 2005). The polymerase genes (Tumpey *et al.*, 2005) and NS (Geiss *et al.*, 2002) have also been implicated in the extreme pathogenesis of this virus. This immune dysregulation and acute pathology has also been observed in H5N1 patients (To *et al.*, 2001) and animal models (Gao *et al.*, 1999), suggesting that the ability to modulate the host immune response, leading to severe acute respiratory distress, may be a common feature of highly pathogenic influenza viruses.

In addition to the unusually severe pathology seen in 1918 H1N1 infection, the pattern of infection was also different to that observed in previous influenza outbreaks. Ordinarily, the most susceptible individuals to the virus are infants and the elderly. However, during the 1918 pandemic, the majority of those succumbing to the virus were healthy young adults, with the 15-35 age bracket being struck down with unusual severity (Wright *et al.*, 2006). This suggests pre-existing cross protective immunity in the elderly, or a reduced capacity to mount the excessive inflammatory response that is thought to have contributed to the extreme morbidity and mortality in younger age groups.

H1N1 viruses continue to circulate in humans and cause seasonal illness. However 2009 saw the outbreak of a pandemic strain of H1N1 influenza virus. This novel virus is derived from a swine virus containing gene segments from human, avian and porcine viruses, leading to its description as a triple reassortant virus (Smith *et al.*, 2009). While both seasonal and pandemic H1N1 viruses express the same subtype of surface glycoproteins, these genes are derived from different origins and are antigenically distinct.

1.3.2 1957 – H2N2

1957 saw the outbreak of a strain of influenza with H2 and N2 subtypes, both acquired from avian viruses and also included an avian PB1 gene (Zamarin *et al.*, 2006). The outbreak was first isolated in Southern China before striking the US and UK, becoming known as Asian influenza. Although mortality rates were less severe than in 1918, infection rates were extremely high, again with younger age groups being the most severely affected. The virus itself was not excessively pathogenic, but still caused the death of over 1 million people worldwide (Wright *et al.*, 2006). It is thought that lack of previous exposure to these viral surface antigens resulted in the high infection and mortality rates observed. The 1957 H2N2 virus expressed the PB1-F2 protein from its avian derived PB1 gene segment. The effect of PB1-F2 on pathogenicity of this virus is unknown but it has been shown that C terminal fragments of this protein led to inflammatory infiltrate and induction of symptoms in mice, indicating a role in disease severity (McAuley *et al.*, 2010a).

1.3.3 1968 – H3N2

The previously circulating H2N2 virus of 1957 was replaced by H3N2 in 1967, causing another pandemic originating in Hong Kong. The H2N2 virus acquired new HA (H3) and PB1 genes by recombination with an avian virus, but retained a similar NA to its precursor. Despite infection rates of up to 40%, mortality was fairly low, most likely due to the majority of the population

having been exposed to a very similar NA antigen 11 years earlier (Wright *et al.*, 2006). Once again, the impact of the avian PB1-F2 is unknown but the C terminal region of this protein induced clinical symptoms and inflammation in the lungs of challenged mice, while failing to induce apoptosis in an in vitro model (McAuley *et al.*, 2010a).

H3N2 viruses continue to infect humans annually and remain in circulation despite the new pandemic H1N1 having effectively outcompeted seasonal H1N1 viruses (Ilyushina *et al.*, 2010).

1.3.4 1977 – H1N1

H1N1 re-emerged at the end of 1977 and caused illness among those under the age of 25. This particular strain was found to be similar to H1N1 viruses that had circulated during the 1950s (Wright *et al.*, 2006) and so the majority of the population had been previously exposed to these surface antigens. Re-emergence of this virus did not replace H3N2 viruses, and both continued to cause illness in humans.

1.3.5 2009 – H1N1

In April of 2009, the most recent influenza pandemic threat arose from a previously unsuspected origin. An H1N1 virus, now thought to have been circulating undetected in swine for as long as a decade (Smith *et al.*, 2009), made the transition to humans in Mexico, rapidly spreading throughout the country and beyond. The 2009 pandemic strain is a triple reassortant virus, containing gene segments derived from avian, human and classical swine viruses of North American and Eurasian origin (Smith *et al.*, 2009). Although it has long been known that pigs can become infected with the virus, most attention has been focused in recent years on avian influenza and so the 'swine flu' outbreak caused some consternation among virologists.

Transmission studies utilising ferrets indicated increased morbidity and viral titres in experimentally infected animals compared to seasonal H1N1, but reduced efficiency of droplet transmission (Maines *et al.*, 2009). Despite this apparently poor transmissibility, the 2009 pandemic virus rapidly spread around the globe between its detection in March 2009 and the World Health Organisation declaration of pandemic status in June of that year.

However, the virus has so far caused relatively mild disease and limited mortality. Although there has been a high incidence of hospitalisations, many of these were due to complications related to underlying conditions, some of which were not previously recognised as risk factors for influenza, such as obesity and diabetes (Louie *et al.*, 2009). Isolates of the 2009 H1N1 virus replicated efficiently in human dendritic cells and macrophages, but induced a weak IFN response, similar to that observed during infection with seasonal H1N1 (Osterlund *et al.*, 2010; Zeng *et al.*, 2011). Furthermore, the 2009 strain appeared to be impaired in its ability to replicate at 33°C, the temperature of the upper respiratory tract, compared with seasonal viruses (Zeng *et al.*, 2011). Strong replicative capacity at 37°C indicates that this virus is adept at causing infection in the lower respiratory tract, confirmed by autopsy data of fatal infection cases which demonstrate strong positivity for virus in the alveoli (Calore *et al.*, 2011). This implies that the reduced severity of disease may be due to inefficient entry to the lower respiratory tract resulting in limited viral replication.

Experimental infections in mice have demonstrated limited immunopathology and lethality, consistent with limited induction of antiviral cytokines (Belser *et al.*, 2010; Maines *et al.*, 2009). However, the 2009 isolates could directly infect mice without prior adaptation (Maines *et al.*, 2009), a trait commonly observed in highly pathogenic strains of influenza virus. In contrast to such viruses, however, the 2009 H1N1 was sensitive to the antiviral action of IFNs, despite avoiding their induction (Osterlund *et al.*, 2010).

Due to the capacity for rapid mutation inherent to RNA viruses, the possibility of this H1N1 obtaining increased virulence is an important concern. As such, several groups have investigated the effect of known virulence factors on the 2009 H1N1 backbone. The currently circulating virus encodes three STOP codons in its PB1-F2 reading frame and therefore expresses a truncated, 11 amino acid long protein. Using reverse genetics to produce a 2009 H1N1 virus expressing a full length PB1-F2 did not result in enhanced virulence (Hai *et al.*, 2010). Similarly, alteration of the STOP codon at position 88 to tryptophan did not increase the pathogenicity of the virus (Ozawa *et al.*, 2011). Recently, however, isolates have been identified with a naturally occurring mutation of the STOP codon at position 12 to lycine, resulting in a 57 residue long PB1-F2 protein. This increased pathogenicity both in vitro and in vivo but was not lethal in mice (Ozawa *et al.*, 2011). Furthermore, mutation of the STOP codon at NS1 position 220 to tryptophan, in concert with an XSEV motif in the final four C terminal amino acids of the NS1 protein results in enhanced virulence of the 2009 H1N1 virus (Ozawa *et al.*, 2011).

Avian and human viruses differ in particular amino acids within the polymerase complex proteins. The consensus human sequence includes lycine and asparagine at positions 627 and 701 respectively in PB2, which is thought to be important for efficient replication in mammals. The 2009 pandemic virus expresses the avian consensus sequence of glutamic acid at 627 and aspartic acid at 701. Mutation of the 2009 PB2 to the consensus human sequence did not enhance replication or disease severity, but did increase viral shedding in ferrets, as did a further mutation to introduce glycine at position 677 (Herfst *et al.*, 2010).

It has been suggested that antigenic shift is more likely than antigenic drift to give rise to a virus with increased pathogenicity. However, given that this virus has effectively outcompeted seasonal viruses, it has been suggested that the

limited capacity for antigenic shift may restrain the emergence of a more pathogenic strain (Ilyushina *et al.*, 2010).

1.3.6 The Threat of an H5N1 Pandemic

In recent years, much attention has been given to the H5N1 strain of avian influenza after the outbreak of this virus in Hong Kong in 1997. This highly pathogenic strain has caused widespread disease in domestic and migratory birds, and has jumped the species barrier to infect humans without apparent recombination of the viral genome (Gao *et al.*, 1999). Direct contact with infected poultry can lead to infection of humans, but despite the highly efficient transmission between birds, human to human transmission appears to be poor (Chan *et al.*, 2005). However, the disease that ensues in infected individuals has been severe with 553 confirmed cases and 323 fatalities to date with a mortality rate of over 80% in some south east Asian countries (WHO, 2011).

The emergence of an avian H5N1 virus with the ability to infect humans with no prior recombination in 1997 was totally unprecedented. All previous influenza viruses of avian origin capable of infecting humans had undergone genetic recombination with human viruses. In 1997, 18 cases of highly pathogenic H5N1 were identified in Hong Kong, of which 6 were fatal (To *et al.*, 2001). All 18 patients were found to have had close, direct contact with poultry, leading to the decision to cull all live poultry in markets in Hong Kong. Human to human transmission appeared to be inefficient, if it occured at all and no further cases were reported at this time. However, in 2001, poultry stocks again became infected with H5N1, resulting in another mass cull. H5N1 was maintained in the wild bird population and in early 2003, a young boy and his father were admitted to hospital in Hong Kong, infected with the H5N1 virus (Peiris *et al.*, 2004). By July 2003, the virus was rife in poultry stocks throughout Asia, leading to the death or culling of over 100 million

farmed birds. The virus has also been identified in various European countries in migratory birds as well as some farmed poultry.

Infection with H5N1 has been observed to lead to dysregulation of the immune system, with greatly elevated proinflammatory cytokine levels and acute respiratory distress syndrome (ARDS), leading to multiple organ failure and haemophagocytosis (To *et al.*, 2001). Much of this pathology is due to disrupted immune regulation caused by the virus and has been the focus of many studies over the last decade. Various viral genes have been implicated in alteration of the host immune response, including the NS and HA genes, as well as PB2 (Gao *et al.*, 1999; Hatta *et al.*, 2001; Li *et al.*, 2005; Seo *et al.*, 2002). H5N1 viruses appear to be resistant to cellular IFNγ and TNFα (Seo *et al.*, 2002), while inducing expression of these and other proinflammatory cytokines from macrophages, $CD4^+$ and $CD8^+$ T cells infiltrating the infected respiratory tract (Chan *et al.*, 2005; Cheung *et al.*, 2002). The production of these cytokines in the context of a virus highly resistant to their actions leads to increased immunopathology in the lung as the inflammatory response causes damage to the lung tissue while attempting to clear the virus. The induction of cytokine production from infected macrophages (Cheung *et al.*, 2002; Zhou *et al.*, 2006) leads to further influx of inflammatory mediators into the tissue and continues to exacerbate the condition, ultimately leading to the severe symptoms observed.

The potential for this highly pathogenic virus to recombine with one capable of efficient human to human transmission and the increasing incidence of human infection makes the emergence of an H5N1 pandemic a serious threat.

1.4 Experimental Influenza Virus Infections in Mice

Several different strains of virus have been utilised in experimental mouse models of influenza virus infection. Perhaps the most commonly studied are the mouse adapted H1N1 strains A/WSN/33 (WSN) and A/PR/8/34 (PR8), both of which result in severe disease. However, two milder H3N2 strains, BJx109 and HKx31, are also frequently used as mice generally recover from these infections. Importantly, these viruses share their internal genes with PR8, differing only by their surface antigens.

1.4.1 A/WSN/33

In 1939 and 1940, two authors published the generation of variant strains of the Wilson-Smith virus (A/WS/33) which had been adapted to stably induce neurological symptoms in mice. The first of these strains was generated by serial passage in embryonic chick chorioallantoic tissue followed by intracerebral inoculation in mice, resulting in neurological symptoms by passage 12 (Stuart-Harris, 1939), and became known as 'A/NWS/33'.

Several other variants were established by Francis and Moore, by serial passage of the Wilson-Smith strain through embryonic chick brain tissue. Following the seventh passage in this tissue, the virus was inoculated intracerebrally into mice, and further serial passage performed until neurological symptoms were evident at passage 12, when the mice were euthanized. A further variant was developed in this laboratory by serial passage through whole chick embryo cultures, which was the standard tissue culture technique for maintenance of influenza viruses at that time. Again, following intracerebral inoculation and serial passage, this virus demonstrated the ability to induce neurological symptoms. The neurotropic capacity of this virus was restricted to intracerebral inoculation, while infection by the intranasal route resulted in pulmonary infection with no evidence of neurological symptoms (Francis & Moore, 1940). However, this virus has now

been shown to induce systemic infection and has been recovered from the brain following intranasal infection (Castrucci & Kawaoka, 1993). This laboratory maintained virus became known as 'A/WSN/33' (WSN) and has been widely used for infection studies in mice.

The NA protein of WSN has been identified as being responsible for the neurotropism of this virus (Goto *et al.*, 2001), and also enables WSN to utilise the ubiquitous protease plasmin to cleave its HA in the absence of trypsin (Goto & Kawaoka, 1998). This increases the pathogenicity and tropism of WSN, as the virus does not contain a polybasic cleavage site in its haemagglutin protein, the presence of which is typical of highly pathogenic viruses and allows cleavage by ubiquitous cellular proteases such as furin (Gao *et al.*, 1999).

1.4.2 A/PR/8/34

The PR8 strain of virus was derived from a human isolate in Puerto Rico in 1934 (Francis, 1934). This isolate was serially passaged in ferrets, followed by passage in mice and further maintenance in chick embryo tissue culture medium, during which time the virus retained its infectivity for mice and ferrets, resulting in pulmonary disease (Francis & Magill, 1935). PR8 has subsequently been shown to be highly pathogenic to mice, inducing excessive inflammation in the lung and death within seven days of infection (Hennet *et al.*, 1992).

1.4.3 HKx31 and BJx109

As antigenic drift alters the surface proteins of circulating seasonal influenza viruses, the annual influenza vaccine must be updated. However, circulating strains are generally inefficient at replicating in tissue culture and so high yielding reassortants, which combine the efficient tissue culture replicative capacity of PR8 with the antigenic determinants of seasonal influenza strains,

are necessary for generation of vaccine strains. Embryonated chicken eggs are coinfected with the seasonal virus and the laboratory strain PR8, resulting in recombinant viruses. The recombinant virus with the highest haemagglutination titre in the presence of anti-PR8 rabbit antisera is selected for further passage through chicken eggs. This is repeated for three passages before antigenic determination of the high growth reassortant virus. Further egg passage is carried out, followed by antigenic characterisation to ensure stable phenotype of the virus before inclusion in the vaccine (described by Robertson *et al.*, 1992).

This technique was successfully pioneered by Dr. E. Kilbourne, generating the HKx31 virus by recombination between PR8 and A/Aichi/2/68 (Kilbourne *et al.*, 1971). Similarly, BJx109 is a high yielding reassortant virus expressing the internal genes of PR8 and the surface proteins of the seasonal strain A/Beijing/353/89, generated for inclusion in the 1991-1992 vaccine (Robertson *et al.*, 1992).

Despite the high growth capacity, and the ability to replicate in mice, these viruses are not as pathogenic as their PR8 parent (Tate *et al.*, 2011), which has been associated with the differential abilities of these viruses to infect macrophages (Reading *et al.*, 2000) and resist the actions of surfactants and collectins (Reading *et al.*, 1997).

1.5 Pathogenesis of Influenza A Virus

Various viral proteins have been implicated in the pathogenicity of influenza viruses, with H5N1 viruses being especially well documented for their ability to cause dysregulation of the immune system. Intensive inflammation of the airways and lungs leading to severe and irreversible pathology is characteristic of this strain.

1.5.1 Haemagglutinin

Highly pathogenic avian influenza (HPAI) H5N1 viruses have been divided into two groups based on their pathogenicity in mice. Group one viruses cause lethal systemic infection in mice and contain a multibasic cleavage site making HA susceptible to cellular proteases such as furin and PC6 (Gao *et al.*, 1999). It has been suggested that this is responsible for allowing the virus to spread beyond the respiratory tract and become cleaved into HA1 and HA2 subunits in many different cell types. Similarly, despite the absence of the polybasic cleavage site, WSN has demonstrated extrapulmonary tropism including neurovirulence, associated with the ability to bind and sequester plasminogen, enabling this virus to utilise plasmin to cleave its HA (Goto & Kawaoka, 1998).

The second group of HPAI viruses are non lethal in mice and remain localised in the respiratory tract (Gao *et al.*, 1999). It was thought that lack of a multibasic cleavage site seen in group one viruses restricts the tropism of these viruses to respiratory cells containing specific proteases. However, some non-lethal viruses placed in group 2 possess multi-basic cleavage sites in their HA, indicating that lethality in mammals is a polygenic trait. However, both groups of viruses cause systemic, lethal infection in chickens. Furthermore, this classification applies only to isolates from the 1997 outbreak of H5N1.

Single gene reassortant virus studies allowed further investigation of the role of HA in H5N1 virulence. HA from group two viruses were found to contain either

serine or isoleucine at position 227, but were still non-lethal regardless of residue at this position. However, introduction of these HA genes onto a group one virus background led to differing properties. The HA containing isoleucine at position 227 successfully attenuated the pathogenicity of the group one virus. The presence of serine however, did not confer any protection and infected mice succumbed to the infection (Hatta *et al.*, 2001). This shows that although amino acid sequence is an important factor in determining attenuation of virulence, this is complicated by the presence of other virulence factors within a viral strain.

1.5.2 Non Structural Protein 1

The NS1 protein has been heavily implicated in the pathogenesis of H5N1 and other influenza virus strains (Figure 1.2). It confers resistance against the anti-viral activity of IFNs and TNFα, while interfering with production of these cytokines from infected cells. It has been shown that recombinant viruses expressing the NS1 gene from H5N1 on an H1N1 background led to increased production of TNFα from infected cells (Cheung *et al.*, 2002; Lipatov *et al.*, 2005). However, pre-treatment with IFN or TNFα, which inhibits replication of other influenza A viruses, had no effect on replication of H5N1 virus. Seo et al showed that the NS1 from lethal H5N1 has a point mutation at position 92. All human strains have aspartic acid (D) at this position. Those derived from the 1997 H5N1, an avian virus, encode glutamic acid (E) at position 92. PR8 H1N1 virus was given only the NS1 from either H5N1/1997 (E at position 92), H5N1/2001 (D at position 92) or a revertant of H5N1/1997 (D at position 92). The viruses encoding D at NS1 position 92 were attenuated, while the remaining virus was pathogenic. Furthermore, NS1 of H5N1 imbued WSN H1N1 virus with the capacity to induce high levels of TNFα, suggesting that this gene is involved in dysregulation of the cytokine response (Cheung *et al.*, 2002). This single amino acid change has also been identified as responsible for viral resistance to cytokines (Seo *et al.*, 2002). This work, however, was

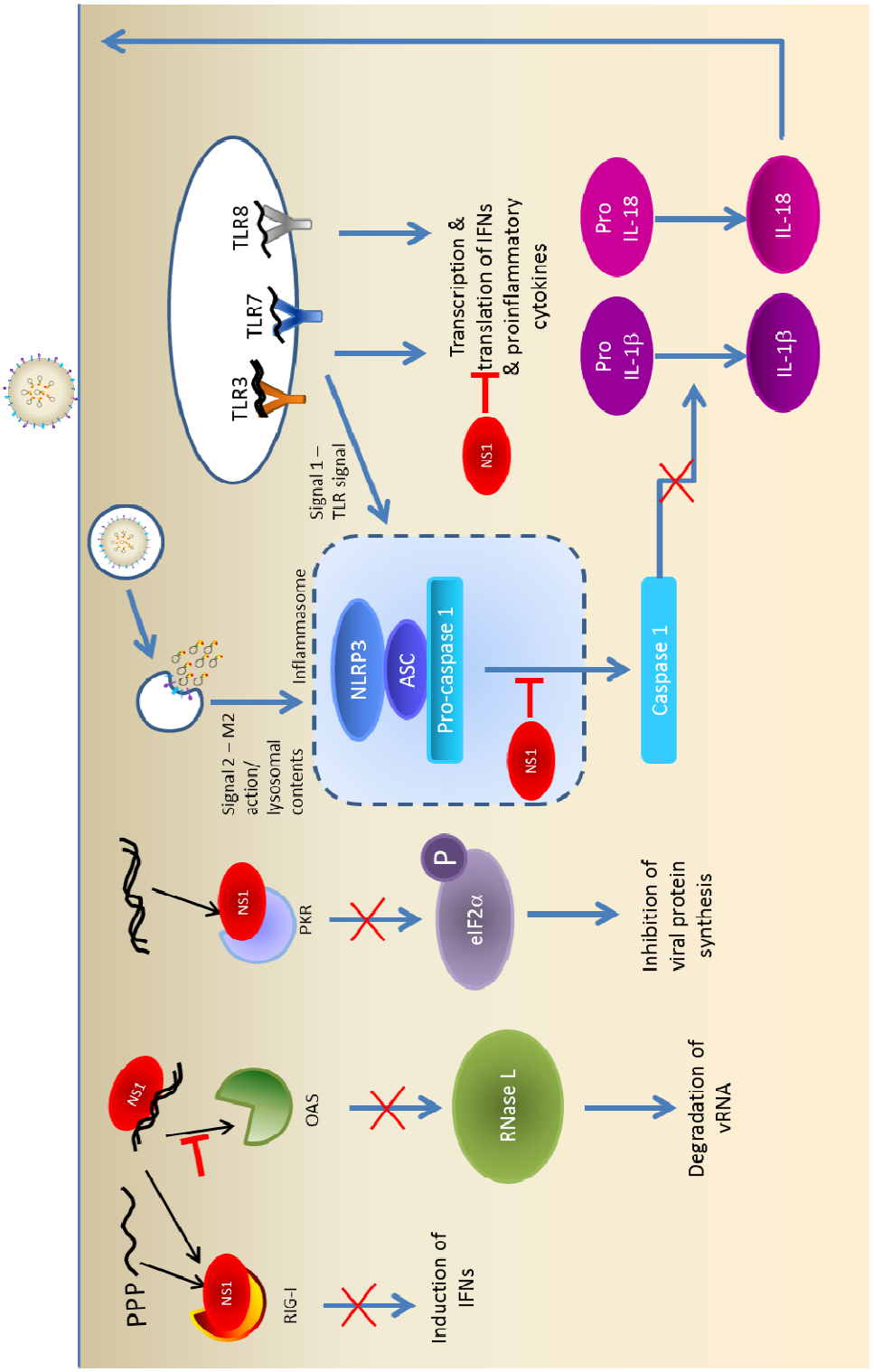
TLR8
TLR7
TLR3
Transcription & translation of IFNs & proinflammatory cytokines
NS1
Signal 1 – TLR signal
Pro IL-18
IL-18
Pro IL-1β
IL-1β
Signal 2 – M2 action/ lysosomal contents
Inflammasome
NLRP3
ASC
Pro-caspase 1
NS1
Caspase 1
NS1
PKR
P
eIF2α
Inhibition of viral protein synthesis
NS1
OAS
RNase L
Degradation of vRNA
PPP
NS1
RIG-I
Induction of IFNs

Figure 1.2 NS1 interacts with cellular defence pathways
The viral protein NS1 interacts and inhibits many pathways involved in cellular recognition and response to influenza virus, including blocking IFNs at both pre and post-transcriptional levels, inhibiting inflammasome dependent cleavage of caspase 1 and binding to viral RNA or host proteins to prevent recognition of the viral genome and thereby facilitates host immune evasion by a multitude of mechanisms.

carried out in porcine lung cells using pre-treatment with swine cytokines rather than a human lung epithelial cell line. A recent study has demonstrated that in human lung explants, H5N1 and seasonal H1N1 viruses are in fact susceptible to the actions of IFNs following pre-treatment, despite efficiently inhibiting post-infection IFN signalling. This indicates that although these viruses can subvert induction of the host immune response, they are not inherently resistant to the actions of IFNs (Jia *et al.*, 2010).

It was thought that the ability of the NS1 protein to bind to double stranded RNA resulted in sequestration of the viral genome from cellular defences such as PKR and 2'-5'-oligoadenylatesynthetase (OAS; Wright *et al.*, 2006). However, while the RNA binding region of NS1 appears to be vital in protecting the virus from the degrading effects of OAS-induced RNAseL (Min & Krug, 2006), this function of the NS1 protein does not seem to be involved in evasion of the PKR pathway. It is now apparent that NS1 can bind to the N terminal region of PKR, inhibiting the conformational change induced by binding of double stranded RNA (Li *et al.*, 2006; Min *et al.*, 2007). NS1 also binds to RIG-I (Mibayashi *et al.*, 2007; Pichlmair *et al.*, 2006), further impairing induction of the host IFN and anti-viral response. NS1 mediated impairment of PKR, OAS and RIG-I results in downstream inhibition of transcription factors such as IRF3 and NFκB, ultimately preventing transcription of IFNs and effective establishment of the antiviral state (Figure 1.2).

In addition to its role in pre-transcriptional impairment of the IFN response, NS1 also mediates post-transcriptional mechanisms of IFN blockade (Figure 1.2). NS1 can inhibit processing and maturation of cellular mRNAs by interacting with host polyadenylation machinery, Cleavage and Polyadenylation Specificity Factor (CPSF) 30 and PolyA Binding Protein II, resulting in inhibition of CPSF30 binding to cellular mRNAs and therefore impaired processing (Nemeroff *et al.*, 1995). Because the virus does not utilise these proteins for polyadenylation, viral mRNAs are unaffected. NS1 is also

responsible for selective translation of viral mRNAs at the expense of cellular mRNAs, in addition to reducing the quantity of mature cellular mRNAs produced. This occurs by interactions between NS1, the 5' UTR of viral mRNAs and host cell protein complexes involved in targeting mRNAs to sites of increased translation. NS1 interacts with subunits of the cellular cap-binding complex, eIF4GI and PABPI, as well as with hStaufen, which is involved in transportation of mRNAs to the polysome, resulting in selective enhancement of viral mRNA translation (Aragon *et al.*, 2000; Burgui *et al.*, 2003; Falcon *et al.*, 1999).

The NLRP3 inflammasome plays a role in the immune response to influenza A virus, resulting in activation of caspase-1, IL-1β and IL-18. Inflammasome activation has been identified as a vital component in the development of functional innate and adaptive responses to influenza A viruses (Allen *et al.*, 2009; Ichinohe *et al.*, 2009; Thomas *et al.*, 2009). However, the RNA binding domain of NS1 has been found to inhibit caspase-1 activation and therefore prevent cleavage of functional IL-1β and IL-18 from their pro- forms (Stasakova *et al.*, 2005), further impairing the host response to infection.

Deletion of NS1 by reverse genetics has further confirmed the role of this protein in escape from the host antiviral response. The delNS1 mutant virus (generated on a PR8 H1N1 background) cannot grow in IFN competent systems (Egorov *et al.*, 1998; Garcia-Sastre *et al.*, 1998), in part due to recognition of viral RNA by PKR in the absence of NS1, and subsequent inhibition of viral protein synthesis (Bergmann *et al.*, 2000). However, this virus can replicate efficiently in IFN deficient cells, therefore showing that NS1 is required not for replication but for interaction and subversion of the host IFN response (Salvatore *et al.*, 2002). IFNα-regulated genes are effectively inhibited by wild type H1N1 virus due to NS1 mediated inhibition of NFκB activation, but the delNS1 mutant fails to do this (Wang *et al.*, 2000) and so is reduced in its ability to subvert host IFN responses. Furthermore, the NS1 protein may

effectively 'buy time' for viral replication by inhibiting induction of the inflammatory burst. Infection with the delNS1 virus resulted in rapid induction of inflammatory responses in C57Bl/6 mice, while this was delayed by up to 48 hours before the host antiviral response was initiated following infection with wildtype virus (Moltedo *et al.*, 2009).

NS1 has also been shown to interact with the p85β subunit of PI3K (Hale *et al.*, 2006). This interaction seems to be important for viral growth but the downstream effects on this diverse signalling pathway are as yet unclear. It is likely however, that this interaction modulates apoptosis, prolonging survival of infected cells (Hale *et al.*, 2006). However, it has recently been shown that failure of mutant NS1 to bind PI3K did not result in increased apoptosis (Jackson *et al.*, 2010) and so the role of this particular interaction remains undetermined.

Despite interacting with the PI3K pathway, NS1 may play a role in induction of apoptosis of host immune cells, although this is not well defined. Again, the delNS1 mutant was utilised to investigate the involvement of NS1 in macrophage apoptosis. delNS1 viruses induce rapid apoptosis in infected cells (Zhirnov *et al.*, 2002), possibly due to the inability of this mutant virus to inhibit IFN-mediated events. However, the wildtype virus shows delayed apoptosis, indicating that NS1 protects the infected cell from undergoing immediate apoptosis and therefore prolonging the time for viral replication. Conversely, in the absence of other viral proteins NS1 has been shown to be sufficient to induce apoptosis in cells (Schultz-Cherry *et al.*, 2001) further illustrating the complexity of the role played by this protein.

1.5.3 PB2

Studies of the two groups of H5N1 viruses with differential lethality in mice have led to the identification of PB2 as a virulence factor for this virus. Introduction of PB2 from a non-lethal H5N1 virus onto a lethal virus

background led to attenuation of the lethal virus. However, introduction of PB2 from a lethal H5N1 virus onto a mild background required expression of serine at position 227 of the HA protein to confer lethality, while the same PB2 gene on the non lethal background containing isoleucine at this position of the HA protein did not lead to death of the animals (Hatta *et al.*, 2001). Taken together, this illustrates the complexity of interplay between influenza virus pathogenicity factors, as sequence specificity on a given gene segment in combination with distinct virulence factors can influence the phenotype of the virus.

The amino acid sequence of PB2 has also been investigated with regards to pathogenicity. Positions 627 and 701 have been implicated (Table 1.2). Single gene reassortant viruses were again utilised to investigate the effect of amino acid polymorphisms at these locations. H5N1 viruses lethal in mice, that usually contain lysine at position 627 were attenuated by the presence of glutamic acid at this residue – normally seen in non-lethal virus PB2. Conversely, the milder viruses could be rendered lethal by substitution of glutamic acid for lysine (Gao *et al.*, 1999; Hatta *et al.*, 2001). Similarly, at position 701, substitution of asparagine for aspartic acid leads to attenuation of lethal viruses, while the reciprocal substitution enables non fatal viruses to become lethal (Li *et al.*, 2005). As asparagine is found mostly in human viruses, it may be a requirement for making the jump from birds to humans. It is highly likely, therefore, that PB2 may play a role in host tropism.

Gene	Background	Amino Acid	Outcome
PB2	Lethal	Lys@627	Death
PB2	Lethal	Glu@627	Survival/attenuation
PB2	Non Lethal	Lys@627	Death
PB2	Non Lethal	Glu@627	Survival
PB2	Lethal	Asp@701	Death
PB2	Lethal	Asn@701	Survival/attenuation
PB2	Non Lethal	Asn@701	Survival
PB2	Non Lethal	Asp@701	Death

Table 1.2 Pathogenic polymorphisms in PB2
Amino acids at positions 627 and 701 are important determinants of PB2 pathogenicity. Insertion of Glu instead of Lys at position 627 leads to attenuation of lethal virus, while the opposite combination makes milder virus lethal. Insertion of Asn instead of Asp at position 701 leads to attenuation of lethal virus, while the opposite combination makes milder virus lethal.

1.5.4 PB1-F2

The PB1 gene segment has been found to be of avian origin in pandemic strains of influenza virus (Zamarin *et al.*, 2006). The avian PB1 gene expresses an alternative open reading frame which encodes a protein termed PB1-F2, which is frequently lost or truncated during long term adaptation in humans (McAuley *et al.*, 2010a). The presence of this avian-derived factor in pandemic strains identifies it as a potential pathogenicity factor in influenza A virus infection.

Although initially implicated in induction of apoptosis in macrophages (Chen *et al.*, 2001), it now appears to play a pleiotropic role in influenza virus pathogenicity. PB1-F2 contains a C terminal mitochondrial localisation sequence, resulting in translocation to this organelle, where it disrupts membrane potential and induces apoptosis dependent on components of the permeability transition pore complex, VDAC1 and ANT3 (Zamarin *et al.*, 2005) and the pro-apoptotic proteins Bax and Bak (McAuley *et al.*, 2010a). This may lead to immunosuppression (Chen *et al.*, 2001), reduced viral clearance and increased opportunity for viral replication (Zamarin *et al.*, 2006). A recent study, however, has indicated that the pro-apoptotic function of PB1-F2 may be virus strain and cell type specific, with the most commonly studied PR8-derived PB1-F2 inducing apoptosis in both macrophage and lung epithelial cell lines. The 1918 PB1-F2 demonstrated the ability to induce apoptosis in macrophages but not epithelial cells, while PB1-F2 from other viruses, including H5N1, failed to induce this phenomenon (McAuley *et al.*, 2010a).

Several groups have further investigated the potential function of this intriguing protein, implying a potential role in enhancing viral replication due to interactions of PB1-F2 with the viral polymerase complex (Mazur *et al.*, 2008). This too appears to be strain and cell type specific with alteration of PR8 PB1-F2 leading to differential polymerase activity in A549 and 293T

epithelial cell lines but similar replication in vivo, while disruption of H5N1 and 1918 PB1-F2 demonstrated decreased polymerase activity in both cell lines without affecting in vivo viral titres. Furthermore, PB1-F2 from an H3N2 virus had no discernable effect on replication in vitro or in vivo (McAuley *et al.*, 2010b).

The role of PB1-F2 may in fact be to regulate the inflammatory response. Both C terminal peptides and full length PB1-F2 proteins from a PR8 and the 1918, 1957 and 1968 pandemic strains of influenza virus resulted in excessive influx of macrophages and neutrophils, concomitant with onset of clinical symptoms following in vivo infection of mice (McAuley *et al.*, 2010a). Consistent with this, a recent study has indicated that a point mutation at position 66, altering asparagine to serine, results in enhanced pathogenesis independent of induction of apoptosis (Conenello *et al.*, 2011). The mutant was shown to depress the host IFN response, while elevating other proinflammatory cytokines, concomitant with increased innate immune cell infiltration early in infection. This implies that the PB1-F2 protein may play a major role in modulation of the innate response. Furthermore, the PB1-F2 has been found to interact with IPS-1, a downstream component of the RIG-I cascade, therefore the mitochondrial targeting of PB1-F2 may not be to induce apoptosis but rather to interfere with IFN induction, a function that is further enhanced in the presence of 66S (Varga *et al.*, 2011).

Recently, a third protein product from the PB1 gene segment has been identified. Initiation of translation downstream of the PB1 protein results in a truncated PB1 related product designated N40 (Wise *et al.*, 2009). Although the function of this novel protein is yet to be elucidated, it is evident that expression is closely interlinked with that of PB1 and PB1-F2. Disruption of the PB1-F2 open reading frame by specific mutations results in altered levels of N40 and PB1, while disruption of the N40 START codon leads to enhanced PB1 during early infection (Wise *et al.*, 2009). Although several of the studies

detailed above have induced PB1-F2 mutations that are silent in both PB1 and N40 proteins (McAuley *et al.*, 2010a; McAuley *et al.*, 2010b), the effect of PB1-F2 disruption must be carefully examined in light of the lack of independent protein expression from this gene segment.

Prolonged circulation in the human population appears to favour truncation or non-functional mutation of PB1-F2 as observed in seasonal human H3N2 and post 1950 H1N1 isolates (McAuley *et al.*, 2010a). As previously discussed, the prototype 2009 pandemic H1N1 virus possesses a human PB1 gene segment without a PB1-F2 protein due to multiple STOP codons within this open reading frame. Furthermore, the naturally occurring 2009 variant virus encoding a truncated PB1-F2 with leucine at position 12 showed some increased pathogenicity but was not lethal in experimentally infected animals (Ozawa *et al.*, 2011). It is therefore likely that PB1-F2 is essential for efficient replication in the avian host, but dispensable in human infection resulting in its subsequent loss of function following sustained adaptation to the human host.

1.6 Immune Detection of Influenza Virus

1.6.1 Toll-Like Receptors

Influenza virus is recognised by infected cells in several ways. Double and single stranded viral RNA is recognised by the intracellular toll-like receptors (TLR) 3 and 7 respectively and both have been implicated in detection of influenza virus infection (Figure 1.3).

TLR7 signals via the MyD88 adaptor protein, resulting in NFκB activation and expression of proinflammatory cytokines. This receptor also employs an alternative signalling pathway in plasmacytoid dendritic cells, via IRF7 activation, leading to IFNα production (reviewed by Kawai & Akira, 2010). Mice

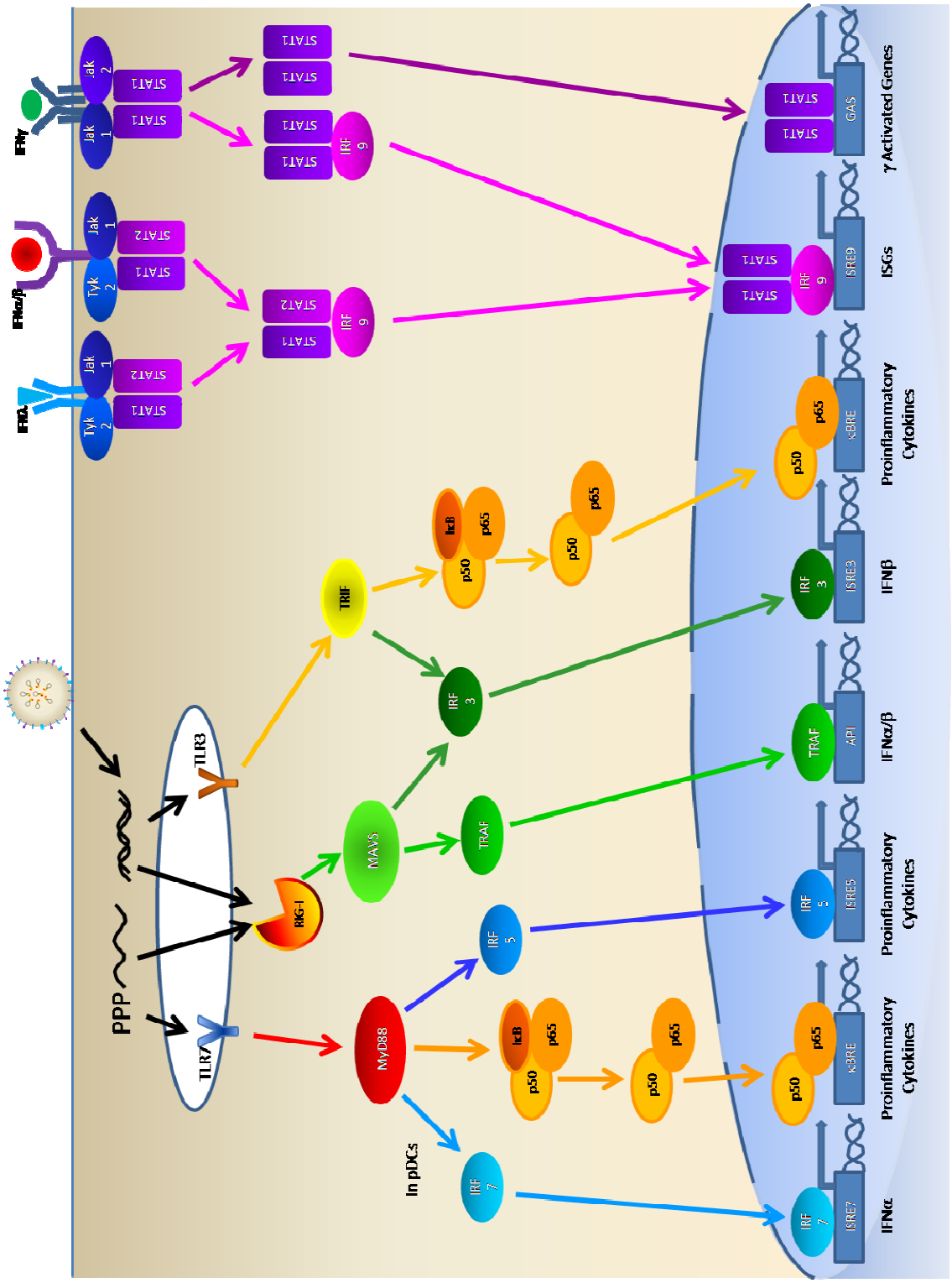
IFNγ
IFNα/β
IFNλ
Jak 2
Jak 1
Tyk 2
STAT1
STAT2
IRF 9
PPP
TLR3
TLR7
RIG-I
MAVS
MyD88
TRIF
TRAF
IRF 3
IRF 5
IRF 7
IκB
p50
p65
In pDCs
GAS
ISRE9
κBRE
ISRE3
API
ISRE5
ISRE7
γ Activated Genes
ISGs
Proinflammatory Cytokines
IFNβ
IFNα/β
Proinflammatory Cytokines
Proinflammatory Cytokines
IFNα

Figure 1.3 Signalling cascades following influenza virus infection
Infection with influenza virus is recognised with many different pattern recognition receptors, resulting in signalling cascades and expression of IFNs and proinflammatory cytokines, ultimately inducing an antiviral state.

lacking TLR7 or MyD88 have been shown to be deficient in their capacity to mount an effective IFNα response following infection both in vitro and in vivo, while exposure to purified single stranded genomic viral RNA was sufficient to induce this response from wildtype plasmacytoid dendritic cells (Diebold *et al.*, 2004; Lund *et al.*, 2004).

TLR3 recognises double stranded RNA and has been implicated in detection of many viral infections. This is the only TLR that does not utilise the MyD88 pathway, signalling instead via TRIF and IRF3 which results in production of IFNβ (reviewed by Kawai & Akira, 2010). Surprisingly, mice deficient in TLR3 expression demonstrate ameliorated disease following infection with influenza virus, exhibiting prolonged survival and decreased inflammatory cytokine expression in the lung (Le Goffic *et al.*, 2006). However, this was at the expense of viral clearance and ultimately all mice succumbed to infection. However, influenza virus does not appear to generate detectable double stranded RNA (Pichlmair *et al.*, 2006). This suggests that the presence of double stranded RNA may be extremely transient, sufficient to activate TLR3 but not be detectable by assay. Alternatively, NS1 incompetent intermediates may be released from dying infected cells, resulting in fragments of double stranded RNA which may activate this TLR. However, the lack of readily detectable double stranded RNA indicates that recognition of single stranded viral RNA may be the most common means of viral detection within the cell.

1.6.2 RIG-I

In addition to endosomal TLRs, the cytoplasmic protein RIG-I has been implicated in detection of influenza virus RNA (Figure 1.3). This receptor has been shown to detect transcribed viral RNA in vitro (Kato *et al.*, 2006) and single stranded viral genomes expressing 5'-phosphates and secondary structure in vivo (Pichlmair *et al.*, 2006; Rehwinkel *et al.*, 2010). Following binding of RNA, RIG-I induces IFNβ expression via IPS-1 and IRF3 (Mibayashi

et al., 2007). The influenza virus protein NS1 has been shown to play a role in inhibition of the IFNβ response to viral RNA, not by sequestering of viral RNA as previously proposed, but by binding to RIG-I and inhibiting activation of downstream transcription factors (Mibayashi *et al.*, 2007; Pichlmair *et al.*, 2006; Talon *et al.*, 2000).

Although both TLR and RIG-I pathways independently induce antiviral cytokine responses, only partial redundancy exists. Functional signalling via both cascades is required for efficient antibody and CTL responses (Kumar *et al.*, 2008).

1.6.3 Inflammasome

Induction of IL-1β and IL-18 following influenza virus infection is an important aspect of the immune response and occurs through activation of the inflammasome (Figure 1.2). Following activation by a two signal mechanism (Pang & Iwasaki, 2011), this cytoplasmic complex of proteins functions to activate caspase 1 which in turn cleaves pro-IL-1β and pro-IL-18 to their active forms (Stasakova *et al.*, 2005). Although some authors have indicated that genomic influenza virus RNA is sufficient for inflammasome activation, implicating TLR signalling as signal 1 (Thomas *et al.*, 2009), others have shown that a second signal in the form of lysosome products and reactive oxygen species are also vital (Allen *et al.*, 2009). The function of the M2 ion channel protein has also been implicated as signal 2 (Pang & Iwasaki, 2011). Mice genetically deficient in inflammasome components NOD-like receptor protein 3, its adaptor molecule ASC, or caspase 1 are unable to activate IL-1β or IL-18, resulting in increased morbidity associated with impaired neutrophil and monocyte recruitment (Allen *et al.*, 2009; Thomas *et al.*, 2009), with another group indicating impaired T cell responses (Ichinohe *et al.*, 2009). Emphasising the importance of inflammasome activation in the antiviral response, the RNA binding properties of the NS1 protein interferes with

inflammasome activation of caspase 1, resulting in impaired IL-1β and IL-18 responses (Stasakova *et al.*, 2005).

1.6.4 Mx Protein

The anti-viral protein Mx1, which is nuclear in mice but cytoplasmic in humans and known as MxA, may play a key role in protection from influenza viruses. Initially identified as a gene product that imbued a strain of laboratory mice with resistance to lethal influenza virus infection (reviewed by Haller *et al.*, 2007), transfection of this protein into $Mx1^{-/-}$ mice conferred resistance to influenza virus infection, even in the absence of IFNs (Staeheli *et al.*, 1986). It now appears that this IFN-induced protein may target the viral nuclear protein, and by means as yet still unclear, interfere with viral RNA transcription (Dittmann *et al.*, 2008). Furthermore, Dittmann and colleagues demonstrated that Mx confers protection in a strain dependent manner, with avian influenza viruses showing greater susceptibility to the inhibitory effects of this protein than those of human origin. Of interest was the finding that the highly pathogenic H5N1 virus was susceptible to the actions of the human Mx protein, while the 1918 H1N1 influenza virus was almost completely resistant (Dittmann *et al.*, 2008). This suggests a possible role for Mx in protection from avian influenza viruses and may offer further insight into the inability of H5N1 to efficiently transmit within the human population.

1.6.5 PKR and OAS

Following initiation of the IFN response, two further cytoplasmic proteins are known to play a role in antiviral defence. PKR, a serine-threonine kinase, inhibits viral protein synthesis by phosphorylating the transcription initiation factor eIF-2 (Murphy *et al.*, 2008). PKR function is inhibited by NS1, allowing the virus to replicate effectively within the IFN competent cell (Bergmann *et al.*, 2000; Li *et al.*, 2006; Min *et al.*, 2007).

Similarly to PKR, OAS is expressed following IFN stimulation. This protein functions to activate RNAse L which degrades viral RNA, destroying the virus (Murphy *et al.*, 2008). However, the presence of NS1 protein once again counteracts this cellular defence mechanism. NS1 binding of viral RNA has been shown to be vital for inhibiting RNAse L activity and protecting the viral genome from degradation (Min & Krug, 2006).

Despite the many fold roles of the NS1 protein in protecting the virus from host cell defences, the virulence of a particular strain is closely related to its ability to dysregulate the ensuing immune response following infection.

1.7 Dysregulation of the Host Immune System

1.7.1 Cytokine Responses

Infection with influenza A virus leads to increased production of proinflammatory cytokines, an immediate result of the host IFN response to generate an antiviral microenvironment and limit viral replication. The infection is usually cleared within a few days and the respiratory tract recovers from inflammation. However, viruses such as H5N1 (Chan *et al.*, 2005; Cheung *et al.*, 2002) and the 1918 H1N1 (Kobasa *et al.*, 2004) induce dramatic increases in proinflammatory cytokines from epithelial and immune cells, leading to debilitating and often irreversible pathology in the lung. In addition to the elevated levels of cytokines observed, H5N1 also appears to be resistant to the effects of these (Seo *et al.*, 2002).

H5N1 has been shown to induce elevated levels of many proinflammatory cytokines as well as chemoattractants (), and is a more potent inducer of these cytokines than other human influenza viruses (Cheung *et al.*, 2002). However, this is not a feature exclusive to the H5N1 viruses. Experimental infection of

mice with the H1N1 strain PR8 results in severe disease characterised by excessive inflammatory infiltration into the lungs, coupled with uncontrolled expression of cytokines such as IL-1, IL-6, TNFα and IFNγ (Hennet *et al.*, 1992). The temporally distinct cellular infiltration and cytokine expression observed provide early evidence of what is now thought of as a 'cytokine storm' following infection with highly pathogenic strains of influenza virus, such as H5N1 (Chan *et al.*, 2005; Cheung *et al.*, 2002). Furthermore, patients succumbing to fatal H5N1 infection demonstrated more extreme cytokinaemia than those who survived (de Jong *et al.*, 2006).

Production of TNFα by infected respiratory epithelial cells and alveolar macrophages is an early response to viral infection. This activates macrophages to produce IFNβ, further TNFα, chemoattractants MIP-1α/β, MCP-1 and RANTES, as well as inducing chemokine expression from epithelial cells (Herold *et al.*, 2006). In turn, this leads to influx of inflammatory cells such as neutrophils as well as B and T cells. The ability of highly pathogenic influenza viruses to induce high levels of cytokine production exacerbates the inflammatory response to infection leading to uncontrolled inflammation and immunopathology.

1.7.2 B and T Cell Response

CD8+ T cells are important mediators of viral clearance, although depletion of this subset does not impair clearance (Eichelberger *et al.*, 1991) indicating that other mechanisms such as antibody mediated clearance can compensate for the absence of these cells (Scherle *et al.*, 1992). Clearance appears to be dependent on the presence of T_H1 $CD4^+$ T cells (Graham *et al.*, 1994; Moran *et al.*, 1999), as depletion of both T cell subsets results in excessive viral load and death (Eichelberger *et al.*, 1991; Scherle *et al.*, 1992). B cell production of neutralising IgG isotypes has been shown to confer protection against influenza driven immunopathology in the lung (Palladino *et al.*, 1995) while IgA

Cytokine	Role	Sources
TNFα	Mediator of inflammatory response Induces cytokine production from various cells	Activated mϕ & lymphocytes
IFNα/β	Antiviral, inhibits cell proliferation Regulates MHC I expression	Lymphocytes, mϕ & epithelial cells
IL-1β	Acts on lymphocytes & monocytes Induces fever & other acute responses	Many including lymphocytes, mϕ & NK cells
IL-4	Alternatively activates mϕ Induces IgG, IgE & class switching	T lymphocytes
IL-6	Stimulates antibody production Regulates inflammatory responses	T lymphocytes & monocytes
IL-10	Inhibits proinflammatory cytokine production	Mϕ & lymphocytes
IL-12	Induces IFNγ from T & NK cells	Activated mϕ, monocytes & B lymphocytes
RANTES	Attracts lymphocytes	T lymphocytes & mϕ
MIP-1α/β	Attracts lymphocytes	Lymphocytes, mϕ & neutrophils
MCP-1	Attracts and activates monocytes	Monocytes & T lymphocytes
IP-10	Attracts Th1 lymphocytes & monocytes	Monocytes & T lymphocytes
TRAIL	Induces apoptosis in tumour cells	Mϕ & lymphocytes

Table 1.3 Cytokines induced during influenza virus infection.
Highly pathogenic influenza virus infection results in upregulation of cytokines and hemokines from immune and epithelial cells.

facilitates protection in the upper respiratory tract (Renegar *et al.*, 2004).

Neutralising antibodies have been isolated from H5N1 survivors, passive immunisation with which resulted in lower viral titres in the lungs of infected mice (Simmons *et al.*, 2007), while vaccination of mice with a mild H5N1 plus alum led to cross reactive protective antibody response to challenge with a lethal H5N1 strain (Lu *et al.*, 1999). Furthermore, immunisation with plasmid-expressed HA from the 1918 H1N1 virus resulted in potent B and T cell responses, while T cell depletion studies indicated that protection was antibody mediated (Kong *et al.*, 2006).

Although H5N1 viruses have demonstrated the ability to induce apoptosis in immune cells, this appears to be specific to the pathogenic group one viruses. Tumpey and colleagues showed that infection with reassortant group one H5N1 led to depletion of circulating lymphocytes by 80%, as well as fewer T cells in the lung, compared with group two viruses. This was due in part to lower levels of chemokine MIP-1α and increased apoptosis in the lung and spleen (Tumpey *et al.*, 2000).

It has been suggested that a frustrated $CD8^+$ T cell response may contribute to the cytokine storm observed during infection (reviewed by La Gruta *et al.*, 2007; Moskophidis & Kioussis, 1998). When virus titres are low, CTL function effectively to clear the infection. However, when titres are elevated, the CTL response struggles to function properly, resulting in more and more cytokines being produced, while very little virus is cleared. This further exacerbates the inflammation in the lung. The speed of viral replication has also been implicated in dysregulation of the T cell response to influenza virus. It has been suggested that rapid replication induces high levels of IL-12p40, which in turn upregulates FasL on dendritic cells in the lymph nodes. This results in Fas:FasL mediated apoptosis of T cells circulating through the lymph node and subsequent depletion of CTL following highly pathogenic, or high dose virus

infection. Lower doses of virus, or slower replication fails to induce this dramatic increase in FasL and therefore an efficient CTL response is mounted (Legge & Braciale, 2005). This is further implied, as infection with a high dose of PR8 results in influx of monocytes and neutrophils but decreased T cell derived IL-10 (Sun *et al.*, 2009).

1.7.3 Macrophages and Apoptosis

Macrophages have been shown to be both essential to clearance of influenza virus but also to contribute to immunopathology in the lung. Inhibition of macrophage recruitment either by disruption of the CCR2 gene or pharmaceutical antagonism of this receptor resulted in ameliorated pathology and improved survival following infection with PR8 virus (Herold *et al.*, 2008; Lin *et al.*, 2011). However, others have shown that alveolar macrophages are essential for limiting disease severity following infection with the low pathogenic strain of influenza virus BJx109 (Tate *et al.*, 2010c).

Macrophages are known to absorb virus to their surface and release it to infect neighbouring cells (Wells *et al.*, 1978) as well as to phagocytose virions, but it appears unlikely that macrophages become productively infected (Rodgers & Mims, 1981). The ability of influenza virus to infect macrophages appears to be strain dependent, resulting in differential cytokine production and related immunopathology (Reading *et al.*, 2010). Reading and colleagues have indicated that the ability of the two closely related viruses PR8 and BJx109 to cause such different severity of disease is a direct result of the ability to infect macrophages (Reading *et al.*, 2010). BJx109 efficiently infects murine macrophages and therefore is readily internalised into the cell where it undergoes abortive infection, essentially limiting the amount of free virus available to cause infection and damage to the lung epithelium (Tate *et al.*, 2010b). Conversely, PR8 poorly infects macrophages, allowing free virus to infect epithelial cells, resulting in a more severe disease (Tate *et al.*, 2010c). This has been attributed to the glycosylation pattern and also the SA

preference of the virus, with PR8 being poorly glycosylated and binding preferentially to α2,3SA, while BJx109 has several glycosylation sites on the HA and NA proteins and a preference for α2,6SA (Tate *et al.*, 2010a; Tate *et al.*, 2010c). This means that BJx109, but not PR8, efficiently binds to SA and lectin domains of receptors such as the macrophage mannose receptor (CD206) (Upham *et al.*, 2010), facilitating efficient uptake into the endosomal compartment in macrophages.

In addition to the ability of H5N1 viruses to induce higher cytokine production from macrophages than do other human influenza A viruses, these viruses appear to actively replicate within human macrophages (Cheung *et al.*, 2002; Mok *et al.*, 2007; Perrone *et al.*, 2008). Infection with H5N1 has also been observed to delay apoptosis of infected cells (Mok *et al.*, 2007), perhaps as a means of allowing a longer window for viral replication. However, this is in contention with reports that suggest H5N1 effectively induces apoptosis in immune cells (Tumpey *et al.*, 2000).

Virus-induced TRAIL expression from macrophages has been implicated in enhanced pathology and damage to epithelial cells following infection with highly pathogenic influenza but not milder strains (Herold *et al.*, 2008). Zhou and colleagues also showed that increased expression of TRAIL from macrophages leads to apoptosis of Jurkat T cells, suggesting the possibility of TNFα regulated apoptosis in functional T cells in vivo via macrophage produced TRAIL (Zhou *et al.*, 2006). This study also showed that human H1N1 was more efficient at inducing apoptosis of T cells than the avian virus, suggesting that although apoptosis may be a mechanism by which H5N1 ultimately affects the immune system, it is delayed in comparison with human viruses.

Production of RANTES (CCL5) by macrophages has been shown to protect these cells from apoptosis as $CCL5^{-/-}$ mice showed decreased viral clearance

alongside increased macrophage apoptosis, despite demonstrating functional lymphocyte recruitment (Tyner *et al.*, 2005). This indicates that macrophages play an important role in viral clearance in addition to their role in cytokine production.

1.8 Macrophages

1.8.1 Differentiation

Macrophages, dendritic cells and neutrophils all derive from the same progenitor cell in the bone marrow, with this common monoblast differentiating into a monocyte which enters the circulation and finally migrates into tissues to become a resident macrophage (van Furth & Cohn, 1968). Monocytes strongly express adhesion molecules on their surface, which facilitate extravasation into the tissues. α integrins CD11b and CD11c interact with the β integrin CD18 to form adhesion molecules. These integrins bind to members of the intercellular adhesion molecule (ICAM) family expressed on endothelial cells, among others, enabling the macrophage to adhere to the endothelial layer and exit the blood stream (Dustin *et al.*, 1986; Rothlein *et al.*, 1986).

Macrophages are responsive to various growth factors in vivo that influence differentiation and survival of this cell type. M-CSF (Stanley *et al.*, 1978) and IL-34 (Lin *et al.*, 2008) stimulate proliferation and survival of macrophages through interactions with the M-CSF receptor, CSF-1R, although they are thought to bind to differing regions (Garceau *et al.*, 2010). GM-CSF gives rise to granulocytes as well as macrophages, and acts through a distinct receptor which shares its β chain with the IL-3 receptor (Kitamura *et al.*, 1991). Interestingly, some populations of tissue macrophages, such as alveolar macrophages are dependent on GM-CSF for function, but not for differentiation and survival (Paine *et al.*, 2001). Further to the requirement for

M-CSF to support survival and proliferation of macrophages, at concentrations that promote maximal proliferation, macrophages actively degrade M-CSF, limiting the proliferative capacity of this growth factor by removing it from the microenvironment (Tushinski *et al.*, 1982). M-CSF has also been shown to be proinflammatory in vitro, priming responses to LPS, while suppressing the response to other TLR ligands such as CpG (Sweet *et al.*, 2002). Conversely, other studies have demonstrated outgrowth of an IL-12^{low}IL-10^{high} regulatory type macrophage in the presence of M-CSF, while GM-CSF resulted in classical IL-12^{high} macrophages (Fleetwood *et al.*, 2007).

1.8.2 Role in Immune System

Macrophages are highly efficient professional phagocytes and antigen presenting cells. They detect, engulf, degrade and present microbial antigen to cells of the adaptive immunity. They have enormous phagocytic capacity and play a vital role in clearance of debris during infection and homeostasis. Differentiation between apoptotic cell turnover and clearance of infection is vital to prevent inappropriate inflammatory responses. Phagocytosis occurs by attachment of a particle to the macrophage via a range of receptors, followed by internalisation and degradation through sequential endosomes. Phagocytic receptors include complement receptors (CR), Fc receptors (FcR), mannose receptors CD206 and DC-SIGN, CD14, scavenger receptor A (SR-A) in the mouse, and SR-A and B in man (Aderem & Underhill, 1999). The receptor(s) involved in internalisation dictate the inflammatory response to phagocytosis. Ligation of FcR, for example, leads to release of TNFα, while CR-mediated phagocytosis does not (Stein & Gordon, 1991; Wright & Silverstein, 1983). However, more recently, macrophages undergoing FcγR ligation have been demonstrated to direct T_H2 polarisation of the immune response, dependent on macrophage derived IL-10 (Anderson & Mosser, 2002). Recognition of mannosylated moieties by CD206 results in production of proinflammatory cytokines including TNFα and IL-12 (Garner *et al.*, 1994; Shibata *et al.*, 1997;

Yamamoto *et al.*, 1997), while uptake of apoptotic cells via CD14 (Devitt *et al.*, 1998) actively inhibits release of LPS-induced inflammatory mediators from macrophages (Fadok *et al.*, 1998; Meagher *et al.*, 1992). This discrimination allows clearance of apoptotic cells without further induction of inflammatory mediators, allowing resolution of inflammation and preventing inappropriate tissue damage.

Macrophages are a vital component of the innate immunity, being one of the first defences encountered by invading pathogens. Early detection of infection by macrophages results in rapid release of cytokines, driving the adaptive immunity into polarised responses. Although initially thought to be poor antigen presenting cells relative to dendritic cells, there is much evidence to suggest the contrary. In recent years the distinctions between macrophages and dendritic cells have become blurred, with both cell types performing overlapping roles and expressing the same surface markers (reviewed by Hume, 2008). Macrophages have demonstrated the ability to present both endogenous and exogenous antigen in association with MHC I and MHC II respectively to $CD4^+$ and $CD8^+$ T cells during primary responses (Desmedt *et al.*, 1998; Pozzi *et al.*, 2005). In addition to this, macrophages possess the ability to cross present antigen to T cells; following uptake of exogenous antigen which by the normal pathway would be presented in complex with MHC II, macrophages can process and present this in complex with MHC I molecules, thereby presenting exogenous antigen directly to $CD8^+$ cells (Kovacsovics-Bankowski *et al.*, 1993; Kovacsovics-Bankowski & Rock, 1994).

Further to their capacity to stimulate T cells following antigen capture, macrophages appear to be capable of priming B cell responses by capturing and presenting native protein to B cells migrating through the subcapsular sinus (reviewed by Martinez-Pomares & Gordon, 2007). The macrophage surface marker sialoadhesin can bind to the soluble form of the mannose receptor CD206, which in turn binds the mannosylated moieties on the surface

of pathogens (Junt *et al.*, 2007; Martinez-Pomares *et al.*, 1999). This allows macrophages to catch lymph-borne particulate antigen and present it to passing B cells, which slow their passage through the subcapsular sinus and form prolonged interactions with macrophages as they proceed deeper into the follicle (Carrasco & Batista, 2007).

Although initially thought to drive T_H1 responses due to their efficient production of IL-12, macrophages are now known to demonstrate a much more complex spectrum of activation phenotypes, resulting in priming of a range of immune responses (Figure 1.4).

1.8.3 Classical Activation

Macrophages have long been known to become activated and increase their anti-microbial capacity and cytokine output following stimulation with IFNγ and LPS or TNFα. Proinflammatory 'classically' activated macrophages produce an array of cytokines and inflammatory mediators including IFNγ, IL-12, TNFα, IL-1β and nitric oxide, which mount a rapid assault on intracellular pathogens and prime T cells for a T_H1 response (Edwards *et al.*, 2006; Nathan *et al.*, 1983). This activation state therefore contributes to type 1 inflammation, characterised by IL-12, IFNγ, TNFα and neutrophilia.

It was originally postulated that two activating signals are required by the macrophage to become classically activated. These are usually IFNγ and TNFα. IFNγ is derived from either $CD4^+$ T helper cells, natural killer cells, or in an autocrine manner from macrophages themselves in response to pathogen (Fultz *et al.*, 1993), while TNFα is induced by TLR ligands such as LPS, and then co-operates with IFNγ to amplify the classical response. However, some TLR ligands are capable of inducing IFNβ which, in the presence of TNFα, can substitute for IFNγ signalling to induce classical activation of macrophages (reviewed by Mosser & Edwards, 2008).

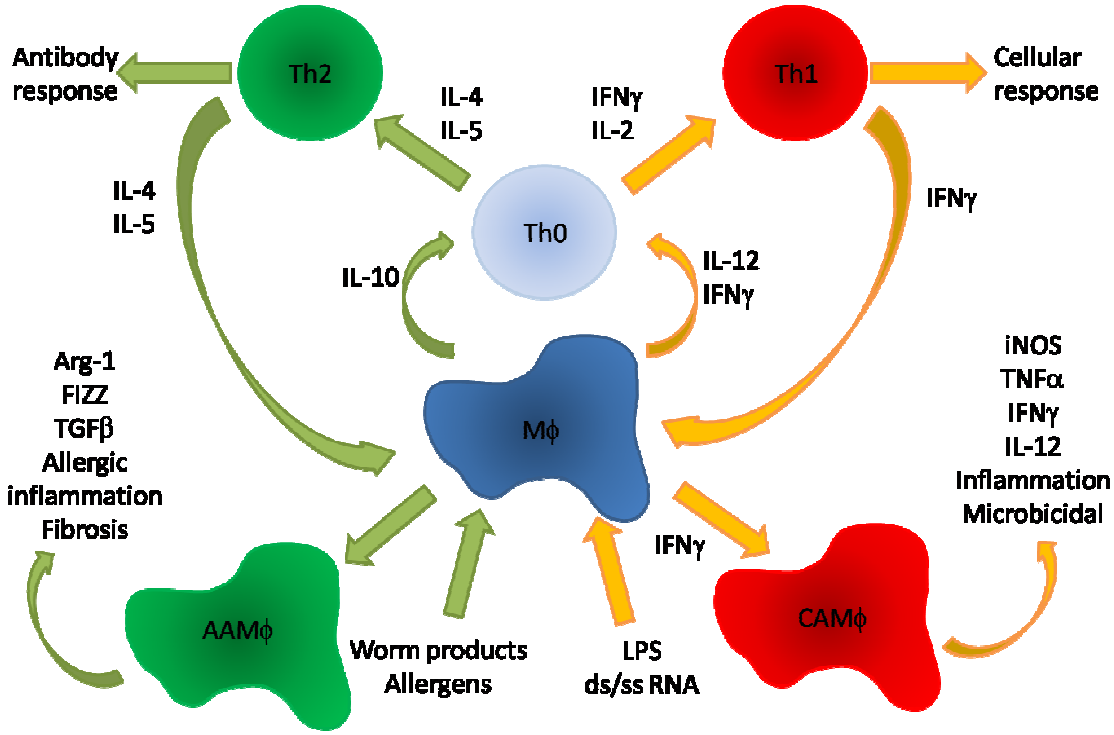

Figure 1.4 Macrophages influence development of T cell subsets
Macrophages activated by differing stimuli influence the development of T_H1 or T_H2 T cells, which in turn further promote outgrowth of classical or alternatively activated macrophages.

Classical activation results in production of proinflammatory cytokines, polarisation of $CD4^+$ T cells into T_H1 cells leading to activation of CTLs, and recruitment of neutrophils and macrophages to the site of infection. Inducible nitric oxide synthetase (iNOS) and IL-12 production are hallmark characteristics of classical activation, providing protection against intracellular pathogens such as *Leishmania*, *Listeria* and *Mycobacteria* spp. Generation of nitric oxide by classically activated macrophages following infection plays such a vital role in protection, that $iNOS^{-/-}$ animals demonstrate reduced survival following infection with such pathogens (MacMicking *et al.*, 1997; Wei *et al.*, 1995), while pharmaceutical inhibition of iNOS results in exacerbated disease in many infections ranging from intracellular bacteria and fungal infections to extracellular helminthic parasites (reviewed by MacMicking *et al.*, 1997). Furthermore, iNOS and nitric oxide have been shown to inhibit replication by coxsackie, vaccinia, ectromelia and herpes simplex viruses (Croen, 1993; Karupiah *et al.*, 1993; Zaragoza *et al.*, 1997). However, iNOS has been implicated in pathological developments in neurological disease such as Borna disease and rabies viruses, as well as experimental herpes simplex virus encephalitis (Akaike *et al.*, 1996; Fujii *et al.*, 1999; Koprowski *et al.*, 1993; Zheng *et al.*, 1993). Similarly, iNOS contributes to the pathogenesis of influenza virus, with ameliorated disease severity demonstrable following inhibition of iNOS metabolism or production (Aldridge *et al.*, 2009; Karupiah *et al.*, 1998).

This highlights an important aspect of classical macrophage activation. Such efficient antimicrobial killing must be tightly controlled to prevent excessive inflammation and tissue damage. IL-10 is upregulated following the respiratory burst induced by LPS stimulation of macrophages (Chang *et al.*, 2007; Wanidworanun & Strober, 1993), resulting in a decrease in proinflammatory cytokine production, as well as inhibiting its own expression by induction of the suppressor of cytokine signalling protein, SOCS3 (O'Shea & Murray, 2008).

1.8.4 Alternative Activation

Many studies have demonstrated that inbred strains of mice demonstrate T_H1 or T_H2 skewing of their immune responses, a system which has been used to dissect the roles played by these polarised T cell subsets in infection (Buchmuller-Rouiller & Mauel, 1986; Heinzel *et al.*, 1989; Mosmann *et al.*, 1986; Schijns *et al.*, 1994; Watanabe *et al.*, 2004). Similarly, these inbred mice also demonstrate differential macrophage activation, with the T_H1 C57Bl/6 mouse demonstrating classical macrophages, while the T_H2 BALB/c mouse shows an alternative macrophage phenotype (Mills *et al.*, 2000; Pradel *et al.*, 2009).

The initial 'alternatively' activated macrophage was demonstrated in response to IL-4 stimulation (Stein *et al.*, 1992), which resulted in upregulation of CD206, while incubation with IFNγ downregulated this marker. Subsequently, alternatively activated macrophages have been indentified following infection with parasitic worms (Anthony *et al.*, 2006; Chakkalath & Titus, 1994; Herbert *et al.*, 2004; Loke *et al.*, 2002), after sterile surgery (Loke *et al.*, 2007) and during allergic airway inflammation and fibrosis (Hancock *et al.*, 1998; Kim *et al.*, 2008; Liu *et al.*, 2004; Prasse *et al.*, 2007), indicating a role in type 2 inflammation, characterised by eosinophilia and expression of T_H2 cytokines IL-4, IL-5 and IL-13.

Originally thought of as a linear polarisation, with classical and alternatively activated macrophages opposing each other, it is now apparent that a spectrum of macrophage activation states exists (reviewed by Mosser & Edwards, 2008). Differences within the 'alternatively' activated population have been identified depending on the stimulus given. IL-4 and IL-13 share a common receptor chain, IL-4Rα (Hilton *et al.*, 1996), and induce alternative activation by signalling through this receptor (reviewed by Gordon, 2003).

Other activation groups are apparent following exposure to IL-5, IL-10 and immune complexes (Edwards *et al.*, 2006; Gerber & Mosser, 2001; Mantovani *et al.*, 2004; Stumpo *et al.*, 2003). Macrophages activated with these stimuli are distinct from the prototypical classical macrophage, but are also distinct from one another, albeit with partially overlapping characteristics. This is exemplified by the range of genes induced following macrophage activation, with 75% of the genes induced by IL-10 being distinct from those upregulated by IFNγ stimulation. 57% of the IL-10 induced genes are also shared by IL-5 activation. However, only 18% of upregulated genes are common to both IL-10 and IL-4 activation, demonstrating the stimulus dependent diversity within the 'alternatively activated' macrophage (Stumpo *et al.*, 2003). Thus, non classical macrophages have now been further divided into groups which represent immunoregulatory and tissue remodelling effector macrophages (Edwards *et al.*, 2006; Mantovani *et al.*, 2004). Expression of IL-10 and IL-12 has been used to distinguish between these groups of macrophages. Classically activated macrophages are generally IL-12^{high} IL-10^{low}, while regulatory macrophages express more IL-10 than IL-12. True alternatively activated macrophages are those activated with IL-4, and are strong producers of arginase, while classically activated macrophages predominantly express iNOS over arginase (Edwards *et al.*, 2006).

Furthermore, newly characterised cytokines are being ascribed roles in various aspects of alternative activation, most notably IL-21 and IL-33. IL-33 synergises with IL-13 to induce IL-5 expression and enhance alternative activation and eosinophilia, thereby contributing to T_H2 mediated airway inflammation (Kurowska-Stolarska *et al.*, 2008; Kurowska-Stolarska *et al.*, 2009). IL-21 is produced by T_H2 cells and enhances alternative activation of macrophages by inducing expression of the shared IL-4 and IL-13 receptor chain while also downregulating expression of the soluble IL-13 decoy receptor, ultimately exacerbating fibrosis and granulomatous inflammation (Pesce *et al.*, 2006).

The defining characteristic of alternative activation is differential metabolism of L-arginine, which further underscores the role played by such macrophages in tissue remodelling and repair. Alternatively activated macrophages produce arginase, leading to metabolism of L-arginine into proline and contributing to collagen deposition (Hesse *et al.*, 2001), while classical macrophages produce nitric oxide by means of iNOS. Although both enzymes may be induced by the same stimuli (Johann *et al.*, 2007), arginase is capable of outcompeting iNOS for substrate (Gobert *et al.*, 2004; Green *et al.*, 1990; Johann *et al.*, 2007). While poorly antimicrobial to intracellular pathogens due to lack of nitric oxide (Modolell *et al.*, 1995), it has now been shown that alternatively activated macrophages are essential for protection against parasites. However, this can be due to differing mechanisms.

Infection with *Leishmania major* drives T_H2 responses as a method of evading the host-protective inflammatory response. iNOS mediates leishmaniacidal activity of macrophages during the obligate intracellular amastigote stage of leishmaniasis (Chakkalath & Titus, 1994; Liew *et al.*, 1990). Inhibition of iNOS, IL-12 or IFNγ results in fatal infection (Mattner *et al.*, 1996; Stenger *et al.*, 1996; Wei *et al.*, 1995), while treatment of susceptible T_H2 skewed strains of mice, such as BALB/c, with exogenous IFNγ renders them resistant to this parasite (Buchmuller-Rouiller & Mauel, 1986; Green *et al.*, 1990).

Schistosoma mansoni also induces alternative activation and T_H2 type responses, yet these appear to be host protective. *Schistosoma* are extracellular trematodes, which lay eggs in the gastro-intestinal tract and lining of the mesenteric veins resulting in granulomatous inflammation and fibrosis. This pathology is T_H2 mediated and induction of a T_H1 response is beneficial in reducing granuloma size and associated pathology (Hesse *et al.*, 2001). However, adopting a T_H1 response to adult worms results in uncontrolled inflammation and failure to expel eggs from the gut (Herbert *et*

al., 2004). Alternatively activated macrophages are vital in modulating the immune response during schistosomiasis (Herbert *et al.*, 2004), with IL-10 expression being key in balancing the excessive T_H1 inflammatory response with the pathologic fibrosis induced by schistosome eggs (Hoffmann *et al.*, 2000).

While the antiparasitic alternatively activated macrophages evidently contribute to fibrosis and tissue repair following the damage inflicted by parasite migration during various stages of the life cycle, alternatively activated macrophages have also been implicated in the pathogenesis of allergic asthma and chronic airway inflammation. Alveolar macrophages have been thought of as a suppressive population, or at the very least quiescent in their ability to mount an inflammatory response to the constitutive barrage of inhaled particles. Several studies have demonstrated the deleterious effect of alveolar macrophage depletion resulting in exacerbated disease severity, prolonged immune responses and inflammation (Broug-Holub *et al.*, 1997; Tate *et al.*, 2010c; Thepen *et al.*, 1989). However, others have indicated that this cell population is essential in protection from pathogens by mounting an IFNγ response, inhibition of which leads to inappropriate type 2 inflammation (Pribul *et al.*, 2008; Tang *et al.*, 2001). These discrepancies may be related to the complex nature of macrophage interactions with pathogens, as macrophages presenting antigen via the MHC pathway commonly stimulate T_H1 responses (Anderson & Mosser, 2002; Tang *et al.*, 2001), while those taking up opsonised particles and apoptotic cells by phagocytosis drive T_H2 responses (Anderson & Mosser, 2002; Johann *et al.*, 2007).

Allergic lung inflammation has been associated with excessive eosinophil infiltration and production of IL-4, IL-5, IL-13 and IgE. This was originally thought of as a T_H2 mediated phenomenon, due to the fact that SCID mice do not develop airway hyperresponsiveness (AHR) (Corry *et al.*, 1996). This was confirmed by the observation that the T_H2 biased BALB/c mouse develops

AHR, while the prototype T_H1 mouse C57Bl/6 is protected (Kearley *et al.*, 2009). This paradigm is complicated, however, by the involvement of IFNγ. Some studies demonstrate protective effects of this cytokine by inducing a T_H1 environment and therefore ameliorating the excessive type 2 response (Kearley *et al.*, 2009; Yoshida *et al.*, 2002). IFNγR$^{-/-}$ mice show prolonged T_H2 cytokines and eosinophilia following sensitisation with ovalbumin (OVA), a well characterised experimental inducer of allergic type inflammation in the mouse, while wildtype animals demonstrate complete resolution of the condition at the same timepoint. This indicates a role for IFNγ in clearance and resolution of eosinophil-mediated inflammation (Coyle *et al.*, 1996). Conversely, others have suggested that IFNγ may exacerbate acute airway inflammation (Koch *et al.*, 2006), leading to non-eosinophilic inflammation and tissue damage (Grattendick *et al.*, 2002).

In addition to the T_H1/T_H2 paradigm leading to lung inflammation, the more recently documented T_H17 phenotype has been heavily implicated in allergic asthma, with alveolar macrophages identified as the main source of IL-17 within the asthmatic lung (Song *et al.*, 2008). Dependent on TGFβ and IL-6, and in humans, IL-1β and IL-23 for development, the T_H17 phenotype is proinflammatory with expression of IL-17 and IL-21, which further induce an inflammatory cascade of CXCL chemokines and contribute to cellular influx and pathogenic inflammation (Basso *et al.*, 2009).

Alternatively activated macrophages play a role in mediating AHR and chronic inflammation in the lung. Atopic patients have demonstrated higher numbers of IL-10$^+$ monocytes that readily differentiate into alternatively activated macrophages in vitro, in addition to elevated alternatively activated macrophages in fibrotic regions of the lung (Prasse *et al.*, 2007). Furthermore, IL-33 has been shown to be increased in human asthma patients and play a role in inducing quiescent alveolar macrophages into alternative activation. In the mouse, IL-33 signalling enhances alternative activation of macrophages

and results in IL-5 mediated lung inflammation due to increased eosinophilia (Kurowska-Stolarska *et al.*, 2009).

In addition to environmental stimuli, viral infections have been implicated in triggering development of AHR. Macrophages have been ascribed a potential role in this type of airway inflammation by means of prolonged activation of invariant NKT cells during low level persistence of the viral infection resulting in iNKT:macrophage interactions and chronic IL-13 and IL-13 receptor expression on the macrophage, ultimately resulting in excessive mucus production and AHR (Kim *et al.*, 2008).

However, alveolar macrophages pulsed with OVA and therefore functioning as APC, have been shown to successfully inhibit allergic airway inflammation by counteracting the T_H2 response (Tang *et al.*, 2001; Vissers *et al.*, 2005). Taken together, macrophages play a complex role in development and resolution of airway inflammation, with induction of alternative activation playing a predominantly pathogenic role, despite the tissue reparative potential of this macrophage subset.

Regulatory macrophages have been observed following clearance of apoptotic neutrophils, which results in TGFβ production from these macrophages and suppression of inflammatory mediators (Fadok *et al.*, 1998). Regulatory macrophages strongly express IL-10, but require two stimulatory signals for this to occur. Apoptotic cells (Johann *et al.*, 2007), exposure to prostaglandins (Strassmann *et al.*, 1994) or immune complexes (Lentsch *et al.*, 1997) in isolation is not sufficient to induce a regulatory macrophage phenotype, but in conjunction with a TLR ligand, IL-10 expression is initiated (Edwards *et al.*, 2006; Gerber & Mosser, 2001).

This regulatory phenotype is likely to be vital in the resolution of inflammation. Phagocytosis of inflammatory neutrophils results in induction of pro-fibrotic

arginase (Johann *et al.*, 2007) and release of TGFβ and prostaglandin E, which are known to inhibit inflammatory mediators and induce IL-10 expression (Fadok *et al.*, 1998; Strassmann *et al.*, 1994). iNOS mRNA is destabilised and degraded, inhibiting production of nitric oxide (Vodovotz *et al.*, 1993), while TNFα expression is downregulated due to inhibition of the transcription factor NFκB by stabilisation of IκK (Lentsch *et al.*, 1997), in addition to the IL-10 mediated induction of SOCS3 and associated suppression of inflammatory cytokine expression (O'Shea & Murray, 2008). Furthermore, ligation of macrophage FcγR has been shown to induce a switch from T_H1 to T_H2, inducing preferential IL-10 production over IL-12 from the macrophage (Gerber & Mosser, 2001; Lentsch *et al.*, 1997). This response is rapid following receptor binding of immune complexes, suggesting that a beneficial inflammatory response is generated during the early phase of infection to maximise pathogen killing, during which time the humoral response is mounted. The presence of immune complexes at the site of infection results in ligation of the macrophage FcγR and downregulation of the inflammatory response.

Despite the differing gene expression induced by the various alternative stimuli and the differing roles played by non-classical macrophages, drawing distinctions between subsets is difficult due to the plastic nature of these cells. Macrophages are known to alter their phenotype depending on stimuli and combinations thereof (Stout *et al.*, 2005), indicating that macrophage activation is in fact a dynamic phenomenon, rather than a commitment to a particular phenotype. Nomenclature within the literature has also been somewhat misleading as some authors use the term 'alternatively activated' to describe macrophages stimulated with any stimuli other than IFNγ, while others have specified this term to refer only to IL-4/-13 stimulated cells. For the purposes of the study detailed herein, the term 'alternatively activated macrophage' shall refer to IL-4 stimulated cells only.

1.9 IFNγ Receptor Deficient Mice

1.9.1 IFNγ

Interferon gamma (IFNγ) is the prototype T_H1 cytokine, involved in inflammatory responses, activation of both the innate and acquired immunity, and protection from invading pathogens. Although originally thought to be produced by T and natural killer cells, IFNγ is now also known to be released by macrophages (Di Marzio *et al.*, 1994; Fultz *et al.*, 1993). This has led to a 'kickstart' mechanism for macrophage activation to be proposed, whereby autocrine IFNγ activates macrophages to produce IL-12 and further IFNγ which results in escalation of macrophage activation and drives T_H1 development from naive $CD4^+$ T cells (Frucht *et al.*, 2001). IFNγ also plays a role in preventing T_H2 responses by inhibiting IL-4 production from $CD4^+$ T cells, and by altering T cell responsiveness to IFNγ. This cytokine has been shown to have anti-proliferative effects on T_H2 polarised $CD4^+$ T cells, resulting in outgrowth of the T_H1 population (Gajewski & Fitch, 1988).

The major role of IFNγ is to activate macrophages, which then secrete large quantities of IL-12 resulting in T_H1 differentiation of T cells, but also demonstrate enhanced anti-microbial activity in the macrophage itself. IFNγ stimulation primes macrophages for upregulation of many proinflammatory mediators including IL-12, IL-18, iNOS and IFNγ itself, following a second stimulus such as TLR ligands or TNFα (Drapier *et al.*, 1988; Lorsbach *et al.*, 1993). T cells respond by producing further proinflammatory cytokines in addition to enhanced expression of surface receptors for IL-12, complement, antibody and both classes of MHC molecules (reviewed by Schroder *et al.*, 2004). SOCS 1 & 3 are induced by IFNγ and limit the IFNγ response even in the absence of infection, thereby limiting inflammation (Song & Shuai, 1998).

In addition to inducing inflammation and activating the immune response, IFNγ has direct antiviral properties. Although the type I IFNs are the most potent inducers of the antiviral state via the signalling cascade involving STATs 1 & 2 ultimately resulting in activation of Interferon stimulated response elements (ISRE) in the promoter regions of IFN stimulated genes (ISG), IFNγ induces many of the same antiviral genes such as PKR and OAS (reviewed by Boehm *et al.*, 1997). PKR contains both ISRE and gamma activated sequence (GAS) elements in the promoter region and is therefore directly induced by IFNγ (Tanaka & Samuel, 1994), while OAS is induced by an indirect mechanism.

IFNγ signals through phosphorylation of STAT1 homodimers following ligation of the IFNγR, resulting in activation of GAS elements in the promoters of ISGs (reviewed by Boehm *et al.*, 1997). One of the genes most strongly induced by IFNγ is Interferon regulatory factor 1 (IRF1), which binds to ISRE thereby inducing ISGs following exposure to IFNγ, resulting in indirect induction of ISGs such as OAS (Coccia *et al.*, 1995). Furthermore, IRF1 is a potent enhancer of IFNβ expression (Pine, 1992) and so many of the antiviral effects of IFNγ are indirect due to upregulation of type I IFN expression. However, IFNγ also upregulates expression of the p48 subunit of the type I IFN transcription factor, Interferon-stimulated gene factor 3 (ISGF3). Interaction of p48 with STAT1 homodimers results in direct IFNγ induced activation of ISRE (Bluyssen *et al.*, 1995). Furthermore, IFNγ induced IRF1 has been shown to be vital to induction of iNOS (Kamijo *et al.*, 1994), which in addition to induction of PKR and OAS, further contributes to the antiviral effects of IFNγ.

Despite its role in mounting a protective response to infection, IFNγ has been implicated in the pathogenesis of autoimmune disease due to its proinflammatory nature. However, some polymorphisms in the IFNγ gene may be beneficial as a dampened inflammatory response may occur. Evidence of this was found by assessment of IFNγ gene sequences in centenarian men and

women, indicating that polymorphisms leading to low IFNγ production may be associated with longevity (Lio *et al.*, 2002).

1.9.2 The IFNγ Receptor

Ubiquitously expressed on the surface of all cells except red blood cells (Farrar & Schreiber, 1993), the IFNγ receptor comprises a homodimeric IFNγRα subunit, which binds IFNγ and then interacts with the signalling subunit, IFNγRβ, also a homodimer. IFNγRα binds and internalises ligand, activating the Jak-STAT pathway. Binding of IFNγ to this subunit leads to phosphorylation of Jak1 and 2, which in turn allows activation of latent STAT1 by the IFNγRα (reviewd by Schroder *et al.*, 2004). Nuclear translocation then occurs with the IFNγRα being transported to the nucleus along with bound IFNγ and STAT1, while IFNγRβ is recycled to the cell surface (Larkin *et al.*, 2000). Older studies indicate that IFNγRα may also be recycled to an intracellular pool of receptor subunits, allowing constitutive repopulation of the plasma membrane with ligand-binding receptor (Celada & Schreiber, 1987).

IFNγRβ has been demonstrated to play a role in T_H1 polarisation. Following exposure to IFNγ, $CD4^+$ T cells downregulate expression of the IFNγRβ chain, and therefore become unresponsive to the IFNγ-induced block on proliferation, resulting in expansion of the T_H1 population (Bach *et al.*, 1995). The β chain has also been implicated in cell survival, with cells expressing high levels of IFNγRβ undergoing apoptosis in response to IFNγ, due to rapid STAT1 activation resulting in high levels of IRF-1. Low level expressing cells, such as T cells, are protected as they undergo more gradual accumulation of IRF-1, which is insufficient to trigger apoptosis (Bernabei *et al.*, 2001).

IFNγRα has five potential N-linked glycosylation sites (Farrar & Schreiber, 1993). Disruption of this glycosylation by treatment with enzymes such as neuraminidase, which destroys SA, renders IFNγRα incapable of binding

ligand, suggesting that glycosylation is essential for maintaining receptor conformation (Fischer *et al.*, 1990).

1.9.3 IFNγ and IFNγR Deficiency

Despite the seemingly critical role played by IFNγ in development of protective T_H1 responses, disruption of either the IFNγ or the IFNγRα gene (referred to herein as IFNγR$^{-/-}$) does not lead to overt immunodeficiency. Although more susceptible to some intracellular infections, IFNγR$^{-/-}$ mice develop normally with similar expression of CD3, 4, 8, MHC I and II and also IgM to wildtype Sv129 animals (Huang *et al.*, 1993). However, lack of IFNγ signalling in mice predisposes the host to more severe disease following infection with *Listeria monocytogenes* (Szalay *et al.*, 1996), pseudorabies (Schijns *et al.*, 1994), vaccinia and lymphochoriomeningitis (LCMV) viruses (Huang *et al.*, 1993). The virological studies, however, documented normal CTL responses to viral infections but reduced IgG_{2a} compared to wildtype Sv129 mice. Survival following infection with a low pathogenic strain of influenza virus (HKx31, H3N2) was not different in IFNγR$^{-/-}$ mice than in wildtype, with similar viral titres, CTL and antibody responses being documented (Price *et al.*, 2000). It has been indicated that the cell type in which the IFNγ signalling deficiency occurs is important in determining response to infection. Reconstitution of LCMV-infected irradiated IFNγR$^{-/-}$ mice with wildtype CTL did not result in protection, but wildtype mice given IFNγR$^{-/-}$ haematopoetic cells displayed milder disease (Henrichsen *et al.*, 2005). This study suggested that induction of an IFNγ-mediated antiviral response in the parenchyma was essential in order to allow efficient cellular protection, while CTL could function independently of IFNγ.

The Sv129 strain of mice, from which IFNγR$^{-/-}$ animals were generated, is a T_H1 predisposed strain as these mice do not express IL-4 from splenocytes stimulated with concavalin A (Schijns *et al.*, 1994). It appears that in the

absence of IFNγ signalling, production of IL-12 results in inhibition of IL-4 expression and allows maintenance of a functional T_H1 response to infection (Bach *et al.*, 1995; Mattner *et al.*, 1996; Schijns *et al.*, 1995; Swihart *et al.*, 1995). However, other studies have documented increased T_H2 cytokines in IFNγR$^{-/-}$ animals (Gangadharan *et al.*, 2008) despite the presence of IL-12 (Szalay *et al.*, 1996). Other cytokines, including IFNα/β can evidently compensate for some functions of IFNγ (Muller *et al.*, 1994), but not for all, as IFNγR$^{-/-}$ fail to upregulate nitric oxide following stimulation with TNFα, IFNα/β or LPS (Kamijo *et al.*, 1993). IFNγR deficiency in humans has been associated with increased severity of mycobacterial and herpes virus infections in childhood (Dorman *et al.*, 1999), while defective IFNγ signalling can result in reduced neutrophil recruitment (Davies *et al.*, 1982).

Taken together, these studies indicate that disruption of IFNγ signalling results in a functional T cell response, a functional antibody response but with altered isotype proportions, but an impaired innate response with decreased neutrophil mobility and poor nitric oxide production, ultimately impairing the immune response to intracellular pathogens.

1.10 Research Aims

1.10.1 Hypothesis

Influenza viruses infect macrophages, altering the cytokine profile and leading to enhanced inflammation with a concomitant increase in immunopathology. This project aims to investigate the hypothesis that alternative activation of macrophages overcomes this scenario by inducing an anti-inflammatory, T_H2-like environment, thereby reducing immunopathology and maintaining organ function.

1.10.2 Research Questions

To address this hypothesis, several research questions must be answered, both in vitro and in vivo. The following questions need to be explored in vitro before any in vivo work can be undertaken.

What are the phenotypes of "alternative" and "classical" macrophages in our hands?

Can alternatively activated macrophages sustain influenza virus infection?

Once infected, can such macrophages maintain their alternative phenotype?

Once these queries have been addressed, the following in vivo questions will be explored.

Does skewing of the immune system away from T_H1 using IFNγ receptor deficient mice lead to protection from immunopathology?

What effect does skewing of the immune system have on viral load and disease progression?

Investigation of these questions will lead to a better understanding of the immunopathological processes involved in influenza virus infection, which is of utmost importance in development of novel therapeutics to this disease.

2 Materials and Methods

2.1 Animals and Macrophage Isolation

2.1.1 Isolation of Bone Marrow for in vitro Culture

6-8 week old mice of wild type 129SvEv (Sv129) and BALB/c backgrounds, IFNγ receptor deficient mice on the 129SvEv background (IFNγR$^{-/-}$) and IL-4 receptor deficient mice on the BALB/c background (IL-4R$^{-/-}$) were culled for macrophage isolation. Both IFNγR$^{-/-}$ and IL-4R$^{-/-}$ mice were congenic as for both strains, the target genes were disrupted in embryonic stem cells which were then implanted into 3.5 day blastocysts. Chimeric males were intercrossed with wildtype females, resulting in heterozygous F1 offspring. These were then intercrossed to obtain IFNγR$^{-/-}$ Sv129 (Huang *et al.*, 1993) or IL-4R$^{-/-}$ BALB/c animals (Noben-Trauth *et al.*, 1997), therefore findings may be directly compared between wildtype and mutant strains of mice. Littermate controls were not used as mutant mice were from distinct but congenic lines. Femurs were removed, cleaned and flushed through with cold Rosewell Park Memorial Institute 1640 medium (RPMI; Gibco) supplemented with 10% foetal calf serum (Invitrogen), using a 25 gauge needle (Microlance) and 10mL syringe (Terumo) to remove the bone marrow. Bone marrow was then centrifuged at 8000g, washed again in supplemented RPMI and resuspended in 40mL complete macrophage medium, as detailed in section 2.2.4.

2.1.2 In vivo Infections

6-8 week old female mice of the Sv129 and IFNγR$^{-/-}$ genotypes were infected intranasally with influenza virus A/WSN/33 at a dose of $1x10^4$ plaque forming units (pfu) per mouse. Mice were weighed daily and culled at days 2, 4, 6 and 8. Lungs were harvested for virus assay and histological analysis. Small pieces of lung were harvested from the most distal point of the left lobe,

consistent between all animals and placed in RNAlater (Qiagen) for RNA extraction. These pieces were initially stored at 4°C to allow the RNAlater solution to penetrate the tissue, followed by longer term storage at -80°C. Collecting tissue from this region of the lung meant that changes in cytokine expression influencing the whole lung could be detected, whereas taking samples from closer to centre of the lung could be heavily influenced by the local presence of infiltrating cells and give a false indication of the extent of cytokine production throughout the entire organ.

2.2 Tissue Culture

2.2.1 Madine-Darby Canine Kidney Cells

Madine-Darby Canine Kidney (MDCK) cells were cultured in tissue culture flasks (Nunc) in Dulbecco's Modified Eagle's Medium (DMEM; Gibco) supplemented with 10% foetal calf serum (Invitrogen), 100U/mL penicillin and streptomycin (Gibco) and 1% L-glutamine (Gibco). Cells were passaged every four days by incubation with trypsin (Gibco) for 20 minutes, centrifuged at 8000g and reseeded in DMEM.

2.2.2 RAW macrophages

RAW 264.7 cells, a murine leukaemic macrophage cell line was cultured in RPMI supplemented with 10% foetal calf serum, 100U/mL penicillin and streptomycin and 1% L-glutamine. Cells were loosely adherent and passaged every four days by gentle scraping, followed by reseeding in new flasks.

RAW cells were infected with A/WSN/33 virus at a multiplicity of 1 and used as positive controls for the staining methods detailed in section 2.8.

2.2.3 L929 fibroblasts

L929 fibroblasts were cultured in RPMI supplemented as described in section 2.2.2. Cells were passaged every four days until a total volume of 2L supernatant was achieved. This was then collected and pooled followed by centrifugation at 8000g to remove cellular debris, and stored at -20°C in 20mL volumes as a source of M-CSF. L929 cells and supernatants were also tested for mycoplasma using a PCR-ELISA detection kit (Roche), as these fibroblasts are known to produce IFNα/β when infected with mycoplasma. Cells and supernatants were pelleted by centrifugation, followed by lysis of the pellet. After neutralisation of the lysis buffer, extracts and controls were incubated with the kit PCR mix and run on the following program: 5 minutes at 95°C, followed by 40 cycles of 30s at 94°C, 30s at 62°C, 1 minute at 72°C with a final 10 minute step at 72°C. 10µL of the PCR product was denatured using the kit denaturation reagent before addition of hybridisation reagent, transfer to ELISA plates and incubation in the dark with gentle agitation for 3 hours at 37°C. Anti-digoxigenin conjugated to peroxidase was added to wells and incubated in the dark for a further 30 minutes at room temperature before addition of 3,3',5,5'-tetramethylbenzidine (TMB) and a final incubation period of 20 minutes in the dark at room temperature. A sulphuric acid stop solution was added and absorbance determined at 450nm. Negative controls should give <0.25Abs, while positive controls should be >1.2Abs. If samples were >0.2Abs after subtraction of the negative control, then samples were considered mycoplasma positive. However, all samples gave final absorbance of <0.2Abs, and so were considered mycoplasma free.

2.2.4 Bone Marrow Derived Macrophages

Isolated bone marrow was cultured in 10mm square bacteriological dishes (Sterilin) for 7 days in complete macrophage media, which contained RPMI supplemented with 10% foetal calf serum (Invitrogen), 100U/mL penicillin and streptomycin (Gibco), 1% L-glutamine (Gibco) and 50% L929 supernatant.

Cultures were initially set up by seeding cells from one femur in each plate. Bone marrow derived macrophages (BMDMϕ) were passaged on day four by the following method: incubation with Dulbecco's Phosphate Buffered Saline (D-PBS; Gibco) for 5 minutes followed by detaching from the plastic by washing vigorously with D-PBS using an 18 gauge needle (Microlance) and syringe (Terumo) and centrifugation at 8000g. Cells from each plate were then reseeded into two new plates in complete macrophage medium supplemented with 5mL original medium. On day 7, BMDMϕ were activated with either 4ng/mL IL-4, or 1ng/mL IFNγ (Peprotech) in complete macrophage medium. Activated BMDMϕ were infected at 16 hours post activation (day 8) by incubation with A/WSN/33 virus at a multiplicity of infection of 10 for 1 hour. Following this, inoculum was removed, the activating medium returned to the plates and culture continued for either 16 hours, or 48 hours to allow multiple rounds of viral replication. BMDMϕ were detached from the plastic, washed and centrifuged into pellets of $5x10^6$ cells and supernatant collected, then stored at -20°C for future analysis.

2.3 Virological Techniques

2.3.1 Influenza Virus Preparation

The mouse adapted influenza A virus strain A/WSN/33 (a gift from Dr D. Jackson, University of St Andrews, UK) was cultured on a monolayer of MDCK cells for 36 hours at a multiplicity of infection of 0.001. The supernatant was then harvested and centrifuged at 8000g before being aliquotted into volumes of 100µL, 500µL and 1mL and stored at -80°C for future use. Virus titre was determined by plaque assay on MDCK cells.

2.3.2 Plaque Assay

Ten fold serial dilutions of virus were made in serum free DMEM and 400µL of dilutions $1x10^{-3}$ to $1x10^{-8}$ were plated in duplicate onto confluent MDCK monolayers in 6 well plates (Nunc). The plates were incubated at 37°C for 1 hour, rocking every 10 minutes to prevent the cells drying out and ensure even spread of inoculum. Virus was removed by aspiration after 1 hour and cells overlaid with 2% agarose (Bioline) in serum free DMEM containing 2µg/mL N-acetyl trypsin (Sigma). Once the agarose had set, plates were inverted and incubated at 37°C for 3 days. Cells were then fixed with 10% neutral buffered formalin (Surgipath), agarose plugs removed and monolayers stained with toluene blue (Appendix 2.3 Recipes) to visualise plaques. Plaques were counted at two dilutions and the average taken, the higher dilution being converted into the lower, giving the plaque count in 400µL of the chosen dilution. This was then multiplied by 2.5 to give plaque count/mL and finally multiplied by the appropriate dilution factor to give final viral titre in pfu/mL.

2.3.3 Haemagglutination Assay

Two fold dilutions of BMDMϕ supernatant were made and 25µL diluted supernatant was added to 25µL 1% human red blood cells (RBC) in round bottom 96 well plates. Plates were incubated at 4°C overnight to allow virus to agglutinate the RBC. Presence of virus particles was detected by inhibition of RBC pellet formation in the bottom of the well. Serially diluted virus stock and media alone were used as positive and negative controls respectively.

2.4 Flow Cytometry

$0.5x10^{6}$ BMDMϕ were aliquotted in 100µL phosphate buffered saline supplemented with bovine serum albumin (PBSA; Appendix 2.3 Recipes). These cells were labelled with rat anti-mouse primary antibodies listed in Table

2.1, washed twice with PBSA then stained with a secondary goat anti-rat antibody labelled with Alexafluor 647 (Molecular Probes) at a dilution of 1:4000. Two further PBSA washes were performed and cells fixed in 200µL 4% paraformaldehyde (PFA; Appendix 2.3 Recipes) for 20 minutes before addition of 300µL PBSA for analysis.

Antibody	Dilution	Cell type	Supplier	Clone	Isotype
CD11b	Neat	Macrophage	In house	5C6	IgG2b
F4/80	1:100	Macrophage	AbD Serotec	Cl:A3-1	IgG2b
CD206	1:200	Macrophage	AbD Serotec	MR5D3	IgG2a

Table 2.1 Flow cytometry antibodies.
Antibody dilutions and target cells for flow cytometry analysis of bone marrow derived macrophages

CD206 labelled BMDMϕ required fixing and permeablisation of the cell membrane prior to labelling. This was carried out by washing cells twice with PBSA, fixing for 10 minutes with 4% PFA followed by permeablising with 0.1% saponin (Sigma) in PBSA for 10 minutes. Primary antibody was then diluted in permeablisation buffer (Appendix 2.3 Recipes) and incubated with the cells for 30 minutes on ice, followed by washing with PBSA and incubation with secondary antibody, again diluted in permeabilsation buffer. Two final washes with PBSA were carried out before the cells were resuspended in 500µL PBSA for analysis.

The labelled cells were then analysed on a FACSCalibur system using CellQuest software (BD Biosciences). Further analysis was also carried out using FlowJo software (TreeStar).

2.5 Enzyme Linked Immunosorbent Assay

IL-12p40 and TGFβ levels in BMDMϕ supernatant and lung homogenates were analysed by Enzyme Linked Immunosorbent Assay (ELISA). TGFβ is found in both latent and activated forms, requiring cleavage to become active. For this ELISA, samples were not subjected to cleavage as the amount of active TGFβ present was under investigation, not the total amount being synthesised. This allowed detection of the extent of bioactive TGFβ present following influenza virus infection. 96 well ELISA plates (Immunolon) were coated with the appropriate capture antibody (RnD Systems), diluted in PBSA, for 16 hours at 25°C. Plates were then washed twice with PBS containing 0.05% Tween20 (National Diagnostics) and blocked with PBSA for 1 hour, followed by two further washes. Samples were plated in duplicate and incubated for 2 hours at room temperature, followed by two further washes and addition of the biotinylated detection antibody (RnD Systems). Plates were incubated for 2 hours at room temperature and washed again before addition of streptavidin-linked horseradish peroxidise (RnD Systems) for 20 minutes in the dark. After three washes, TMB substrate solution (RnD Systems) diluted in 100mM sodium acetate, (Sigma) containing 2μL 30% hydrogen peroxide (Sigma), was added to the wells for 20 minutes in the dark. Finally, the reaction was terminated using 2M sulphuric acid (BDH). Absorbance was measured at 450nm, with reference wavelength of 540nm and plotted using Prism software (Graphpad).

2.6 Inducible Nitric Oxide Synthetase Bioassay

Active inducible nitric oxide synthetase (iNOS) was investigated using the Greiss reagent bioassay, which results in production of nitrite and a colour change from colourless to pink in the presence of enzyme. 100μL Greiss

reagent (Appendix 2.3 Recipes) was added to 100µL BMDMϕ supernatant or 100µL sodium nitrite standard (Sigma) and absorbance read at 540nm.

2.7 Arginase-1 Bioassay

Bioactive Arginase-1 was measured in its ability to convert L-Arginine to urea as follows. $1x10^5$ BMDMϕ were plated onto 96 well flat bottomed plates (Nunc), washed with PBS and lysed with 0.1% Triton-X (Sigma). The lysate was then removed to sterile eppendorfs. After addition of 100µL 25mM Tris-HCl and 20µL 10mM $MnCl_2$, tubes were incubated at 56°C for 10 minutes. 100µL of each sample was transferred to fresh eppendorfs and incubated with 100µL 0.5M L-Arginine for 2 hours. During this time a standard dilution series of urea was made. Following the incubation step, 800µL sulphuric/phosphoric acid solution (Appendix 2.3 Recipes) was added along with 40µL isonitropropiophenone, mixed by vortexing and incubated at 95°C for 30 minutes. Once cooled, samples and standards were plated in a 96 well plate and absorbance read at 540nm.

2.8 Immunohistochemistry

2.8.1 Immunofluorescence

$1x10^5$ infected BMDMϕ were cultured on 8 well chamber slides (BD Falcon), medium aspirated and cells washed with PBS. All incubations were performed for 30 minutes at room temperature, and antibodies were used at concentrations detailed in Table 2.2. BMDMϕ were fixed with 4% PFA before blocking with Cas block (Invitrogen). Slides were incubated with polyclonal goat anti-influenza antibody (AbD Serotec; Table 2.2), or polyclonal sheep anti-NS1 antibody (a gift from Dr. D. Jackson, University of St Andrews, UK)

followed by washing twice with PBS. Rabbit anti-goat/sheep Alexafluor 488 labelled secondary antibody (Molecular Probes), along with DAPI (Invitrogen) was added again followed by two wash steps. The chamber portion of the slide was then removed, the slides mounted in mowiol (Appendix 2.3 Recipes) and sealed with nail polish. Slides were stored in the dark at 4°C.

Target	Host	Dilution	Supplier	Clone
Influenza virus	Goat	1:200	AbD Serotec	Polyclonal
NS1	Sheep	1:200	Dr D. Jackson	Polyclonal
Mouse F4/80	Rat	1:100	AbD Serotec	A3-1
Mouse Ly6G	Rat	1:100	Biolegend	1A8
Sheep/Goat IgG - Alexafluor 488	Rabbit	1:1000	Invitrogen	Polyclonal
Rat IgG - Alexafluor 594	Rabbit	1:1000	Invitrogen	Polyclonal
DAPI	-	1:1000	-	-
Rat IgG - Horseradish peroxidase	Goat	1:100	Invitrogen	Polyclonal

Table 2.2 Immunohistochemistry antibodies.
Host and target species and dilutions of antibodies used for immunohistochemistry staining of sections and cells.

2.8.2 Dual immunofluorescent stain

Virus positive macrophages were detected by dual immunofluorescent staining for the macrophage marker F4/80 and influenza antigens. Lungs were inflated and coated with OCT compound (VWR) and frozen rapidly in isopentane over dry ice. Sections were prepared on coated slides and stored at -80°C. Incubations were performed for 30 minutes at room temperature, unless otherwise stated, and antibodies were used at the concentrations detailed in Table 2.2. At time of staining, sections were fixed in acetone for 10 minutes, followed by washing briefly in PBS and blocking with Cas block. Incubation with polyclonal goat anti-influenza antibody was followed by washing with PBS and addition of the second primary antibody, rat anti-F4/80 (AbD Serotec). Subsequently, sections were incubated with a cocktail of Alexafluor-linked

secondary antibodies (Table 2.2), allowing detection of both antigens and counterstain with DAPI to be performed in a single incubation. Sections were then washed thoroughly and mounted with mowiol, sealed with nail polish and stored in the dark at 4°C.

2.8.3 Immunohistochemistry

Paraffin wax embedded lung sections were stained for neutrophil marker Ly6G Biolegend), or virus antigens, followed by detection with DAB substrate. Briefly, sections were dewaxed in xylene (BDH) followed by rehydration in increasing concentrations of alcohol. Slides were then placed in a sodium citrate antigen retrieval solution (Appendix 2.3 Recipes) and microwaved in a pressure cooker for 20 minutes to break crosslinking of antigens caused by the paraffin wax embedding process. Slides were cooled in running tap water before being blocked with Cas block for 30 minutes and washed twice with TBS containing 0.05% Tween 20 (Appendix 2.3 Recipes). Sections were incubated with primary goat anti-influenza, or rat anti-Ly6G (Biolegend) antibody (Table 2.2) for 2 hours at room temperature, followed by two washes and blocking of endogenous peroxidases by incubation with H_2O_2:methanol (Appendix 2.3 Recipes) for 5 minutes. Species specific horseradish peroxidase labelled secondary antibody (AbD Serotec;Table 2.2) was added for 1 hour at room temperature followed by washing. Sections were then incubated with diaminobenzidine substrate solution (DAB; Sigma) for 10 minutes followed by two further washing steps. Slides were mounted in Vectamount (Vector) permanent mounting medium and stored at room temperature.

2.9 RNA Extraction

2.9.1 RNA Extraction from BMDMϕ

RNA was extracted from cell samples using a RNeasy Mini Kit (Qiagen) as per the manufacturer's instructions. Briefly, pellets of $5x10^6$ BMDMϕ were disrupted by addition of 350µL RLT Buffer (lysis buffer, containing β-mercaptoethanol) followed by addition of 350µL 70% ethanol. The homogenised lysate was then mixed by pipetting, placed in a spin column and centrifuged at 8000g for 15 seconds. 700µL RW1 Buffer (first wash buffer) was then added to the column and centrifuged, followed by two washes of 500µL RPE (second wash buffer, containing ethanol). 30-50µL nuclease free water was then added directly to the membrane in the spin column and centrifuged at 8000g to elute RNA. RNA concentration was determined using a spectrophotometer and quality of RNA estimated by running 2µL on a 1% agarose gel to visualise 18S and 28S ribosomal RNA bands.

2.9.2 RNA Extraction from Whole Lungs

Lung pieces in RNAlater were removed from -80°C and placed in sterile eppendorfs on dry ice. 100µL RLT buffer was added and lungs ground using a plastic pestle (Anachem) until completely homogenised. 600µL RLT buffer was added, the homogenate placed in a Qiashredder column (Qiagen) and centrifuged at 8000g for two minutes. 700µL 70% ethanol was added to the effluent from the Qiashredder and RNA extraction continued as described above.

2.10 DNase Treatment and Reverse Transcription

1000 or 2000ng RNA was DNase treated with 1µL DNA-free (Ambion) plus 1µL buffer and incubated at 37°C for 30 minutes. 1µL inactivation reagent (Ambion) was then added and incubated at room temperature for two minutes before brief centrifugation to pellet the inactivation reagent. Reverse transcription using the Superscript III system (Invitrogen) was then performed. DNase treated RNA was incubated at 65°C with 50ng random primers (Invitrogen) or 0.2µM oligodT (Ambion) and 0.5mM dNTPs (Roche) for five minutes followed by one minute on ice. Superscipt III enzyme, 5x first strand buffer, DTT and RNaseOUT (all Invitrogen) were added and the following heating cycle performed: 25°C for five minutes; 50°C for 60mins; 70°C for 15mins. cDNA was stored at -20°C.

2.11 Gene Cloning

Primers were designed as listed in Table 2.3 using NetPrimer and Primer3 software. Specificity was confirmed by performing a search on NCBI Nucleotide BLAST. The genes detailed in Table 2.3 were amplified with a high fidelity DNA polymerase (Finnzyme) and cloned using a Zero Blunt II Topo PCR Cloning Kit (Invitrogen) and Beta 10 competent cells (New England Biolabs). Briefly, 1µL amplified product was incubated at room temperature with 1µL pCR Blunt II TOPO plasmid along with salt solution and water for 10 minutes. Following this, the plasmid/product mixture was added to a tube of Beta 10 cells, mixed gently and incubated on ice for 10 minutes. Heat shocking was carried out at 42°C for 30 seconds and the cells replaced on ice. 250µL SOC medium (Invitrogen) was added to the tube of cells and shaken for 1 hour at 37°C. Cells were then streaked onto kanamycin plates (Appendix 2.3 Recipes), incubated overnight and colonies picked for further analysis.

Several clones were also purchased from GeneService and are detailed in Table 2.4. These were streaked onto plates containing appropriate antibiotic and single colonies picked for analysis.

Cloned products were purified using a Miniprep DNA Purification Kit (Qiagen). Briefly, picked colonies were amplified in 5mL kanamycin or ampicillin medium (Appendix 2.3 Recipes) and incubated shaking overnight at 37°C. Amplified cultures were pelleted, supernatant removed and the pellet resuspended in Buffer P1 (resuspension buffer). Cells were transferred to microfuge tubes where 250µL Buffer P2 (alkali lysis buffer) was added with gentle mixing, followed by addition of 350µL Buffer N3 (neutralisation buffer). Lysates were centrifuged at 12,000g for 10 minutes and supernatants applied to a QiaPrep spin column. Columns were centrifuged, effluent discarded and column washed with Buffer PB (binding buffer). Effluent was again discarded and a second wash step performed using Buffer PE (wash buffer), followed by further centrifugation to remove effluent and residual buffer. Bound DNA was eluted by addition of 50µL water directly to the membrane of the column and spinning for one minute.Products were sequenced, linearised with restriction enzymes (Promega), listed in Table 2.4, or with HinDIII for all Blunt Topo plasmids, and used as template DNA for qPCR.

Template DNA for the influenza A virus gene M1 was generated in the same manner by Mr Ian Bennet.

Gene	Forward	Reverse	Region	Accession No
Arg-1	ggaacccagagagagcatga	ggagaaaggacacaggttgc	87-547	NM_007482
CD206	caccagagcccacaacaac	ctggtggattgtcttgtgga	2003-2494	NM_008625
CNX	ttagttgaccagtctgttg	cctttcatcccaatcttcag	694-803	L23865
IL-10	gcttctattctaaggctggc	ctgggggatgacagtagg	949-1148	NM_010548
iNOS	atgctaatgcgaaaggtca	tttggtgtggtgtaggac	1744-2563	NM_010927
SDHA	gctcctactgatgaaacctg	aactcaatcccttacagcaa	2017- 2189	NM_023281
TNFa	gggattatggctcagggtc	ggctggctctgtgaggaagg	979-1277	NM_013693

Table 2.3 Primers for cloning of genes of interest.
Primers were designed using the freely available programs Primer3 and NetPrimer then checked for specificity on NCBI Blast.

Gene	Accession No	Plasmid	Linearised	Antibiotic
FIZZ	BC029248	pCMV SPORT6	HinDIII	Amp
IL-1b	BC011437	pCMV SPORT6	EcoRI	Amp
IL-6	BC132458	pCR Blunt TOPO	HinDIII	Kan/Amp
IL-12p40	BC103608	pCR4-TOPO	NotI	Kan

Table 2.4 Details of purchased clones.
Clones were purchased from Gene Service Ltd and grown on plates containing antibiotic before pickingof individual colonies, overnight culture and DNA purification alongside in-house cloned products. Amp, Ampicillin; Kan, Kanamycin.

2.12 Quantitative Polymerase Chain Reaction

2.12.1 Generation of standard curves

Standard curves were generated from the purified template DNA of each gene of interest by calculating the number of gene copies per µL (Equation 2.1) and making serial ten fold dilutions.

$$\text{Copies}/\mu L = \frac{6.02 \times 10^{23} \times \text{concentration } \{g/\mu L\}}{\text{Total vector size } \{bp\} \times 660}$$

Equation 2.1 Calculation of gene copy number per µL cloned plasmid

2.12.2 Optimisation of reaction conditions

Primers were designed for each gene of interest as previously described and are detailed in Table 2.5. Reaction conditions for SybrGreen qPCR (SybrGreen, Biogene; PCR reagents, Roche) were optimised by first using a constant concentration of $MgCl_2$ and altering the primer concentration. Once optimal primer concentration had been established, $MgCl_2$ concentration was titrated for each set of primers. Annealing temperature was also altered based on the melt temperatures of the primers. A trial standard curve was then performed to ensure that all conditions were successfully optimised. This will be discussed fully in Chapter 3. Reaction conditions for each gene of interest are detailed in Table 2.6.

2.12.3 Analysis and Normalisation of Quantitative RT-PCR data

Two housekeeping genes were used to normalise the genes of interest. A panel of primers for 12 genes (Quantace) was tested, and will be discussed in Chapter 3. The two genes with most stable expression were selected; calnexin (CNX) and succinate dehydrogenase A (SDHA). Primers were designed, again

using NetPrimer and Primer3 software (Table 2.5), product was amplified by high fidelity PCR, purified by Qiagen Miniprep, cloned as described in 2.11 and reaction conditions optimised.

Relative expression of genes between samples and non activated controls was calculated using Genex software (MulitD Analyses), based on Equation 2.2, taking efficiency of the reaction and expression of housekeeping genes into consideration. Relative expressions were then plotted using Prism Graphpad software (GraphPad Software) or R (R-project.org).

$$\frac{\text{Sample A}}{\text{Sample B}} = \frac{\left[\frac{(1+E_{Ref})^{Ct\ Ref}}{(1+E_{Sample\ A})^{Ct\ Sample\ A}}\right]}{\left[\frac{(1+E_{Ref})^{Ct\ Ref}}{(1+E_{Sample\ B})^{Ct\ Sample\ B}}\right]}$$

Equation 2.2 Calculation of relative gene expression between activation groups.

2.13 Statistical Analysis

Data is presented as mean ± standard error of the mean (SEM), or as box and whisker plots representing the median, 25th and 75th percentile, minimum and maximum values. Outliers have been included in the statistical analysis and plotted as single points outwith the whiskers of the main data set. Histograms were plotted using Prism 4.0 for Windows (GraphPad). Analysis of variance (ANOVA) was performed using the statistical package R (R-project.org), which was also used to display box and whisker plots. Statistical significance was graded as * $P<0.05$, ** $P<0.005$, *** $P<0.0005$.

Gene	Forward	Reverse
CNX	tta gtt gac cag tct gtt g	cct ttc atc cca atc ttc ag
SDHA	gct cct act gat gaa acc tg	aac tca atc cct tac agc aa
Arg-1	ggc ctt tgt tga tgt ccc ta	atg ctt cca act gcc aga ct
CD206	tga acc caa atg tcc aga aa	ctc gta atc agc ctc caa atc
FIZZ	act ggg tgt gct tgt ggc ttt gcc t	agc agg gta aat ggg caa ta
IL-1b	cga caa aat acc tgt ggc ct	gag gca agg agg aaa aca ca
IL-6	gta cca tag cta cct gga gt	gga gag cat tgg aaa ttg g
IL-10	ctt tgc tat ggt gtc ctt tca	atc tcc ctg gtt tct ctt cc
IL-12p40	gga agc acg gca gca gaa ta	ttg agg gag aag tag gaa tgg
iNOS	tgc tac tga gac agg gaa g	gac agt ctc cat tcc caa
TNFa	cac cac cat caa gga ctc aa	gac aga ggc aac ctg acc ac
Influenza M1	ctc tct atc gtc ccg tca gg	gag cgt gaa cac aaa tcc ta

Table 2.5 qPCR primers (All MWG Eurofins)

Gene	Forward	Reverse	MgCl	Anneal
CNX	400nm	400nm	3.0mM	62°C
SDHA	400nm	400nm	2.5mM	62 °C
Arg-1	400nm	400nm	3.0mM	62 °C
CD206	400nm	400nm	3.0mM	62 °C
FIZZ	400nm	400nm	2.5mM	66 °C
IL-1β	300nm	300nm	2.5mM	62 °C
IL-6	400nm	400nm	2.5mM	62 °C
IL-10	500nm	500nm	2.5mM	62 °C
IL-12p40	400nm	400nm	2.5mM	62 °C
iNOS	400nm	500nm	3.0mM	62 °C
TNFα	400nm	500nm	3.0mM	65 °C
Influenza M1	400nm	500nm	2.5mM	62 °C

Table 2.6 Optimised qPCR conditions

Appendix 2.1 Suppliers

AbD Serotec	MorphoSys UK Ltd, Endeavour house, Langford Business Park, Langford Lane, Kidlington, Oxford, OX5 1GE, UK www.abdserotec.com
Ambion	Applied Biosystems/Ambion, 2130 Woodward St., Austin, TX 78744-1832, USA www.ambion.com
Anachem	Anachem House, 1 & 2 Titan Court, Laport Way, Luton, LU4 8EF, UK www.anachem.co.uk
BD Biosciences	21 Between Towns Rd, Cowley, Oxford, OX4 3LY, UK www.bdbeurope.com
BDH	Supplied by VWR www.vwr.com
Bioline	16 The Edge Business Centre, Humber Rd, London, NW2 6EW, UK www.bioline.com
Biogene	BioGene House, 6 The Business Centre, Harvard Way, Kimbolton, Cambs, PE28 0NJ, UK www.biogene.com

BioLegend UK Ltd	Munro House, Trafalgar Way. Bar Hill,Cambridge, CB23 8SQ, UK www.biolegend.com/uk
Eurofins MWG Operon	Anzingerstr. 7a, 85560 Ebersberg, Germany www.eurofinsdna.com
Finnzyme	Keilaranta 16 A, 02150 Espoo, Finland www.finnzymes.com
Fisher Scientific	Bishop Meadow Rd, Loughborough, Leicestershire, LE11 5RG, UK www.fishersci.com
GeneService Ltd	Source BioScience, Units 24 & 25, William James House, Cowley Road, Cambridge, CB4 0WU, UK www.geneservice.co.uk
Gibco	Supplied by Invitrogen www.invitrogen.com
GraphPad Software Inc.	2236 Avenida de la Playa, La Jolla, CA 92037 USA www.graphpad.com
Immunolon	Supplied by VWR www.vwr.com

Invitrogen	3 Fountain Drive, Inchinnan Business Park, Paisley,PA4 9RF, UK www.invitrogen.com
Microlance	Supplied by SLS www.scientificlabs.co.uk
Molecular Probes Inc (Invitrogen)	29851 Willow Creek Rd, Eugene, OR 97402, USA www.invitrogen.com
MultiD Analyses	Odinsgatan 28, SE-411 03, Göteborg, Sweden www.multid.se
National Diagnostics	Supplied by Fisher Scientific www.fishersci.com
New England Biolabs	75-77 Knowl Piece, Wilbury Way, Hitchin, Herts SG4 0TY, UK www.neb.com
Nunc	Supplied by SLS www.scientificlabs.co.uk
PeproTech	PeproTech House, 29 Margravine Rd, London, W6 8LL, UK www.peprotechec.com
Promega	Delta House, Southampton Science Park, Enterprise Rd, Southampton SO16 7NS, UK www.promega.com

Qiagen	Qiagen House, Fleming Way, Crawley, West Sussex, RH10 9NQ, UK www.qiagen.com
Quantace	Rowlandson House, 289-293 Ballards Lane, Finchley, London N12 8NP, UK www.quantace.com
R-project	The R Foundation for Statstical Computing www.r-project.org
RnD Systems	19 Barton Lane, Abingdon Science Park, Abingdon, Oxford, OX14 3NB www.rndsystems.com
Roche	Charles Avenue, Burgess Hill , West Sussex , RH15 9RY, UK www.roche.com
Scientific Laboratory Supplies (SLS)	Orchard House, The Square, Hessle, East Riding of Yorkshire, HU13 0AE, UK www.scientificlabs.co.uk
Sigma Aldrich	The Old Brickyard, New Road, Gillingham, Dorset, SP8 4XT, UK www.sigmaaldrich.com
Sterilin	Supplied by SLS www.scientificlabs.co.uk

Surgipath	Venture Park, Stirling Way, Bretton, Peterborough, Cambridgeshire, PE3 8YD, UK www.surgipath.com
Thermo Scientific	Pierce Biotechnology, PO Box 117, 3747 N. Merdian Rd, Rockford, IL 61105, USA www.thermoscientific.com
Tree Star Inc.	340 A Street #101, Ashland, OR 97520, USA www.treestar.com
Vector Laboratories	3 Accent Park, Bakewell Rd, Orton, Southgate, Peterborough, PE2 6XS, UK www.vectorlabs.com
VWR	Hunter Boulevard, Magna Park, Lutterworth, Leicestershire, LE17 4XN, UK www.vwr.com

Appendix 2.2 Equipment

Automatic pipettor	Express, Falcon
Balances	Fine: AE163, Mettler Medium: EK-200G, AND
Centrifuges	TJ-6, Beckman 1-15P, Sigma 113, Sigma
Flow cytometer	FACSCalibur, Becton Dickinson
Gel documentation system	FluorChem HD2, Alpha Innotech
Gel electophoresis system	Mini-Sub Cell GT, Bio-Rad
Haemocytometer	SLS
Heating Block	Dri-Block, Techne
Histology camera	AxioCam MRc, Zeiss
Humidity chamber	Sandrest
Incubators	25°C: 4536, Forma Scientific 37°C humidified: MCO-20AIC, Sanyo
Microbiological safety cabinets (Class II)	Envair

Microscopes	Axioskop 2 Plus, Zeiss Observer D1, Zeiss
Microwave	NN-E442W, Panasonic
PCR machine	T3 Thermocycler, Biometra
pH meter	CD500, WPA
Pipettes	Pipetman, Gilson
Plate reader	Modulus Microplate, Turner Biosystems
Pressure cooker	Tendercook, Nordic Ware
Real time PCR machine	R-3000 Rotorgene, Corbett
Refrigeration	4°C: Silverline, LEC; PL167GWA, Proline -20°C: Scandinova -80°C: U410 Premium, New Brunswick Scientific
Spectrophotometer	ND-1000, NanoDrop
Stirrer	Stuart Scientific
Waterbath	Grant Instruments
Vortex	Whirlimixer, FSA Laboratory Supplies

Appendix 2.3 Recipes

Greiss Reagent	5.8% (v/v) H_3PO_4 1% (w/v) Sulfanilamide 0.1%(w/v) N-(1-Naphthyl)ethylenediamine dihydrochloride
Kanamycin agar	LB medium 1.5% (w/v) bacto-agar 30µg/mL kanamycin
Kanamycin medium	LB medium 30µg/mL kanamycin
LB medium (pH7.4)	1% (w/v) tryptone 0.5% (w/v) yeast extract 1% (w/v) NaCl
Paraformaldehyde (pH7.4)	PBS 4% (v/v) paraformaldehyde 1% (v/v) 1M NaOH
PBS pH 7.4	137mM NaCl 2.7mM KCl 4.3mM Na_2HPO_4 1.4mM KH_2PO_4
PBSA	PBS 1% (w/v) bovine serum albumin 0.1% (w/v) sodium azide

Permeablisation buffer	PBSA 0.1% (w/v) saponin
Peroxidase block	TBS 70% (v/v) methanol 3% (v/v) H_2O_2
Mowiol	1% (w/v) Mowiol 4-88 25% (v/v) Glycerol 50% (v/) 0.2N TrisHCl pH8.5
Sodium citrate antigen retrieval buffer (pH 6.0)	10mM $Na_3C_6H_5O_7.2H_2O$ 0.05% (v/v) Tween 20
Sulphuric/phosphoric acid	10% (v/v) H_2SO_4 30% (v/v) H_3PO_4
TBS (pH7.4)	0.8% (w/v) $NaCl_2$ 0.05% (w/v) KCl 0.3 % (w/v) Trisma base
Toluene Blue	1% (w/v) Toluene Blue 5% (v/v) methanol to dissolve

Appendix 2.4 Technique Development

Macrophage Culture

Bone marrow derived macrophages (BMDMϕ) were initially cultured as described by several authors (Qin *et al.*, 2007; Turnbull *et al.*, 2006), on tissue culture plastics in DMEM or RPMI, supplemented with 100U/ml penicillin and streptomycin, 1% L-Glutamine, 10% foetal calf serum and recombinant macrophage colony stimulatory factor (rM-CSF). According to the literature, cells were then removed from plastic with versene and downstream analysis or manipulation performed. However, it rapidly became evident that this method of culture was inappropriate, if not completely unsuccessful. Retrieval of BMDMϕ from tissue culture plastic using either versene or trypsin proved extremely difficult, with loss of the majority of viable cells, rendering further analysis impossible. Both plastic and growth medium required adjustment in order to obtain viable cultures of BMDMϕ in sufficient numbers for further analysis.

Tissue culture plastic

After limited success in establishing macrophage cultures using published methods, advice was sought from Dr Dave Sester and Prof. David Hume at the Roslin Institute, both of whom have considerable experience in macrophage culture and manipulation. It was recommended that BMDMϕ be grown on bacteriological dishes (Sterillin) as the tissue culture coating on Nunc brand plastics leads to extremely strong adherence of BMDMϕ and removal of viable cells in large numbers is highly unlikely. As such, BMDMϕ were then grown in uncoated 100mm square dishes and removed easily by washing with magnesium, calcium free PBS using a needle and syringe. Following optimisation of the growth medium, this allowed harvest of large quantities of

viable cells, which were then either reseeded for activation and infection, or harvested for FACS analysis or RNA extraction.

Growth medium optimisation

M-CSF is an essential growth factor required for outgrowth and maintenance of macrophage cultures (Metcalf, 1986; Tushinski *et al.*, 1982). rM-CSF is available from several suppliers, with R&D Systems and Peprotech being the most commonly used. As such, rM-CSF was purchased from Peprotech and titrated on freshly extracted bone marrow, starting with the manufacturer's recommended concentration of 1ng/ml. However, even at 10ng/ml, BMDMϕ were sparse on the plate, with no evidence of proliferation and many floating cells. rM-CSF purchased from R&D Systems was titrated in the same manner, yielding similar results (Figure 2.1a). This was not an inherent inability of bone marrow cells to respond to cytokine, as substantial BMDMϕ outgrowth was observed in response to 'in house' rM-CSF, a kind gift from Prof. David Hume for use as a positive control. As it was evident that commercial rM-CSF was ineffective at inducing macrophage outgrowth from bone marrow, at least at financially viable concentrations, an alternative source of growth factor was sought.

The murine fibroblast cell line, L929, is known to be a potent producer of M-CSF (Ladner *et al.*, 1988) and media supplemented with L929 supernatant has been frequently used in the past to grow macrophages. However, the inherent difficulty with this approach is the soup of cytokines and growth factors that are likely to be present in the supernatant, detailed analysis of which has never been published. However, macrophages would be exposed to a complex cytokine milieu in situ, rather than M-CSF in isolation and therefore, by comparing activated samples with controls exposed to supplemented medium only, this source of M-CSF was deemed appropriate and may bear some physiological relevance to the in vivo cytokine environment experienced by res-

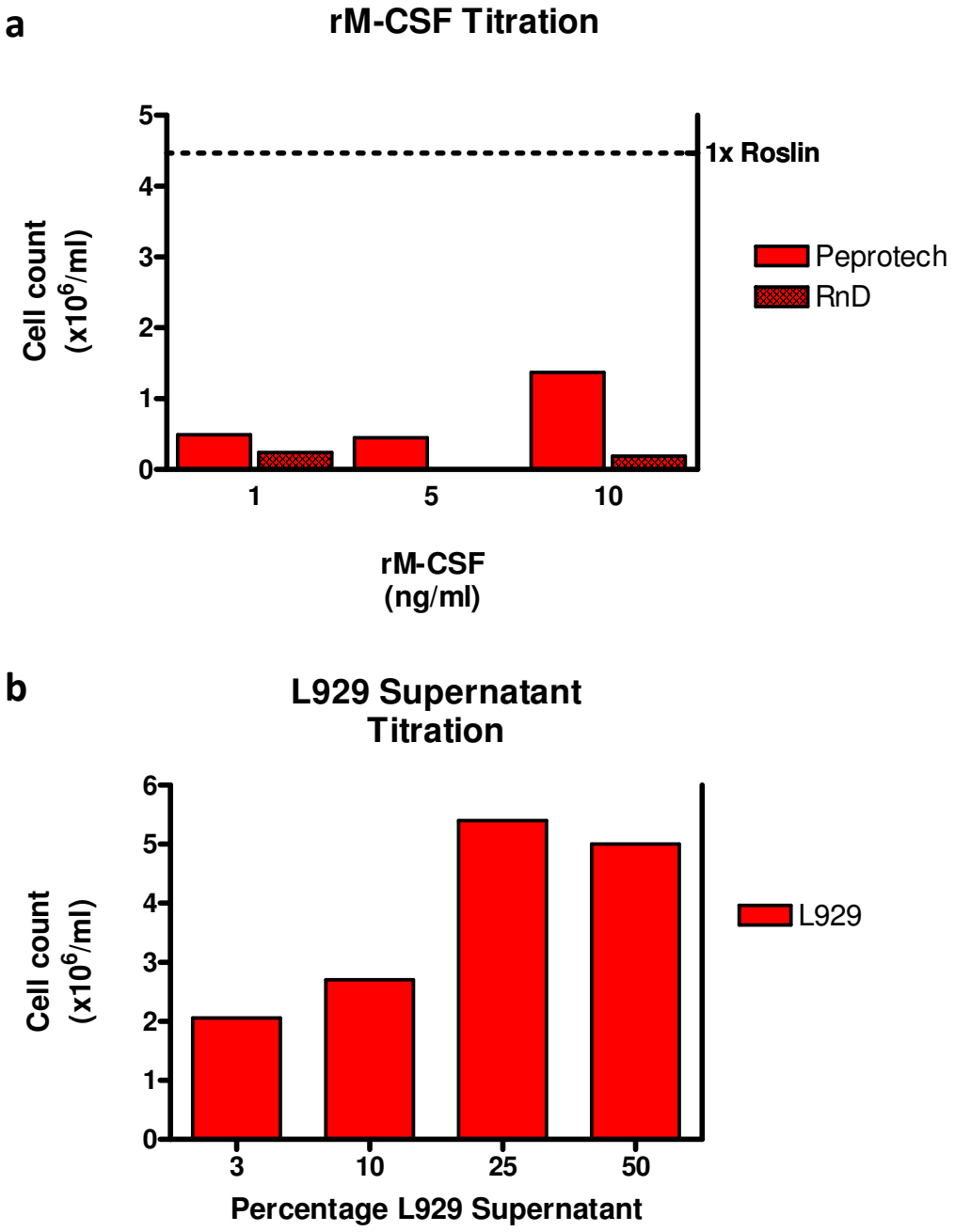

Figure 2.1 Titration of commercial and in house M-CSF.
RPMI media was supplemented with 10% foetal calf serum, 1% L-Glutamine and 100U/mL penicillin and streptomycin, along with a) commercially available rM-CSF from Peprotech or R&D Systems at 1, 5 or 10ng/ml. rM-CSF from the Roslin Institute was used at 1x concentration as a positive control (dotted line). b) RPMI was supplemented with 3, 10, 25 or 50% supernatant harvested from L929 murine fibroblast cells.

ident tissue macrophages. As such, RPMI supplemented with L929 supernatant was titrated (Figure 2.1b). Strong outgrowth of BMDMϕ was achieved with concentrations of supplemented media above 10% v/v. However, given the difficulties experienced establishing this system, the highest concentration of 50% L929 supernatant v/v was selected as optimal growth conditions for BMDMϕ in our laboratory.

Immunohistochemistry

Several unsuccessful attempts were made to stain for the macrophage marker F4/80 on paraffin wax embedded material. These tissues are unsuitable for fluorescent staining due to high levels of autofluorescence caused by this manner of processing. Therefore, colorimetric stains were investigated. As the lungs were inflated with 10% neutral buffered formalin, antigen retrieval was required to break cross linking of surface antigens. Citrate buffer at pH 6.0 was used for heat induced antigen retrieval, both by microwaving and by heating more gently in a water bath at 90^{o}C. As it was likely that F4/80 may be a fragile surface antigen, the process of dewaxing and rehydration through sequential alcohols may have caused damage which prevented the antibody from binding. Therefore, rehydration through decreasing concentrations of acetone was attempted. However, only very weakly positive antigen was detected. This was of no use as it would be overshadowed by strong viral staining when attempting to perform the dual stain. A biotinylated antibody was employed to add an amplification step to the protocol, but this too proved ineffective.

It was then decided to repeat the animal experiments and inflate lungs with OCT compound, followed by fast freezing and cutting of frozen sections. This effectively bypassed the damage caused by paraffin wax embedding and subsequent downstream processing, allowing staining with fluorescent antibodies. This resulted in strong positive staining with the biotinylated

F4/80 antibody, but also some non specific staining in the secondary antibody control slide. Further investigation indicated the presence of endogenous biotin activity in these sections. Attempts were made to block this with streptavidin solutions, but these large complexes also appeared to sterically hinder specific binding of antibody to the macrophages, which were also likely to possess endogenous biotin activity. A rat anti-mouse F4/80 antibody, which was previously shown to specifically detect macrophages by flow cytometry, was successfully employed on these frozen sections in conjunction with goat anti-rat Alexafluor 488. The ability of this antibody to detect macrophages by flow cytometry, and the strong staining obtained when used against RAW macrophages indicated that this antibody was highly specific for macrophages. Furthermore, when positive staining was compared to cell morphology, it appeared that this antibody successfully detected any macrophages present within the sections examined.

Once specificity of both the anti-macrophage and anti-influenza antibodies had been established, attempts were made to perform a dual stain for these markers. However, further problems ensued due to conflicting species specificities of secondary antibodies conjugated to particular Alexafluors that could be visualised by the confocal microscope. The goat anti-influenza virus was detected with a rabbit anti-goat Alexafluor 488, while the confocal microscope could visualise Alexafluors 488 and 546 in addition to the DAPI counterstain. However, it was not possible to purchase an Alexfluor 546 conjugated antibody without species conflictions and so a rabbit anti-rat Alexafluor 594 was purchased. Dr Trudi Gillespie at the IMPACT confocal facility was able to image this Alexafluor using a far red laser which gave a visible but less intense red emission, therefore enabling the dual stain for virus and macrophages within lung tissue to be performed. Although it may have been possible to purchase an anti-influenza virus antibody raised in an alternative species, at the time of development, the influenza virus stain was extremely reliable and so there was less inclination to change this unless

absolutely necessary. Furthermore, purchasing an anti-rat secondary antibody would benefit the laboratory as a whole more than altering the influenza stain, as many of the primaries used are raised in rat, in addition to saving on the cost involved in purchasing 3 new antibodies rather than the anti-rat Alexafluor only.

The results of failed immunohistochemistry experiments were assessed by microscopy but not photographed, either due to non specific staining or lack of signal.

Quantitative PCR

Selection of reference genes

Appropriate reference genes were required for normalisation of qPCR data. Appropriate reference genes should be stably expressed across the range of tissue types and infection or treatment models under investigation to provide a reliable standard to normalise RNA concentration against. The program NormFinder (available through Genex software) was utilised to select two housekeeping genes with the most stable expression across a panel of activated BMDMϕ. To do this, a standard curve for each of a panel of housekeeping genes (Table 2.7) was generated and a panel of samples run (Table 2.8).

Standard curves for each housekeeping gene were set up using high fidelity PCR products from genomic DNA, generated with PFU polymerase (NEB) and the primer pairs supplied in the Quantace Normalisation Gene Panel. These products were then gel purified using a Qiagen Gel Purification Kit. Concentration of the products was assessed using a Nanodrop spectrophotometer and copy number per microlitre calculated (Equation 2.1).

This DNA was then used in serial dilution for generation of standard curves, under the conditions recommended by the manufacturer (Table 2.9).

NormFinder then calculated the variability between samples, based on the point at which each crossed the threshold set in the standard curve, allowing selection of the most stably expressed genes as reference genes (Figure 2.2). The two genes with most stable expression were CNX and SDHA, and so these were carried forward as reference genes.

Optimisation of genes of interest

For each gene to be analysed, primer and $MgCl_2$ concentrations were optimised, along with annealing temperature to ensure optimal reaction conditions. iNOS is detailed here as a worked example of the optimisation procedure applied to each gene. Primer sequences for all genes are listed in Table 2.5.

Initially a panel of primer concentrations were tested with a constant concentration of $MgCl_2$ (2.5mM) in a 20µL reaction volume (Table 2.10). The optimal combination of forward and reverse primer concentrations was that which gave highest product yield with a narrow single peaked melt curve. Figure 2.3a depicts the product yield, showing that all concentrations of primers give a similar yield of product. However, some combinations result in fluorescent intensity achieving 100% at an earlier cycle, and therefore the most efficient was selected as the optimum combination of primer concentrations. For iNOS, this was 400nM forward, 500nM reverse primer (Figure 2.3e). A single peak was observed when the products were melted (Figure 2.3c), demonstrating that these primers were specific, and generated a single product. However, there was a small shoulder to the left of this melt curve due to suboptimal primer concentrations. When conditions are fully optimised, this shoulder will no longer be present.

Abbreviation	Gene
CNX	Calnexin
SSDHA	Succinate dehydrogenase complex, subunit A
GAPDH	Glyceraldehyde-3-phosphate dehydrogenase
G ACTIN	Gamma actin, cytoplasmic
RN18s	18S Ribsomal RNA
PGK	Phosphoglycerate kinase 1
UBQC	Ubiquitin C
RPL13A	Ribosomal protein L13a
B2MG	Beta-2 microglobulin E

Table 2.7 Panel of qPCR reference genes
Gene panel assessed for selection of reference genes to be used for normalisation of qPCR data.

Tissue	Timepoint	Activation
BMDMϕ	Day 7	M-CSF
BMDMϕ	Day 8	M-CSF + IFNγ
BMDMϕ	Day 8	M-CSF + IL-4
BMDMϕ	Day 8	M-CSF + IL-13
BMDMϕ	Day 6	M-CSF
BMDMϕ	Day 7	M-CSF + IFNγ
BMDMϕ	Day 7	M-CSF + IL-4

Table 2.8 Panel of stimulated BMDMφ assessed for selection of stable reference genes.

Step	Temp	Time
Enzyme activation	95°C	10min
Anneal	95°C	15sec
Extend	55°C	20sec
Denature	72°C	20sec

Table 2.9 Reaction conditions for Quantace Normalisation Gene Panel primer pairs, performed at 2.5mM $MgCl_2$.

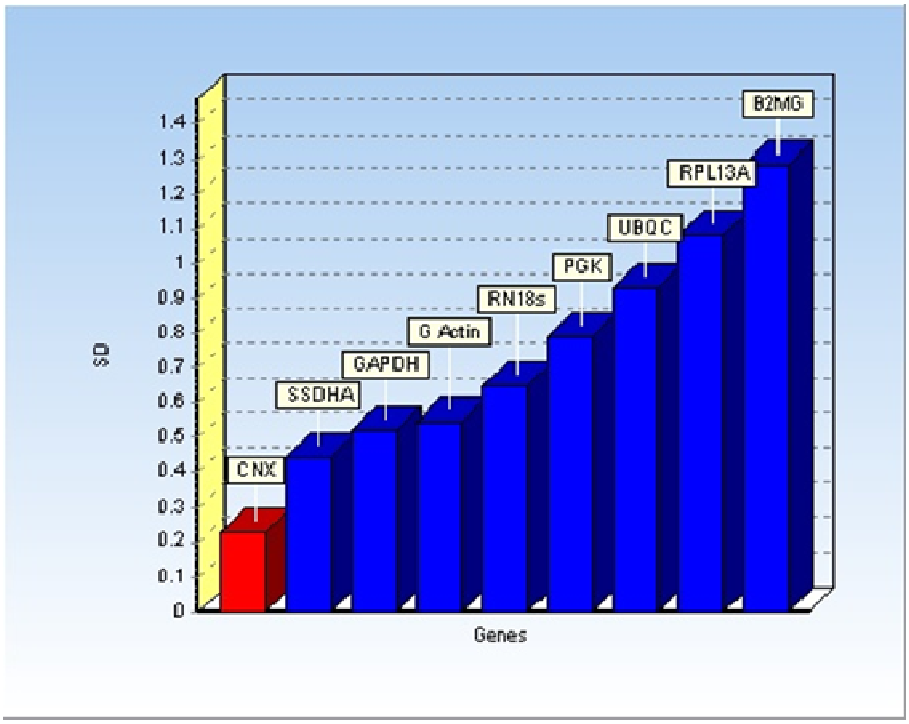

Figure 2.2 NormFinder analysis of reference gene expression across cell panel.
Standard deviation of Ct values are assessed across the range of cells tested and those genes with least variation are selected as reference genes with most stable expression.

Forward	Reverse	Forward	Reverse
300	300	500	300
300	400	500	400
300	500	500	500
300	600	500	600
400	300	600	300
400	400	600	400
400	500	600	500
400	600	600	600

Table 2.10 Primer concentration matrix.
Optimum primer concentration was selected by testing each combination of forward and reverse primer concentrations.

Tube	Concentration
1-3	2.0mM
4-6	2.5mM
7-9	3.0mM
10-12	3.5mM

Table 2.11 $MgCl_2$ concentration optimisation.
Optimum concentration was selected in combination with the previously established optimum primer concentration.

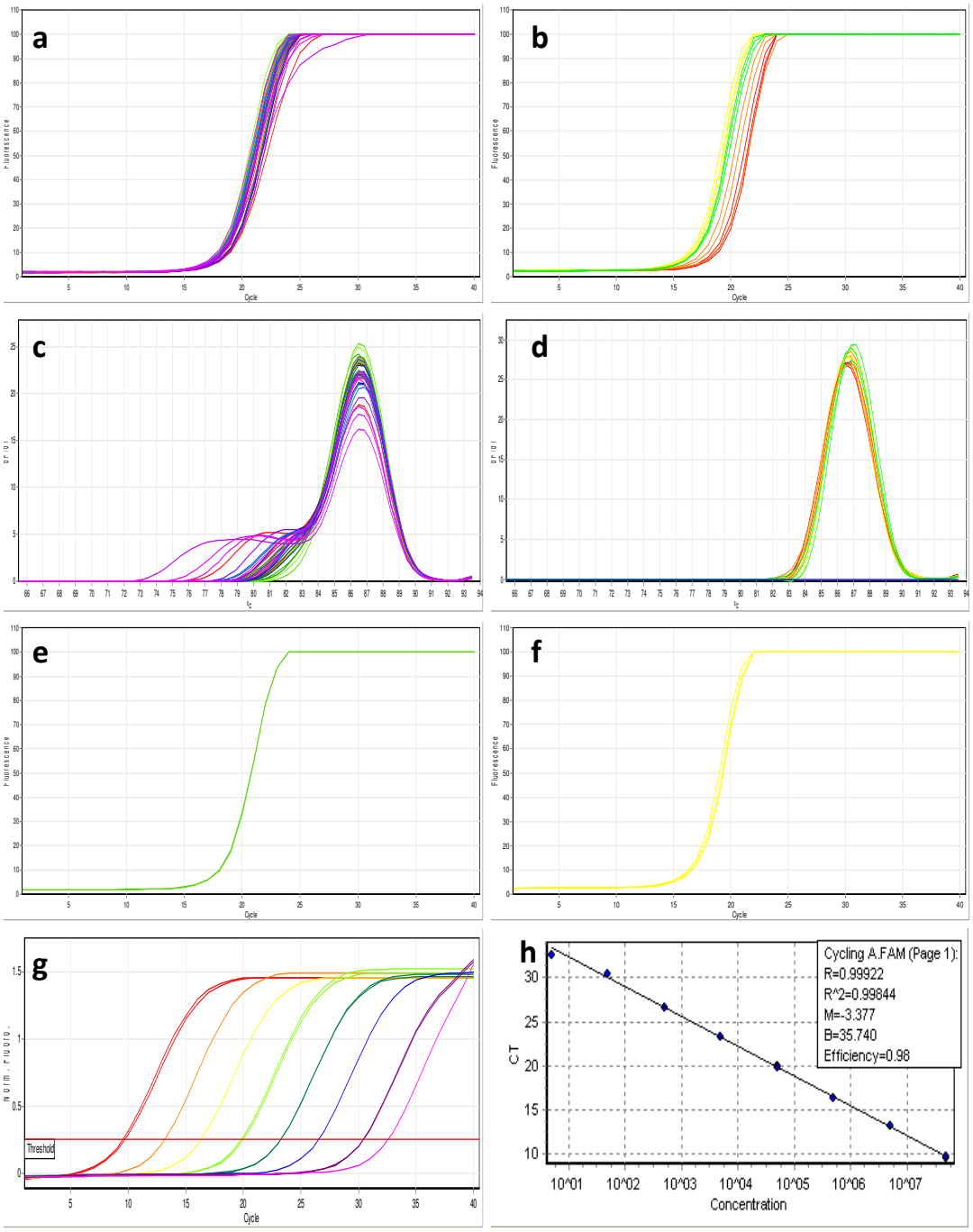

Figure 2.3 qPCR optimisation for iNOS.
Primer concentration was optimised, by assessment of a) product yield and c) melt curve, followed by selection of the combination of concentrations that gave highest product yield with a clean melt curve (e). $MgCl_2$ was then assessed in the same manner (b, d & f). A standard curve was performed (g) resulting in an efficient reaction under these conditions (h).

Once optimal primer concentration had been established, $MgCl_2$ concentration was addressed. Increasing $MgCl_2$ concentration enhances specific binding. Primers had been carefully designed to minimise primer dimer and cross dimers, so only a narrow range of $MgCl_2$ concentrations were assessed (Table 2.11).

$MgCl_2$ was optimised in the presence of the previously established primer concentration, again with product yield and melt curve being assessed. In the case of iNOS, and the majority of genes investigated, a concentration of 3.0mM (Figure 2.3f) most rapidly achieved 100% fluorescence (Figure 2.3b) with a single peaked melt curve (Figure 2.3d). The melt curve shoulder observed in Figure 2.3c was absent following primer optimisation (Figure 2.3e), indicating appropriate primer concentrations had indeed been selected. Finally, a standard curve was performed to ensure an efficient reaction could be obtained under the newly optimised conditions (Figure 2.3g&h).

Primer pairs for each gene of interest were subjected to this optimisation process, in addition to which, annealing temperature was altered if necessary. Fully optimised conditions are detailed in Table 2.6. Despite detecting the template used for generation of a standard curve, the initial set of IL-12p40 primers failed to detect product in samples and so these primers were redesigned using Primer3 and NetPrimer software, resulting in successful detection of IL-12p40 in samples.

Optimisation of cDNA dilutions

Establishment of a suitable dilution of cDNA was required to ensure the most reliable results were obtained. If the cDNA used is too concentrated or too dilute, this can affect the quality of the reaction. This must be balanced against finding a suitable dilution to give sufficient quantities of cDNA to complete reactions for all genes of interest.

cDNA was generated from BMDMϕ exposed to M-CSF alone, IFNγ or IL-4 in vitro, along with mock and virus infected lung homogenates. Samples were pooled by activation group before undergoing serial dilution, beginning at 1:10 and continuing to 1:50. A standard curve for each gene of interest was generated from the cloned template material as described in Chapter 2.12.1 to obtain a threshold to apply to the pooled samples. The serial dilutions of cDNA were run under the appropriate conditions for each gene as described in Table 2.6 and the point at which each dilution crossed the threshold (Ct value) was plotted against dilution (Figure 2.4). A suitable common dilution (1:20) was selected from the straight line region of these plots.

Statistical analysis

Statistical analysis was performed using the software package R (R Foundation for Statistical Computing). Linear mixed effect models were applied to assess differences in mean relative gene expression between activation and infection groups, as well as between Sv129 and IFNγR$^{-/-}$ backgrounds for survival, infection rates and relative gene expression.

This type of model incorporates what are described as 'fixed' and 'random' effects. A fixed effect is a variable which alters the mean of a group, allowing comparisons between groups, or in other words, generates informative data, for example cytokine treatment. A random effect is one which influences the variation within a dataset and is generally uninformative. For example, mice within the same treatment group will have some variation but the difference between individual mice within a group is not of interest when investigating the differences between treatment groups. However, although not inherently of interest, this effect must still be taken into account (Crawley, 2007).

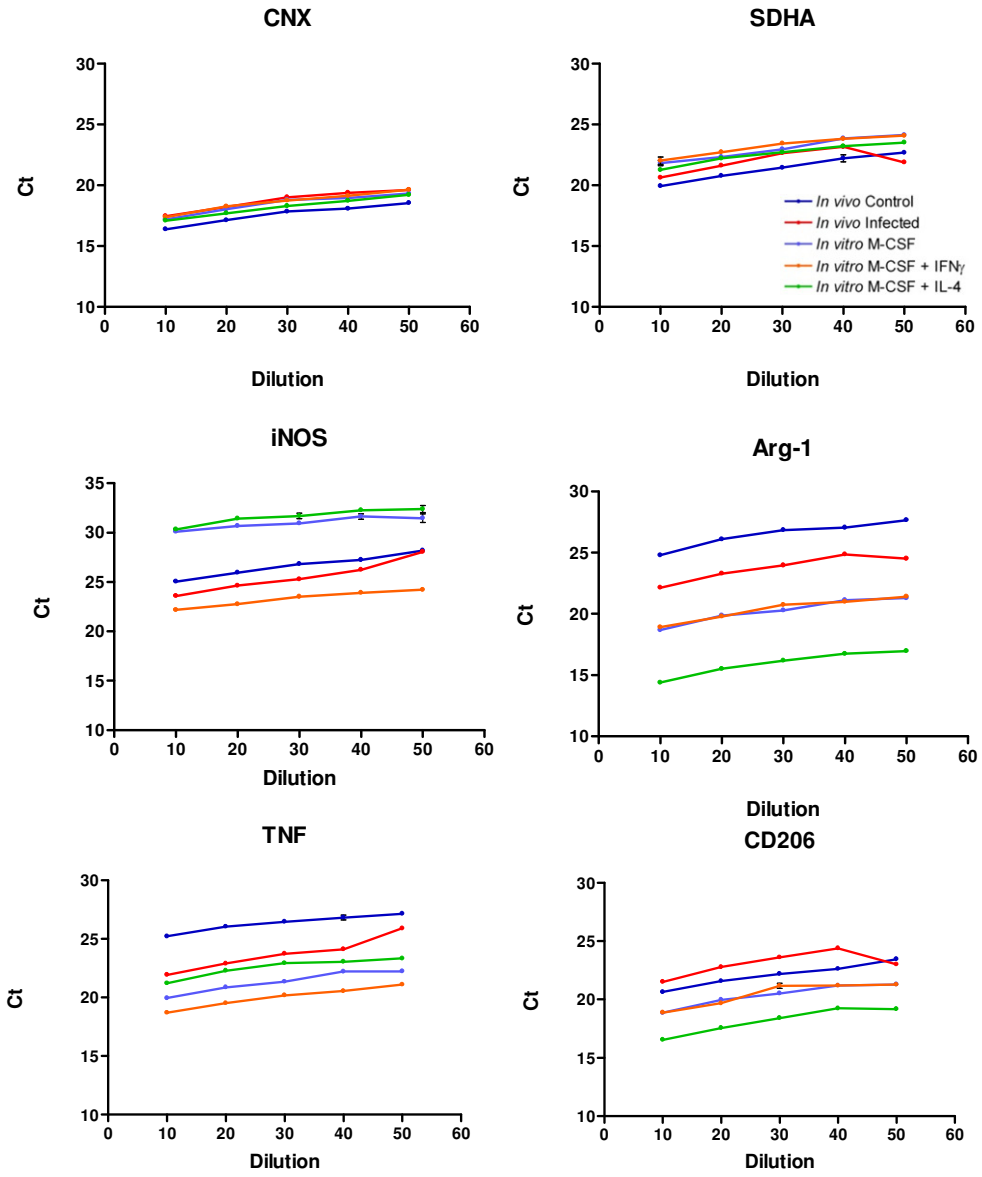

Figure 2.4 Selection of optimal cDNA concentration.
Samples were pooled by activation group and diluted prior to performing Q-PCR for genes of interest. Lowest common dilution within the straightest portion of the graph for each gene was selected (1:20).

In this section, development of the model will be outlined fully, using in vitro generated relative gene expression data for iNOS at the 48 hour timepoint (Chapter 4.2.1) as a worked example of this statistical analysis method. This shall begin with an introduction to the factors under investigation, followed by basic analysis of each factor in turn. Finally, all factors will be incorporated together, taking reverse transcription efficiency (RT) and repeated measures from the same animal (mouse effect) into account in the final full model. Statistics presented in results chapters are those generated from the full linear mixed effect model.

Factors under investigation

The experiments performed aimed to establish whether activation with IFNγ or IL-4 led to different responses to infection with influenza virus A/WSN/33, and whether this was different between the two strains of mice being studied. In order to do this, bone marrow from each mouse was split into six groups;

M-CSF alone
M-CSF + IFNγ
M-CSF + IL-4
M-CSF + WSN
M-CSF + IFNγ + WSN
M-CSF + IL-4 + WSN

Therefore each individual animal appeared in every group, introducing repeated measures to the sampling process. This allowed comparison of the same mice for differing cytokine treatments and infection (fixed effects) but also meant that the inherent variations between individual mice (random effect) must be taken into account, ie accounting for a mouse that may be a consistently low cytokine producer, but follows the same trend as the rest of the population sampled.

It was also important to discover whether any interactions existed between the factors under investigation, for example is response to virus in one strain of mouse dependent on cytokine treatment? Interactions will be discussed in subsequent sections.

Therefore the factors under investigation were strain of mouse, cytokine treatment and infection status, each of which yielding informative data that affects the mean of each group, and so were treated as fixed effects. However, these factors were additionally influenced by differing reverse transcription efficiencies (RT effect), which also had to be taken into account as a fixed effect. As previously described, the repeated measures from individual mice introduced random variation into the dataset and therefore mouse effect was treated as a random effect, and ultimately led to use of linear mixed effect models for this analysis (Crawley, 2007).

Single factor analysis

In order for the data to be analysed successfully, it was first compiled into one spreadsheet, with each factor heading a column. The dataset was created, manipulated to order the factors, exclude missing values and named (eg Data 1). Data were expressed as gene expression relative to the M-CSF alone control group, so this group had already been taken into account prior to analysis and was therefore excluded from the analysis. This approach allowed for initial investigation of each factor in isolation, prior to assessment of any other effects or interactions.

A one way ANOVA was performed for each factor (RT, Figure 2.5a; strain, Figure 2.5b; cytokine treatment, Figure 2.5c; infection status, Figure 2.5d) and the distribution of the residuals was checked for normality and followed by log transformation if necessary. This was required for the iNOS example described here. Each one way ANOVA generated an output indicating whether there was

a statistical difference between groups independent of any other factor. For example, there was a significant difference between Sv129 and IFNγR$^{-/-}$ BMDMϕ in their ability to express iNOS ($p<0.0001$) irrespective of infection or cytokine treatment (Figure 2.5e, Figure 2.5b).

As each factor was assessed in isolation by one way ANOVA, the influence of one factor on another was not addressed and required further investigation. There were clear differences between reverse transcription reactions, with batch 3 demonstrating a higher median than the previous two (Figure 2.5a).

The variation in RT would influence the remaining factors under investigation unless taken into account prior to further analysis and so must be incorporated as a fixed effect. Mouse effect was not included at this stage of the analysis.

Integration of reverse transcription as a fixed effect

In order to allow comparison between samples reverse transcribed at different times, RT effect was taken into account as a fixed effect, prior to assessing the other factors. To do this, a new dataset was created from the residuals of the RT factor column following the initial ANOVA. A residual is the difference between an individual sample value and the mean value of the group. Therefore, the residuals carried forward into the next stage of the analysis represent the variation in the data that remains after correcting for RT effect.

The residuals were plotted on a boxplot, followed by ANOVA for the remaining factors taking RT into account. This means that the effect of strain on iNOS expression could be interpreted, having already taken into account the effect of RT (Figure 2.6a & b). The output obtained demonstrated that although there was a significant difference between reverse transcriptions ($p<0.001$; Figure 2.6c, 'RT'), there was also a significant difference between Sv129 and IFNγR$^{-/-}$

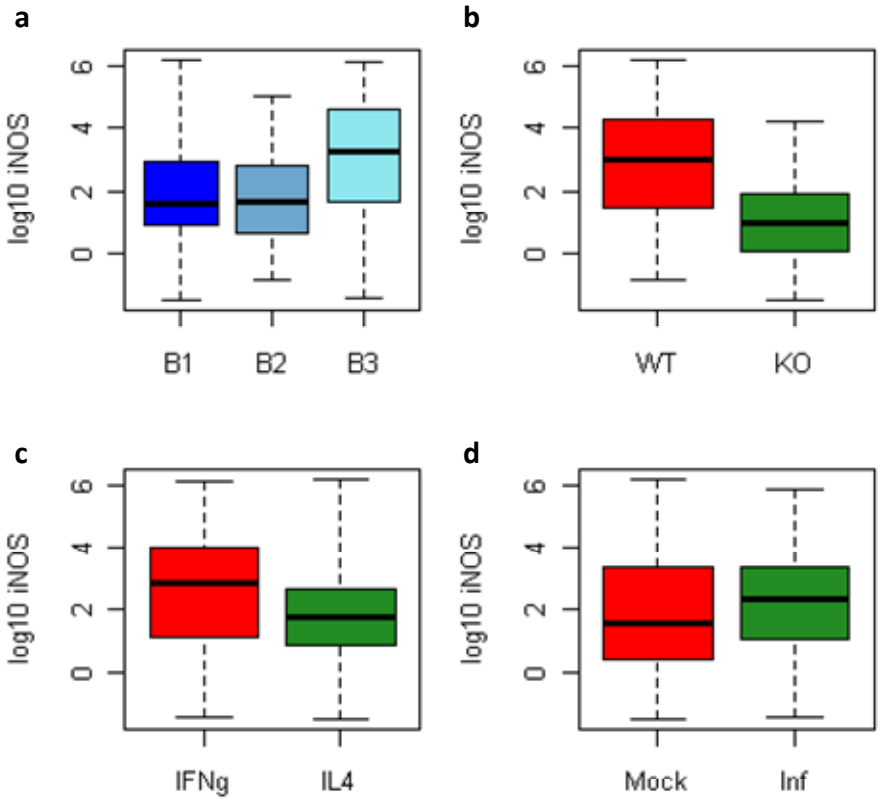

e

```
summary(aov(log10iNOS~Strain,data=Data1)

                Df        P
Strain          1         <0.0001***
Residuals       119
```

Figure 2.5 Factors under investigation.
Reverse transcription batch (a); strain of mouse (b); cytokine treatment (c) and infection status (d) were plotted independently of each other, demonstrating differences in mRNA expression within each factor, but not taking into account the influences of the other factors.
e) Example of R command and readout for ANOVA for mouse strain data. R was given the summary of ANOVA command (aov) which resulted in the output detailing a significant difference in iNOS expression between Sv129 and IFNγR$^{-/-}$ mice with 119 residuals remaining. (Df = degrees of freedom)

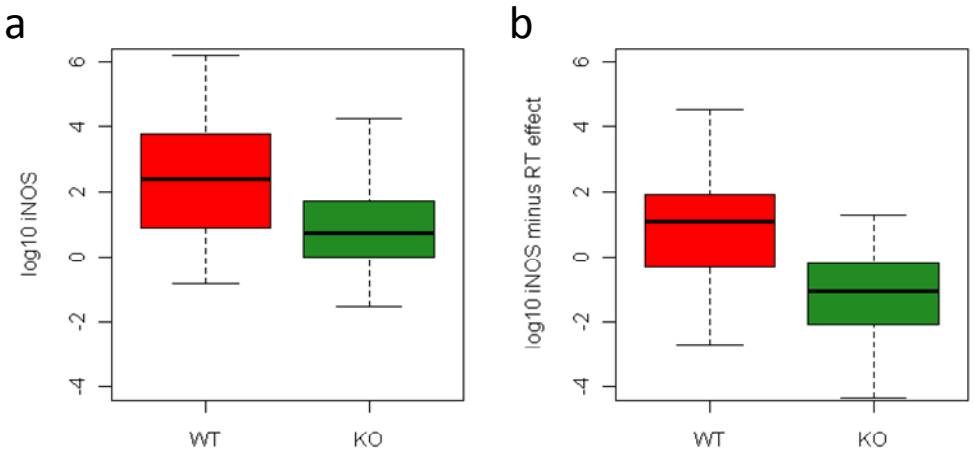

c

```
summary(aov(log10iNOS~RT+Strain,data=Data1))

             Df        P
RT           2      <0.001
Strain       1      <0.0001
Residuals    117
```

Figure 2.6 Example of data for mouse strain, taking RT effect into account.
a) ANOVA of strain in Data1 prior to accounting for RT effect, as plotted in Fig 2.5b
b) Residuals following ANOVA of RT factor were used to plot differences in iNOS mRNA expression between strains of mice, taking RT effect into account.
c) ANOVA of iNOS mRNA expression between strains of mice, taking RT effect into account, indicates a significant difference between Sv129 and IFNγR$^{-/-}$ BMDMϕ.

BMDMϕ in their ability to express iNOS irrespective of cytokine treatment or infection ($p<0.0001$; Figure 2.6c, 'Strain'). Genetic background of the BMDMϕ was significant prior to taking RT into account (Figure 2.5e & Figure 2.6a), but by incorporating RT as a fixed effect in this manner, the effect of this variable was removed when assessing the effect of the remaining variables, allowing more accurate interpretation of the data.

Single cytokine analysis

Having integrated RT effect into the model as a fixed effect, further analysis of the remaining factors was undertaken to determine the effect of cytokine treatment and infection on the two strains of mice. This involved splitting the original dataset, Data 1, into subsets for the two cytokines under investigation, IFNγ and IL-4. The remaining factors, namely strain and infection status, within each subset were assessed and any interaction between these factors was investigated (Figure 2.7a). This demonstrated that, as expected, genetic background of the BMDMϕ led to a significant difference in iNOS expression following stimulation with IFNγ, having taken RT into account ($p<0.0001$; Figure 2.7a, 'Strain'). It was also apparent that there was no significant difference between mock and infected BMDMϕ in iNOS expression following IFNγ stimulation, or in other words, infection failed to significantly upregulate iNOS expression over that observed in response to IFNγ alone ($p=0.67$; Figure 2.7a, 'MockInf').

Analysis of interactions between factors answers the following question: is response to virus influenced by genetic background, following exposure to IFNγ or IL-4? If there was a significant interaction between strain and infection status for the IFNγ stimulated subset, this would indicate that the relationship between mock and infected Sv129 BMDMϕ for iNOS expression was different to the relationship between mock and infected IFNγR$^{-/-}$ counterparts, in the presence of IFNγ. If the interaction between strain and infection status was not

significant, then this suggests that both strains respond in a similar manner to infection with regards to iNOS expression following stimulation with IFNγ. What was actually observed was that neither strain significantly upregulated iNOS expression in response to infection over that seen for IFNγ alone, therefore there was no interaction between strain and infection ($p=0.29$; Figure 2.7a, Strain:MockInf), but that IFNγR$^{-/-}$ BMDMϕ showed significantly lower iNOS expression than their wildtype counterparts ($p<0.0001$, Figure 2.7a 'Strain' & c). The interaction was excluded and the model repeated to ensure that the interaction did not mask factor effects (Figure 2.7b). Exclusion of the interaction did not alter the degree of significance observed.

Integration of mouse as a random effect

As yet, individual mouse effect had not been taken into account, and so was incorporated into the model as a random effect. This was because each individual mouse was present in every group, giving rise to repeated measures. The differences between individual mice were not of interest for comparisons between groups but must be accounted for due to the variation they introduced into the dataset. Most statistical models assume independence of data but as repeated measures are present in this dataset, this assumption is incorrect. Therefore, the repeated measures must be explicitly incorporated into the analysis by means of the linear mixed effect model. The full model was run for each cytokine subset, taking RT effect into account as a fixed effect and mouse effect into account as a random effect, along with assessment of interactions between the remaining factors (Figure 2.8) although only the IFNγ stimulated subset is discussed here.

a

```
 summary(aov(log10iNOS~RT+Strain+MockInf+Strain:MockInf,
          data=Data1,subset=Ck=="IFNg"))

                    Df        P
RT                  2         0.05
Strain              1         <0.0001
MockInf             1         0.67
Strain:MockInf      1         0.29
Residuals           55
```

b

```
   summary(aov(log10iNOS~RT+Strain+MockInf,data=Data1,
          subset=Ck=="IFNg"))

                    Df        P
RT                  2         <0.05
Strain              1         <0.0001
MockInf             1         0.67
Residuals           56
```

c

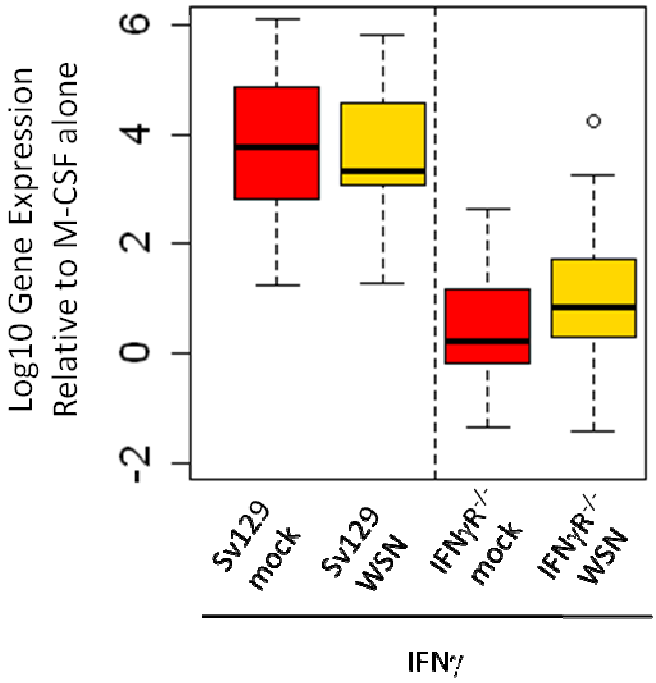

Figure 2.7 ANOVA for IFNγ-activated subset for mouse strain and infection status.
a) ANOVA for the IFNγ stimulated subset of data demonstrated a significant difference between Sv129 and IFNγR$^{-/-}$ mice in response to IFNγ, but not in response to infection. There was no significant interaction between infection status and strain of mouse.
b) Excluding the interaction from the analysis did not alter the degree of significance observed previously for the factors investigated.
c) Relative iNOS expression minus RT effect demonstrating differences between Sv129 and IFNγR$^{-/-}$ BMDMϕ following stimulation with IFNγ ($p<0.0001$) and that neither strain significantly upregulate expression upon infection ($p=0.67$). o, outlier.
As both strains respond in the same manner to infection, ie by failing to further upregulate iNOS expression, there is no significant interaction between strain and infection status ($p=0.29$).

This analysis demonstrated that iNOS mRNA expression was significantly different in Sv129 BMDMϕ compared to IFNγR$^{-/-}$ BMDMϕ upon activation with IFNγ, as would be expected ($p<0.0001$; Figure 2.8a, 'Strain'). Furthermore, this analysis also showed that there was no significant difference in iNOS mRNA expression between mock and virus infected BMDMϕ in the presence of IFNγ ($p=0.52$; Figure 2.8a, 'MockInf'), and that there was no interaction between the two factors ($p=0.49$; Figure 2.8a, 'MockInf:Strain').

However, this did not allow investigation of differences between strains following polarisation and infection, ie, to answer the question 'is there a difference between classically and alternatively activated infected IFNγR$^{-/-}$ BMDMϕ and wildtype counterparts?' required further analysis.

Full mixed effect model

Finally, the dataset was once again assessed as a whole to investigate interactions between cytokine treatment and mouse strain, or cytokine treatment and infection status, with both RT and mouse effect taken into account (Figure 2.9). As previously indicated (Figure 2.5) there were significant differences in iNOS mRNA expression between mock and virus infected BMDMϕ, ie overall, the mean iNOS expression for infected cells (classical and alternatively activated BMDMϕ of both strains together) was significantly higher than for uninfected cells ($p<0.01$; Figure 2.9a 'MockInf'). There were also significant differences between Sv129 and IFNγR$^{-/-}$ BMDMϕ ($p<0.0001$; Figure 2.9a, 'Strain'), and between IFNγ and IL-4 activated BMDMϕ ($p<0.0001$; Figure 2.9a, 'Ck'), independently of any other factor, as plotted in Figure 2.5. Obviously this was not particularly useful as genetic background and activation group must be separated, and so interactions between these factors were investigated. As previously discussed, there was no interaction between strain and infection in the presence of IFNγ. However, significant interactions were evident between infection status and cytokine treatment ($p=0.001$; Figure

a

```
    anova(lme(log10iNOS~RT+MockInf+Strain+MockInf:Strain,
      data=Data1,subset=Ck=="IFNg",random=~1|Mouse.ID))

                      Df   P
RT                    2    0.09
MockInf               1    0.52
Strain                1    <0.0001
MockInf:Strain        1    0.49
```

b

```
anova(lme(log10iNOS~RT+MockInf+Strain,data=Data1,subset=Ck==
                "IFNg",random=~1|Mouse.ID))

                      DF    P
RT                    2    0.10
MockInf               1    0.52
Strain                1    <0.0001
```

c

```
    anova(lme(log10iNOS~RT+MockInf+Strain+MockInf:Strain,
      data=Data1,subset=Ck=="IL-4",random=~1|Mouse.ID))

                      Df   P
RT                    2    <0.01
MockInf               1    <0.01
Strain                1    <0.05
MockInf:Strain        1    0.64
```

d

```
anova(lme(log10iNOS~RT+MockInf+Strain,data=Data1,subset=Ck==
                "IL-4",random=~1|Mouse.ID))

                      DF    P
RT                    2    <0.01
MockInf               1    0.01
Strain                1    0.05
```

Figure 2.8 Inclusion of mouse as random effect.
Mouse effect was integrated into the model as a random effect using the mixed effect model command 'lme' (a), which did not alter the significance of results obtained in Fig. 3.7. Exclusion of the interaction between infection status and mouse strain (b) did not affect the significance of the factors investigated. The model was repeated for the IL-4 stimulated subset (c & d).

Figure **2.9**a, 'MockInf:Ck'), or in other words, initial cytokine treatment of BMDMϕ had a significant effect on response to virus infection in both strains. Similarly, mouse strain and cytokine treatment showed a significant interaction ($p<0.0001$; Figure 2.9a 'Strain:Ck'), or rather that response of BMDMϕ to cytokine was influenced by genetic background.

Taken together, these interactions indicate that IFNγR$^{-/-}$ BMDMϕ respond differently with regards to iNOS expression than do Sv129 cells in the presence of IFNγ, but not IL-4 (Figure 2.9a; 'Strain:Ck' & b) and that although IFNγ treated IFNγR$^{-/-}$ BMDMϕ show lower iNOS expression than their wildtype counterparts ($p<0.0001$; Figure 2.9a, 'Strain' & Figure 2.9b), infection does not significantly further increase expression in either strain ($p=0.49$; Figure 2.8a, 'MockInf:Strain' & Figure 2.9b). However, in the presence of IL-4, both strains demonstrate upregulated iNOS expression following infection ($p<0.05$; Figure 2.8c 'Strain' & Figure 2.9b), but as this meant that both strains responded in a similar manner to virus, there was again no interaction between strain and infection status with regards to iNOS expression ($p=0.64$, Figure 2.8c, 'MockInf:Strain'). The final interaction to be interpreted was that of infection status and cytokine, or in other words, does inital cytokine treatment affect response to virus? This interaction was statistically significant ($p=0.001$; Figure 2.9a, 'MockInf:Ck'), indicating that iNOS expression is different between classical and alternatively activated BMDMϕ following infection.

a

```
anova(lme(log10iNOS~RT+MockInf+Strain+Ck+
MockInf:Strain+MockInf:Ck+Strain:Ck,data=Data1,random=~1|Mouse
                                .ID))

                        Df          P
RT                      2           0.05
MockInf                 1           0.01
Strain                  1           <0.0001
Ck                      1           <0.0001
MockInf:Strain          1           0.40
MockInf:Ck              1           0.001
Strain:Ck               1           <0.0001
```

b

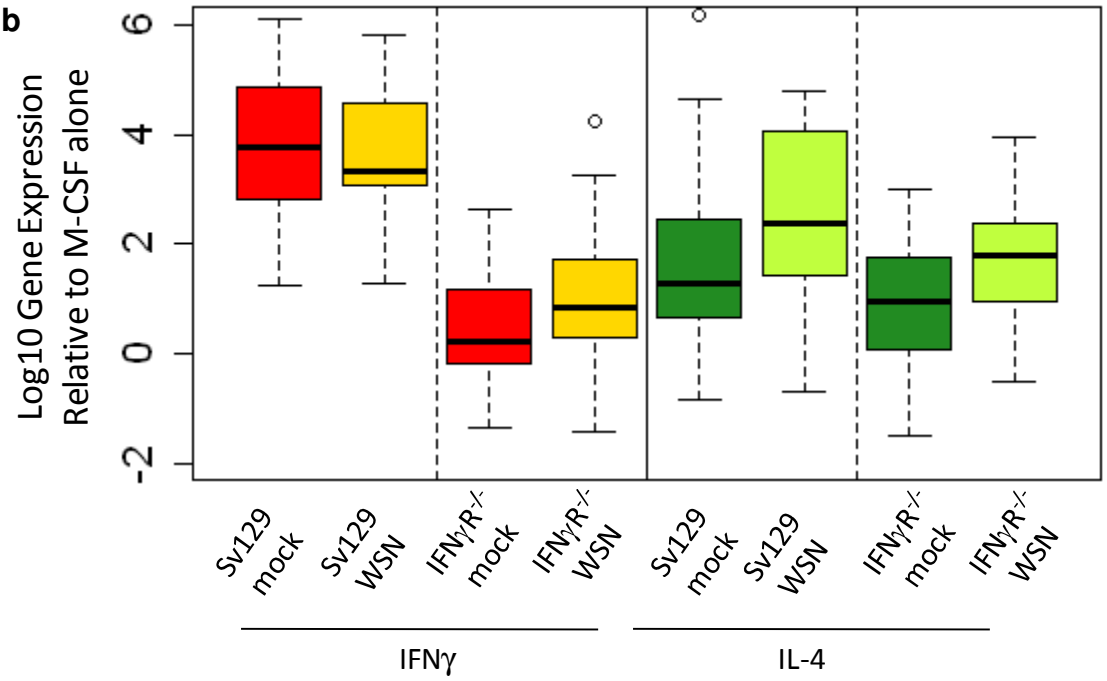

Figure 2.9 Full mixed effect model for in vitro iNOS mRNA expression.
a) Full mixed effect model, taking RT and mouse effects into account as a fixed and random effect respectively, followed by investigation of factors as fixed effects and interactions between factors.
b) Boxplot output of whole data for *in vitro* iNOS mRNA expression, demonstrating differential iNOS expression in a factor dependent manner. o, outlier.
This data is discussed fully in the context of other genes in Chapter 4.

In terms of statistical interpretation with regards to iNOS expression, virus infected IFNγ stimulated BMDMϕ are not different from mock infected IFNγ stimulated BMDMϕ, but virus infected IL-4 stimulated BMDMϕ are different from mock infected IL-4 stimulated BMDMϕ, indicated by the significant 'MockInf:Ck' interaction. IFNγR$^{-/-}$ BMDMϕ do not respond to IFNγ treatment, while Sv129 do but both strains respond similarly to IL-4, and so the 'Strain:Ck' interaction is significant. Infected BMDMϕ of either strain do not respond differently to mock BMDMϕ in the presence of either cytokine, which was established within single cytokine subsets where the 'MockInf:Strain' interaction is not significant. However, as the 'MockInf:Ck' and 'Strain:Ck' interactions are significant, this shows that Sv129 and IFNγR$^{-/-}$ BMDMϕ respond differently to cytokine treatment and that cytokine treatment influences response to infection, so it can therefore be inferred that there is a difference in iNOS expression between classically and alternatively activated Sv129 BMDMϕ and identically treated IFNγR$^{-/-}$ counterparts following infection.

Exclusion of the non-significant interaction (MockInf:Strain) did not affect the significance of any other. These data will be presented fully, in their proper context in Chapter 4.

This procedure was applied to all genes investigated both in vitro and in vivo, while a slightly modified method excluding RT effect was applied to the survival and infection data in Chapter 5.1.1.

3 In vitro infection of bone marrow derived macrophages

Infection with influenza virus leads to a classical proinflammatory response from macrophages and other cells of the immune system, resulting in elevated levels of inflammatory mediators which can be detrimental to the host, resulting in cytokine storms and organ failure. It has previously been shown that reducing infiltration of dendritic cells and macrophages during influenza infection leads to ameliorated disease (Aldridge *et al.*, 2009; Herold *et al.*, 2008), most likely due to lower levels of inflammatory mediators such as iNOS and TNFα in the lung. It has also been shown that the T_H1 or T_H2 bias of C57Bl/6 and BALB/c mice respectively results in differing responses to some pathogens. A T_H2 response is essential for expulsion of helminth worms in the BALB/c mouse (Else *et al.*, 1994), but the ability of C57Bl/6 mice to mount an efficient local inflammatory response affords protection from bacterial infection and sepsis (Watanabe *et al.*, 2004).

Disruption of genes encoding receptors for key mediators which influence the T_H1 or T_H2 bias of the immune system, IFNγ and IL-4 respectively, results in a skewed cytokine response. This project sought to identify the role that altering the cytokine profile produced by macrophages has on influenza virus infection. These preliminary experiments aim to establish and optimise the experimental conditions and procedures that will be used to profile the response of BMDMϕ from 129SvEv (Sv129), IFNγR$^{-/-}$, BALB/c and IL-4R$^{-/-}$ mice to influenza virus by investigating BMDMϕ responses from a small number of animals. As such, no statistical analysis will be carried out.

3.1 Characterisation of polarised bone marrow derived macrophages

Macrophages have been experimentally infected with influenza virus in vitro, with differing efficiency depending on the strain of virus (Tate *et al.*, 2010c) and the manner of macrophage isolation (Rodgers & Mims, 1981). However, the macrophage response to influenza virus in the Sv129 strain of mice has not been previously reported in the literature. Similarly, infection of IFNγR$^{-/-}$ macrophages on this genetic background requires characterisation in vitro.

3.1.1 Characterisation of the bone marrow derived macrophage population

Macrophages were generated from Sv129 mouse bone marrow as described in Chapter 2.2.4. After 7 days culture with M-CSF, mature BMDMϕ were characterised by flow cytometry (Figure 3.1). BMDMϕ were assessed for macrophage markers F4/80 and CD11b, isotype controls and secondary antibody alone were included to control for non-specific binding and fluorescence. Greater than 90% of cells stained positive for F4/80 and CD11b (Table 3.1), confirming that culture of bone marrow cells with M-CSF for 7 days gives rise to a population of macrophages.

3.1.2 Generation of classical and alternatively activated macrophages

Sv129 BMDMϕ were harvested, counted and reseeded followed by culture with activating cytokines for 16 hours as described in Chapter 2.2.4. Figure 3.2 depicts the experimental procedure followed for generation and infection of polarised macrophages. Both IFNγ and IL-4 were titrated to determine the optimal activating concentration to achieve polarised BMDMϕ (Figure 3.3).

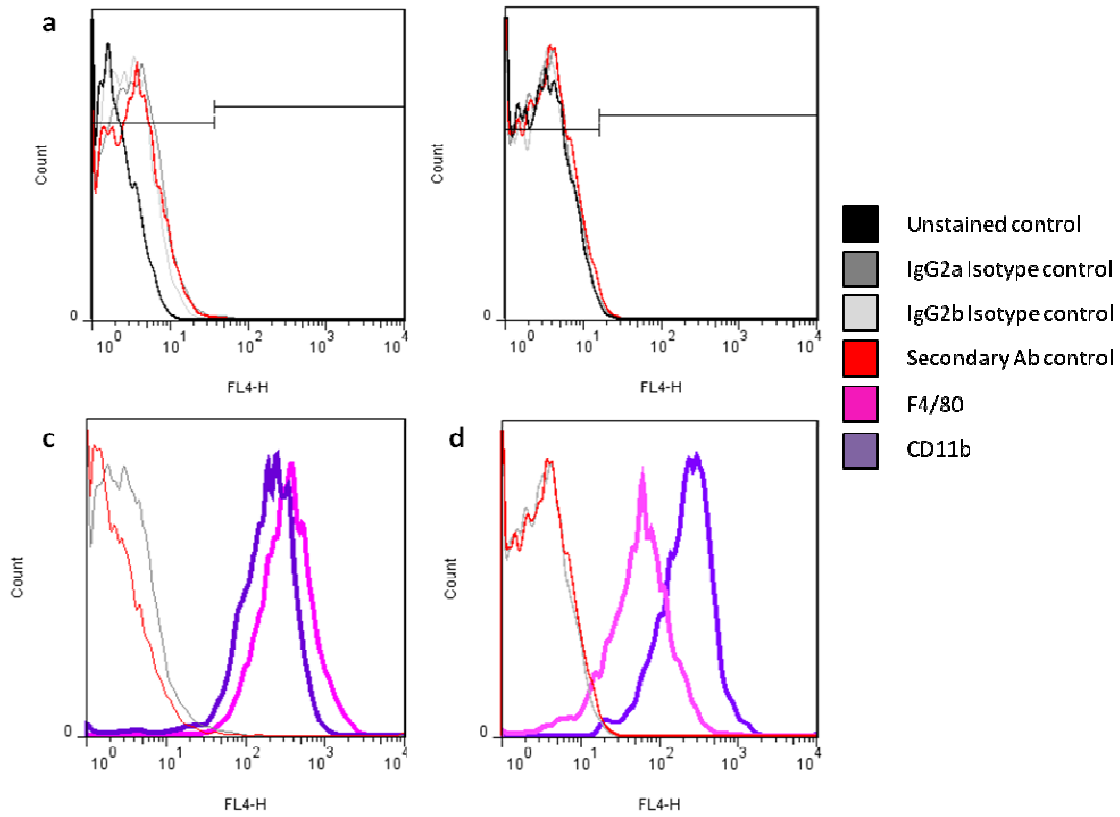

Figure 3.1 Flow cytometric analysis of 7 day BMDMϕ.
Sv129 (a&c) and IFNγR$^{-/-}$ (b&d) BMDMϕ were assessed for expression of surface markers indicative of macrophage lineage, along with isotype fluorescent controls.

Marker	Percentage Positive	
	Sv129	IFNγR$^{-/-}$
Secondary Control	0.32	0.60
F4/80	99.25	91.34
CD11b	95.21	93.96

Table 3.1 Flow cytometric analysis of 7 day BMDMϕ.
Percentage of cells staining positive for each surface marker..

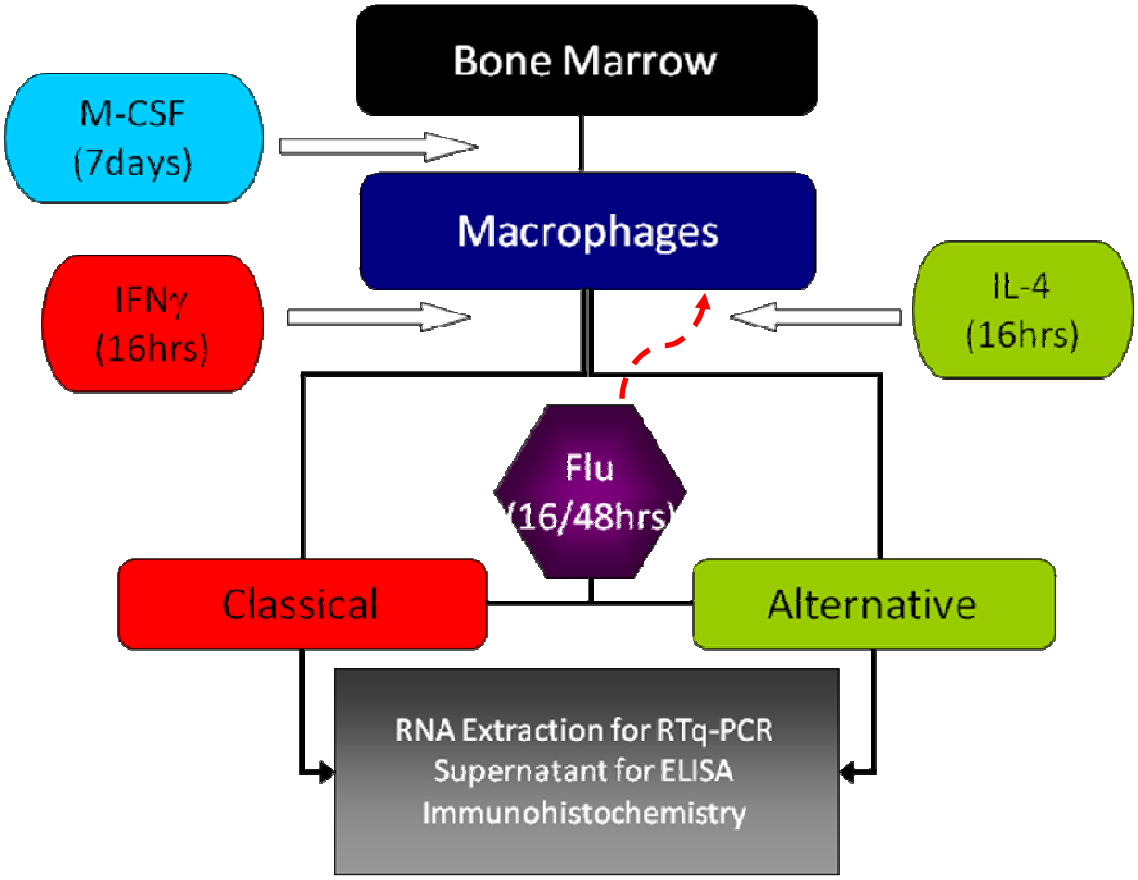

Figure 3.2 Experimental procedure
Bone marrow was harvested from femurs and cultured in the presence of M-CSF for 7 days. Cells were then split and incubated with activating cytokine for 16 hours to generate polarised macrophage subsets. These were then either characterised directly, or infected with influenza virus at an MOI of 10 for 16 or 48 hours before characterisation. For optimisation of infection conditions, macrophages were infected following 7 days culture in M-CSF but prior to polarisation (red hatched arrow)

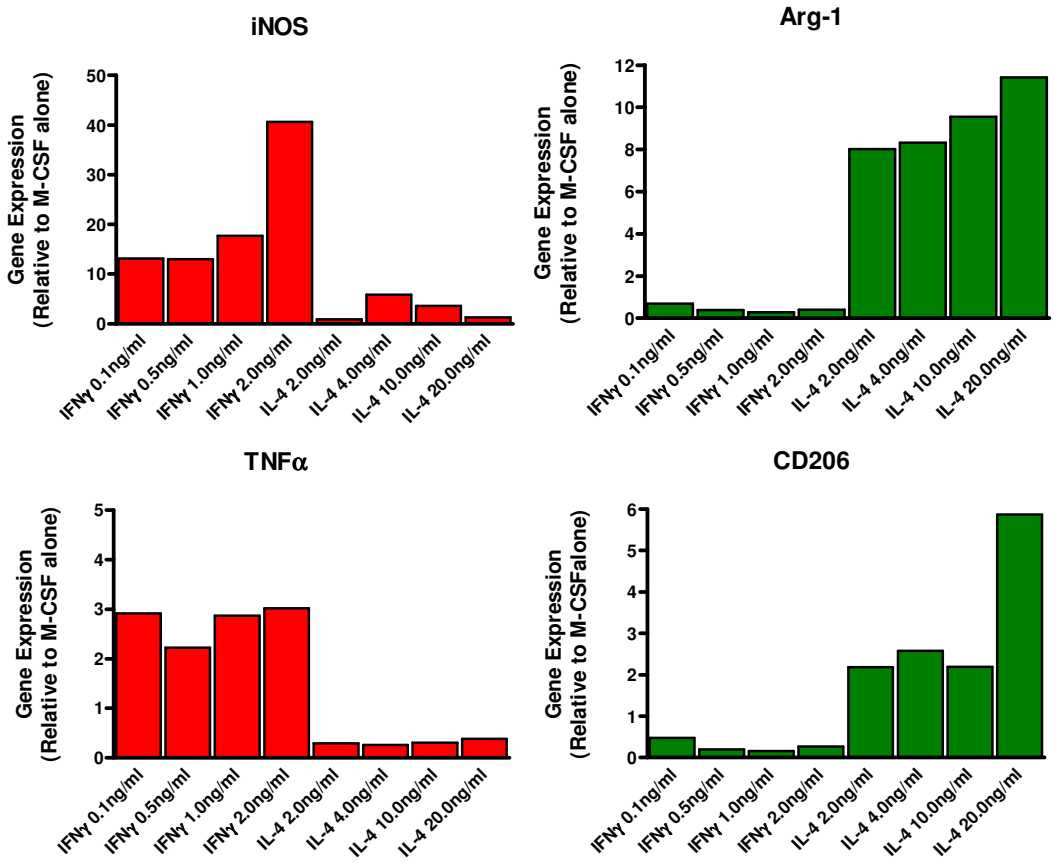

Figure 3.3 Titration of activating cytokines IFNγ and IL-4.
mRNA expression of iNOS & TNFα (classical activation) and Arg-1 & CD206 (alternative activation) were assessed by qPCR at increasing concentrations of IFNγ and IL-4. Samples were normalized against BMDMϕ stimulated with M-CSF alone. Gene expression was normalized against two housekeeping genes, CNX and SDHA. n=1

mRNA expression of iNOS and TNFα, indicative of classical activation, along with Arg-1 and CD206, alternative activation markers, was quantified by qPCR to assess polarisation. Incubation with all concentrations of IFNγ for 16 hours led to elevated iNOS and TNFα, but not Arg-1 or CD206 mRNA expression. Conversely, activation with IL-4 resulted in elevated Arg-1 and CD206 mRNA, but low expression of the two classical markers. This confirmed the generation of polarised macrophages following incubation with either IFNγ or IL-4. Concentrations of 1ng/mL IFNγ and 4ng/mL IL-4 were selected to complete a timecourse to establish the optimal incubation period for polarisation of Sv129 BMDMϕ.

Polarised phenotypes were established rapidly upon incubation of BMDMϕ with activating cytokine. As early as 1 hour post activation, iNOS and TNFα mRNA was upregulated in response to IFNγ (Figure 3.4), while IL-4 activated macrophages showed upregulation of alternative markers Arg-1 and CD206 mRNA, but not iNOS or TNFα.

Interestingly, IL-10 mRNA expression was upregulated at early timepoints after IL-4 activation, peaking at 8 hours followed by subsequent decline. However, upon activation with IFNγ, expression of this mRNA was low at 8 hours but increased until 24 hours, in contrast to the response seen to IL-4. This suggests that IL-10 expression is upregulated upon prolonged exposure to proinflammatory stimulus, in order to return the inflammatory microenvironment to homeostasis. In response to IL-4, however, IL-10 is induced early, amplifying the overall T_H2 microenvironment, but expression subsequently wanes in the absence of further stimulation.

IL-12p40 was not detected by qPCR, but was successfully detected by ELISA (Figure 3.5). IL-12p40 concentration increased with time in response to IFNγ but not to IL-4, confirming that IL-4 does not drive expression of this classical T_H1 cytokine. TGFβ, however, was detectable at 1 hour post activation, but

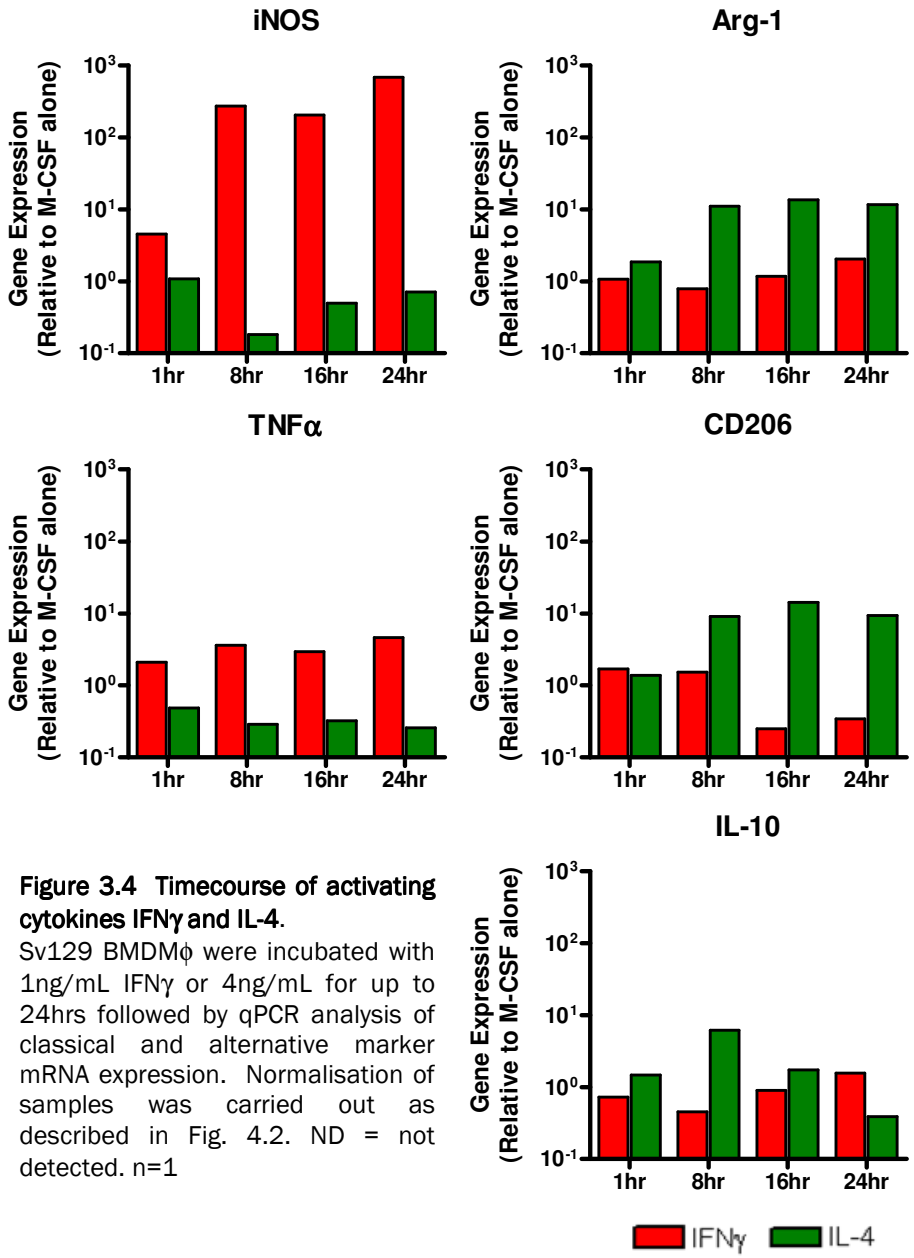

Figure 3.4 Timecourse of activating cytokines IFNγ and IL-4.
Sv129 BMDMϕ were incubated with 1ng/mL IFNγ or 4ng/mL for up to 24hrs followed by qPCR analysis of classical and alternative marker mRNA expression. Normalisation of samples was carried out as described in Fig. 4.2. ND = not detected. n=1

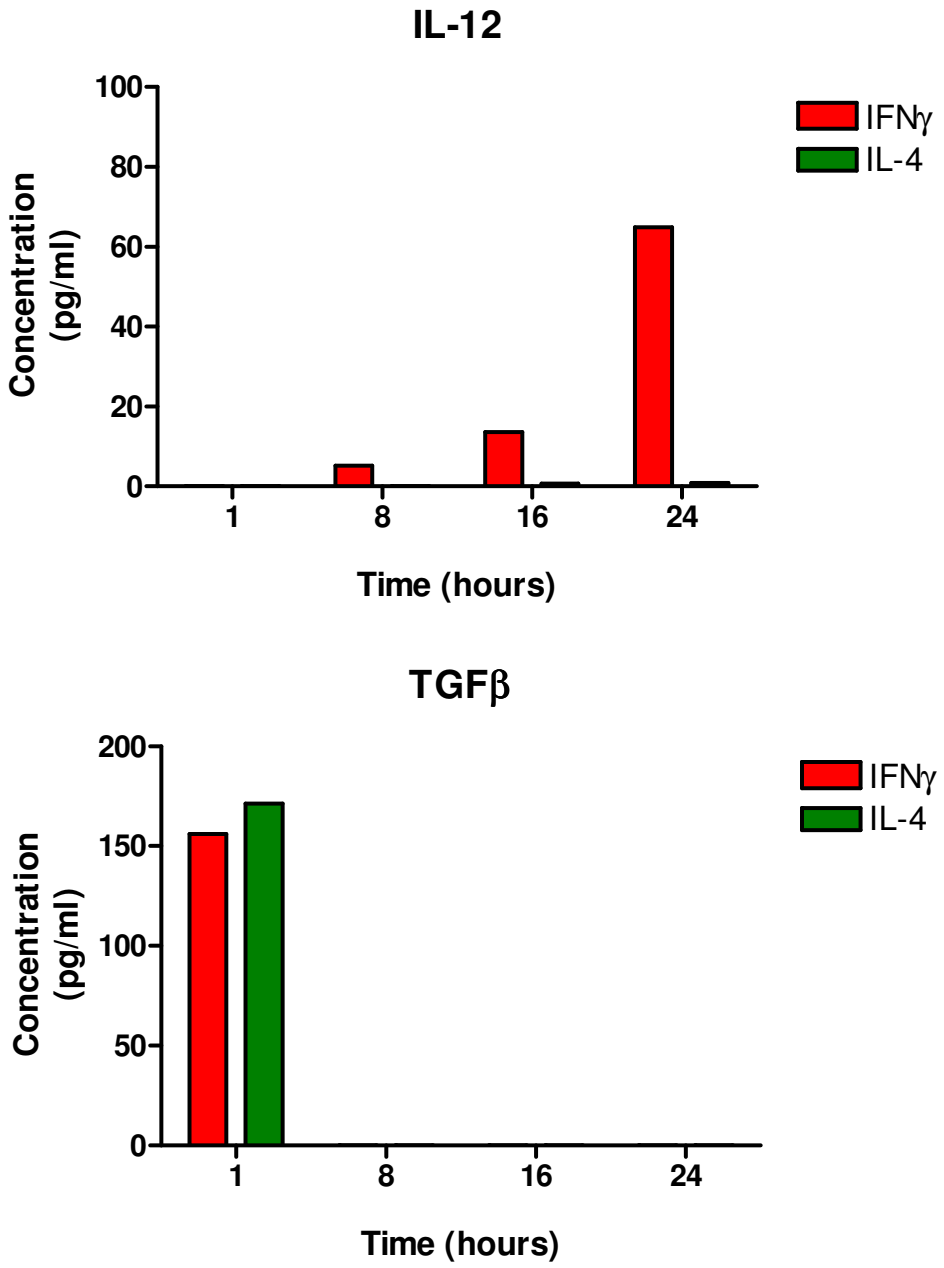

Figure 3.5 ELISA detection of IL-12p40 and TGFβ.
Sv129 supernatants were harvested and assessed for presence of IL-12p40 and TGFβ by ELISA. Optical density was read at 450nm, corrected at 540nm and concentration extrapolated from a standard curve. n=1

downregulated by both IFNγ and IL-4 to undetectable levels at all later timepoints.

Based on these data, an incubation period of 16 hours was selected as this timepoint gave a marked difference in all markers observed, with the exception of TGFβ.

3.1.3 Polarisation of IFNγR$^{-/-}$ bone marrow derived macrophages

In order to determine whether IFNγR$^{-/-}$ BMDMϕ could be polarised, 7 day mature BMDMϕ from IFNγR$^{-/-}$ mice were incubated with 1ng/mL IFNγ or 4ng/mL IL-4 for 16 hours, alongside Sv129 BMDMϕ. iNOS and Arg-1 bioassays were performed to determine successful polarisation (Figure 3.6).

As expected, Sv129 BMDMϕ were successfully polarised by activation with IFNγ and IL-4, confirming the earlier qPCR data (Figure 3.3). The IFNγR$^{-/-}$ BMDMϕ activated with IL-4 showed upregulated Arg-1 activity, consistent with alternative activation. However, incubation of IFNγR$^{-/-}$ BMDMϕ with IFNγ failed to induce iNOS activity, with similar levels observed for both IFNγ and IL-4 stimulation. This confirms that IFNγR$^{-/-}$ BMDMϕ are unable to respond to IFNγ and so fail to become classically activated.

3.1.4 Characterisation of the mRNA expression profile of polarised BMDMϕ

In order to further investigate the capacity of IFNγR$^{-/-}$ BMDMϕ to become polarised, a panel of genes indicative of classical or alternative activation was assessed by qPCR, at 16 hours post activation for Sv129 and IFNγR$^{-/-}$ BMDMϕ. Proinflammatory markers iNOS, TNFα, IL-6 and IL-1β were measured, along

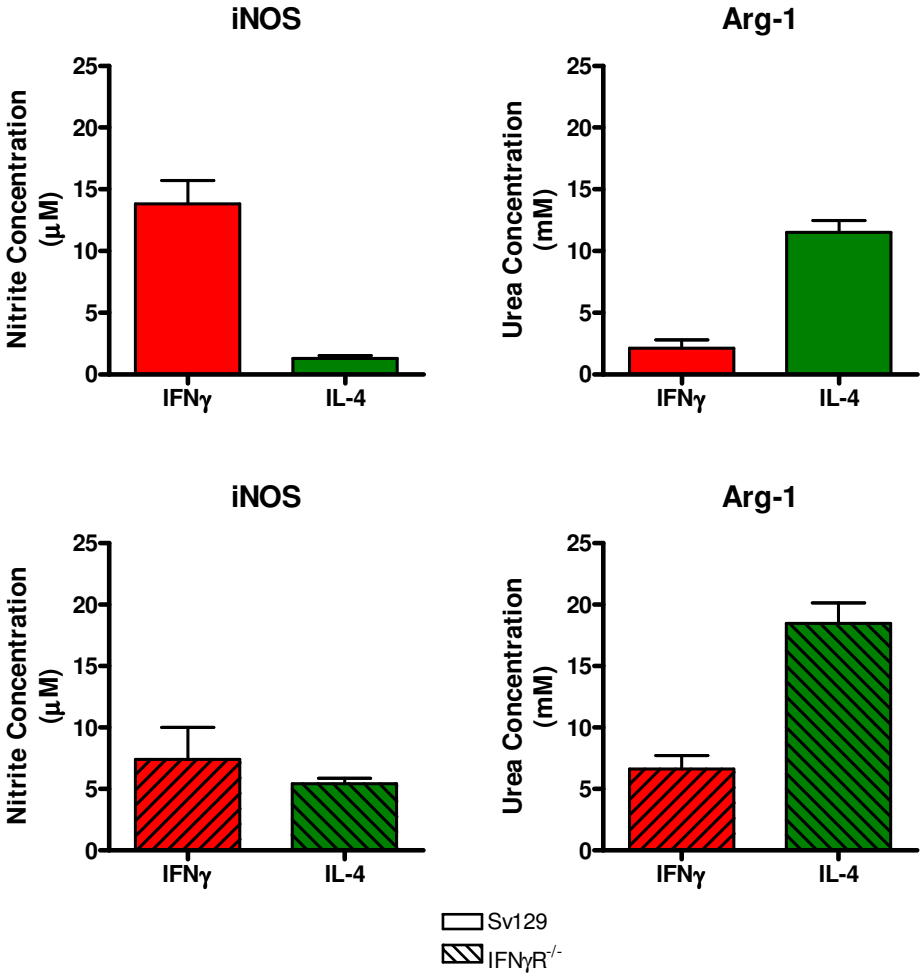

Figure 3.6 Bioassays for iNOS and Arg-1 activity.
Sv129 and IFNγR$^{-/-}$ polarised BMDMϕ were assayed for differential iNOS and Arg-1 activity. Optical density was read at 450nm and corrected at 540nm, concentrations were extrapolated from a standard curve. n=3 per strain.

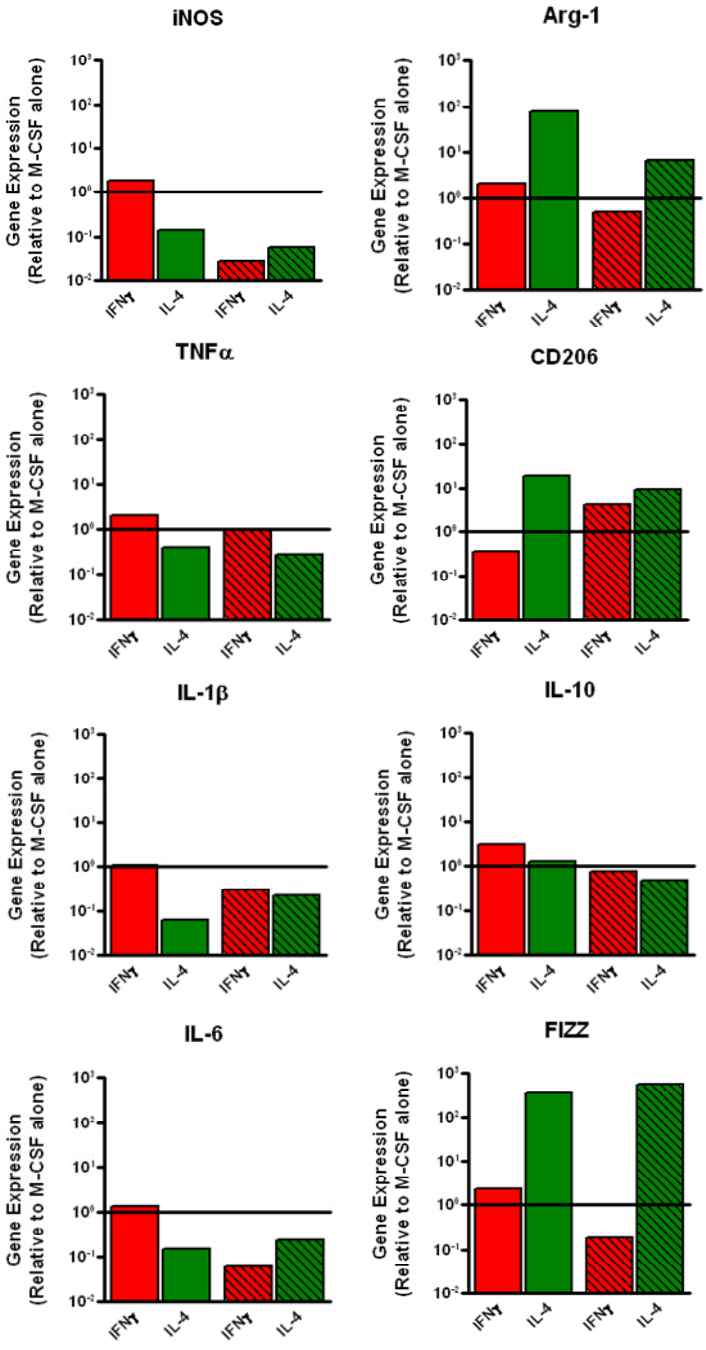

Figure 3.7 mRNA expression profile of polarised BMDMϕ.
16 hr polarised Sv129 and IFNγR-/- BMDMϕ were assessed for expression of a panel of genes indicative of classical or alternative activation by qPCR, and normalised against housekeeping genes CNX and SDHA, followed by normalisation against M-CSF controls to obtain relative expression of each gene. n=1 per strain.

with markers of alternative activation Arg-1, CD206, FIZZ and IL-10 (Figure 3.7). IFNγ stimulation of Sv129 BMDMϕ (Figure 3.7, solid red bar) showed higher expression of iNOS, TNFα, IL-1β and IL-6 mRNA than their IL-4 stimulated counterparts (Figure 3.7, solid green bar). However, these increases were only slightly upregulated from baseline, demonstrating less than a 2 fold increase in expression (Figure 3.7, solid line). The response to IL-4 was more robust in this instance, with the classical markers being downregulated and Arg-1, CD206 and FIZZ mRNA all strongly increased. IL-10 was the exception, with neither IFNγ or IL-4 having a strong effect. However, it should be noted that these data are from a preliminary experiment, where n=1 and thus require further experiments to confirm these findings.

As expected, IFNγR$^{-/-}$ BMDMϕ failed to upregulate any of the classical genes in response to IFNγ (Figure 3.7, hatched red bar). However, expression of iNOS, IL-6 and FIZZ mRNA was quite strongly downregulated relative to M-CSF alone. This was surprising, but may be due to an anomaly within the single mouse investigated during establishment of the techniques in this section. IL-4 (Figure 3.7, hatched green bar) induced successful upregulation of Arg-1, CD206 and FIZZ mRNA, but failed to upregulate IL-10. IL-10 induced by IFNα/β following TLR stimulation results in upregulation of SOCS 3 and subsequent control of inflammatory cytokine signalling, thereby limiting the inflammatory cascade and restoring homeostasis (reviewed by O'Shea & Murray, 2008). The lack of proinflammatory gene expression may be the reason for poor IL-10 expression, as the cytokine microenvironment is not strongly dysregulated following exposure of IFNγR$^{-/-}$ BMDMϕ to IFNγ.

Interestingly, in the absence of IFNγ mediated inhibition, IFNγR$^{-/-}$ BMDMϕ appear to upregulate CD206, while their wildtype Sv129 counterparts downregulate this receptor.

Taken together, these data suggest that IFNγR$^{-/-}$ are impaired in their capacity to mount a classical proinflammatory response, but can be successfully driven into an alternatively activated state.

3.2 Preliminary infection of polarised BMDMϕ with influenza virus

Previous studies have experimentally infected macrophages with varying efficiencies depending on strain of influenza virus and method of macrophage isolation. Reading and colleagues have demonstrated infection of alveolar and peritoneal macrophages differed between virulent and avirulent influenza strains (Reading *et al.*, 2000; Tate *et al.*, 2011), while Rodgers and Mims showed differing infectivity between alveolar and peritoneal macrophages, but no differences between virus strains (Rodgers & Mims, 1981). It was therefore important to establish the optimal infection conditions with the virus to be used prior to attempting infection of polarised macrophages.

3.2.1 Optimisation of A/WSN/33 virus infection

The mouse adapted strain of influenza A virus, A/WSN/33 (WSN) was used to infect BMDMϕ. This virus was initially titrated on MDCK cells in a standard plaque assay as described in Chapter 2.3.2, to determine the concentration of virus in plaque forming units in this cell type. This virus stock was then used to infect BMDMϕ at varying multiplicities of infection (MOI) to establish the optimal viral dose to induce cytopathic effect. In vivo experiments within our laboratory have previously shown BALB/c mice to be more susceptible to infection with this virus than Sv129 (Y. Ligertwood, personal communication) and so the virus was titrated on BMDMϕ from both BALB/c and Sv129 mice.

Seven day mature, non-activated BMDMϕ were infected with WSN (Figure 3.2, red hatched arrow). Infections were carried out on glass chamber slides and stained at 48 hours post infection.

The virus was titrated at MOI of 1 (Figure 3.8a&e), 5 (Figure 3.8b&f), 10 (Figure 3.8c&g) and 15(Figure 3.8d&h) for Sv129 (Figure 3.8a-d) and BALB/c BMDMϕ (Figure 3.8e-h). MOI of 1 gave rise to very low levels of infection (Figure 3.8a&e), while higher MOI resulted in more efficient infection.

MOI of 10 was selected for further infections as this resulted in a robust infection in BMDMϕ from both strains of mice. A timecourse was then performed to determine the optimal duration of infection prior to harvesting BMDMϕ for analysis. Sv129 BMDMϕ were generated and infected as previously described then harvested for cytospins at 1, 8, 16 and 24 hours post infection. These cytospins were stained with polyclonal anti-influenza antibody, followed by visualisation with Alexafluor 488, as described in Chapter 2.8.1 (Figure 3.9). At 1 hour post infection, no staining was seen (Figure 3.9a). However, by 8 hours post infection, strong staining was observed in some cells (Figure 3.9b). The staining pattern altered between 8 and 16 hours to show low level staining in the majority of cells with some more intensely positive macrophages (Figure 3.9c) and was still apparent at 24 hours post infection (Figure 3.9d). The distribution of viral antigen also appeared to change throughout the course of this infection. At 8 hours, the cytoplasm appeared to be staining most strongly, while by 16 and 24 hours post infection, the strongest staining was localised beneath the plasma membrane. Given that a polyclonal anti-influenza antibody was used, it is likely that antibody is predominantly binding to HA and NA.

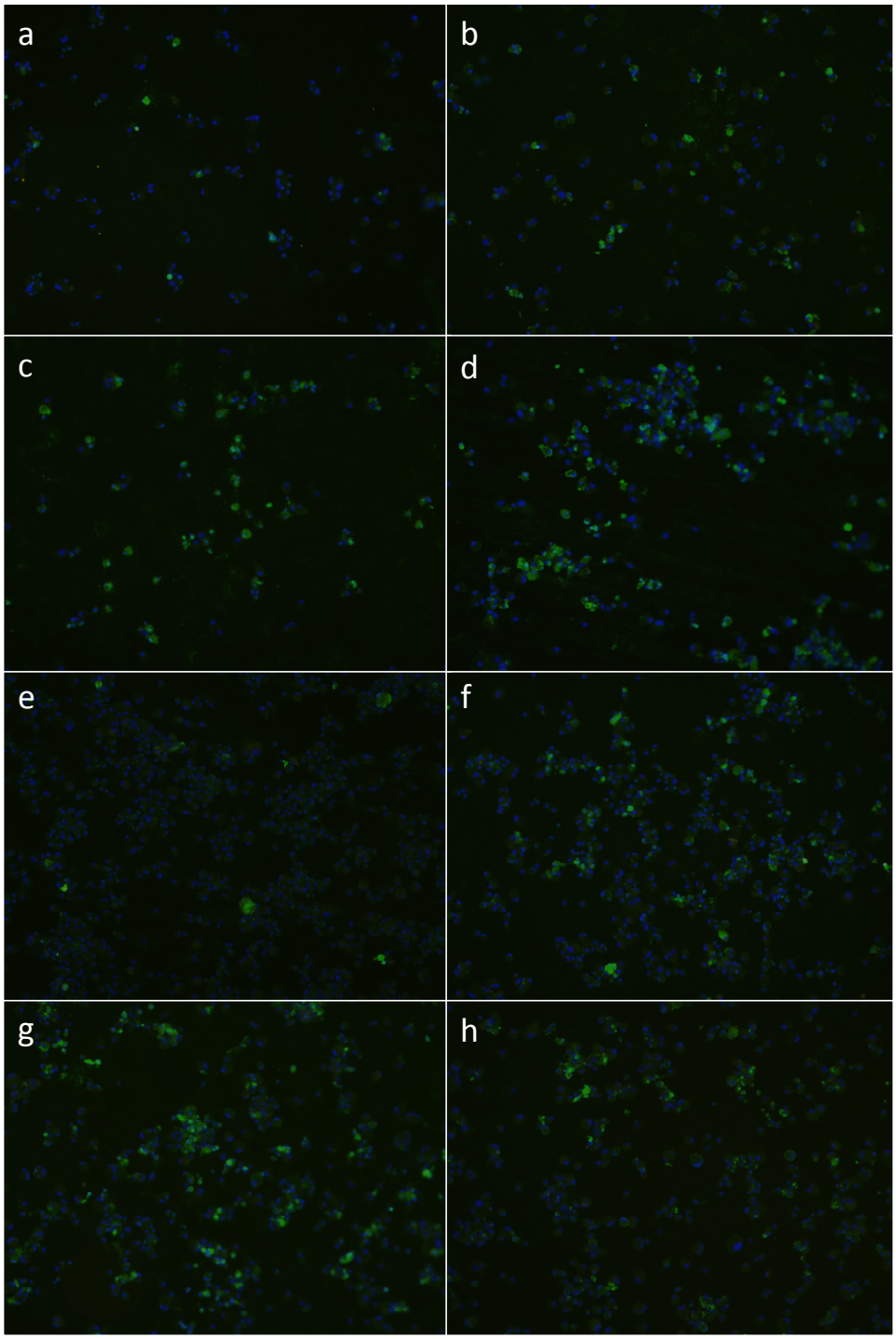

Figure 3.8 Titration of A/WSN/33 on Sv129 and BALB/c BMDMϕ.
A/WSN/33 was titrated at MOI 1, 5, 10 & 15 on BMDMϕ from Sv129 (a-d) and BALB/c (e-h) mice. BMDMϕ were grown on glass chamber slides and stained with polyclonal anti-influenza antibody and Alexafluor 488, along with DAPI nuclear counterstain. Mock infected BMDMϕ were stained as controls.
x5 magnification, representative of n=2 per strain

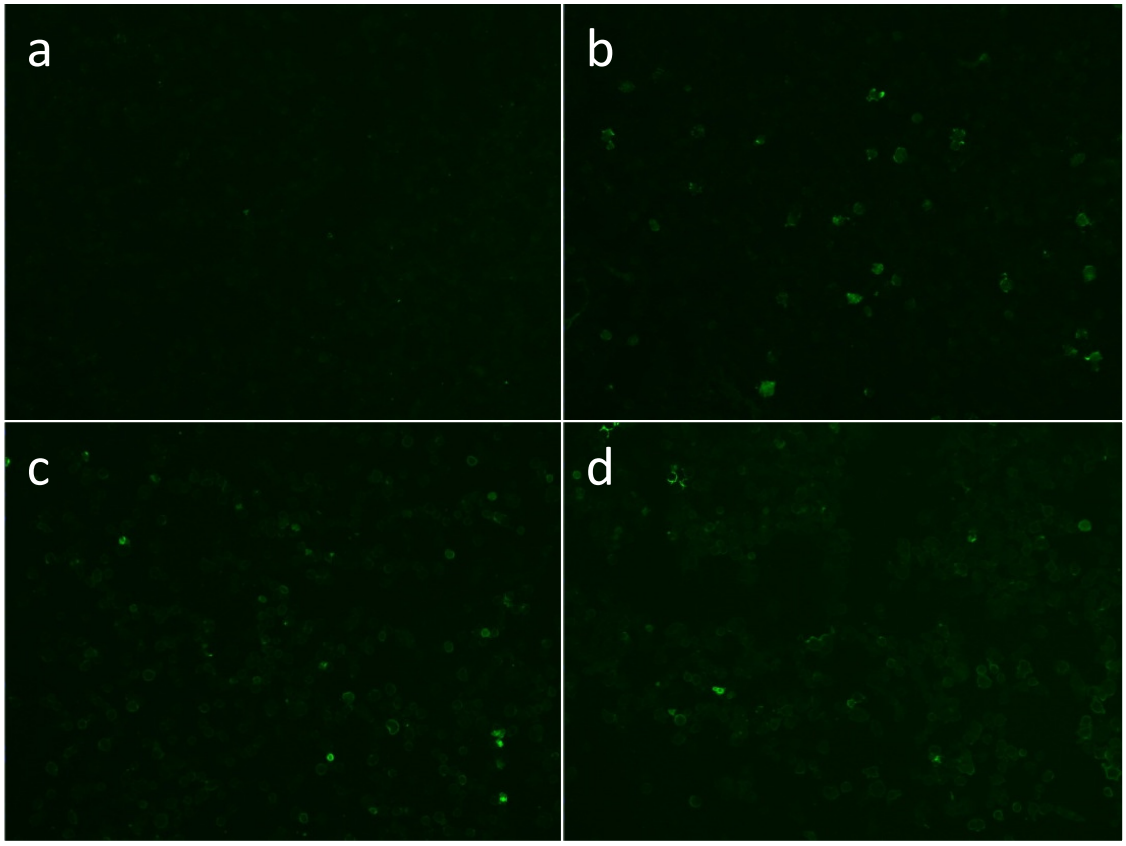

Figure 3.9 A/WSN/33 infection timecourse.
Sv129 BMDMϕ were infected with MOI 10 A/WSN/33 and harvested for cytospins at 1 (a), 8 (b), 16 (c) and 24 (d) hours post infection followed by staining with a polyclonal anti-influenza A antibody and Alexafluor 488.
x5 magnification, n=1

It has been previously reported that macrophages do not support productive infection (Rodgers & Mims, 1981). This pattern of staining suggests that a proportion of BMDMϕ become infected but do not release infectious virus, as an accumulation of viral antigen is detected at the plasma membrane and neighbouring cells express only low levels of staining. It was also evident that the method of preparing infected cells for staining had an important impact on the extent of infection observed. BMDMϕ grown on chamber slides prior to fixation and staining showed stronger staining than those grown on plates and harvested for cytospin analysis. One explanation for this may be mechanical destruction of fragile infected cells during the cytospin process. Taking this into consideration, together with the staining obtained at 48 hours post infection during the virus titration, the timepoints of 16 and 48 hours post infection were selected for further investigation of the effects of influenza virus infection on BMDMϕ grown on chamber slides.

3.2.2 Characterisation of mRNA expression profile in infected polarised Sv129 and IFNγR$^{-/-}$ bone marrow derived macrophages

Polarised Sv129 and IFNγR$^{-/-}$ BMDMϕ were infected and harvested for RNA extraction at 48 hours post infection. The mRNA expression profile was then examined by qPCR.

As previously observed, IFNγ activation of Sv129 BMDMϕ led to an upregulation of mRNA for proinflammatory markers iNOS, TNFα, IL-1β and IL-6 (Figure 3.10, first solid red bar) relative to baseline expression levels in non-activated, uninfected control BMDMϕ (Figure 3.10, solid line). IL-12p40 mRNA was also successfully detected by qPCR and was found to be elevated by IFNγ activation, consistent with the ELISA data (Figure 3.5).

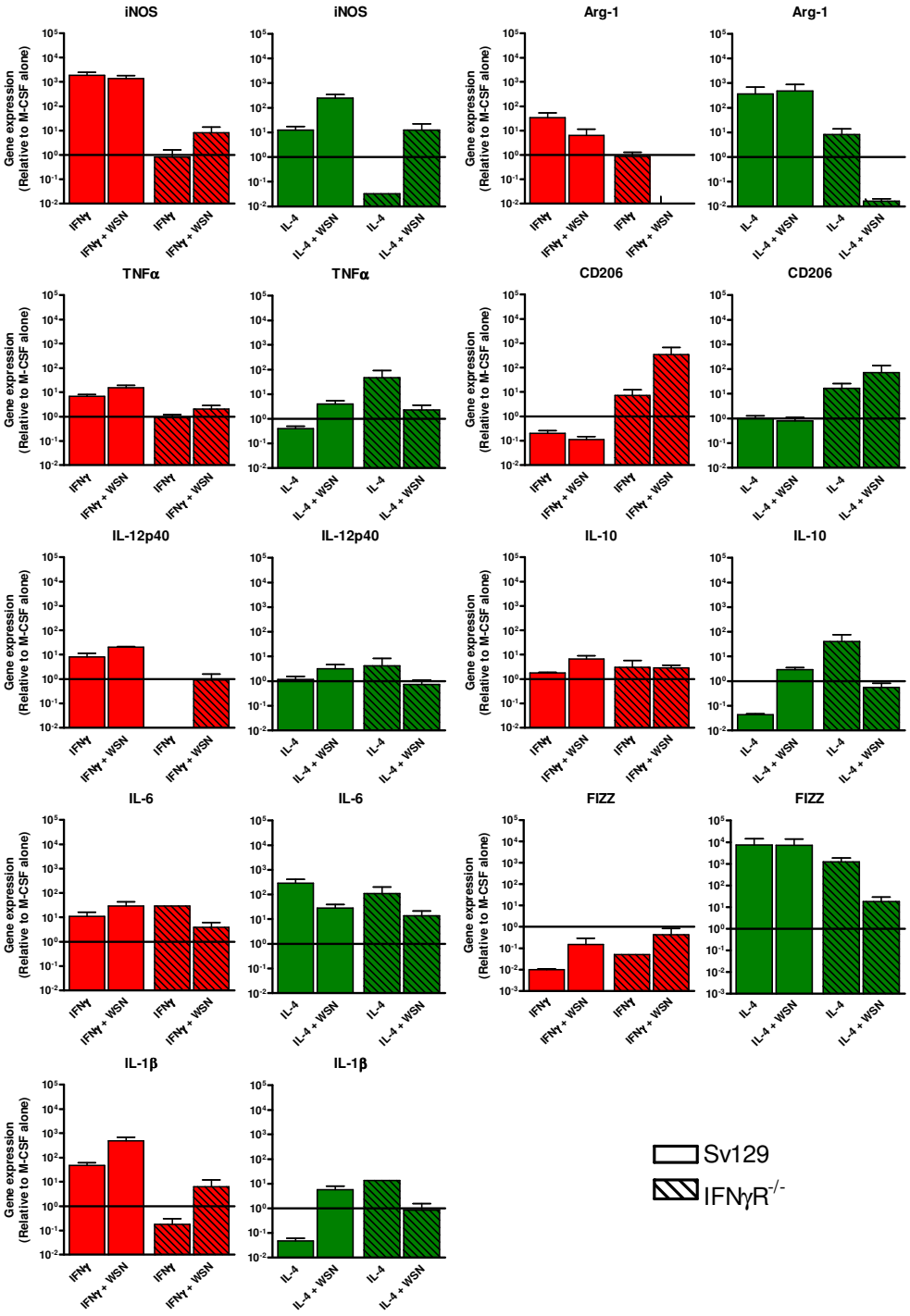

Figure 3.10 mRNA expression analysis of infected polarised BMDMϕ.
Infected polarised Sv129 and IFNγR$^{-/-}$ BMDMϕ were harvested at 48 hours post infection for RNA extraction and qPCR analysis. Samples were normalised against mock infected BMDMϕ stimulated with M-CSF alone and gene expression was normalised against housekeeping genes CNX and SDHA as previously described. n=4 per strain

Arg-1 mRNA was also increased in the IFNγ activated group (Figure 3.10, first solid red bar), but this was to a much lower level than iNOS, a 70 fold increase in Arg-1 versus a 2000 fold increase in iNOS, indicating that the BMDMϕ response was predominantly classical in nature.

Incubation with IL-4 (Figure 3.10, first solid green bar) led to an increase in Arg-1 and FIZZ mRNA, consistent with alternative activation, while CD206 mRNA expression was unaltered. Surprisingly, IL-6 and iNOS expression were also upregulated by IL-4 as well as by IFNγ. IL-10 mRNA, however, was downregulated, perhaps due to absence of proinflammatory TNFα and IL-12p40.

Infection of classically activated Sv129 BMDMϕ (Figure 3.10, second solid red bar) resulted in a further upregulation of TNFα, IL-12p40, IL-1β, IL-6 and IL-10 mRNA expression. iNOS mRNA expression remained high, and surprisingly, FIZZ mRNA was increased slightly when compared with IFNγ alone, but remained lower than baseline levels. Arg-1 mRNA was also elevated from baseline, but to a lesser extent than in response to IFNγ alone, and again remained lower than iNOS in the infected group.

Alternatively activated Sv129 BMDMϕ also exhibited upregulation of iNOS, TNFα, IL-12p40 and IL-1β mRNA upon infection with WSN (Figure 3.10, second solid green bar). This suggests that infection with virus is sufficiently proinflammatory to drive expression of classical markers despite the initial IL-4 signal. However, a mixed phenotype was observed in this population, as Arg-1 and FIZZ mRNA expression remained at similar high levels to those observed with IL-4 alone (Figure 3.10, solid green bars). IL-10 was also upregulated in the infected IL-4 stimulated group, consistent with the suggestion that as proinflammatory cytokines are induced, IL-10 expression increases in order to control this inflammatory response.

IFNγR$^{-/-}$ BMDMϕ, consistent with previous data, showed no classical response to IFNγ (Figure 3.10, first hatched red bar). However, BMDMϕ from one mouse expressed elevated IL-6 mRNA, but this cytokine was undetectable in BMDMϕ from the remaining three mice.

Upon infection of IFNγ stimulated IFNγR$^{-/-}$ BMDMϕ, mRNA for inflammatory markers iNOS, TNFα, IL-12p40 and IL-1β was upregulated, as was IL-6 expression in all four mice (Figure 3.10, second hatched red bar), demonstrating that WSN is capable of driving a proinflammatory response even in the absence of IFNγ signalling. FIZZ was also slightly upregulated, but remained below baseline, similar to wildtype Sv129 BMDMϕ. Interestingly, CD206 mRNA expression was strongly increased upon infection.

IL-4 activation of IFNγR$^{-/-}$ BMDMϕ increased expression of Arg-1 and FIZZ mRNA (Figure 3.10, first hatched green bar), with CD206 expression remaining similar between both IFNγ and IL-4 activated populations (Figure 3.10, first hatched red and green bars respectively). An increase in inflammatory markers TNFα, IL-12p40, IL-1β and IL-6 was also observed and may be responsible for the elevated IL-10 expression in this population.

Infection of the alternatively activated IFNγR$^{-/-}$ BMDMϕ (Figure 3.10, second hatched green bar) showed decreased expression in all markers compared to IL-4 alone, with the exception of iNOS, which was upregulated upon infection, and CD206, which was also elevated. Despite being lower than IL-4 stimulation alone, TNFα mRNA levels were still higher than baseline, as were those for IL-6 and FIZZ. The observation that Arg-1 mRNA expression is almost completely abrogated and FIZZ mRNA is reduced compared to IL-4 activation alone suggests that IL-4 is incapable of maintaining a dominant effect on this strain of macrophage in the presence of WSN.

Similar to wildtype Sv129 BMDMϕ, IFNγR$^{-/-}$ BMDMϕ showed a mixed phenotype upon infection, with expression of both classical and alternative markers. Interestingly, CD206 was elevated in all IFNγR$^{-/-}$ populations assessed and showed the highest degree of upregulation in the infected groups. This receptor has been implicated in attachment and entry of influenza virus to macrophages (Reading *et al.*, 2000) and so this may be an influential factor in the pathogenesis of the virus in this strain of mouse.

3.2.3 Characterisation of mRNA expression profile in infected polarised BALB/c and IL-4R$^{-/-}$ bone marrow derived macrophages

As IFNγR$^{-/-}$ BMDMϕ cannot become classically activated, it was of interest to compare the response to infection with BMDMϕ that were inhibited in their ability to become alternatively activated. As such, IL-4R$^{-/-}$ mice on the BALB/c background were utilised and BMDMϕ from this strain of mice compared to wildtype BALB/c BMDMϕ.

BALB/c BMDMϕ responded to IFNγ activation by upregulation of all classical markers (Figure 3.11, first solid red bar), although the increase in IL-1β and IL-6 was modest. Arg-1 was also upregulated, but to a much lesser extent than iNOS, similar to that observed in Sv129 BMDMϕ. Together with the absence of FIZZ, the overall response to IFNγ appeared to be classical in nature.

Conversely, activation with IL-4 resulted in upregulation of all alternative markers, including IL-10 and decreased expression of proinflammatory cytokines (Figure 3.11, first solid green bar), indicating successful alternative activation.

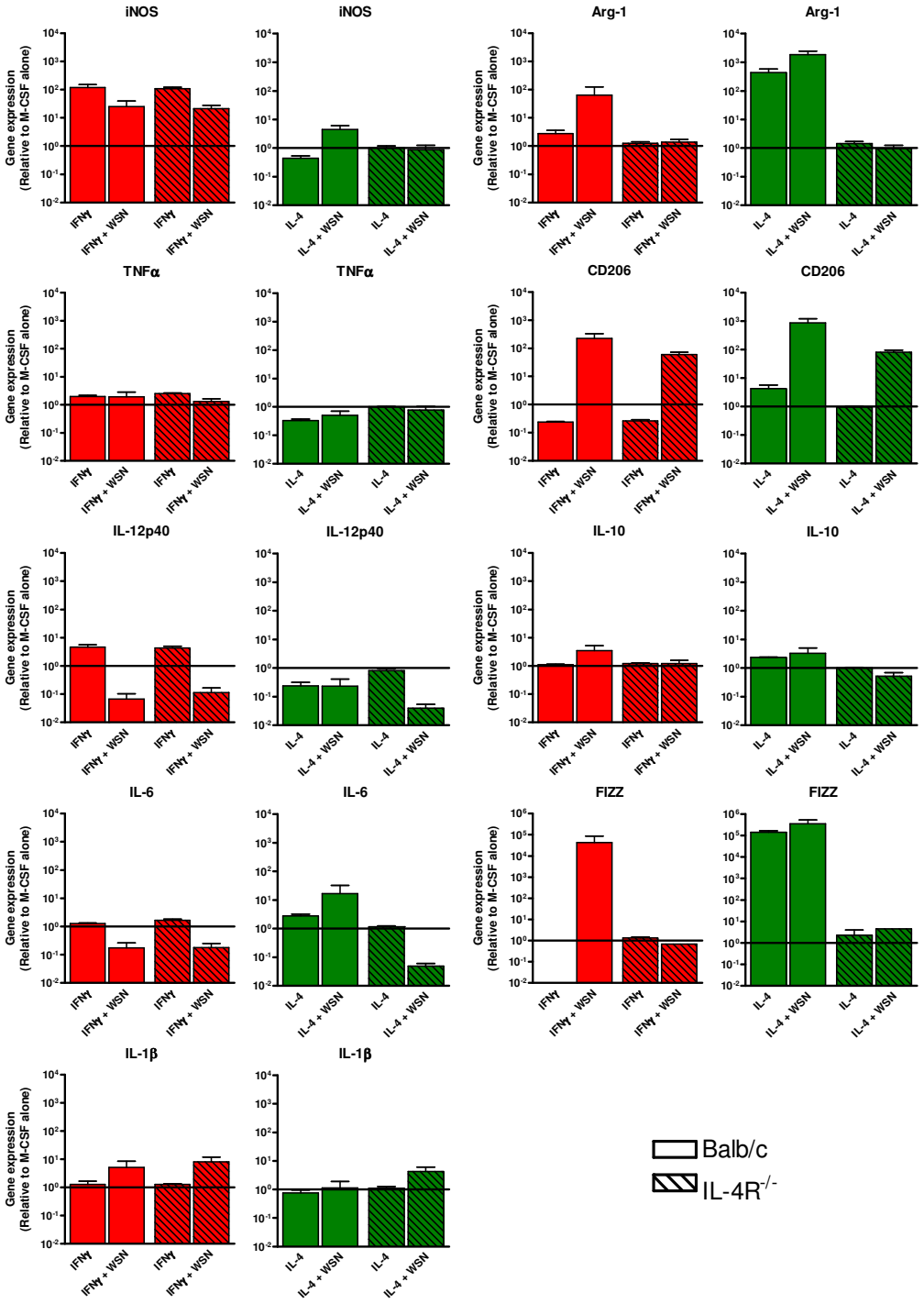

Figure 3.11 mRNA expression analysis of infected polarised BMDMϕ.
Infected polarised BALB/c and IL-4R$^{-/-}$ BMDMϕ were harvested at 48 hours post infection for RNA extraction and qPCR analysis. Samples were normalised against mock infected BMDMϕ stimulated with M-CSF alone and gene expression was normalised against housekeeping genes CNX and SDHA as previously described. n=4 per strain

Infection of the classically activated population resulted in elevated expression of IL-10, TNFα, IL-1β and iNOS mRNA, although in the case of iNOS, this was to a lesser extent than IFNγ alone (Figure 3.11, second solid red bar). Surprisingly, Arg-1, CD206 and FIZZ mRNA expression was also strongly increased in response to IFNγ plus WSN. This strain of mice is more T_H2 biased and so macrophages may adopt a 'wound healing' type role during challenge, hence explaining the observed elevation in Arg-1 and FIZZ expression. Also unexpected was the decline in IL-12p40 mRNA expression. Along with the increase in IL-10 expression, it is suggestive of a less inflammatory response to virus than that seen in the Sv129 BMDMϕ, despite priming with IFNγ.

Alternatively activated BALB/c BMDMϕ showed upregulation of iNOS and IL-6 mRNA in response to infection (Figure 3.11, second solid green bar) but no increase in any other proinflammatory marker. However, expression of alternative markers Arg-1 and CD206 was increased and high expression of FIZZ was maintained. This suggests that, unlike Sv129 BMDMϕ, this strain of macrophage may be more capable of maintaining a dominant alternative phenotype even in the presence of a strong proinflammatory stimulus such as influenza virus.

IFNγ activation of IL-4R$^{-/-}$ resulted in a response indistinguishable from the wildtype BALB/c BMDMϕ (Figure 3.11, first hatched red bar), as did infection of classical BMDMϕ of this strain (Figure 3.11, second hatched red bar), with the exception of Arg-1 and FIZZ, which were markedly lower in the infected IL-4R$^{-/-}$ BMDMϕ than the wildtype BALB/c cells.

Stimulation of IL-4R$^{-/-}$ BMDMϕ with IL-4 failed to induce any response, evidenced by expression of baseline levels of every marker examined. Upon infection, the IL-4R$^{-/-}$ retained their 'non-activated' baseline phenotype, with

very little change in mRNA expression (Figure 3.11, second hatched green bar). IL-1β and FIZZ showed slight upregulation in response to virus, but the increased iNOS and IL-6 observed in wildtype BALB/c BMDMϕ was notably absent. CD206, however, was strongly upregulated during infection consistent with BALB/c BMDMϕ.

3.3 Summary of results and discussion

It has previously been documented that BALB/c and C57Bl/6 mice show markedly differing responses to stimuli such as LPS, whereby C57Bl/6 mice are able to produce high levels of iNOS, TNFα and IL-12, but BALB/c mice are impaired in their ability to do so (Watanabe *et al.*, 2004). Conversely, BALB/c mice have been shown to be higher producers of Arg-1 in response to IL-4 stimulation (Pradel *et al.*, 2009).

The preliminary data presented herein suggest that BMDMϕ on the Sv129 background are primed towards inflammation, similar to the C57Bl/6 background, and appear to be more T_H1 oriented than their BALB/c counterparts. Some degree of proinflammatory cytokine mRNA expression was driven by the virus upon infection of BMDMϕ on the Sv129 background, even in the absence of IFNγ signalling. In contrast to this, infection of IFNγ primed BALB/c and IL-4R$^{-/-}$ BMDMϕ failed to drive expression of inflammatory markers.

While sufficient to induce an alternatively activated phenotype from Sv129 and IFNγR$^{-/-}$ BMDMϕ, IL-4 did not appear capable of maintaining this activation state upon infection with WSN. Macrophages are known to alter their phenotype in response to sequential stimulation (Stout *et al.*, 2005) and therefore it is perhaps not surprising that infection may lead to mixed expression of classical and alternative markers. Infection did not achieve 100% efficiency, even at an MOI of 10 in these BMDMϕ populations, and so

infected cells may upregulate inflammatory genes while uninfected cells may remain alternatively activated.

The data suggest that BALB/c BMDMϕ were able to maintain an alternatively activated phenotype following IL-4 activation and virus infection, or in the absence of IL-4 signalling, BMDMϕ maintained a non activated phenotype. However, similar to the IFNγR$^{-/-}$ BMDMϕ, both BALB/c and IL-4R$^{-/-}$ macrophages demonstrated elevated CD206 mRNA expression following infection. Whether this is a result of infection or of differing levels of endogenous interferon specific to each strain requires further investigation, but enhanced CD206 expression may be influential in the ability of WSN to infect BMDMϕ.

Influenza virus causes damaging immunopathology due to a highly reactive inflammatory response. As IFNγR$^{-/-}$ BMDMϕ seemed impaired in their ability to mount a functional inflammatory response compared to that observed in wildtype Sv129 BMDMϕ, this strain was used to further investigate the effect of the inflammatory response on WSN infection of BMDMϕ (Chapter 4), and continued in a whole mouse model (Chapter 6).

The aim of this chapter was simply to establish the in vitro model systems to be used. The number of replicates in these preliminary experiments was limited and therefore no definitive conclusions can be drawn from the data presented here. However, techniques for culture, activation and infection of BMDMϕ have been established here allowing the study of larger groups of mice in order to investigate the aims of the project in detail.

4 Infection of Sv129 and IFNγR$^{-/-}$ bone marrow derived macrophages

4.1 Infectivity of A/WSN/33 for Sv129 and IFNγR$^{-/-}$ bone marrow derived macrophages

As previously shown in Chapter 3, influenza virus A/WSN/33 can infect Sv129 BMDMϕ and elicit a cytokine response from both Sv129 and IFNγR$^{-/-}$ BMDMϕ (Chapter 3.2.2.) In this chapter, the effect that inhibiting IFNγ signalling could have on influenza virus infection of BMDMϕ and on the characteristic inflammatory response was further investigated.

4.1.1 Evaluation of A/WSN/33 infection of BMDMϕ

BMDMϕ of both strains were generated, activated and infected as described in Chapter 2.2.4, on 8 well glass chamber slides or 100mm uncoated dishes. Macrophages were fixed and stained at 16 and 48 hours post infection with either anti-NS1 or polyclonal anti-influenza antibodies to determine the ability of WSN to infect BMDMϕ as opposed to being detected as phagocytosed virions and infected debris. NS1 is synthesised early in infection and so positive staining for this viral protein indicates active replication, while the anti-influenza antibody may detect viral envelope proteins on phagocytosed particles in addition to any newly expressed viral proteins.

Classically activated Sv129 BMDMϕ demonstrated very strong NS1 staining in the cytoplasm at 16 hours (Figure 4.1a), which diminished by 48 hours, when the NS1 stain appeared condensed in nature and colocalised with the nuclear counterstain (Figure 4.1e). This is consistent with early and abundant expression of NS1 followed by nuclear localisation but no new synthesis of this

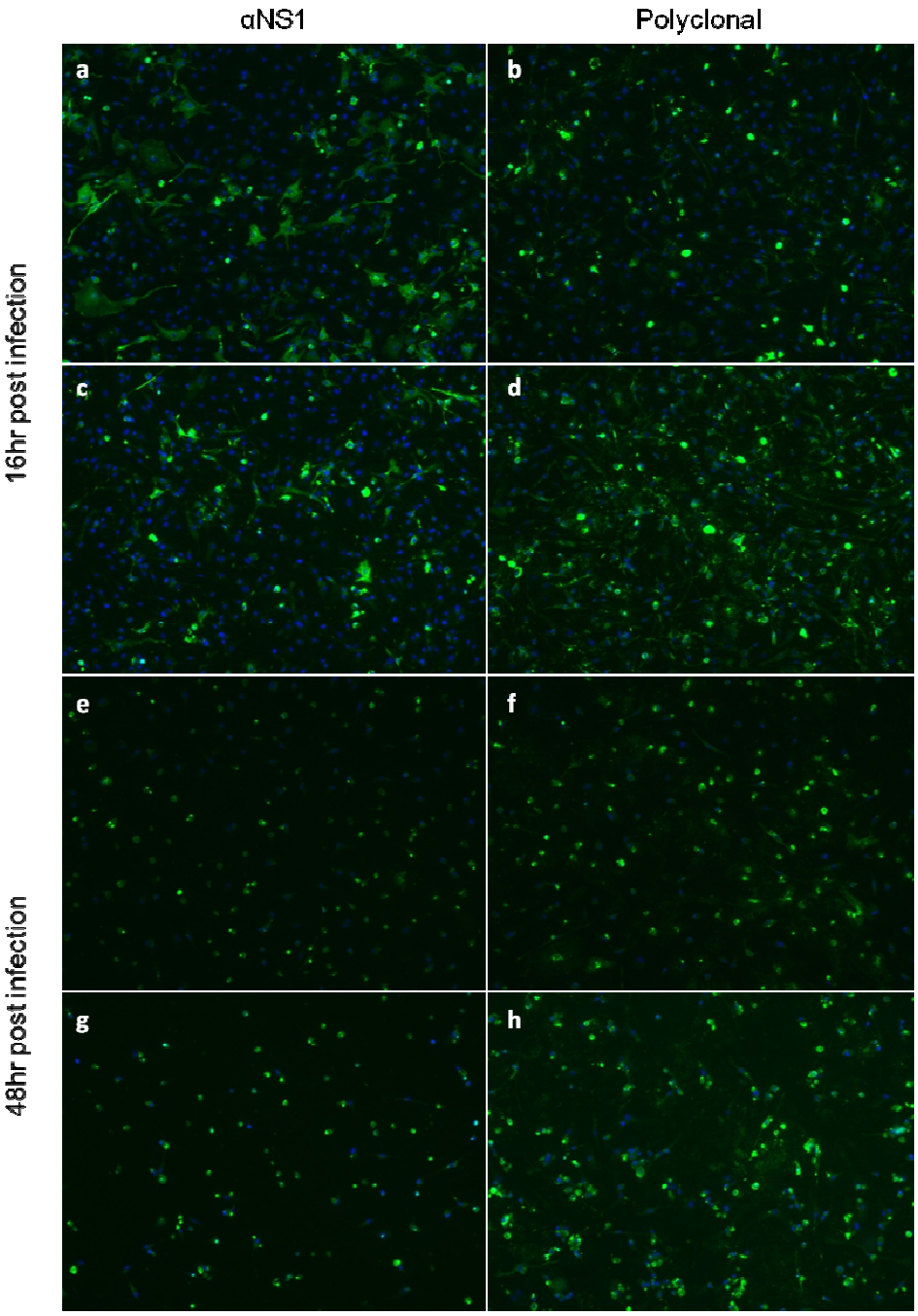

Figure 4.1 Immunofluorescent staining for influenza virus in Sv129 BMDMϕ.
Classical (a,b,e&f) and alternatively activated (c,d,g&h) Sv129 BMDMϕ were stained with an NS1 (a,c,e&g) or polyclonal anti-influenza antibody (b,d,f&h), followed by detection with alexafluor 488 at either 16 (a-d) or 48 hours (e-f).
x20 magnification, 2 fields of vision counted, data are representative of 3 independent experiments.

protein at later stages of non-productive infection. Had replication been ongoing within the cell, NS1 would remain detectable in the cytoplasm at 48 hours. The anti-influenza antibody detected viral antigens at both 16 and 48 hours (Figure 4.1b&f) but was strongest at 48 hours, consistent with an accumulation of viral proteins and particles.

Infection of alternatively activated Sv129 BMDMϕ showed weaker NS1 staining at 16 hours than classically activated BMDMϕ, but stronger positivity with the anti-influenza antibody at this timepoint (Figure 4.1c&d). NS1 staining at 48 hours was sparse but appeared to be predominantly nuclear (Figure 4.1g), while the anti-influenza antibody staining remained strong (Figure 4.1h). These data demonstrate that classical and alternatively activated macrophages exhibit differing infection profiles.

IFNγ and IL-4 stimulated IFNγR$^{-/-}$ BMDMϕ were very similar in their staining patterns, with NS1 staining strongly in both at 16 hours (Figure 4.2a&c), and the anti-influenza antibody most strongly at the later timepoint (Figure 4.2f&h). Similar to their Sv129 counterparts, IL-4 stimulated IFNγR$^{-/-}$ BMDMϕ appear to show stronger polyclonal staining at 16 hours than the IFNγ stimulated population (Figure 4.2b&d), along with slightly weaker NS1 staining, although this was not as pronounced as in the wildtypes. This further suggests differing kinetics of infection between activation groups.

The percentage of cells becoming positive for viral protein by 48 hours was then quantified. Sv129 BMDMϕ showed a significantly higher percentage of cells staining positive for viral protein at 16 hours than IFNγR$^{-/-}$ macrophages (Figure 4.3a, $p<0.05$), but by 48 hours, both strains demonstrated similar levels of positivity (Figure 4.3b). However, IL-4 stimulation led to greater numbers of positive staining cells in both Sv129 and IFNγR$^{-/-}$ BMDMϕ (Figure 4.3a&b, green bars), reaching statistical significance by 48 hours ($p<0.05$).

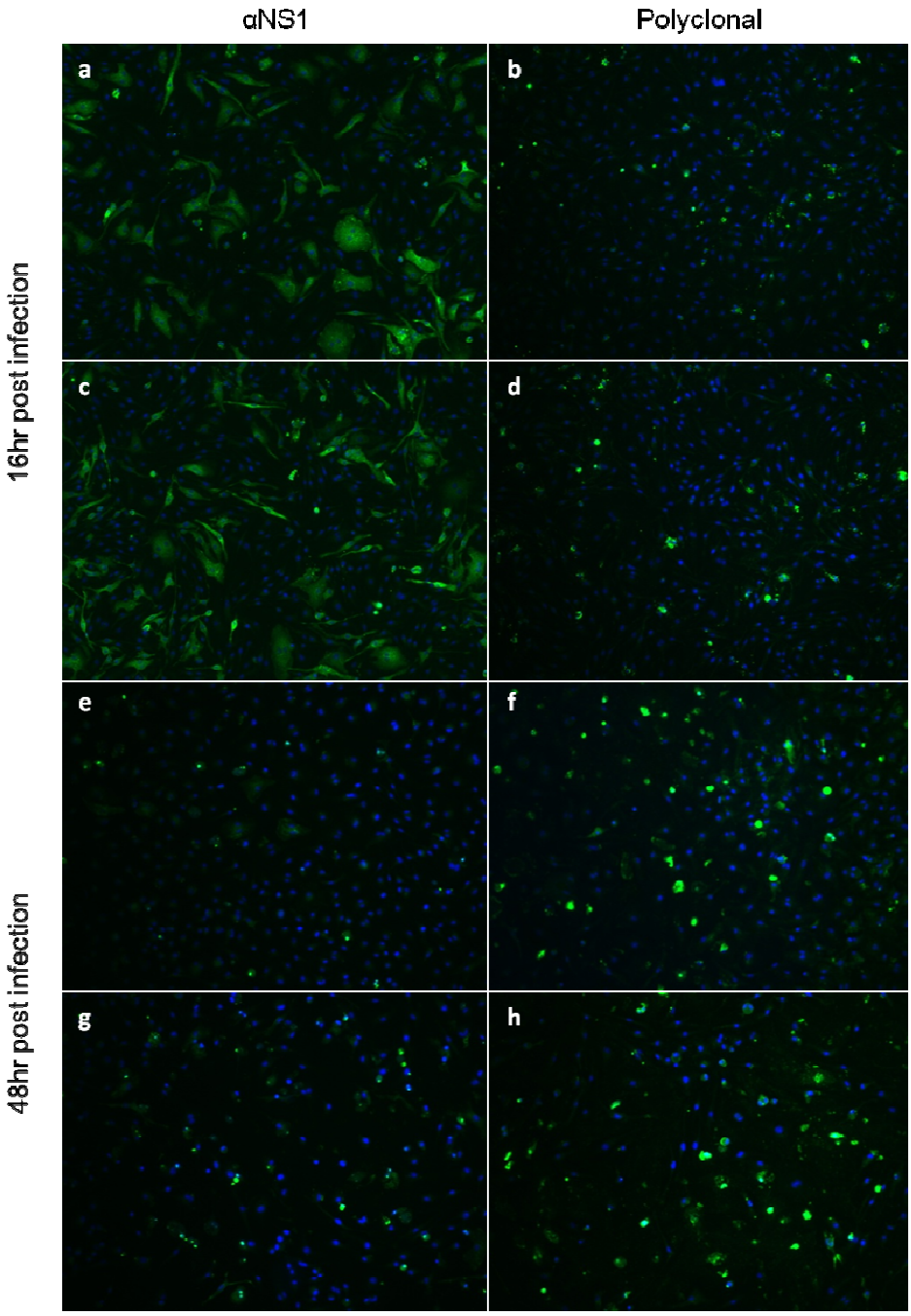

Figure 4.2 Immunofluorescent staining for influenza virus in IFNγR$^{-/-}$ BMDMϕ.
Classical (a,b,e&f) and alternatively activated (c,d,g&h) IFNγR$^{-/-}$ BMDMϕ were stained with an NS1 (a,c,e&g) or polyclonal anti-influenza antibody (b,d,f&h), followed by detection with Alexafluor 488 at either 16 (a-d) or 48 hours (e-f).
x20 magnification, 2 fields of vision counted, data are representative of 3 independent experiments.

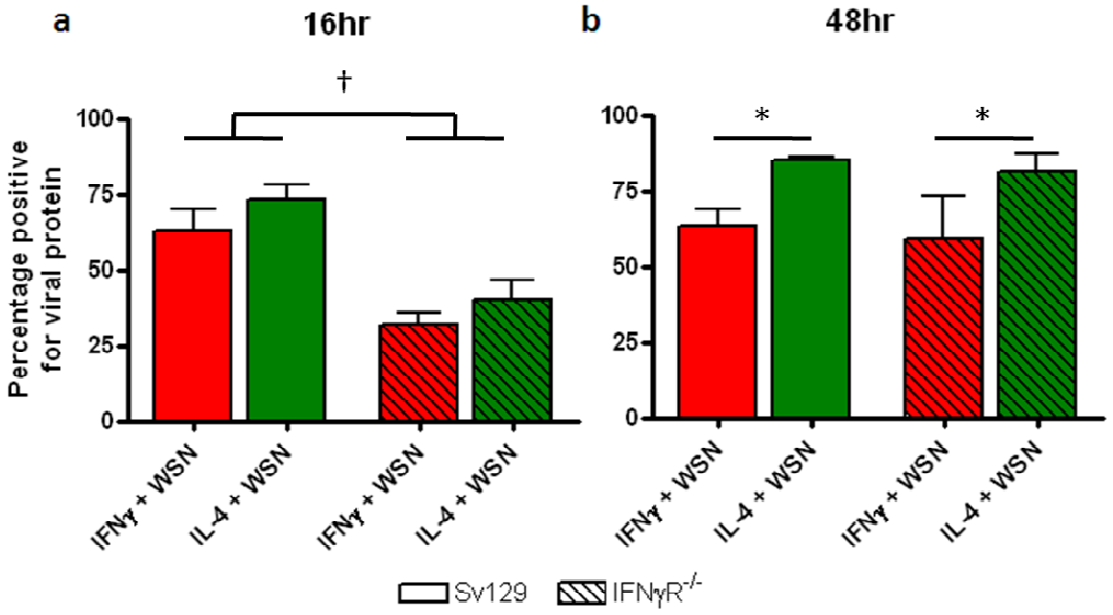

Figure 4.3 Percentage of polarised BMDMϕ infected.
Polarised Sv129 (n=3) and IFNγR$^{-/-}$ (n=3) were infected with MoI 10 WSN, stained with polyclonal anti-influenza A or NS1 antibody and the percentage of positive cells was calculated at 16 (a) and 48 (b) hours post infection. NS1 positive BMDMϕ were counted at 16 hours, while cells positive for anti-influenza antibody were counted at 48 hours. 2 fields of vision were counted.
* indicates statistical significance between cytokine treatment ($p<0.05$)
† indicates statistical significance between Sv129 and IFNγR$^{-/-}$ BMDMϕ ($p<0.05$)

This observation suggests that wildtype Sv129 BMDMϕ are permissive for rapid establishment of infection, with the alternatively activated group being most readily infected. Classically activated BMDMϕ did not demonstrate any further increase in staining for viral proteins at 48 hours, suggesting that IFNγ signalling prevents propagation of the infection, while the alternatively activated group show some increase in positive cell numbers by 48 hours. It was also evident that fewer IFNγR$^{-/-}$ BMDMϕ were positive for viral proteins early in infection, but by 48 hours reached levels similar to wildtype BMDMϕ, suggesting that WSN encounters a restriction on either entry or early protein synthesis in IFNγR$^{-/-}$ BMDMϕ. However, this block is overcome and by 48 hours, similar levels of viral proteins are observed in both Sv129 and IFNγR$^{-/-}$.

qPCR analysis of M1 expression at 48 hours post infection further emphasised the differing effect of IFNγ and IL-4 activation on WSN infection of BMDMϕ. mRNA is synthesised in the infected cell so detection of this RNA species is indicative of active viral replication. Quantification of M1 mRNA copy number, normalised against the housekeeping gene calnexin, showed the alternatively activated group of both strains to contain more M1 mRNA than their IFNγ stimulated counterparts (Figure 4.4, $p<0.0005$). Together with the percentage positivity calculated from the immunofluorescent staining, it may be inferred that alternatively activated macrophages are more permissive for influenza virus infection than their classical counterparts.

Despite lower levels of infection, IFNγR$^{-/-}$ BMDMϕ also showed significantly poorer survival than the wildtype Sv129 cells (Figure 4.5, $p<0.05$ at 16 and 48 hours). By 16 hours post infection, only 55% IFNγ stimulated IFNγR$^{-/-}$ BMDMϕ remained viable by trypan blue exclusion assay, which is similar to survival rates of IFNγR$^{-/-}$ M-CSF only control BMDMϕ following infection with WSN, while 90% of classically activated Sv129 BMDMϕ were viable at this timepoint (Figure 4.5a, red bars).

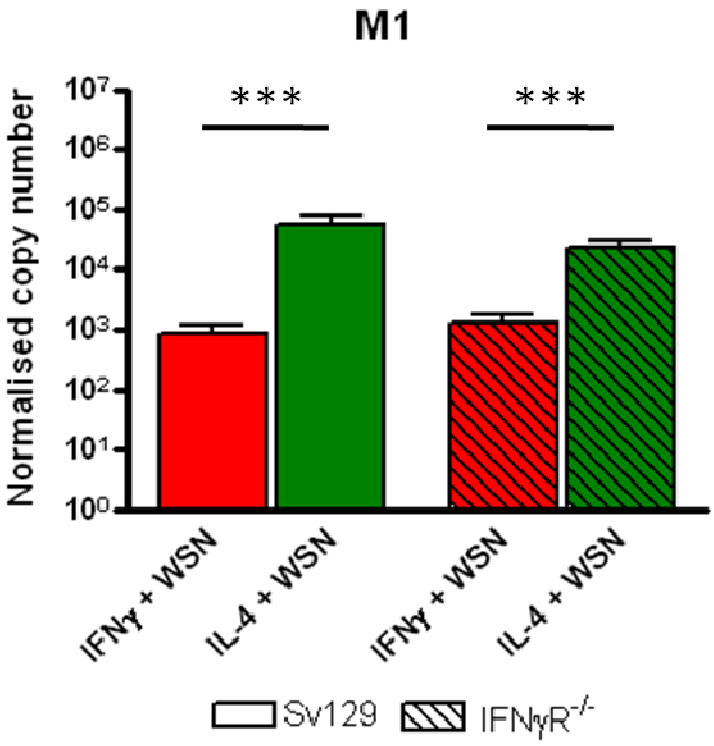

Figure 4.4 Real-time PCR for Influenza M1 mRNA.
M1 mRNA was assessed by qPCR at 48hrs post infection and copy number was normalised against strain matched infected controls activated with M-CSF alone. Data are expressed as copy number per 10^3 copies of the housekeeping gene CNX to normalise for amount of input RNA, as it was unknown how many copies of the M1 mRNA were produced per input virus. n=5 per strain.
*** indicates statistical significance between cytokine treatments ($p<0.0005$)

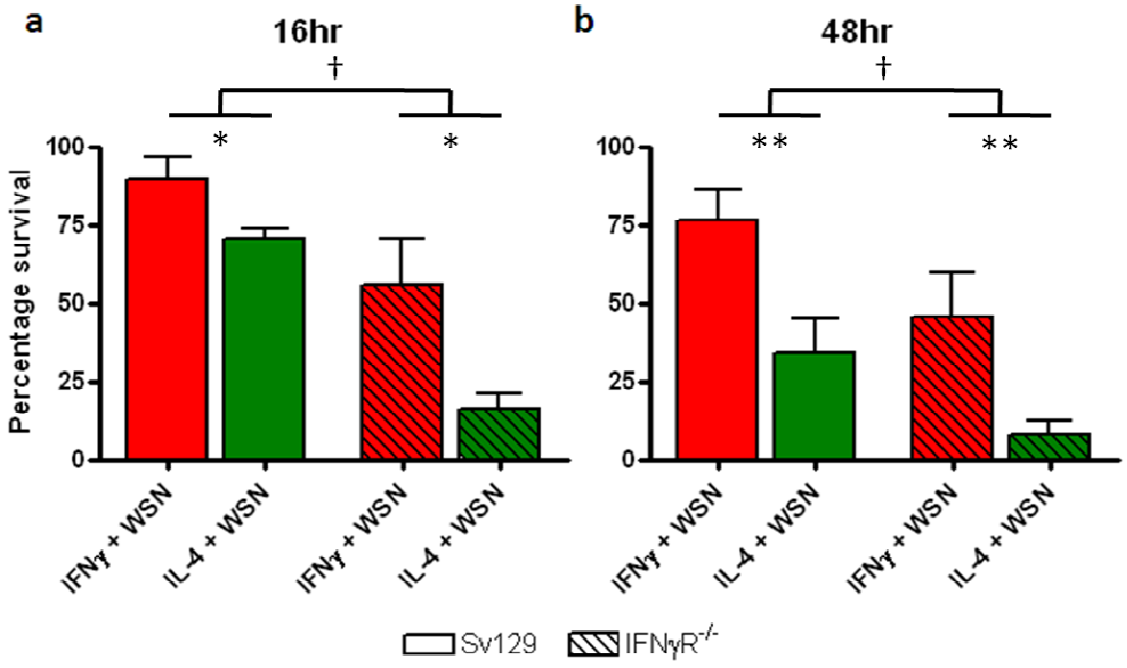

Figure 4.5 Percentage of polarised BMDMϕ surviving infection.
BMDMϕ were harvested and counted. Survival of polarised Sv129 (solid bars) and IFNγR$^{-/-}$ (hatched bars) following infection with MoI 10 WSN was assessed by trypan blue exclusion assay at 16 (a) and 48 hours (b), and normalised against strain matched mock infected polarised BMDMϕ. n=3 per strain at 16 hrs, n=6 per strain at 48 hrs.
* indicates statistical significance between cytokine treatments
(* $p<0.05$, ** $p<0.005$)
† indicates statistical significance between Sv129 and IFNγR$^{-/-}$ BMDMϕ ($p<0.05$)

BMDMϕ survival was further reduced by 48 hours (Figure 4.5b, red bars). BMDMϕ derived from both strains showed significantly lower survival following infection of IL-4 activated macrophages compared to the IFNγ stimulated group (Figure 4.5a&b, green bars, $p<0.05$ & $p<0.005$ at 16 and 48 hours respectively), consistent with the higher rates of infection in these populations. The alternatively activated IFNγR$^{-/-}$ BMDMϕ appeared to be most severely affected suggesting an interaction between strain and cytokine effect upon resilience to infection, but this did not achieve statistical significance ($p=0.07$). Taken together with the NS1 staining data, this suggests that IL-4 activation renders BMDMϕ more permissive for WSN, allowing rapid progression of infection and ultimately resulting in more cell death in the alternatively activated population.

4.1.2 Assessment of viral propagation in BMDMϕ

Despite the presence of NS1 being indicative of active infection, very little infectious virus was released into the supernatant of BMDMϕ from either strain or activation group (Figure 4.6). Supernatant was collected at 48 hours post infection and used to inoculate MDCK cells in a standard plaque assay as described in Chapter 2.3.2. Slightly higher titres were retrieved from IFNγR$^{-/-}$ BMDMϕ supernatant than from Sv129, but both were still markedly lower than the amount of input virus, (Figure 4.6, dashed line). This is consistent with previous studies that found influenza virus infection to be non-productive in macrophages (Rodgers & Mims, 1981; Wells *et al.*, 1978), despite being permissive for viral protein synthesis.

It is possible that infection of macrophages with WSN results in production of replication defective viral particles, as it is evident that NS1 and other viral proteins are being produced, but little infectious virus released. This was investigated by haemagglutination assay, whereby the presence of haemagglutinin-bearing virions causes agglutination of red blood cells regard-

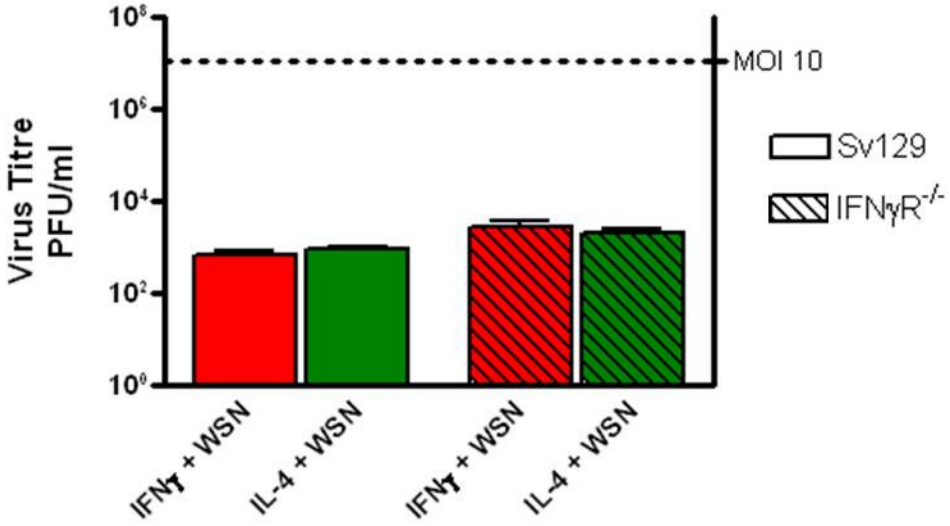

Figure 4.6 Virus titre retrieved from BMDMϕ supernatant.
Serial dilutions of supernatants from polarised infected BMDMϕ harvested at 48 hours post infection were assessed by plaque assay on MDCK cells. Following incubation with the supernatants for 1 hr, MDCK cells were washed, overlaid with agarose and assessed for plaque formation after 72hrs. The dotted line indicates input virus at an MoI of 10 used to infect the BMDMϕ. n=7 per strain

less of infectivity of the particles. Defective particles were not detected in these experiments as incubation of BMDMϕ supernatant with red blood cells did not result in haemagglutination (Figure 4.7). Supernatants had been subjected to two prior freeze, thaw cycles and so it is possible that some particles may have been destroyed. However, it is unlikely that high titres would be affected by several freeze thaw cycles, and haemagglutination would be observed in undiluted supernatant. As this did not occur, it suggests that high numbers of defective particles are not released from BMDMϕ and that influenza virus infection is truly abortive in this cell type.

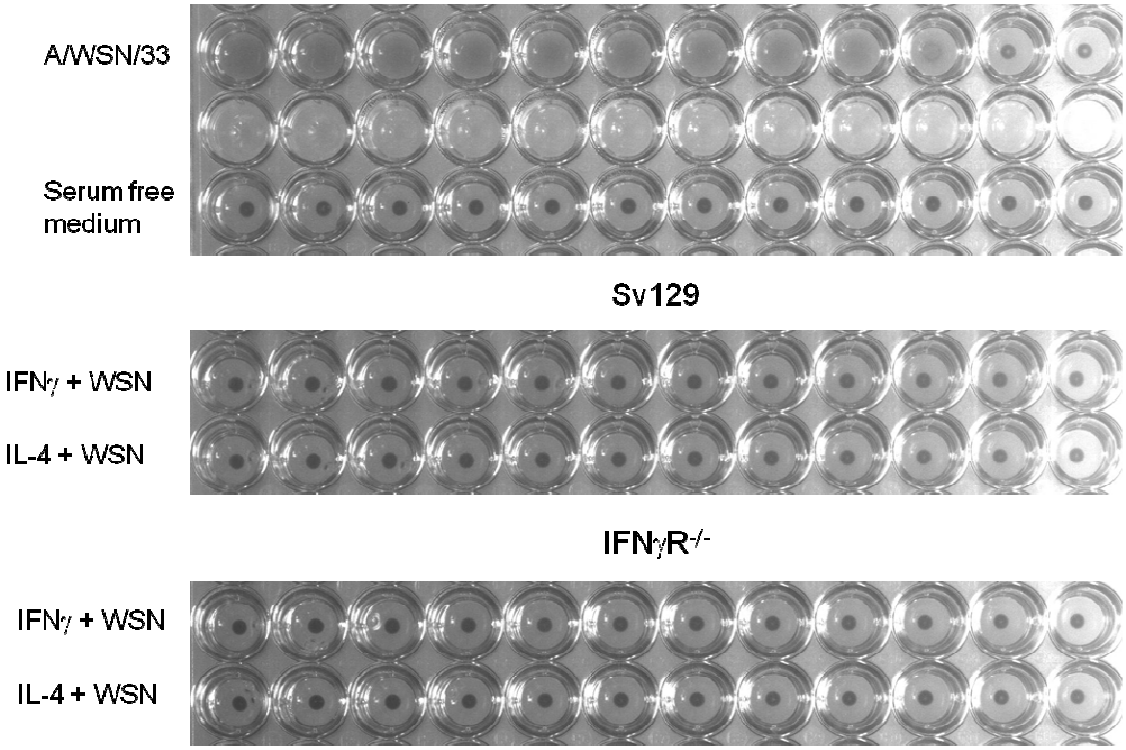

Figure 4.7 Haemagglutination assay with supernatants from infected polarised BMDMϕ
Serial dilutions of supernatants from infected polarised BMDMϕ harvested at 48 hour post infection were incubated with human red blood cells to assess presence of defective influenza virus particles. Diluted stock virus and serum free medium were used as positive and negative controls respectively

4.2 Cytokine response to influenza virus infection

Further to the preliminary data presented in Chapter 3.2.2, the inflammatory response to influenza virus infection of Sv129 and IFNγR$^{-/-}$ was investigated. Again, qPCR was used to assess mRNA expression of key markers, along with ELISA and functional bioassays to assess the levels of protein being produced.

4.2.1 mRNA expression profile in Sv129 and IFNγR$^{-/-}$ BMDMϕ upon infection with A/WSN/33

The cytokine response to WSN was investigated by infecting BMDMϕ of both strains after activation with either IFNγ or IL-4, as described in Chapter 2.2.4, and extracting RNA at either 16 or 48 hours post infection, along with RNA from activated mock infected control BMDMϕ. RNA was reverse transcribed into cDNA and diluted 1 in 20 before being assessed for gene expression by qPCR. The resulting data were analysed using Genex software and statistical analysis was carried out using the software package R, as described in Appendix 2.4. R was also used to present the data. Additionally, these data are summarised in Table 4.1 indicating up or downregulation in gene expression relative to strain matched BMDMϕ cultured in M-CSF alone. Relative expression data in its full context along with statistical significance are presented in Figure 4.8 and Figure 4.9.

In response to IFNγ, Sv129 BMDMϕ demonstrated upregulated iNOS mRNA expression at both 16 and 48 hours (Figure 4.8a&b, 1st panel, 1st box). Expression remained high, but was not further enhanced by infection with WSN (Figure 4.8a&b, 1st panel, 2nd box). As expected, IFNγ failed to induce significant iNOS expression from IFNγR$^{-/-}$ BMDMϕ at either timepoint (Figure 4.8a&b, 2nd panel, 1st box), indicating a significant difference between Sv129 and IFNγR$^{-/-}$ BMDMϕ ($p<0.05$ & $p<0.0005$ at 16 and 48hrs respectively).

16hr	IFNγ				IL-4			
	Sv129		IFNγR$^{-/-}$		Sv129		IFNγR$^{-/-}$	
Virus	-	+	-	+	-	+	-	+
iNOS	↑↑	↑↑	↑	↑↑	↑	↑↑	↑	↑↑
TNFα	↑	↑	↑	↑	↓	↑	↓	↔
IL-12p40	↑↑	↑↑	↔	↔	↔	↑↑	↑	↑
IL-6	ND	↑↑	ND	↑↑	↑↑	↑↑	↑↑	↑↑
Arg-1	↑	↔	↔	↔	↑	↑	↑	↑
CD206	↓	↓	↑	↔	↑	↔	↑	↔
IL-10	↔	↑	↔	↑	↔	↑	↔	↑
FIZZ	ND	↑↑	ND	↑↑	↑↑	↑↑	↑↑	↑↑

48hr	IFNγ				IL-4			
	Sv129		IFNγR$^{-/-}$		Sv129		IFNγR$^{-/-}$	
Virus	-	+	-	+	-	+	-	+
iNOS	↑↑	↑↑	↔	↑	↑	↑↑	↑	↑↑
TNFα	↑	↑	↔	↔	↓	↑	↓	↔
IL-12p40	↑↑	↑↑	↑	↑	↔	↑	↔	↔
IL-6	↑↑	↑↑	↓	↑	↔	↑	↑↑	↑
Arg-1	↑	↔	↔	↔	↑	↑	↑	↑
CD206	↓	↓	↔	↔	↔	↓	↑	↓
IL-10	↑	↑	↔	↔	↔	↑	↓	↔
FIZZ	↔	↔	↓	↔	↑↑	↑↑	↑↑	↑↑

Table 4.1 Summary of mRNA expression data.
mRNA expression was assessed by qPCR, followed by normalisation against stably expressed housekeeping genes and expressed as fold change relative to mock infected control BMDMϕ. Relative increases and decreases in expression following activation and infection of BMDMϕ are summarised here for each gene of interest.

ND, not detected;
↔, No change from M-CSF only controls (baseline);
↑ Marginal increase from baseline;
↑, <100 fold increase from baseline expression;
↑↑, >100 fold increase from baseline expression;
↓, Decreased expression from baseline

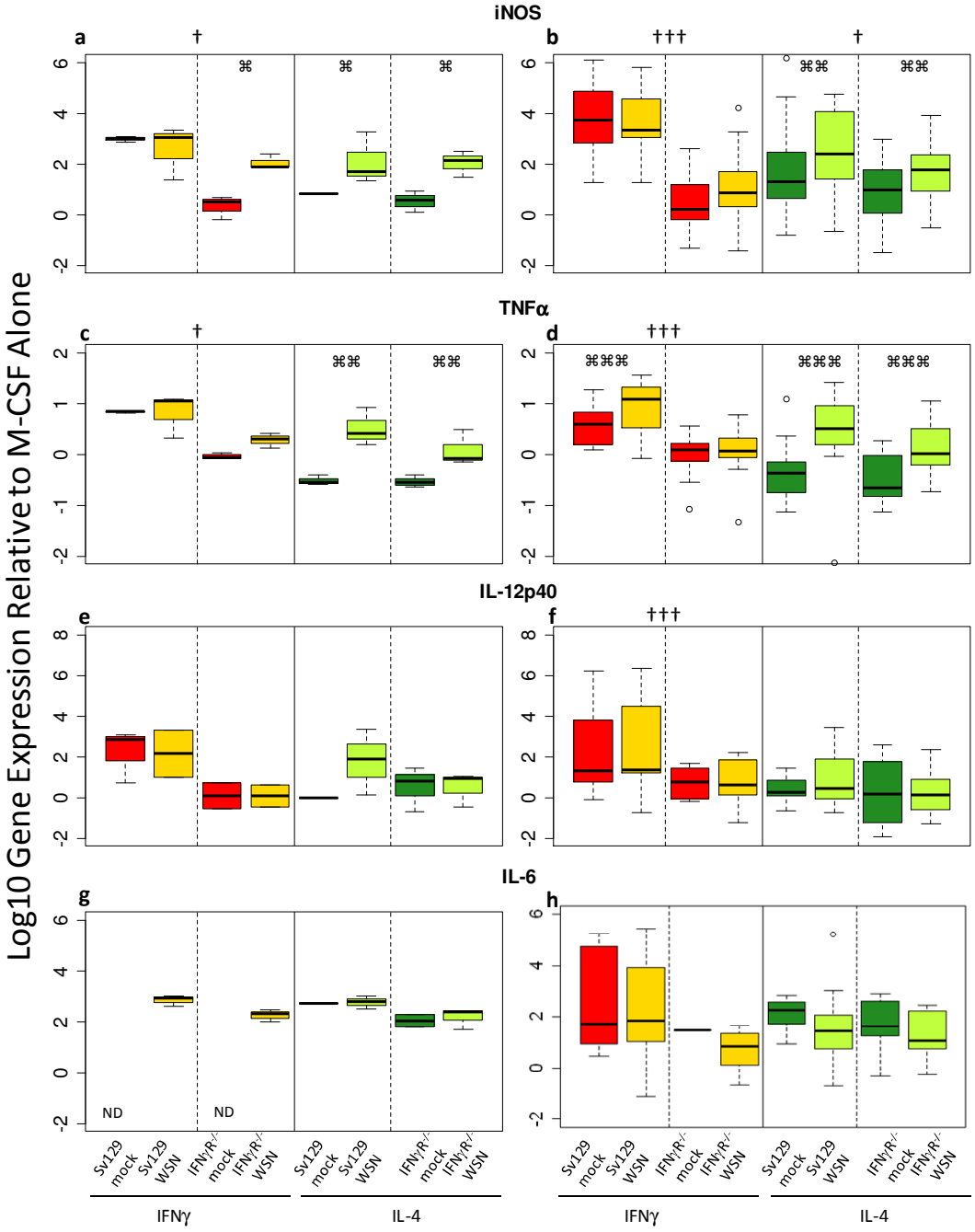
iNOS
TNFα
IL-12p40
IL-6
a
b
c
d
e
f
g
h
Log10 Gene Expression Relative to M-CSF Alone
ND
ND
Sv129 mock
Sv129 WSN
IFNγR-/- mock
IFNγR-/- WSN
IFNγ
IL-4

Figure 4.8 qPCR analysis of 'classical' gene expression.
mRNA was extracted and reverse transcribed to cDNA followed by qPCR assessment of gene expression at 16 hrs (a, c, e, g) and 48 hrs (b, d, f, h). Each gene was normalised against a standard curve and each sample was normalised against two housekeeping genes to account for discrepancies in RNA concentration. Each sample was then normalised against strain matched mock infected controls, activated with M-CSF only to obtain the fold change in mRNA expression relative to baseline levels. Data are expressed as Log10 gene expression relative to controls. n=3 per strain at 16hrs, Sv129 n=22 & IFNγR$^{-/-}$ n=19 at 48hrs, except IL-6 where n=13 & n=10 for Sv129 &IFNγR$^{-/-}$ respectively.
† indicates statistical significance between Sv129 and IFNγR$^{-/-}$ BMDMϕ († $p<0.05$, †† $p<0.005$, ††† $p<0.0005$)
⌘ indicates statistical significance between mock and infected BMDMϕ. Significance was graded as for †.

Infection of IFNγR$^{-/-}$ BMDMϕ with WSN, however, led to a significant upregulation of iNOS expression at 16 hours (Figure 4.8a, 2nd panel, 2nd box, $p<0.05$). This increase in expression was not maintained, however, and by 48 hours levels were not significantly different from the IFNγ only group (Figure 4.8b, 2nd panel, 2nd box). However, there was substantial variability in iNOS mRNA expression, indicating that a proportion of IFNγR$^{-/-}$ BMDMϕ were driven to express iNOS mRNA following infection. Despite the elevated iNOS expression observed early in infection, IFNγR$^{-/-}$ BMDMϕ were significantly impaired in their classical response, regardless of infection ($p<0.05$ & $p<0.0005$ at 16 and 48 hours respectively).

IL-4 stimulation of both Sv129 and IFNγR$^{-/-}$ BMDMϕ failed to induce significant iNOS expression (Figure 4.8a&b, 3rd & 4th panels, 1st box), but again, infection led to a significant increase at both timepoints (Figure 4.8a&b, 3rd & 4th panels, 2nd box, $p<0.05$ & <0.005 at 16 and 48 hours respectively). Additionally, IFNγR$^{-/-}$ BMDMϕ expressed significantly less iNOS mRNA compared to wildtype counterparts at 48 hours, even in the presence of virus ($p<0.05$). WSN infection appears to override the alternative activation induced by IL-4, causing iNOS mRNA to be expressed. Infection with WSN is sufficiently proinflammatory to drive iNOS expression from IFNγR$^{-/-}$ BMDMϕ, although this is impaired in the absence of IFNγ signalling.

A similar pattern of expression was observed for TNFα, with Sv129 BMDMϕ expressing elevated levels in response to IFNγ, which were further enhanced following infection with WSN (Figure 4.8c&d, 1st panel), and reached statistical significance at 48 hours ($p=0.0005$). As expected, IFNγR$^{-/-}$ BMDMϕ were significantly impaired in TNFα expression following exposure to IFNγ (Figure 4.8c&d, 2nd panel, 1st box, $p<0.05$ & $p<0.0005$ at 16 and 48 hours respectively), but at 16 hours, demonstrated elevated TNFα expression following infection (Figure 4.8c, 2nd panel, 2nd box). Similar to iNOS

expression, TNFα mRNA had returned to baseline expression by 48 hours in both mock and infected BMDMϕ.

IL-4 activation downregulated the TNFα response from both strains of macrophage, as expected (Figure 4.8c&d, 3rd & 4th panels, 1st box), but infection of IL-4 stimulated BMDMϕ with WSN resulted in significantly elevated TNFα mRNA in both strains of BMDMϕ when compared to mock infected alternatively activated macrophages (Figure 4.8c&d, 3rd & 4th panels, 2nd box, $p<0.005$ & $p<0.0001$ at 16 and 48 hours respectively). This again demonstrates the ability of WSN to drive an inflammatory response in the presence of alternatively activating stimuli. There was also a statistically significant interaction between infection and strain ($p<0.05$), demonstrating that although the virus is capable of driving a TNFα response from both strains of BMDMϕ, this is impaired in the IFNγR$^{-/-}$ cells compared to wildtype Sv129 BMDMϕ.

IL-12p40 mRNA expression was elevated in Sv129 BMDMϕ in response to IFNγ. Following infection, no further increase was seen compared with IFNγ alone (Figure 4.8, e&f, 1st panel). As expected, IFNγR$^{-/-}$ BMDMϕ showed an impaired inflammatory response at both timepoints compared to wildtype counterparts (Figure 4.8e&f, 2nd panel, 1st box, $p<0.0001$ at 48 hours). IL-12p40 mRNA was not detected in one mouse of each strain at 16 hours, despite this primer pair generating a standard curve with similar efficiency and limit of detection to primers for other genes of interest. Therefore the difference between strains did not reach statistical significance at this timepoint.

IL-4 stimulation failed to induce IL-12p40 mRNA expression from Sv129 BMDMϕ (Figure 4.8e&f, 3rd panel, 1st box), but induced variable expression of this mRNA in IFNγR$^{-/-}$ BMDMϕ (Figure 4.8e&f, 4th panel, 1st box). At 16 hours, these BMDMϕ displayed slightly elevated IL-12p40 expression, and by 48 hours substantial variation existed within this population. However, upon

infection of alternatively activated macrophages, IL-12p40 expression remained low with the exception of Sv129 BMDMϕ at 16 hours post infection, where expression was increased by the virus (Figure 4.8e, 3rd panel, 2nd box). It was surprising to note that IL-12p40 was poorly induced by WSN, when both iNOS and TNFα were efficiently upregulated following infection. However, these data are consistent with the preliminary mRNA expression data presented in Chapter 4.2.2, which showed a very modest increase in IL-12p40 mRNA expression following infection, and a variable response following IL-4 stimulation of IFNγR$^{-/-}$ BMDMϕ (Figure 3.10).

IL-6 was strongly upregulated at 16 hours post infection by both strains of BMDMϕ following infection with WSN but was undetectable in the mock infected IFNγ treated group (Figure 4.8g, 1st and 2nd panels). Furthermore, BMDMϕ from only one wildtype and two knockout mice activated with IL-4 showed expression of this mRNA (Figure 4.8g, 3rd and 4th panels, 1st box). However, infected BMDMϕ from both strains displayed greatly elevated IL-6 mRNA expression, regardless of activating cytokine. By 48 hours, IL-6 mRNA was detectable in all groups, but was highest in Sv129 BMDMϕ (Figure 4.8h, 1st panel, 1st box), although expression was highly variable. Expression in this group was not increased following infection (Figure 4.8h, 1st panel, 2nd box), while IFNγR$^{-/-}$ BMDMϕ were impaired in IL-6 mRNA expression in both mock and infected groups (Figure 4.8h, 2nd panel). IL-4 stimulation led to upregulated IL-6 mRNA in both Sv129 and IFNγR$^{-/-}$ BMDMϕ, with infection resulting in a modest decrease in both strains (Figure 4.8h, 3rd & 4th panels). The considerable variation within these groups, however, prevented these alterations in expression level between mock and infected BMDMϕ reaching statistical significance.

Taken together, the ability of IFNγR$^{-/-}$ BMDMϕ to mount a proinflammatory response to IFNγ stimulation is severely impaired, yet influenza virus is capable of inducing expression of proinflammatory mRNAs from IFNγR$^{-/-}$ BMDMϕ and

from alternatively activated Sv129 BMDMϕ. However, this inflammatory mRNA expression is induced to a lower level in the knock out macrophages compared with their wildtype counterparts and therefore inhibition of IFNγ signalling may be important in vivo in dampening the detrimental inflammatory response that leads to severe immunopathology.

As IFNγR$^{-/-}$ BMDMϕ exhibited a less proinflammatory cytokine response to influenza virus, it was likely that they may express markers of alternative activation to a greater extent than the wildtype Sv129 BMDMϕ. This was also investigated by qPCR. IL-4 activation induced significantly higher levels of Arg-1 mRNA expression from both strains of BMDMϕ at 16 and 48 hours, than did IFNγ (Figure 4.9a&b, all panels, 1st box, $p<0.005$ & $p<0.0001$ at 16 and 48 hours respectively). However, infection led to a slight decrease of this mRNA in all groups, reaching statistical significance at 48 hours post infection (Figure 4.9b, all panels, 2nd box, $p<0.005$). There appeared to be no difference between IFNγR$^{-/-}$ and Sv129 BMDMϕ in their capacity to retain Arg-1 mRNA expression in the face of viral infection, despite the reduced expression of iNOS in IFNγR$^{-/-}$ macrophages.

IL-4 stimulation significantly increased CD206 expression, compared with IFNγ in Sv129 BMDMϕ at both 16 and 48 hours (Figure 4.9c&d, 1st & 3rd panels, 1st box, $p<0.05$ & $p<0.005$). Additionally, CD206 mRNA was more strongly expressed in IFNγR$^{-/-}$ BMDMϕ regardless of activating stimulus when compared with identically treated wildtype BMDMϕ (Figure 4.9c&d, 2nd & 4th panels, 1st box, $p=0.05$, $p<0.0001$, IFNγ at 16 and 48 hrs respectively & $p<0.05$, IL-4 at 48 hours). However, upon infection, CD206 expression was markedly reduced in all groups investigated, significantly so in IL-4 stimulated BMDMϕ at 48 hours (Figure 4.9d, 3rd & 4th panels, $p<0.0001$). This contradicts the preliminary data

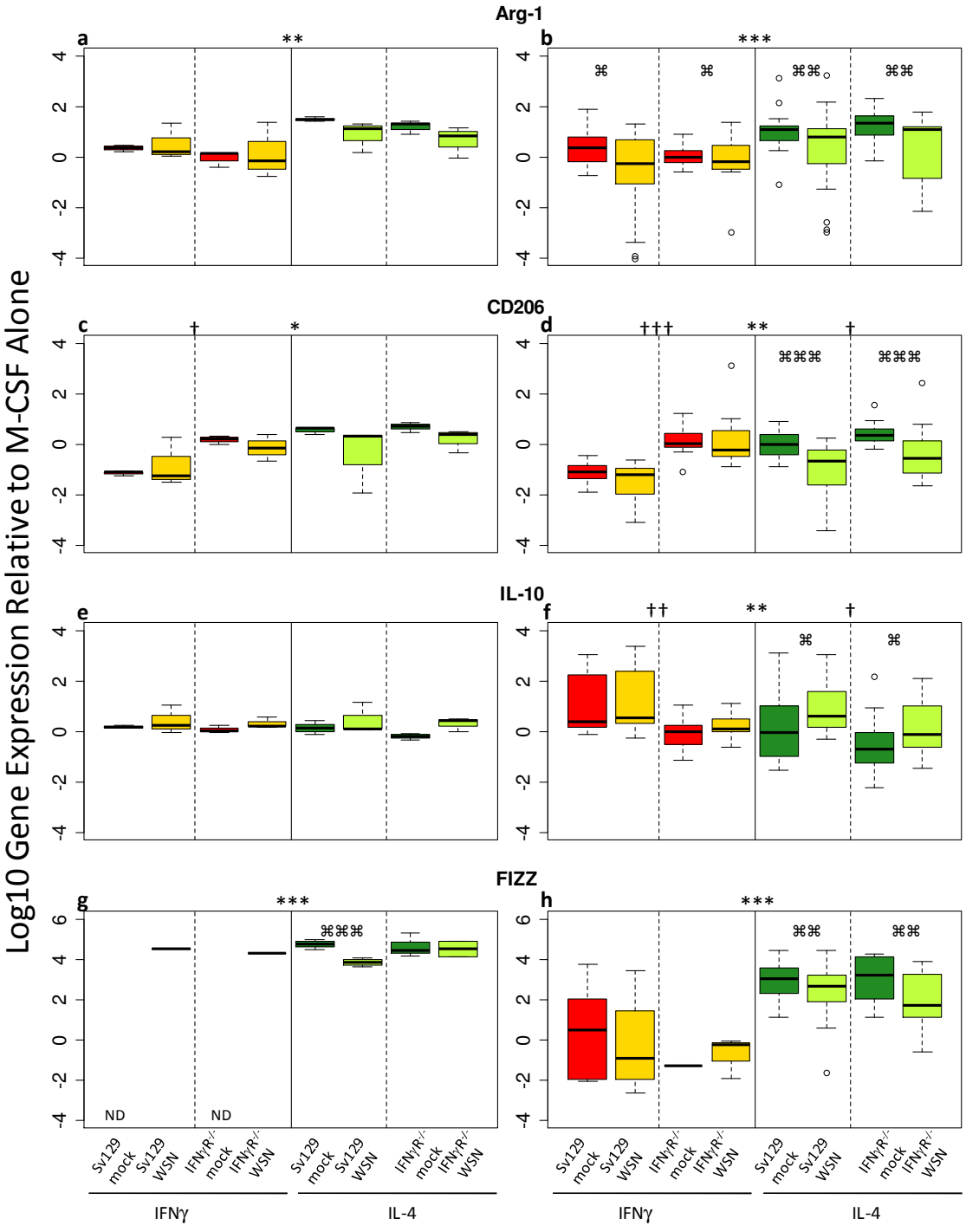
Arg-1
CD206
IL-10
FIZZ
a
b
c
d
e
f
g
h
Log10 Gene Expression Relative to M-CSF Alone
ND
ND
Sv129 mock
Sv129 WSN
IFNγR-/- mock
IFNγR-/- WSN
IFNγ
IL-4

Figure 4.9 qPCR analysis of 'alternative' gene expression.
As for Figure 4.8, RNA was extracted and reverse transcribed, followed by qPCR analysis. Gene specific standard curves and two independent housekeeping genes were used to normalise the data, before fold change relative to non-activated, mock infected controls was calculated.
Data are expressed as Log10 gene expression relative to controls. n=3 per strain at 16hrs (a, c, e, g), Sv129 n=22 & IFNγR$^{-/-}$ n=19 at 48hrs (b, d, f, h), except for FIZZ where n=13 & n=10 for Sv129 & IFNγR$^{-/-}$ respectively.
* indicates statistical significance between cytokine treatments
(* $p<0.05$, ** $p<0.005$, *** $p<0.0005$)
† indicates statistical significance between Sv129 and IFNγR$^{-/-}$ BMDMϕ
⌘ indicates statistical significance between mock and infected BMDMϕ. Significance was graded as for *.

which showed elevated CD206 expression following infection, but may reflect the small sample size of the preliminary experiments. The data also showed a statistically significant interaction between infection and cytokine ($p<0.005$), indicating that the response to infection was significantly different depending on which activating cytokine had been given.

At 16 hours post infection, IL-10 mRNA expression remained around baseline, with a marginal increase observed following infection in all groups (Figure 4.9e). However, by 48 hours, IFNγR$^{-/-}$ BMDMϕ demonstrated significantly lower IL-10 expression than their wildtype counterparts following IFNγ (Figure 4.9f 1st and 2nd panels, 1st box, $p<0.005$) and IL-4 stimulation (Figure 4.9f, 3rd & 4th panels, 1st box, $p<0.05$). Infection led to significantly enhanced IL-10 mRNA expression in alternatively activated BMDMϕ of both strains (Figure 4.9f, 3rd & 4th panels, 2nd box, $p<0.05$). There was also a significant interaction between infection and cytokine ($p=0.05$), indicating that the IL-10 mRNA response to virus differed between alternative and classically activated BMDMϕ. The upregulation of IL-10 in infected BMDMϕ may be a result of type I IFN signalling following detection of the virus and upregulated proinflammatory cytokine mRNA such as TNFα and iNOS, resulting in induction of IL-10 to return the cytokine microenvironment to homeostasis.

BMDMϕ from only one mouse of each strain expressed FIZZ in response to IFNγ followed by virus at 16 hours post infection, while IL-4 alone resulted in strong expression in both strains at this timepoint, as expected. However, the alternatively activated Sv129 BMDMϕ showed a significant decrease in FIZZ mRNA upon infection (Figure 4.9g, 3rd panel, 2nd box, $p<0.0005$). By 48 hours, IFNγ stimulated BMDMϕ demonstrated varying levels of FIZZ expression, and infection induced no significant alterations (Figure 4.9h, 1st and 2nd panels). IL-4 activated macrophages expressed significantly elevated FIZZ mRNA at 48 hours compared to IFNγ stimulated cells (Figure 4.9h, 3rd and 4th panels, 1st box, $p<0.005$), but expression was significantly downregulated compared to the

IL-4 only group following infection (Figure 4.9h, 3rd and 4th panels, 2nd box, $p<0.005$). It is interesting that FIZZ mRNA expression appears to be elevated transiently at early timepoints following exposure to IL-4, but declining by 48 hours. In vivo, this protein is thought to play a role in wound healing; expression of FIZZ is upregulated following surgery but not sustained in the absence of pathogen driven T cell help (Loke *et al.*, 2007). It would appear that FIZZ may be rapidly upregulated following macrophage activation but in the absence of suitable T cell stimulation, expression wanes. IL-4 stimulation may be sufficient to induce FIZZ expression but the very high expression observed at 16 hours is not sustained.

Taken together with the Arg-1 mRNA expression data, this demonstrates that influenza virus downregulates the alternative activation phenotype in both strains of BMDMϕ, while inducing a proinflammatory response from these cells. Despite being less capable of mounting an inflammatory reaction, IFNγR$^{-/-}$ BMDMϕ could not sustain an alternatively activated response in the presence of virus, similar to their wildtype counterparts.

4.2.2 Functional cytokine response to A/WSN/33 infection in Sv129 and IFNγR$^{-/-}$ BMDMϕ

Bioassays for functional iNOS and Arg-1 showed little increase in iNOS activity at 16 hours following IFNγ activation of Sv129 BMDMϕ (Figure 4.10a, first solid red bar) when compared to non activated controls (Figure 4.10a, solid grey bar). IFNγ stimulation resulted in a modest increase in iNOS activity, while mRNA expression was strongly upregulated. A further modest increase in iNOS activity was observed following infection, but this failed to reach statistical significance (Figure 4.10a, solid red bars). iNOS was substantially elevated by 48 hours post infection, but showed no difference between mock and infected BMDMϕ (Figure 4.10b, solid red bars). IL-4 stimulation failed to

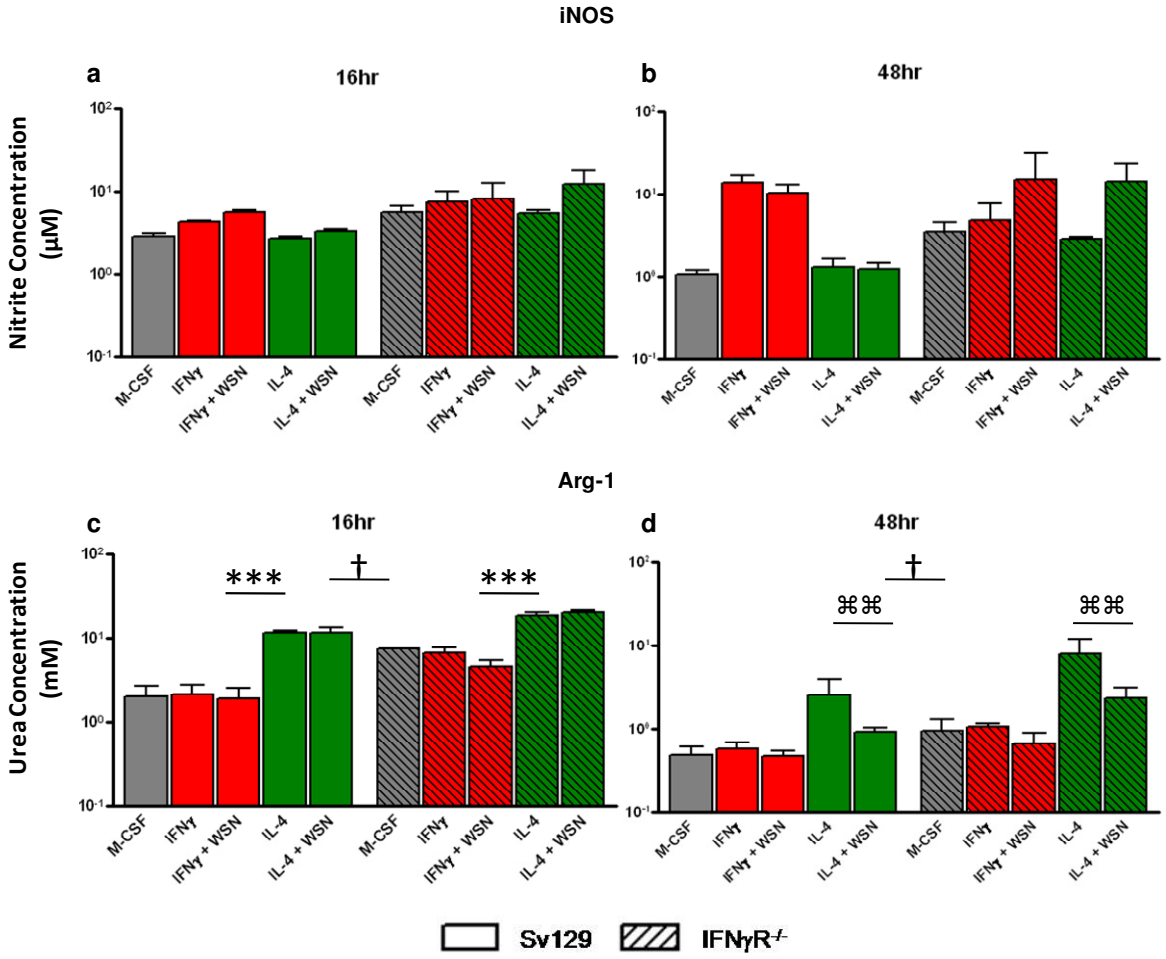

Figure 4.10 Bioassay for functional iNOS and Arg-1.
iNOS and Arg-1 activity in each BMDMϕ population was assessed by bioassay. iNOS activity was measured by incubating supernatants with Greiss reagent, while cell lysates were incubated with L-Arg to determine Arg-1 activity, as described in Chapter 2.6 & 2.7.
Non-activated mock infected controls have been included as grey bars to indicate baseline activity of each enzyme.
n=3 per strain at 16 hour, n=6 per strain at 48 hours
* indicates statistical significance between cytokine treatments (* $p<0.05$, ** $p<0.005$, *** $p<0.0005$)
† indicates statistical significance between Sv129 and IFNγR$^{-/-}$ BMDMϕ
⌘ indicates statistical significance between mock and infected BMDMϕ. Significance was graded as for *

increase iNOS activity at either timepoint (Figure 4.10a&b, first solid green bar), consistent with the qPCR data. However, at 16 hours, there was an increase in functional iNOS in the infected IL-4 activated Sv129 BMDMϕ (Figure 4.10a, 2nd solid green bar), consistent with the PCR data which showed upregulation of iNOS mRNA in this population, although to a much greater extent. However, by 48 hours post infection, iNOS activity was not elevated above baseline (Figure 4.10b, 2nd solid green bar).

Levels of iNOS at 16 hours post infection in both IFNγ and IL-4 IFNγR$^{-/-}$ BMDMϕ were comparable to M-CSF controls (Figure 4.10a, hatched bars). This was marginally enhanced upon infection of the IL-4 stimulated group (Figure 4.10a, hatched green bars), whereas mRNA data showed a two log increase in expression following infection of both classical and alternative BMDMϕ at this timepoint (Figure 4.8a, 2nd & 4th panels). At 48 hours post infection, influenza virus caused enhanced iNOS activity in both the IFNγ and IL-4 stimulated infected groups, which did not acheive statistical significance, while IL-4 alone remained unable to increase iNOS activity (Figure 4.10b, hatched bars). The discrepancies between mRNA expression and protein activity indicate that mRNA levels do not necessarily correlate with functional protein, as there is a delay in translation of mRNA to newly synthesised protein and also the sensitivity of the bioassay is much lower than that of qPCR.

In Sv129 BMDMϕ, Arg-1 activity remained around baseline in response to IFNγ at both 16 and 48 hours (Figure 4.10c&d, solid red bars). Although activity increased significantly in response to IL-4 at both timepoints (Figure 4.10c&d, 1st solid green bar, $p<0.0005$) and remained elevated upon infection at 16 hours, by 48 hours following infection Arg-1 activity was elevated to a significantly lesser extent than that observed for IL-4 alone in Sv129 BMDMϕ (Figure 4.10c&d, 2nd solid green bar, $p<0.005$).

Consistent with the mRNA data (Figure 4.9a&b, 2nd panel), Arg-1 activity was not increased in IFNγR$^{-/-}$ BMDMϕ by treatment with IFNγ alone or following infection, as expected (Figure 4.10c&d, hatched red bars). IL-4 stimulation resulted in significantly increased Arg-1 activity at 16 hours compared with non-activated M-CSF controls ($p<0.0005$), and maintained elevated levels upon infection of the IL-4 activated group at 16 hours post infection (Figure 4.10c, hatched green bars). However, similar to Sv129 BMDMϕ, IFNγR$^{-/-}$ macrophages showed significantly less Arg-1 activity in the infected IL-4 group than for IL-4 alone at 48 hours (Figure 4.10d, hatched green bars, $p<0.005$). These findings indicate that infection with WSN drives BMDMϕ towards a classical, proinflammatory phenotype even in the absence of IFNγ signalling, yet a proportion of cells remain alternatively activated when given a secondary challenge with inflammatory stimuli. As shown in Figure 4.3, complete infection of the BMDMϕ population was not achieved and therefore it is possible that the uninfected population of cells are capable of maintaining their alternative phenotype and continue to exhibit Arg-1 activity despite the presence of influenza virus. It is also interesting that decreased Arg-1 activity does not appear to occur until later in infection. This indicates that although a percentage of cells may remain uninfected and therefore alternatively activated, the protein half-life of Arg-1 will have an effect on the activity observed at the later timepoint. The estimated half-life of Arg-1 is 30 hours and so by 48 hours, much of the protein induced by IL-4 will be degrading in the infected population.

IL-12p40 and TGFβ were assessed by ELISA at both 16 and 48 hours post infection. Consistent with the mRNA expression data, IL-12p40 concentration was significantly increased in Sv129 BMDMϕ in response to IFNγ and not IL-4 ($p<0.005$), but was very slightly enhanced upon infection at 16hrs (Figure 4.11a, solid red bars). IL-4 failed to upregulate IL-12p40, with a non-significant elevation observed in response to virus (Figure 4.11a, solid green bars), while mRNA expression showed a two log increase (Figure 4.8e, 3rdpanel)

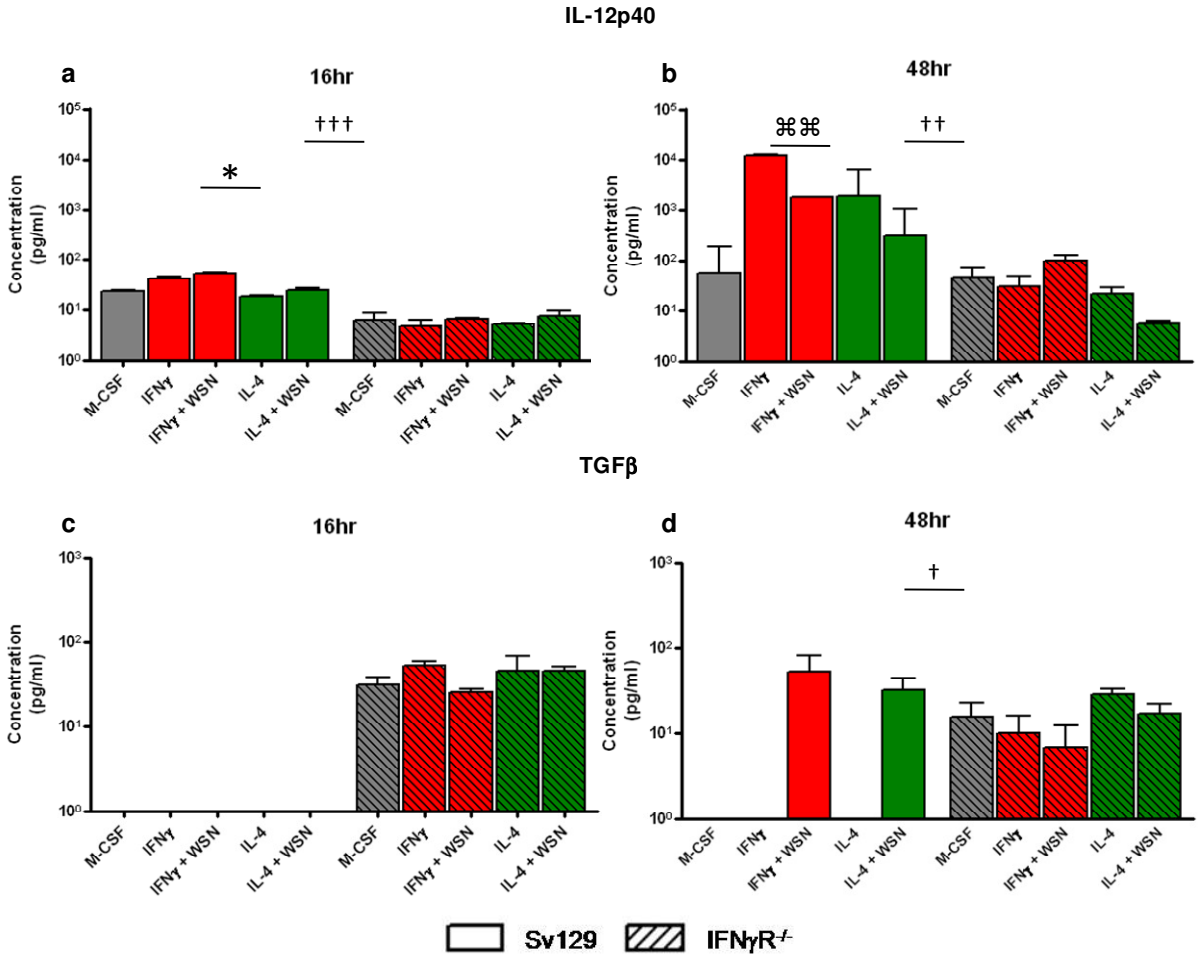

Figure 4.11 ELISA detection of IL-12p40 and TGFβ.
IL-12p40 and TGFβ concentrations in the supernatant were measured by ELISA. Baseline levels for each strain of BMDMϕ are indicated by grey bars.
n=3 per strain at 16 hour, n=6 per strain at 48 hours
* indicates statistical significance between cytokine treatments (* p<0.05, **p<0.005, *** p<0.0005)
† indicates statistical significance between Sv129 and IFNγR$^{-/-}$ BMDMϕ
⌘ indicates statistical significance between mock and infected BMDMϕ. Significance was graded as for *

By 48 hours post infection, all groups demonstrated greatly elevated IL-12p40 concentrations (Figure 4.11b, solid bars), with the biggest increase being in the classically activated population. Infected groups showed lower concentrations of IL-12p40 when compared to cytokine alone, which achieved statistical significance in the IFNγ treated Sv129 BMDMϕ only ($p<0.005$), although levels remained higher than baseline. There was some variability within infected populations at the mRNA level, and mRNA expression may not necessarily relate to new protein synthesis.

IFNγR$^{-/-}$ BMBMϕ exhibited significantly lower IL-12p40 concentrations than Sv129 cells in all groups at 16 hours (Figure 4.11a, hatched bars, $p<0.0005$), consistent with the mRNA expression data (Figure 4.8e). At 48 hours, increased concentration was evident in the infected IFNγ exposed BMDMϕ only (Figure 4.11b, second hatched red bar), while the IL-4 stimulated cells showed decreased IL-12p40 (Figure 4.11b, 2nd hatched green bar), consistent with the qPCR data (Figure 4.8f, 2nd & 4th panels), although neither reached statistical significance. As the alternatively activated BMDMϕ showed a decrease in IL-12p40 upon infection (Figure 4.11b, second hatched green bar), this suggests a reduced inflammatory response to the virus and maintenance of the alternative phenotype in this group, consistent with the iNOS and Arg-1 bioassay data. Overall, the ELISA data shows an impairment of IFNγR$^{-/-}$ BMDMϕ to produce IL-12p40 in response to A/WSN/33 at both 16 and 48 hours post infection, compared with Sv129 BMDMϕ.

TGFβ was also assessed, but was below the level of detection at 16 hours in wildtype Sv129 BMDMϕ (Figure 4.11c). By 48 hours post infection, TGFβ could be readily detected in infected macrophages of both classical and alternative populations (Figure 4.11d, solid bars). In contrast, IFNγR$^{-/-}$ BMDMϕ showed significantly higher levels of TGFβ compared to wildtype macrophages ($p<0.05$) and maintained similar concentrations in all populations assessed at 16 hours (Figure 4.11c, hatched bars). By 48 hours, differences between groups were

emerging with infection of IL-4 activated BMDMϕ maintaining TGFβ concentration, while infected IFNγ primed BMDMϕ demonstrated a decrease, perhaps due to decreased cleavage activation of the protein or enhanced protein shut off induced by the virus in this population. Interestingly, this cytokine appears to be constitutively expressed by IFNγR$^{-/-}$ BMDMϕ with relatively little change between activated groups, while only induced late in infection in Sv129 macrophages indicating underlying discrepancies between these two strains of mice.

Influenza virus is known to shut off host protein synthesis enabling it to produce viral proteins. In both strains of BMDMϕ, all infected groups demonstrated decreased protein concentrations or activities at 48 hours, with the exception of iNOS in IFNγR$^{-/-}$ cells. As this consistently occurred at the later timepoint, it indicates that after the virus has shut off new protein synthesis, degradation of remaining cellular protein may be responsible for the observed decline in concentration. The upregulated iNOS activity at 48 hours post infection may be a result of initial virus induced protein remaining active in the supernatant as, taking into account the variability between samples, levels of activity are similar at both 16 and 48 hours. The lack of IFNγ signalling prevents an increase following exposure to IFNγ and so the infected groups demonstrate higher levels of activity due to virus induced iNOS prior to host protein shut off.

4.3 Summary of results and discussion

Immunofluorescent staining highlighted differing patterns of infectivity between alternative and classically activated macrophages. The weaker anti-NS1 staining observed in IL-4 primed Sv129 BMDMϕ at 16 hours, concurrent with stronger polyclonal antibody staining suggests that alternative activation renders BMDMϕ more readily infectable and so the infection progresses more rapidly. There may be little NS1 protein remaining in the cytoplasm at this

timepoint, perhaps having already begun translocation to the nucleus. The stronger polyclonal staining indicates that greater quantities of viral proteins may have been generated early in infection. This is consistent with other studies demonstrating that nitric oxide can limit viral replication (Croen, 1993; Karupiah *et al.*, 1993; Zaragoza *et al.*, 1997), which may enable the virus to survive and replicate more efficiently within the alternatively activated macrophages. Alternatively, it is possible that the enhanced phagocytic capacity of alternatively activated macrophages (Loke *et al.*, 2007; Tiemessen *et al.*, 2007) enables them to take up viral particles and debris more efficiently than their classically activated counterparts and so there are more viral envelope proteins within the alternatively activated BMDMϕ, which are then readily stained. Priming with IL-4 led to enhanced infection and poor viability in both Sv129 and IFNγR$^{-/-}$ BMDMϕ but despite this, very little infectious virus was retrieved from the supernatant of any population investigated. It also appears unlikely that formation of defective particles was responsible for the polyclonal staining observed at late timepoints infection, rather that immunodominant proteins, most likely HA and NA, accumulate within the cell but do not assemble into virions. HA and NA are known to assemble in rafts below the cell membrane at regions where budding occurs (Takeda *et al.*, 2003). It is likely that this process occurs in infected BMDMϕ as the polyclonal anti-influenza antibody detects clusters of antigen which are predominantly cytoplasmic, suggesting accumulation of protein. However, what prevents these accumulated proteins from assembling into virions is unknown.

Interestingly, activated IFNγR$^{-/-}$ BMDMϕ show constitutively higher expression of CD206 mRNA than Sv129 macrophages (Figure 4.9c&d). This surface receptor has been implicated in influenza virus attachment and infection of macrophages. Reading and colleagues have demonstrated that the efficiency with which a given strain of virus can infect macrophages directly correlates with the ability to bind CD206, and that infection can be inhibited by competitive binding of mannan, a known ligand for CD206 (Reading *et al.*,

2000). The ability to bind and subsequently infect macrophages is dependent on the presence of glycosylation sites on the head regions of HA and NA proteins. Reading et al demonstrated that the H1N1 influenza virus, PR8, possessed poorly glycosylated HA and NA proteins and hence was inefficient at infecting macrophages. BJx109, a virus which shares all internal gene segments with PR8 but expresses H3N2 on its surface, infected macrophages efficiently and demonstrated glycosylated surface proteins (Reading *et al.*, 2000). Although sialic acid is known to be the target receptor for influenza virus binding, these interactions do not necessarily lead to infection. Recently a model has been proposed whereby the virus initially binds to sialic acid which brings it into close proximity with endocytic receptors such as CD206, which require an additional interaction via glycosylated residues to occur prior to efficient internalisation and infection (Tate *et al.*, 2010a; Upham *et al.*, 2010). Despite the elevated CD206 mRNA expression, IFNγR$^{-/-}$ BMDMϕ demonstrate less efficient early infection than their Sv129 counterparts. WSN virus is derived from the parent virus A/WS/33, and was generated by serial passage through mouse brain (Francis & Moore, 1940), during which time it obtained neurovirulence in mice. A similar derivative was also generated, NWS/33 (Stuart-Harris, 1939), which is known to contain only one glycosylation site on its HA, while glycosylation is absent from the HA of the parent strain WS/33 (Job *et al.*, 2010). Sequence comparison between these and the WSN strain confirms that WSN has only two glycosylation sites on the HA head, and the absence of a conserved site on WSN NA has been implicated in the neurovirulence displayed by this virus (Li *et al.*, 1993). This indicates that the glycosylation pattern displayed by WSN HA & NA is unlikely to facilitate binding to the mannose receptor and so upregulation of this sialylated surface receptor would not contribute to viral infection.

IFNγR$^{-/-}$ BMDMϕ demonstrated lower percentage positivity for viral proteins early in infection, but by 48 hours, were comparable to wildtype counterparts. This impaired early infection observed in IFNγR$^{-/-}$ BMDMϕ may be due to poor

entry of the virus into the cell or a non-permissive environment upon infection. As previously discussed, influenza virus binds sialic acid, and the role of this interaction may be to bring the virus into juxtaposition with endocytic receptors, rather than facilitate entry in its own right. Similar to CD206, the IFNγ receptor becomes endocytosed into acidified vesicles where it releases its ligand and joins a cellular pool to be recycled back to the cell surface (Farrar & Schreiber, 1993), making it a candidate receptor for influenza virus attachment and entry. Glycosylation of the IFNγ receptor has been shown to be vital for ligand binding, while removal of sialic acid by treatment of cells with neuramindase abrogated binding, implicating sialic acid in functional binding of IFNγ to its receptor (Fischer *et al.*, 1990). It is possible that the absence of the IFNγ receptor may result in a lack of suitable sialylated endocytic receptors and therefore restrict the amount of virus able to enter the cell and consequently lower levels of viral staining are observed at 16 hours post infection.

However, by 48 hours post infection, the percentage of BMDMϕ staining positive for viral proteins were similar in both wild type and receptor deficient macrophages. Taken together with the PCR data that showed IFNγR$^{-/-}$ BMDMϕ to be capable of mounting an early but unsustained inflammatory response to WSN, it is likely that IFNγR$^{-/-}$ BMDMϕ become more permissive for viral replication as time progresses, as in the absence of IFNγ signalling, neither iNOS or IL-6 expression is maintained. Sv129 BMDMϕ also generated a rapid inflammatory response to infection and yet viral proteins were readily detected at 16 hours post infection, further suggesting that IFNγR$^{-/-}$ BMDMϕ are less permissive for viral attachment and entry. However, once inside, the lack of a sustained inflammatory response allows the virus to rapidly attain equivalent levels of viral positivity as those seen in wildtype Sv129 BMDMϕ. In addition to this, IL-4 stimulated BMDMϕ of both strains show enhanced positivity, consistent with a less inflammatory environment being more permissive for infection. Although alternatively activated BMDMϕ are known to have greater

phagocytic capacity than their classically activated counterparts (Tiemessen *et al.*, 2007), this is unlikely to contribute to the elevated positivity observed at 16 hours postinfection in this group of cells as at this timepoint, NS1 positive cells were assessed. NS1 is synthesised during active replication within the cell and so phagocytosed debris and virions would not result in significant detection of this protein, although it is possible that this phagocytic property of the alternative BMDMϕ may enhance the level of staining observed at 48 hours using the polyclonal anti-influenza antibody.

Conversely, it may be possible that viral entry is not altered or impaired by the absence of the IFNγ receptor but that differing metabolism of wildtype and IFNγR$^{-/-}$ macrophages following infection has an effect on viral permissiveness. Classical Sv129 BMDMϕ are primed with IFNγ prior to infection, which results in enhanced ability to rapidly express antiviral and proinflammatory mediators (Nathan *et al.*, 1983). Furthermore, these cells are capable of responding to autocrine IFNγ induced by IL-12 (Di Marzio *et al.*, 1994; Fultz *et al.*, 1993), therefore amplifying a positive feedback loop by which these macrophages remain activated. Following WSN infection, Sv129 BMDMϕ rapidly increase expression of proinflammatory mRNAs, a response which is sustained throughout the duration of the timecourse investigated. However, IFNγR$^{-/-}$ BMDMϕ demonstrate a reduced respiratory burst early in infection as these cells could not become primed by exposure to exogenous IFNγ (Figure 4.8). This limited burst is further impaired with time as the cells are unable to respond to either exogenous or autocrine IFNγ. The influenza virus polymerase complex has been shown to localise with active RNA polymerase II in order to efficiently steal caps from cellular mRNAs undergoing synthesis (Engelhardt *et al.*, 2005). The reduced mRNA expression observed in IFNγR$^{-/-}$ cells may impede early virus replication as the cellular machinery utilised by the virus does not undergo the rapid and prolonged burst of activity that occurs within wildtype cells, ultimately limiting the amount of replicating virus observed at 16 hours post infection. However, this restriction may be overcome with time

due to the absence of antimicrobial mediators such as nitric oxide, allowing the virus to accumulate to comparable levels in the IFNγR$^{-/-}$ BMDMϕ.

Despite upregulated expression of inflammatory mediators iNOS and IL-12p40 mRNA early in infection in both Sv129 and IFNγR$^{-/-}$, corresponding increases in protein were not necessarily observed. Surprisingly, IFNγR$^{-/-}$ BMDMϕ showed higher baseline levels of functional iNOS and Arg-1 than their wildtype Sv129 counterparts at both timepoints (Figure 4.10a&b, grey bars), but Sv129 BMDMϕ did not demonstrate increased iNOS activity following infection, while IFNγR$^{-/-}$ BMDMϕ showed some enhancement demonstrating that the virus was capable of driving iNOS activity despite the absence of IFNγ signalling. Both strains continued to demonstrate some Arg-1 activity in infected alternatively activated macrophages, suggesting that although strong, the proinflammatory signal given by influenza virus is not overwhelming and also that both strains of BMDMϕ are capable of altering their phenotype in response to sequential stimuli. Furthermore, infection of BMDMϕ did not result in positive staining in every cell. Between 15 and 30% of Sv129 and IFNγR$^{-/-}$ BMDMϕ respectively remained negative for viral proteins at 48 hours post infection. It is likely that these cells are capable of maintaining their alternative phenotype and exhibiting Arg-1 activity despite influenza virus infection in neighbouring cells, especially in the IFNγR$^{-/-}$ cells which are unable to respond to paracrine IFNγ.

The differing levels of cell death and infection seen between strains and polarised groups, necessitate a cautious approach to interpretation of the qPCR data. mRNA expression may not be fully representative of the whole population of cells, only the surviving proportion. Therefore it is not possible to infer with certainty the effect that virus has on polarised BMDMϕ as those surviving may be those remaining uninfected, or those most readily able to alter their phenotype.

In addition to this, it must be remembered that this source of macrophages is heterogeneous by nature. When the bone marrow is harvested from femurs and macrophages isolated by adherence in the presence of M-CSF, a variety of maturational stages are present and it takes several days for all the monocyte progenitors to acquire a mature BMDMϕ phenotype and adhere to the plastic. This may be of some importance in preventing 100% infection, as it has previously been shown that culture of elicited macrophages on plastic for three or seven days alters the total number of cells that can become infected (Rodgers & Mims, 1981). The longer the cells remained in culture, the more permissive they were to infection. This study used thioglycollate elicted peritoneal macrophages, which are more uniform in maturation than BMDMϕ and so this suggests that the degree of maturation may be important in deciding the relative resistance of the cell to influenza virus infection. This in turn is likely to have a downstream effect on the ability of a given cell to maintain its activated phenotype following infection.

TGFβ appeared to be constitutively active in IFNγR$^{-/-}$ macrophages but only detectable late in infection in Sv129 BMDMϕ. This difference in baseline TGFβ expression between Sv129 and IFNγR$^{-/-}$ BMDMϕ is intriguing as it appears that these strains of mice may have differing resting phenotypes of macrophage, or at least differing background expression of certain genes. Previous studies utilising IFNγR$^{-/-}$ mice generated on the Sv129 background have found no discrepancies between these and wildtype animals with regards to lymphocyte composition or natural killer cell activity. IgM responses were found to be normal, as was expression of both MHC I and II. However, upon viral infection, the IgG_{2a} response was impaired in the IFNγR$^{-/-}$ animals (Huang *et al.*, 1993). However, no study has addressed the role or the phenotype of macrophages derived from these mice, and consequently cytokine responses have also been ignored. Therefore it is completely unknown whether disruption of the IFNγ receptor results in altered cytokine expression from macrophages and other cell types. The data presented herein would suggest

that there is a difference in baseline levels at least in iNOS (Figure 4.10a & b), Arg-1(Figure 4.10c & d) and TGFβ (Figure 4.11c & d). This may influence the ability of these BMDMϕ to respond to virus and be important in the impeded early establishment of infection observed. Each protein examined here demonstrated enhanced baseline levels in comparison with Sv129 cells, and so it may be simply that these mice are higher producers with no relative change in protein expression. However, it may be important to further investigate baseline differences in protein expression and activity when making direct comparisons between IFNγR$^{-/-}$ and Sv129 BMDMϕ in the future.

In light of the data presented, it appears likely that the overall impairment of the proinflammatory response in influenza virus infected IFNγR$^{-/-}$ BMDMϕ may have important implications in vivo, as a 'cytokine storm' like scenario may be avoided upon inhibition of IFNγ signalling.

5 In vivo infection of Sv129 and IFNγR$^{-/-}$ mice

Influenza virus infection of Sv129 or IFNγR$^{-/-}$ mice has not previously been documented, although B and T cell responses have been investigated in mice lacking the IFNγ gene on C57B/6 and BALB/c backgrounds (Bot *et al.*, 1998; Graham *et al.*, 1993). These studies showed functional cellular and humoral responses following challenge, but did not address the role played by the innate immunity. The following experiments aim to address this by infecting Sv129 and IFNγR$^{-/-}$ mice with A/WSN/33 and investigating differences in clinical outcome, viral load, immunopathology and cytokine expression profile between these strains of mice.

5.1 Pilot infections of Sv129 and IFNγR$^{-/-}$mice

As demonstrated in Chapter 4, IFNγR$^{-/-}$ BMDMϕ show an impaired inflammatory response when infected with influenza virus A/WSN/33. It was also apparent that the kinetics of viral infection differed between the wildtype and knockout strains of BMDMϕ. These findings could have important implications in vivo, with the possibility of subverting the damaging 'cytokine storm' scenario.

5.1.1 Clinical outcome of infection with A/WSN/33

Due to the absence of information in the literature regarding infection of these strains of mice with influenza virus, it was first necessary to titrate the viral dose based on the available data for C57Bl/6 and BALB/c mice (Hashimoto *et al.*, 2007; Jackson *et al.*, 2008). As such, a series of pilot experiments were performed with a range of infectious doses.

Sv129 mice were infected intranasally under anaesthesia with 1x10^3, 5x10^3 or 1x10^4 pfu of WSN in 40µl PBS, as described in Chapter 2.1.2, and monitored daily for weight loss and clinical symptoms. These included, in order of presentation, ruffling of the fur, hunched posture, increased respiratory rate and immobility. Mice were euthanized at 2, 4, 6, and 8 days post infection, or upon loss of 30% of their starting weight, in accordance with terms of the UK Home Office project licence.

Severity of disease increased in a dose dependent manner in Sv129 mice, as evidenced by weight loss and diminishing clinical score. Mice infected with 1x10^3 and 5x10^3 pfu displayed limited clinical symptoms (Table 5.1) and lost less than 20% of their initial body mass during the course of infection (Figure 5.1a). Those infected with the lowest infectious dose appeared to regain some weight by day 8 which, coupled with the lack of clinical symptoms, suggests these mice successfully recover from infection. However, mice infected with 1x10^4 pfu demonstrated rapid weight loss, with several mice losing up to 30% of their starting weight by day 7 (Figure 5.1a), when this pilot experiment was terminated due to the severity of illness. Clinical symptoms manifested earlier and with greater intensity in these mice, compared with those infected at lower doses (Table 5.1).

IFNγR$^{-/-}$ BMDMϕ displayed poorer viability upon infection with WSN, compared with their Sv129 counterparts, and so it was possible that in the absence of a functional antiviral response, IFNγR$^{-/-}$ mice might display more severe disease, due to inability to control viral replication. As such, IFNγR$^{-/-}$ mice were infected with the lowest dose of 1x10^3 pfu. This, however, led to no observable symptoms and the infected mice maintained their starting body mass, although they failed to gain weight in line with mock infected controls (Figure 5.1b). This supports the hypothesis proposed in Chapter 4.3, that the absence of IFNγ signalling results in an impaired inflammatory response and therefore ameliorated disease.

		Ruffled fur	Hunched posture	Increased respiratory rate	Immobility
1x10^3 PFU	d2	-	-	-	-
	d4	-	-	-	-
	d6	-	-	-	-
	d8	+	-	-	-
5x10^3 PFU	d2	-	-	-	-
	d4	+	+	-	-
	d6	+	+	-	-
	d8	+	+	-	-
1x10^4 PFU	d2	-	-	-	-
	d4	+	+	+	+
	d6	+	+	+	+
	d8	+	+	++	++

Table 5.1 Clinical symptoms in Sv129 mice following infection with WSN at varying dose.
Clinical symptoms were monitored daily and scored on the scale – (no clinical symptoms) to +++ (severe presentation). Mock infected mice consistently showed no clinical symptoms, while infected animals presented increasingly severe symptoms with time in a dose dependent manner. Average score of n=3/timepoint is presented.

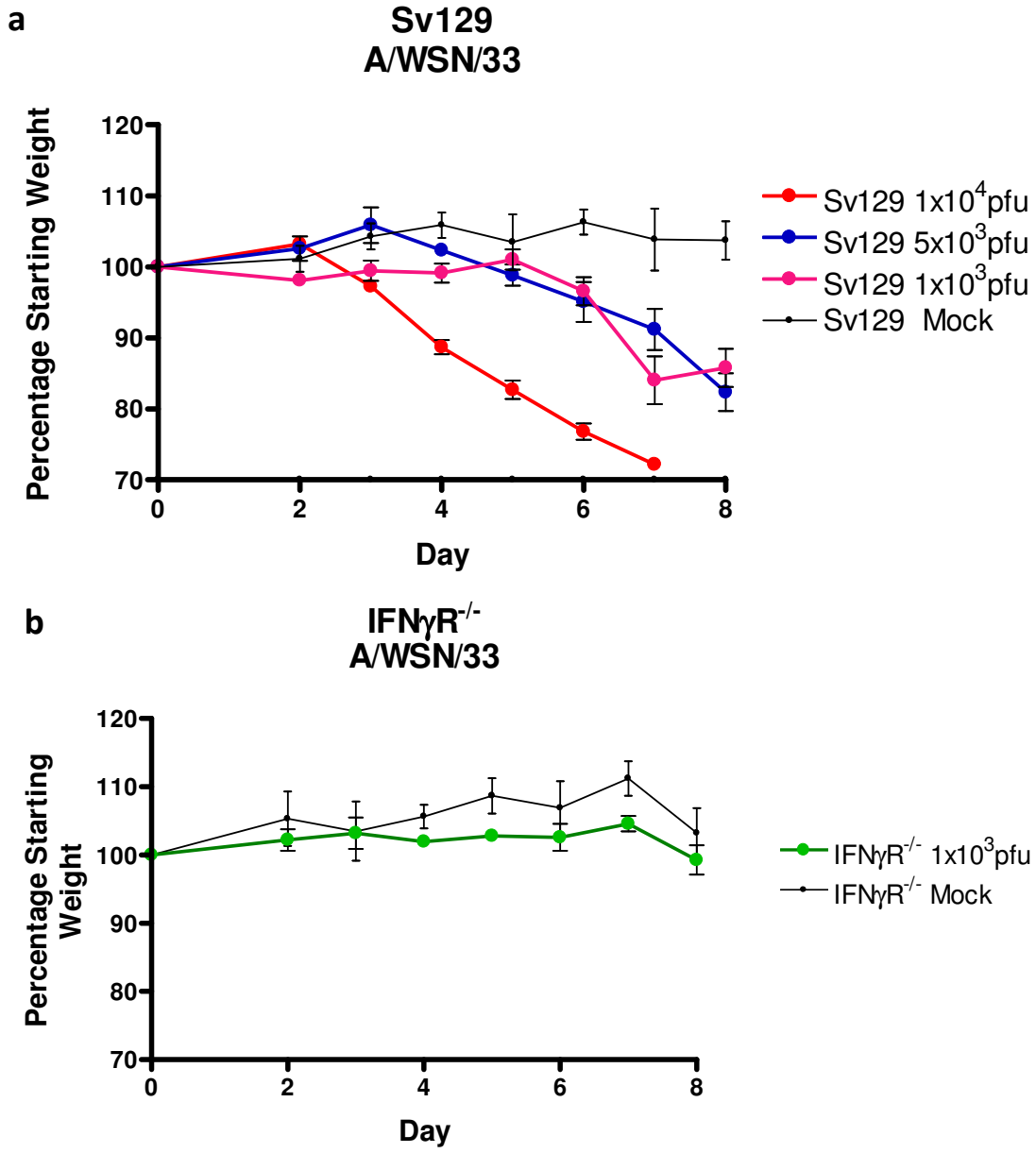

Figure 5.1 Weight loss following infection with varying infectious dose.
Sv129 and IFNγR-/- mice were infected with WSN to establish appropriate infectious dose for future infections. Weight loss was monitored daily as an indication of disease severity. Mock infected mice were inoculated intranasally with 40µl PBS as controls. n=3 per timepoint.

5.1.2 Immunopathology following A/WSN/33 infection

Lungs were harvested following euthanasia of infected and control mice at day 8 post infection. Tissues were fixed and processed to sections as described in Chapter 2.8, followed by staining with haematoxylin and eosin to assess tissue damage as a result of infection.

Infected Sv129 animals demonstrated congestion of the airspaces in a dose dependent manner, compared with mock infected controls (Figure 5.2a-d). Those infected with the lowest dose showed very slight congestion in small areas of the lung, but this increased in density and size with increasing infectious dose, until most of the lung was affected in the $1x10^4$ pfu infected mice.

Surprisingly, IFNγR$^{-/-}$ mice showed several areas of substantial cellular infiltration compared with mock infected controls (Figure 5.2e&f), which was not reflected in the clinical score. The absence of clinical symptoms and weight loss suggested that these mice easily recovered from a subclinical infection, while the histology shows tissue damage at day 8 post infection.

However, as this dose was insufficient to cause observable clinical symptoms in the IFNγR$^{-/-}$ mice, $1x10^4$ pfu was selected for further experiments. Although this led to severe disease in wildtype Sv129 animals, it was necessary to use an infectious dose that would cause manifestation of symptoms in the knockout mice.

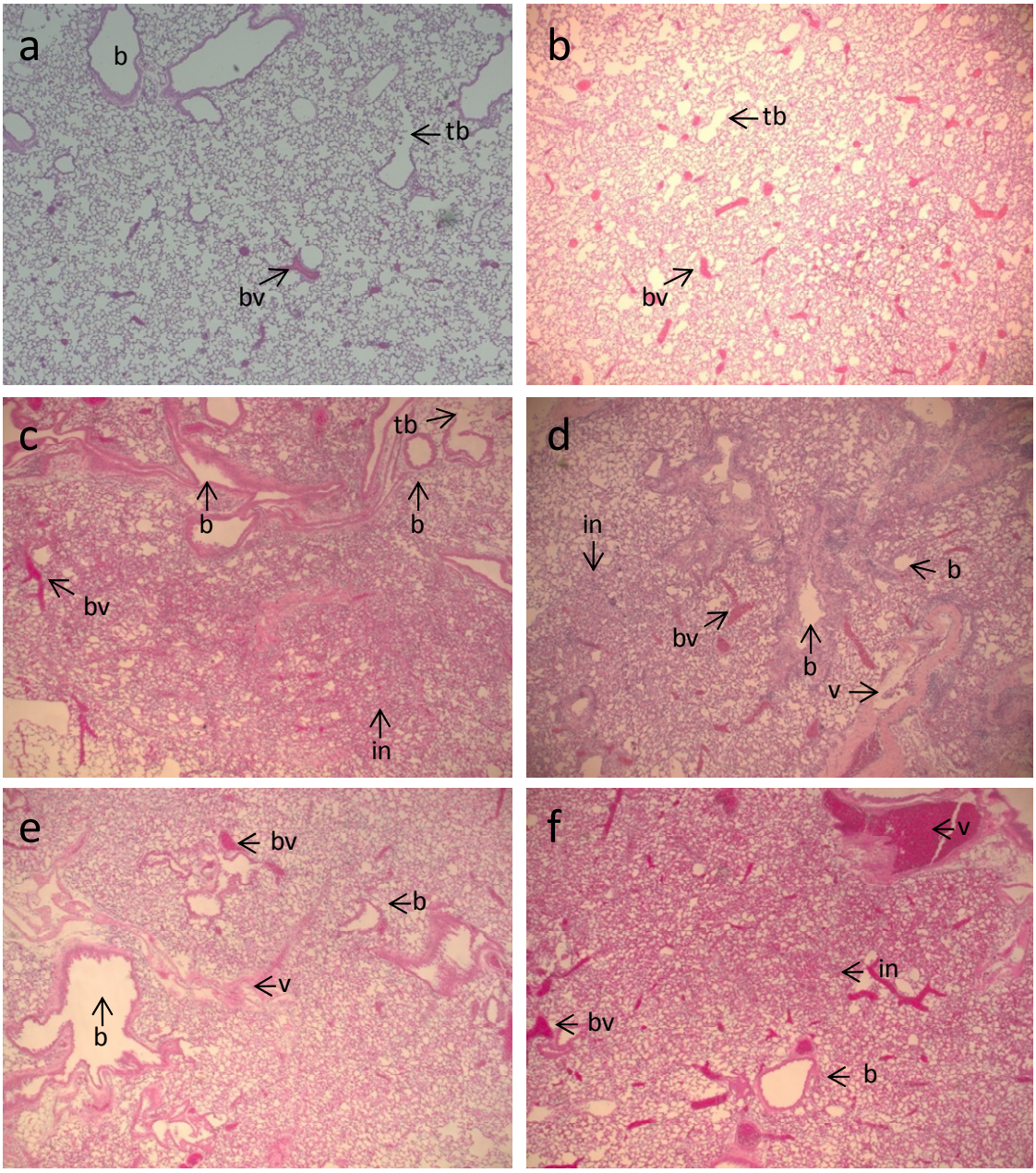

Figure 5.2 Immunopathology in the lung following infection with varying infectious dose.
Sv129 mice inoculated with infectious dose of 1x10^3 (b), 5x10^3 (c) or 1x10^4 (d) demonstrated cellular infiltration into the lungs compared to mock infected animals (a) in a dose dependent manner. IFNγR$^{-/-}$ also demonstrated congestion in the lungs following infection with a low infectious dose, 1x10^3 (f), compared to strain matched mock controls (e). All x5 magnification.
b, bronchiole; tb, terminal bronchiole; v, vein; bv, blood vessel; in, inflammation
n=4 per timepoint

5.2 Infection of Sv129 and IFNγR$^{-/-}$ mice

Following the pilot studies described above, larger groups of mice of both backgrounds were infected with 1x10^4 pfu and the experiments repeated (n=7 at each timepoint). Lungs were harvested for virus titre, RNA extraction and histology following euthanasia at days 2, 4, 6 and 8 post infection.

5.2.1 Clinical outcome of infection with A/WSN/33

As demonstrated in the pilot studies, Sv129 mice infected with 1x10^4 pfu suffered severe disease, with early onset of clinical symptoms (Table 5.2). These mice rapidly lost weight and had reached around 75% of their original body mass by day 8 post infection (Figure 5.3a). IFNγR$^{-/-}$ mice however, showed very little weight loss during the course of the infection, and had begun to recover their starting weight by day 8 (Figure 5.3a). Similarly, only mild clinical symptoms were observed in these mice (Table 5.2), suggesting ameliorated disease and recovery.

Lungs were harvested and homogenised for virus plaque assay, which revealed differences in lung virus titre between the two strains of mice (Figure 5.3b). IFNγR$^{-/-}$ mice demonstrated lower viral titres at each timepoint assessed compared with wildtype Sv129 mice. However, both strains showed declining titres towards the end of the experiment, suggesting that both were capable of clearing the virus. These strain discrepancies were also reflected in the viral M1 gene qPCR results (Figure 5.4), whereby IFNγR$^{-/-}$ animals showed significantly lower expression of this viral mRNA in the lungs than Sv129 mice ($p=<0.0005$). Consistent with the virus titres, IFNγR$^{-/-}$ mice showed declining expression by day 8, but interestingly, elevated expression between days 4 and 6 post infection was coincident with the point at which these mice showed most substantial weight loss, before beginning to recover concurrent with reduced titres and M1 expression. Also of interest, IFNγR$^{-/-}$ BMDMϕ were infec-

		Ruffled fur	Hunched posture	Increased respiratory rate	Immobility
Sv129	d2	-	-	-	-
	d4	++	+	-	+
	d6	++	++	+	+
	d8	+++	++	+	+
IFNγR$^{-/-}$	d2	-	-	-	-
	d4	-	-	-	-
	d6	+	+	-	+
	d8	+	+	+	+

Table 5.2 Clinical symptoms following infection with 1x10^4 PFU WSN.
Sv129 mice demonstrated early onset of symptoms which became increasingly severe throughout the course of infection. IFNγR$^{-/-}$ animals, however, displayed mild symptoms following infection with the same infectious dose, onset of which were delayed until day 6 post infection. Mock infected control animals of both strains presented no clinical symptoms. Average scores presented, n=7 per timepoint.

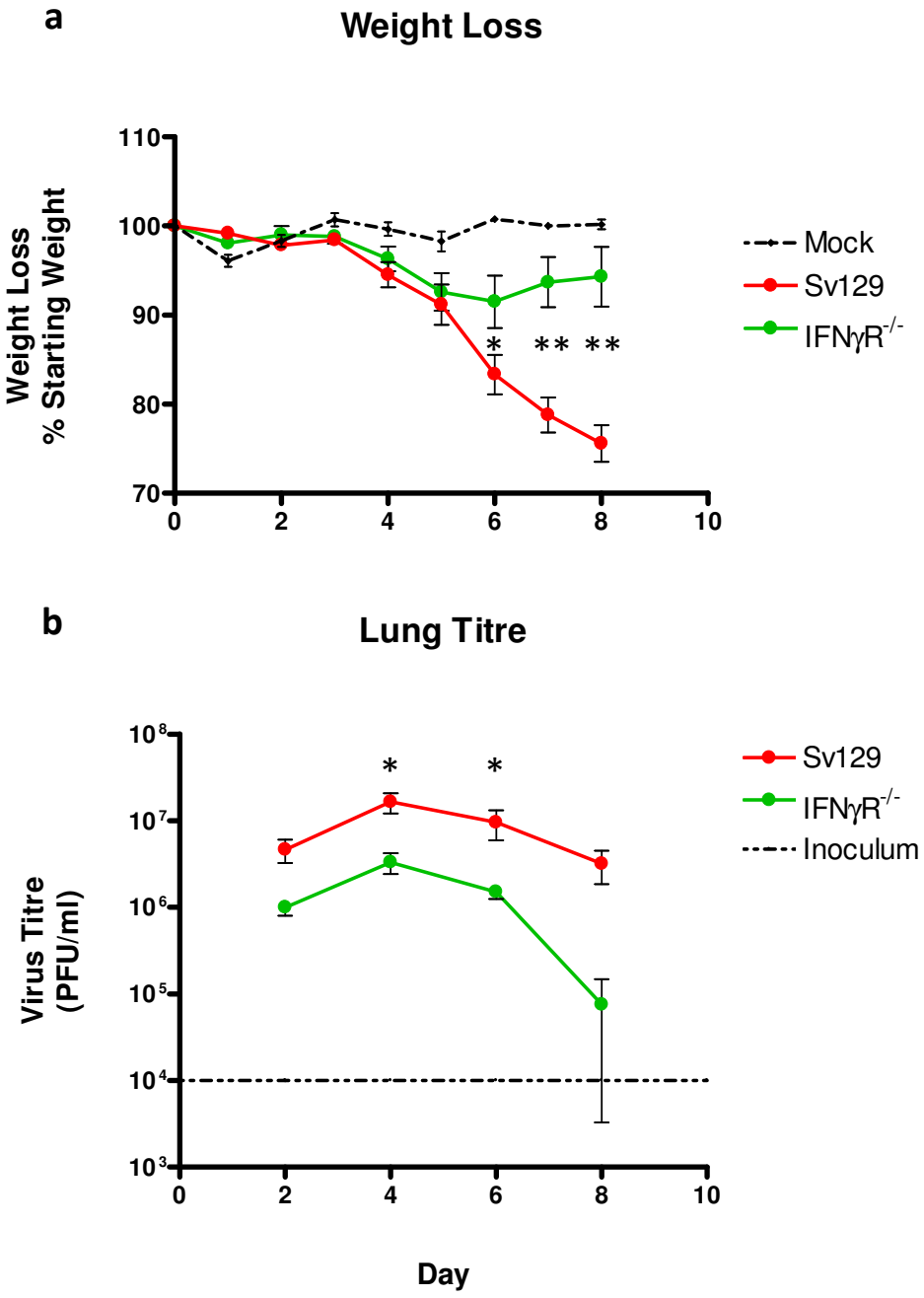

Figure 5.3 Weight loss and viral titre following infection with 1x10^4 PFU WSN.
a) Sv129 mice rapidly lost weight following infection, while weight loss in IFNγR$^{-/-}$ was less severe, having slowed by day 6. Following this timepoint, IFNγR$^{-/-}$ began regaining weight, indicating recovery, while their wildtype counterparts continued to deteriorate.
n=4 per timepoint, representative of 3 independent experiments
b) Viral titres from homogenised lungs were higher in Sv129 animals than IFNγR$^{-/-}$ mice.
n=7 per timepoint
* <0.05, ** <0.005

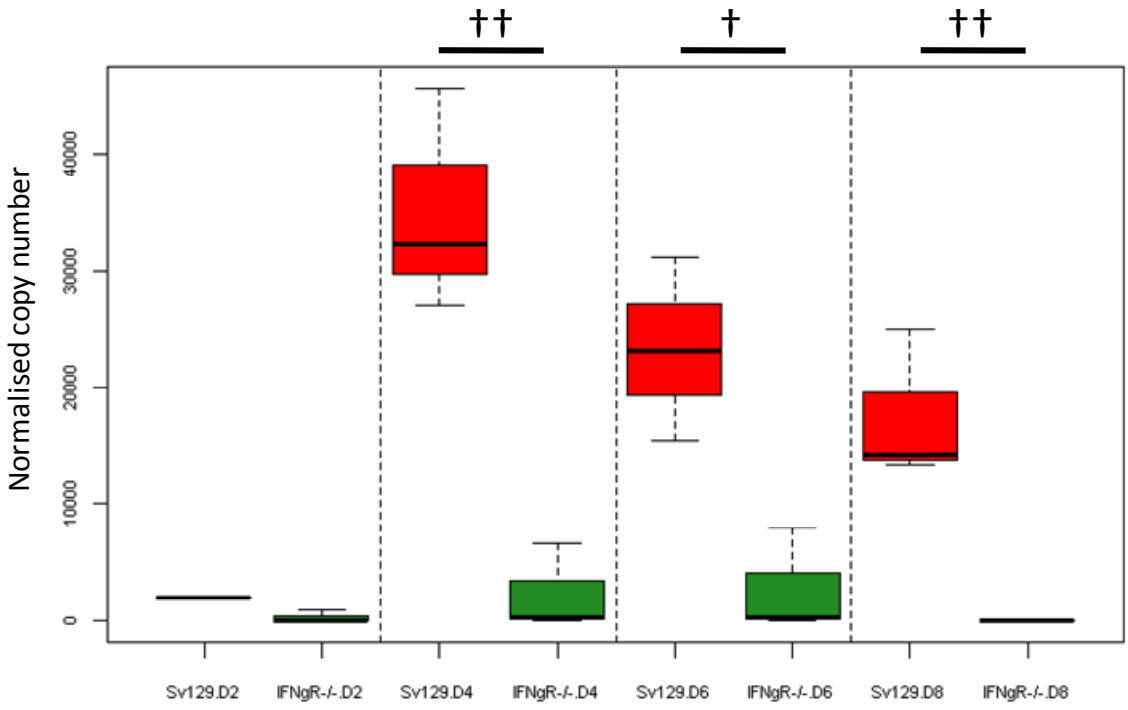

Figure 5.4 Expression of M1 viral mRNA following infection with 1x10^4 PFU WSN.
RNA was extracted from lungs of Sv129 and IFNγR$^{-/-}$ mice and M1 mRNA expression was assessed. Absolute quantification of copy number was applied and normalised against housekeeping gene CNX (M1 copy number per 10^3 copies CNX). At each timepoint examined, Sv129 animals demonstrated significantly higher expression of this viral mRNA than did IFNγR$^{-/-}$ mice († = <0.05, †† = <0.005), which resulted in the overall difference in expression between Sv129 and IFNγR$^{-/-}$ mice being highly significant (p = <0.0005). This indicates that Sv129 mice are more permissive for viral replication than their IFNγR$^{-/-}$ counterparts.
n=3 per timepoint

ted at lower levels than Sv129 cells, implying that the IFNγR$^{-/-}$ background results in reduced viral positivity in different cell types, both in vitro and in vivo.

Together, these data show that disruption of IFNγ signalling leads to mild disease in vivo. As discussed previously, it is possible that this is due to a net loss of sialylated residues on the surface of IFNγR$^{-/-}$ cells and so the virus is less able to gain entry and cause infection. However, it is also possible that in the absence of IFNγ signalling, the immune system is able to generate a functional antibody and T cell response to the virus, as indicated by previous studies (Bot *et al.*, 1998; Graham *et al.*, 1993), resulting in viral clearance while avoiding the excessive inflammation and immunopathology driven by IFNγ. This was further investigated by assessment of immunopathology and cytokine expression.

5.2.2 Influenza virus associated immunopthology

H&E staining revealed stark differences between infected Sv129 and IFNγR$^{-/-}$ mice. The lungs from wildtype animals showed substantial inflammatory infiltrate into the tissue, while the knockout mice demonstrated comparatively little congestion. This was especially marked at day 4 post infection (Figure 5.5a&e). Infected Sv129 mice demonstrated thickening of the alveolar airspace walls and heavy cellular infiltration into the lung tissue and bronchioles. At higher magnification, strong infiltration was seen around the bronchioles, which also demonstrated sloughing of the epithelial cell lining and appeared to contain cellular debris. (Figure 5.5b). IFNγR$^{-/-}$ mice, however, showed minimal thickening of the airspace walls, with some cellular infiltration appearing in a focal pattern, compared to the diffuse congestion observed in the wildtype Sv129 mice (Figure 5.5e). Under higher magnification, this infiltration was seen to be within the alveolar airspaces only (Figure 5.5f) rather than within

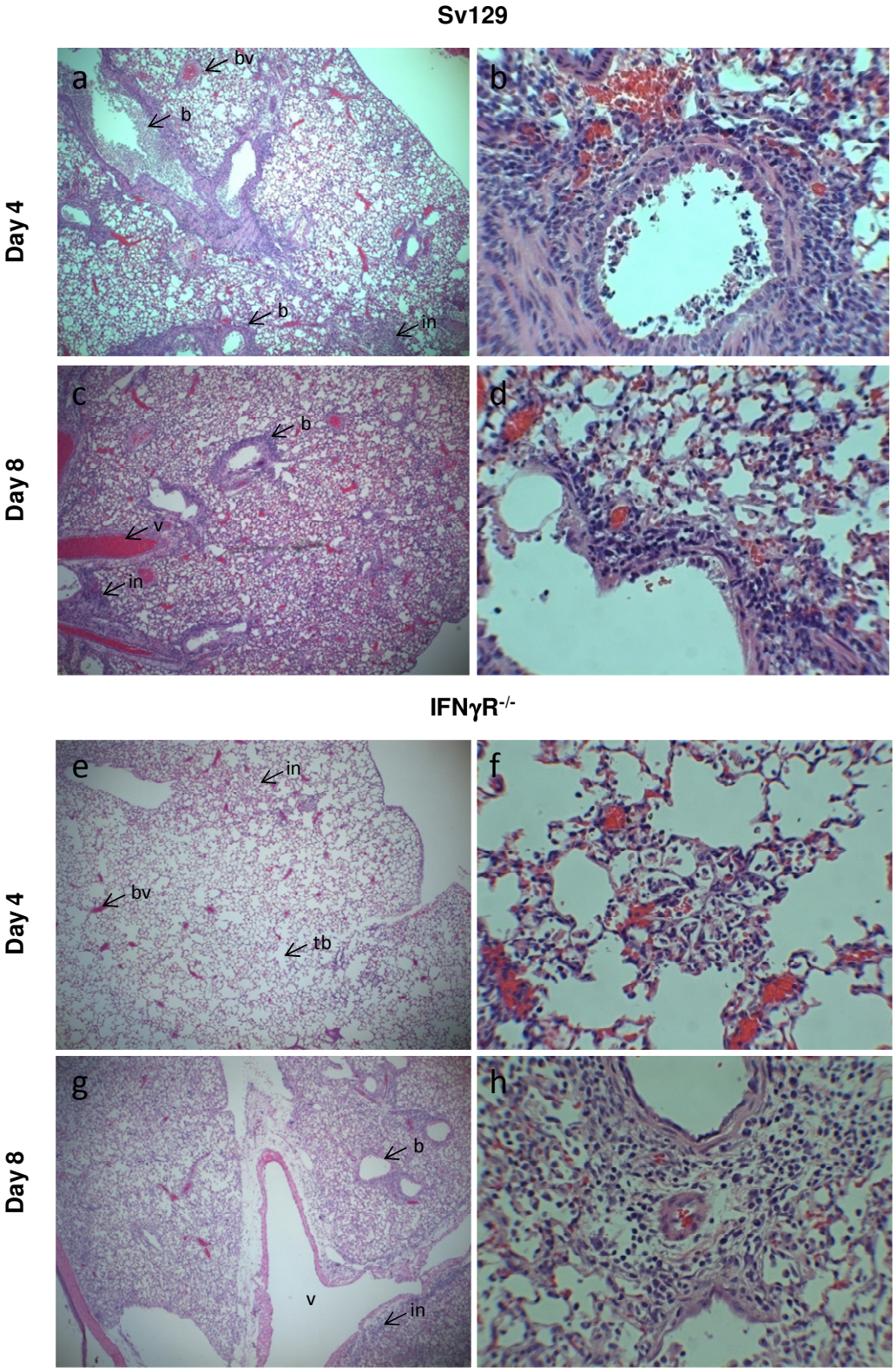
Sv129
Day 4
Day 8
a
bv
b
b
in
b
c
b
v
in
d
IFNγR-/-
Day 4
Day 8
e
in
bv
tb
f
g
b
v
in
h

Figure 5.5 Immunopathology following infection with 1x10^4 PFU WSN.
Infected Sv129 lungs under x5 magnifcation (a&c) and at x40 magnification (b&d), at days 4 and 8 respectively, showed intense and diffuse cellular infiltrate. IFNγR$^{-/-}$ lungs ((e) x5, day 4; (f) x40, day 4; (g) x5, day 8; (h) x40, day 8) displayed reduced infiltration compared to wildtype counterparts. Mock infected controls of both strains failed to demonstrate infiltration.
Representative of n=6 per timepoint.
b, bronchiole; tb, terminal bronchiole; v, vein; bv, blood vessel; in, inflammation

bronchioles, again highlighting a difference in infection kinetics between wildtype and IFNγR$^{-/-}$ mice By day 8 post infection, both strains of mice demonstrated more extensive congestion within the lungs, but the wildtype Sv129 mice were most severely affected. Lungs from these mice showed diffuse thickening of the alveolar airspace walls, with extreme cellular infiltration and oedema in every area examined (Figure 5.5c). Higher magnification showed severe damage to the bronchiolar epithelium, with very few cells remaining intact and many inflammatory cells penetrating the alveolar airspaces (Figure 5.5d). IFNγR$^{-/-}$ mice showed more diffuse infiltration and thickening of the alveolar airspace walls than had been observed at day 4, but this was less severe than that seen in wildtype mice. Moderate congestion with infiltrating cells was observed throughout the majority of the IFNγR$^{-/-}$ infected lung (Figure 5.5g), and under x40 magnification, strong infiltration was seen around the bronchioles. Similar to Sv129 mice, the bronchioles also showed evidence of damage to the epithelial layer.

The delayed onset of cellular infiltration in the lungs of infected IFNγR$^{-/-}$ mice, together with the limited weight loss and clinical symptoms observed in Chapter 5.2.1 suggested differing patterns of infection in these mice compared to wildtype Sv129 animals. This was further investigated by staining for influenza virus using either a broad spectrum polyclonal anti-influenza antibody, along with HRP detection or a polyclonal anti-NS1 antibody followed by detection with Alexfluor 488, as described in Chapter 2.8.

Immunofluorescent staining for NS1 immediately highlighted differing patterns of infection in the two strains of mice. At day 2 post infection, Sv129 mice demonstrated patches of positive staining cells throughout the lung, with bronchiolar epithelium staining very strongly (Figure 5.6a). In contrast, IFNγR$^{-/-}$ showed smaller groups of positive cells, with limited involvement of the epithelial lining (Figure 5.6b). By day 4, both strains showed stronger positivity for virus, with the majority of bronchiolar epithelial cells becoming

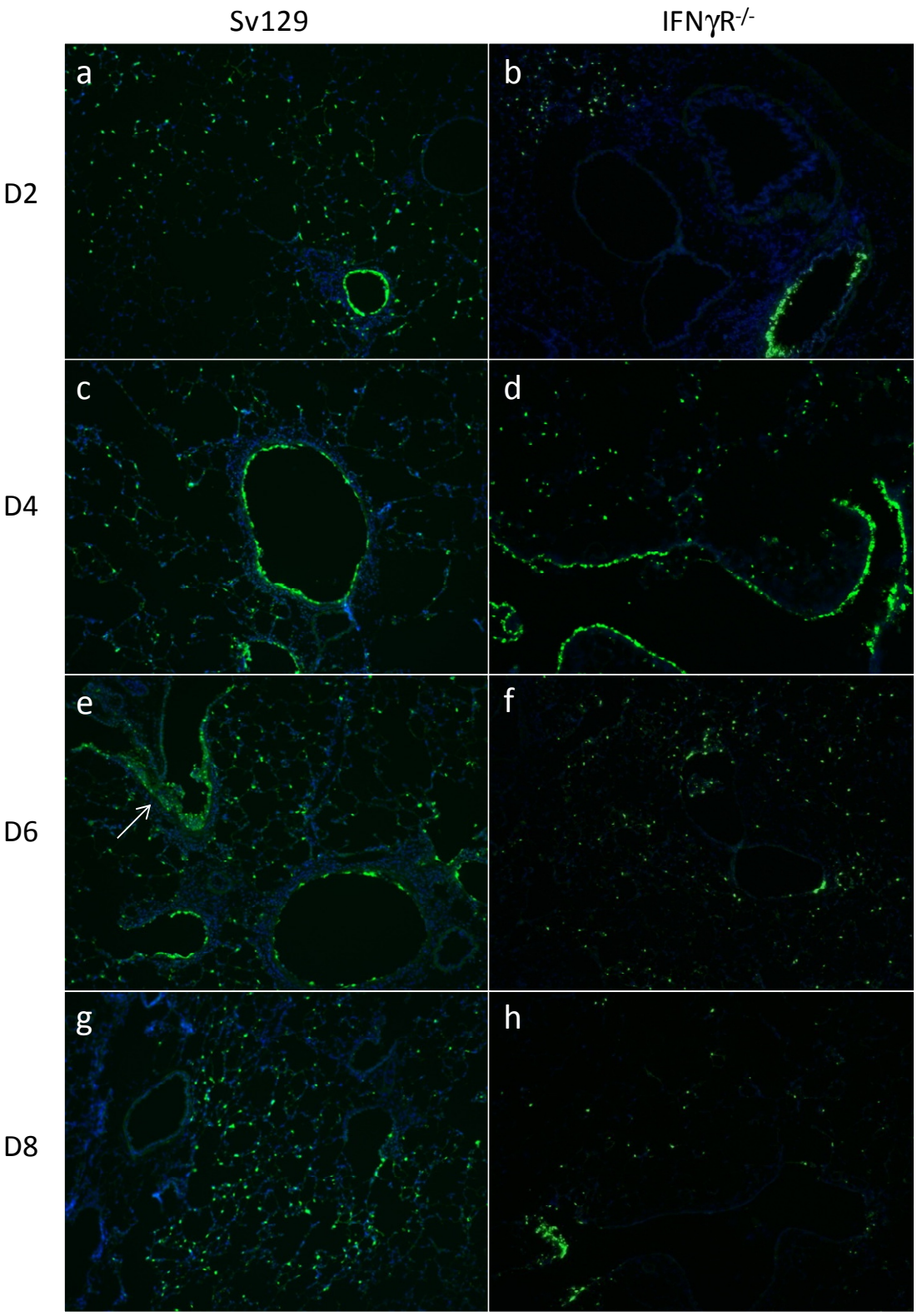
Sv129
IFNγR-/-
D2
D4
D6
D8
a
b
c
d
e
f
g
h

Figure 5.6 Immunofluorescent staining of NS1 viral protein.
Sv129 mice demonstrated stronger staining for NS1 in the lungs at all timepoints examined, in addition to a different pattern of localisation compared with IFNγR$^{-/-}$ animals. (a, c, e, g) Sv129 at days 2, 4, 6 and 8 respectively, (b, d, f, h) IFNγR$^{-/-}$ at days 2, 4, 6 and 8 respectively. Mock infected lungs from both strains of mouse were negative for NS1 staining.
Representative of n=3 per timepoint

positive for NS1 (Figure 5.6c&d). At this timepoint, more NS1 was detected in the alveolar airspaces in both strains of mice. However, by day 6 post infection, Sv129 mice demonstrated intense and diffuse positivity for NS1 protein in the alveolar spaces and in the bronchioles (Figure 5.6e). Some positive staining was still visible in the bronchiolar epithelium, but this was reduced compared to previous days. However, debris and sloughed epithelial cells were apparent indicating extensive damage to the bronchioles in Sv129 mice (Figure 5.6e, white arrow). In contrast to this, IFNγR$^{-/-}$ mice showed very little staining within the bronchioles, with no visible debris (Figure 5.6f). However, there was a diffuse pattern of NS1 staining throughout the lungs indicating that the virus had successfully infected the tissue. By day 8, however, very few NS1 positive cells remained within the IFNγR$^{-/-}$ lung (Figure 5.6h), indicating that limited new viral synthesis was ongoing at this timepoint, and that IFNγR$^{-/-}$ animals had successfully controlled the infection. Sv129 mice continued to demonstrate intense NS1 staining at day 8, although there was no evidence of bronchiolar infection at this timepoint (Figure 5.6g). This demonstrates that Sv129 mice are more permissive for viral replication than IFNγR$^{-/-}$ animals, with infection becoming established early and viral replication continuing throughout the course of infection in this strain of mice. Conversely, IFNγR$^{-/-}$ mice demonstrate a delayed onset of widespread viral replication, which is subsequently brought under control by day 8 post infection.

The anti-NS1 staining was followed with detection of virus using the polyclonal anti-influenza antibody. Due to the broad specificity of this antibody, virus particles and proteins remaining in the lung can be visualised after active replication has ceased, in order to determine the full extent of infection. Similar to the NS1 stained sections, at day 4 Sv129 mice demonstrated infection of the bronchiolar epithelium with occasional positive cells within the alveolar airspaces (Figure 5.7a). By day 8 however, the infection had progressed, with the alveolar walls themselves showing strong positive staining

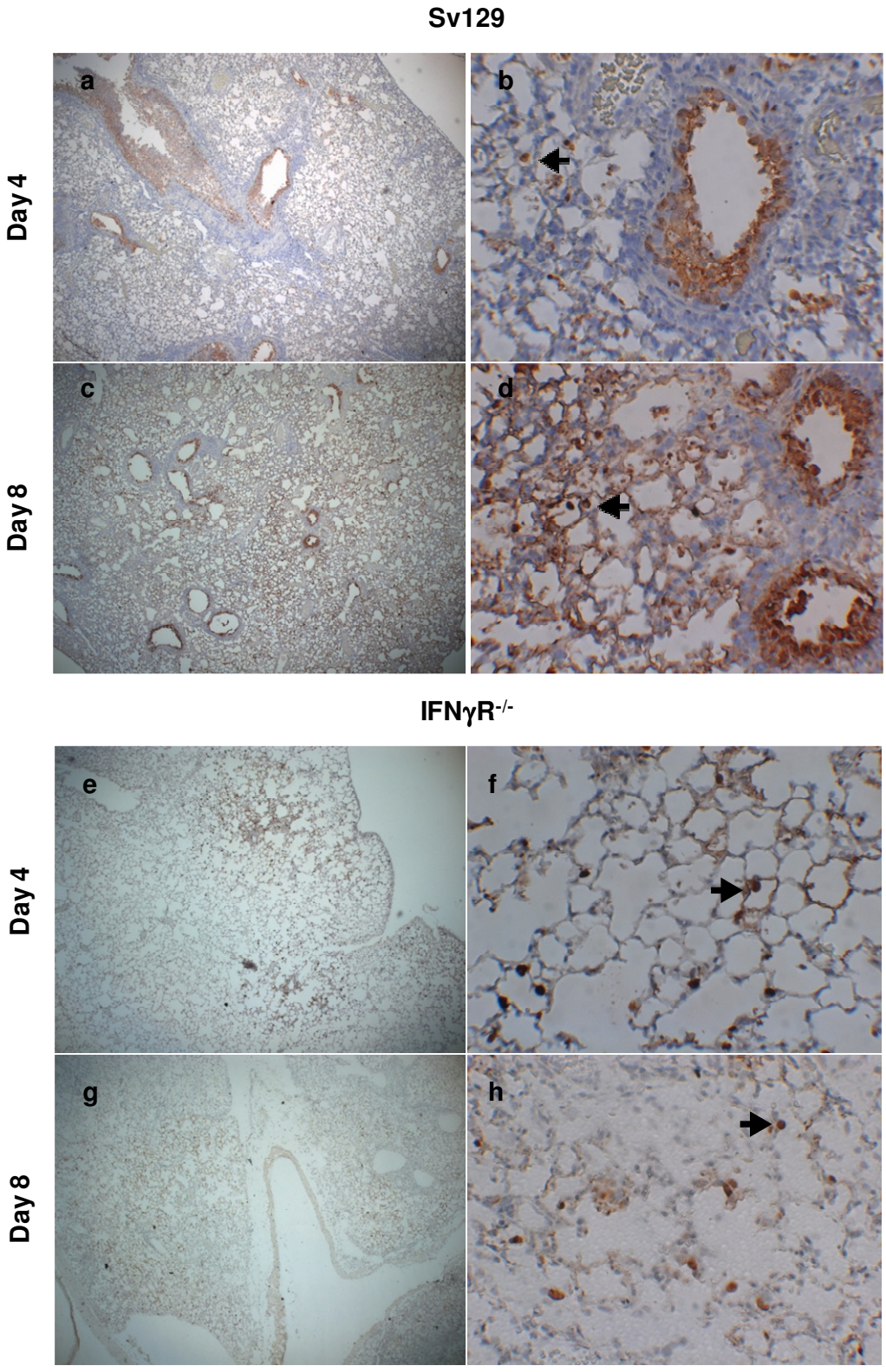
Sv129
Day 4
Day 8
a
b
c
d
IFNγR-/-
Day 4
Day 8
e
f
g
h

Figure 5.7 Immunohistochemistry for influenza virus proteins.
Infected Sv129 lungs under x20 magnifcation (a&c) and at x40 magnification (b&d), at days 4 and 8 respectively, showed intense and diffuse staining for influenza virus proteins. IFNγR$^{-/-}$ lungs ((e & g) x20, day 4 and 8; (f & h) x40, day 4 and 8) displayed less positivity for viral proteins compared to wildtype counterparts. Black arrows indicate cells with macrophage-like morphology and strong staining for viral proteins. Mock infected controls of both strains were negative for viral staining.
Representative of 3 independent experiments

staining for virus (Figure 5.7c). Under higher magnification it became evident that the bronchiolar epithelium was heavily infected but also undergoing strong inflammatory infiltration at day 4 (Figure 5.7b), while by day 8, all remaining epithelial cells were infected and the bronchioles were congested with debris (Figure 5.7d). This is consistent with the pattern of infection observed with the NS1 antibody, whereby the infection progresses from the bronchioles to the lung tissue as a whole, with excessive damage to the epithelium.

The virus staining pattern seen in IFNγR$^{-/-}$ lungs closely mimicked the pattern of infiltration seen in the H&E stained sections. The walls of the alveolar airspaces were positive for viral proteins at both timepoints, and this was focal in nature at day 4 (Figure 5.7e) but more diffuse by day 8 (Figure 5.7g). However, this positivity was substantially weaker than that demonstrated by the wildtype Sv129 animals. Under higher magnification, it was apparent that the alveolar walls were thickened, but less heavily infected than their wildtype counterparts.

In addition to this, both strains of mice demonstrated very strongly positive cells within the alveolar airspaces (Figure 5.7b, d, f, g, black arrow), which were most pronounced at day 8. The position and morphology of these cells was suggestive of macrophages, either infected or phagocytosing infected material. This was further investigated by staining for virus and the macrophage marker F4/80, followed by detection with Alexafluor 488 and Alexafluor 594, labelling the virus green and macrophages red (Chapter 2.8.2). Although DAPI was included as a counterstain, it was omitted from these images as it obstructed a clear view of the colocalised Alexafluor signals.

Low numbers of alveolar macrophages were present in the lungs of mock infected Sv129 mice (Figure 5.8, white arrow). However, even early in infection there was evidence of macrophages homing to the lung and exiting the blood at

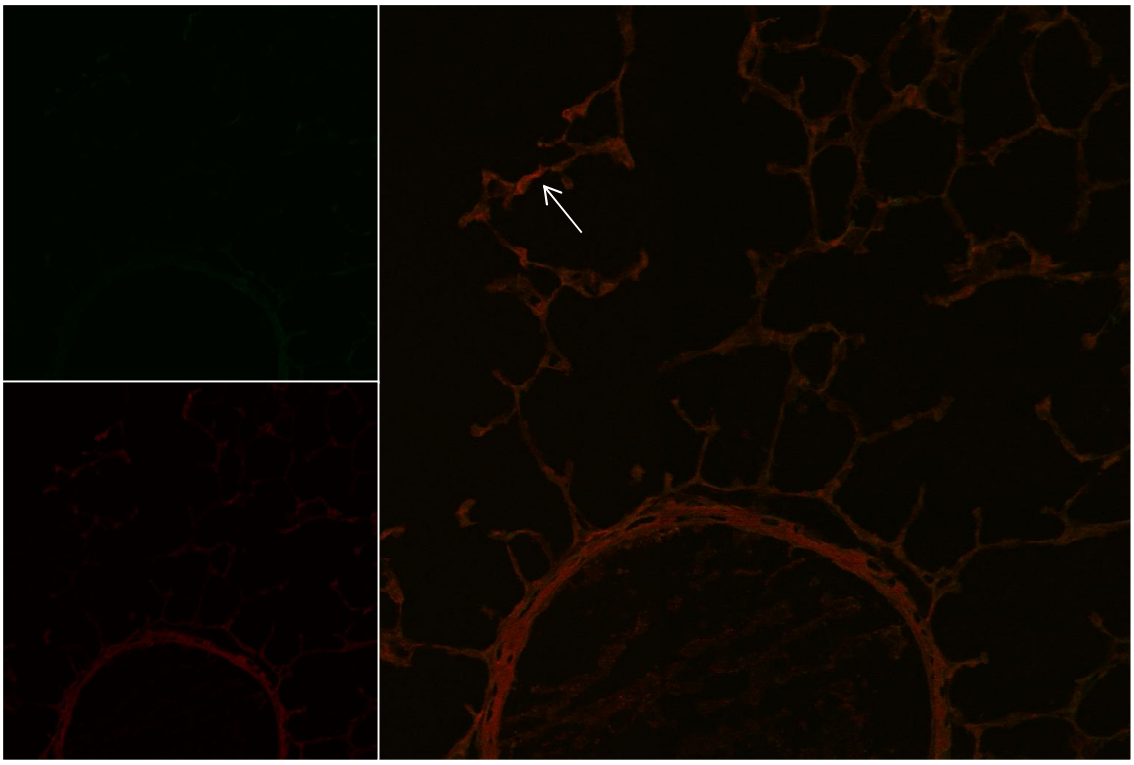

Figure 5.8 Immunofluorescence for virus positive macrophages; Sv129 mock
Mock infected Sv129 displayed low levels of macrophages (white arrow) within the lung in the absence of virus. Top left panel: anti-influenza virus + alexafluor 488; bottom left panel: anti-F4/80 + alexafluor 594; right panel: overlaid image.
Representative of n=2

the site of infection (Figure 5.9). At high magnification, virus was seen in the epithelial cells lining the alveolar spaces but also in macrophages (Figure 5.9b, white arrow), with infiltrating macrophages gathering at the interface of the blood stream and the lung. By day 4 post infection, Sv129 showed vast numbers of cells leaving the blood and entering the lung, forming large perivascular cuffs around blood vessels (Figure 5.10a). This infiltrate contained many macrophages (Figure 5.10a white arrows), which migrated towards the infected epithelium and contributed to thickening of the alveolar space walls (Figure 5.10b). In addition to this intense inflammatory infiltration, these mice demonstrated strong infection and destruction of the bronchiolar epithelium (Figure 5.11a). Once again, macrophages were seen to successfully home to these areas and were present in large numbers (Figure 5.11a), localising below the epithelial layer (Figure 5.11b, white arrow). Migration of macrophages to the bronchioles continued through day 6 post infection (Figure 5.12a), when macrophages became visible within the bronchioles, engulfing infected debris within the airways (Figure 5.12b, white arrows). By the end of the experiment, there was diffuse F4/80 positivity within the Sv129 lung, coinciding with the pattern of polyclonal virus staining observed in Figure 5.7, demonstrating that macrophages remained present in high numbers within the lung for the duration of infection and contributed in no small measure to the congestion and thickened appearance of the alveolar walls. Much of the virus detected appeared to be localised with the macrophages, suggesting that these cells have successfully scavenged debris and infected epithelial cells, while some virus remained associated with epithelium alone (Figure 5.13b white arrows). The presence of such numbers of macrophages within the airspace lining, along with other infiltrating cells, is likely to compromise gas exchange and contribute to the morbidity of these mice.

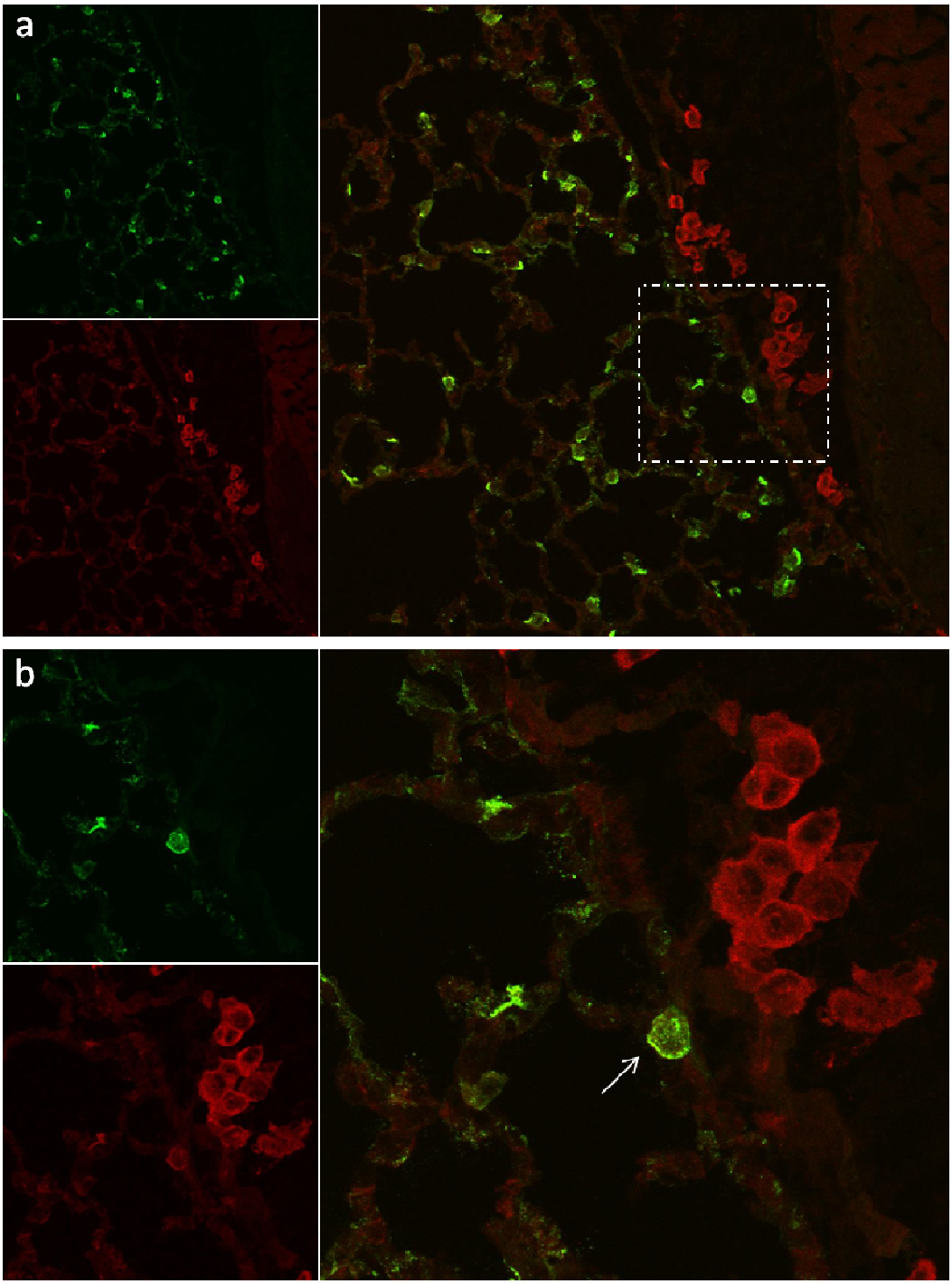

Figure 5.9 Immunofluorescence for virus positive macrophages; Sv129 d2.
Sv129 mice demonstrated macrophages infiltrating from blood stream into the lung at day 2 post infection, with some double positive cells at this early timepoint (white arrow). (a) x20 magnification, (b) x63 magnification. Top left panel: anti-influenza virus + alexafluor 488; bottom left panel: anti-F4/80 + alexafluor 594; right panel: overlaid image.
Representative of n=3

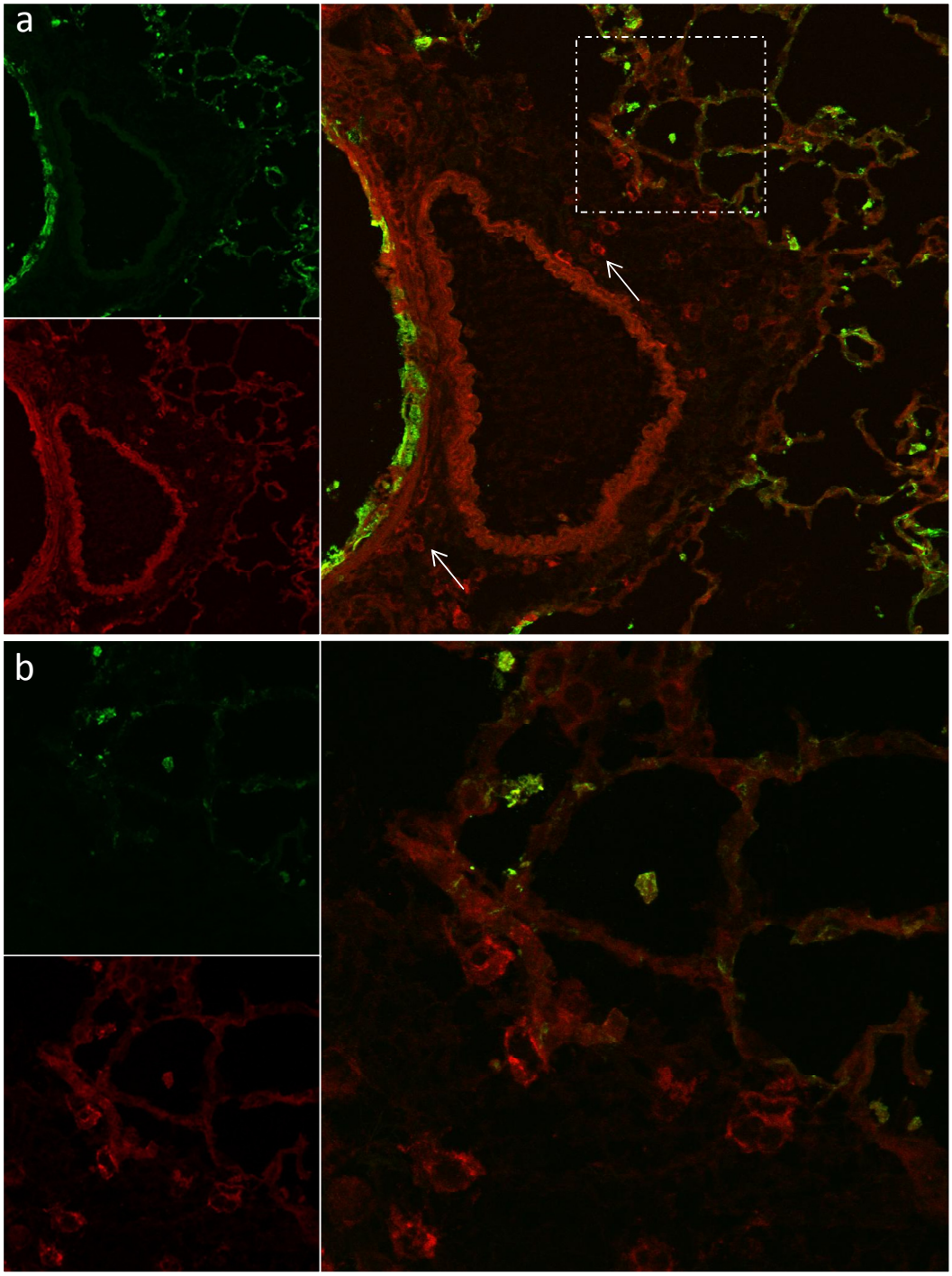

Figure 5.10 Immunofluorescence for virus positive macrophages; Sv129 d4.
At day 4 post infection, large numbers of macrophages could seen surrounding the blood vessels and bronchioles, migrating towards infected epithelium (white arrows). (a) x20 magnification, (b) x63 magnification. Top left panel: anti-influenza virus + alexafluor 488; bottom left panel: anti-F4/80 + alexafluor 594; right panel: overlaid image.
Representative of n=3

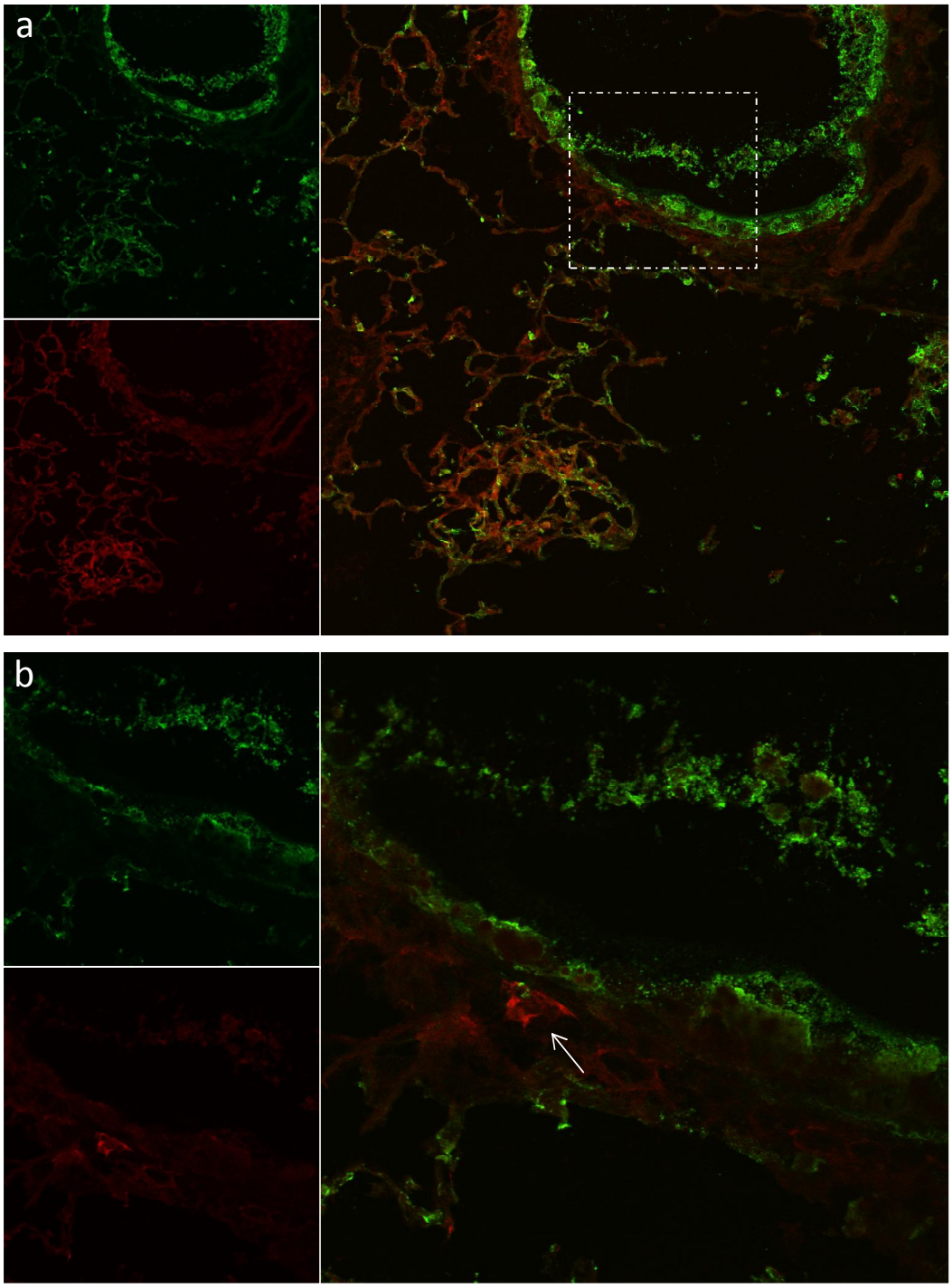

Figure 5.11 Immunofluorescence for virus positive macrophages; Sv129 d4.
At day 4 post infection, destruction of bronchiolar epithelium was evident, with macrophages localising beneath the epithelial layer (white arrows). (a) x20 magnification, (b) x63 magnification. Top left panel: anti-influenza virus + alexafluor 488; bottom left panel: anti-F4/80 + alexafluor 594; right panel: overlaid image.
Representative of n=3

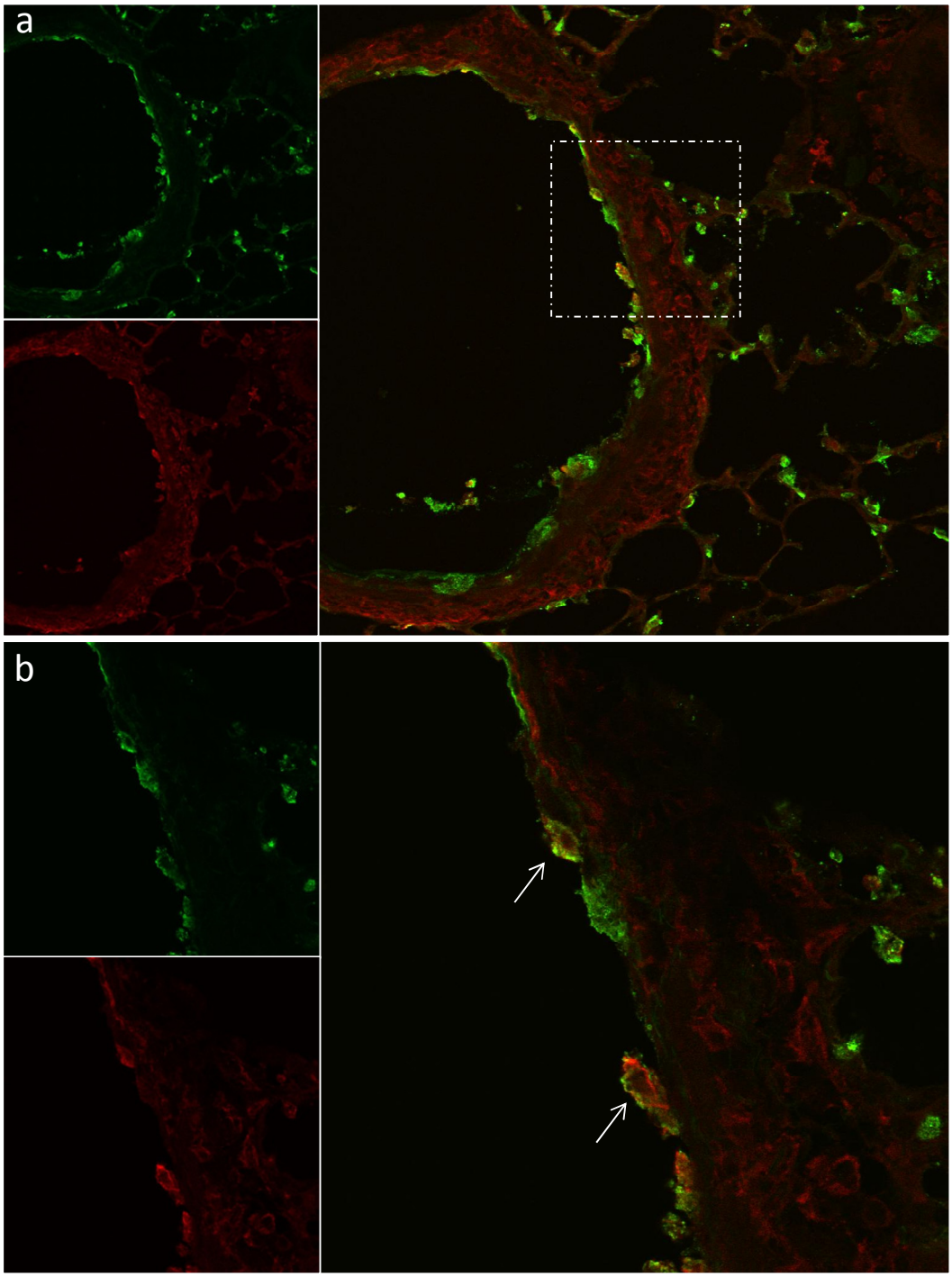

Figure 5.12 Immunofluorescence for virus positive macrophages; Sv129 d6.
At day 6 post infection, macrophages could be seen within the bronchioles, engulfing infected epithelial cells (white arrows). (a) x20 magnification, (b) x63 magnification. Top left panel: anti-influenza virus + alexafluor 488; bottom left panel: anti-F4/80 + alexafluor 594; right panel: overlaid image.
Representative of n=3

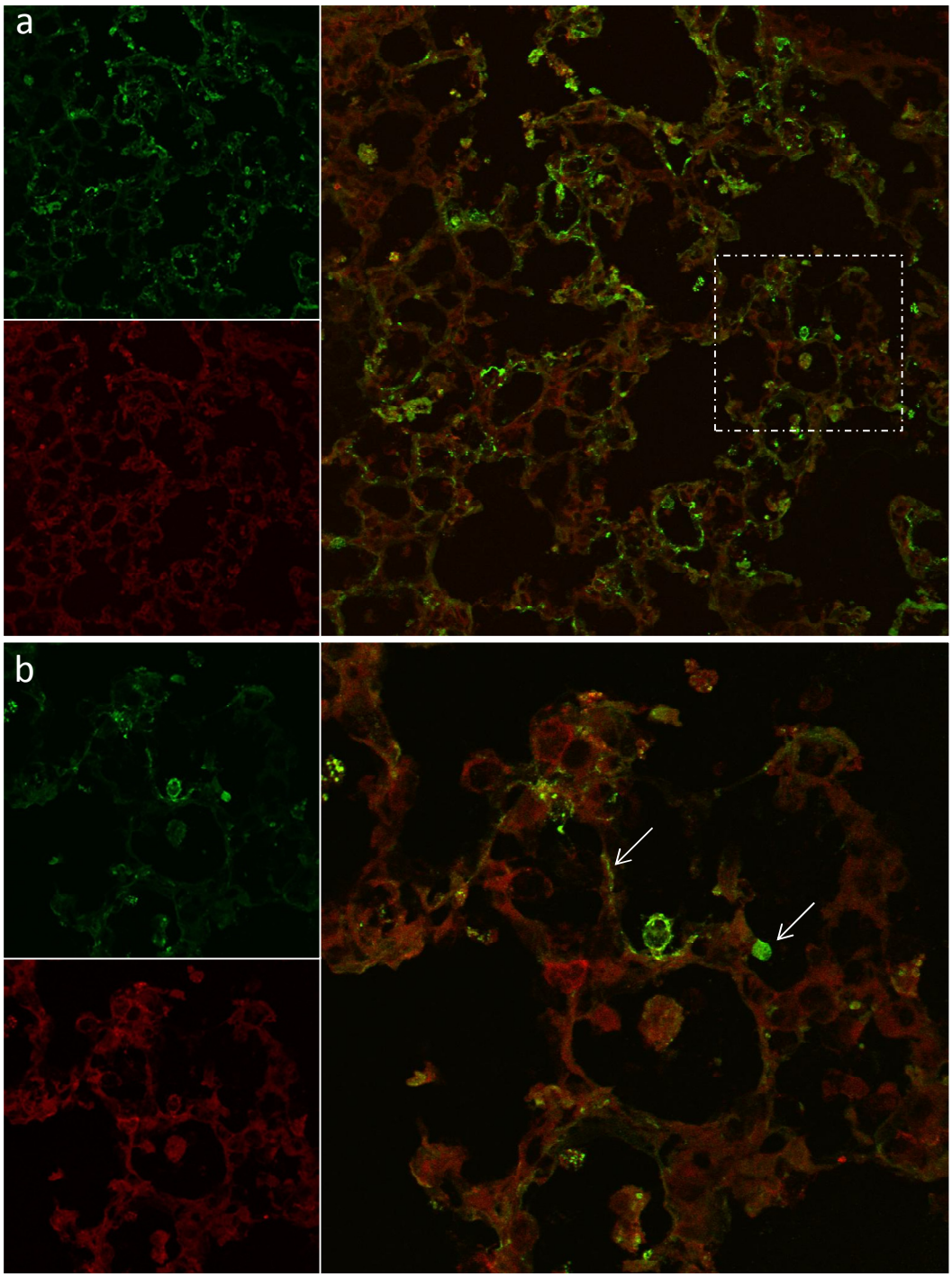

Figure 5.13 Immunofluorescence for virus positive macrophages; Sv129 d8.
At day 8 post infection, macrophages were seen throughout the lung, thickening the alveolar space walls. Much of the remaining virus localised with macrophages but some remained associated with epithelium alone (white arrows). (a) x20 magnification, (b) x63 magnification. Top left panel: anti-influenza virus + alexafluor 488; bottom left panel: anti-F4/80 + alexafluor 594; right panel: overlaid image.
Representative of n=3

Mock infected IFNγR$^{-/-}$ mice appeared to demonstrate higher numbers of F4/80 positive cells than their wildtype counterparts (Figure 5.14 white arrows), suggesting a potential difference in resident alveolar macrophage numbers between the two strains of mice, although this was not confirmed by quantitative analysis. Upon infection, macrophages appeared to home rapidly to the site of infection with no evidence of infiltration from the vasculature. At day 2 post infection, small patches of infected cells were visible within the lung and many macrophages were already present (Figure 5.15a). Under higher magnification, macrophages could clearly be seen alongside infected epithelial cells and several were themselves strongly positive for virus (Figure 5.15b, white arrow), although many remained negative for virus even in close proximity to infected cells. Similar to Sv129 animals, by day 4 strong infection was visible in the epithelial lining of the bronchioles, with large numbers of macrophages infiltrating into this region (Figure 5.16a). These infiltrating macrophages were seen to converge on regions of infected epithelium and again, many were positive for virus while others appeared to be moving towards the infected regions (Figure 5.16b). Day 6 post infection saw a further increase in macrophages numbers, with large cuffs forming around the bronchioles and thickening of the alveolar space walls (Figure 5.17a), similar to the wildtype Sv129 lung. Infected epithelium and debris was observed in the larger bronchioles, in contrast to the NS1 stain. However, this is likely to be late stage proteins and whole virions detected by the broad spectrum polyclonal antibody, indicating that antigen remains at these sites after viral replication has ceased and macrophages localise here to clear the debris. Under higher magnification, the thickened alveolar walls could be clearly seen and were strongly positive for viral proteins (Figure 5.17b). Macrophages appeared to be infiltrating these regions and engulfing infected material (Figure 5.17b, white arrow) and therefore contributing to congestion of the lungs. However, by day 8 post infection, very little viral staining was evident in the IFNγR$^{-/-}$ lung with a concurrent reduction in macrophage numbers. F4/80 positive cells remained around blood vessels (Figure 5.18a), but fewer were ob-

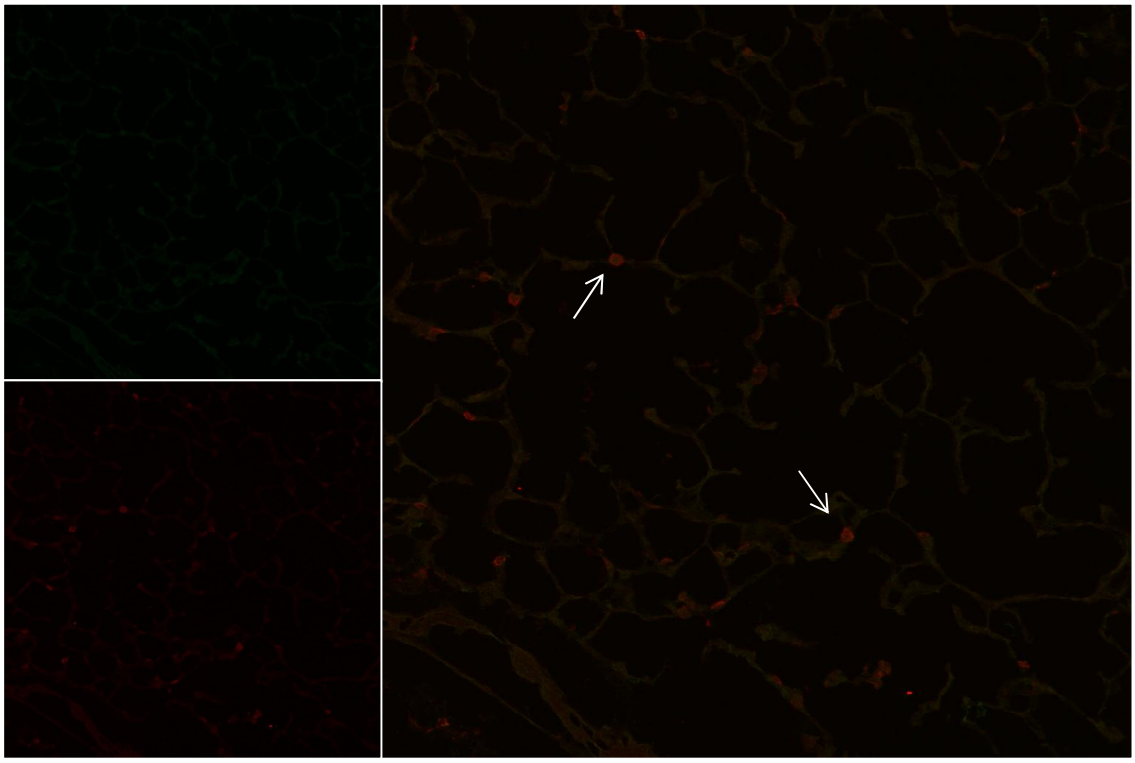

Figure 5.14 Immunofluorescence for virus positive macrophages; IFNγR$^{-/-}$ mock.
IFNγR$^{-/-}$ mice displayed higher numbers of macrophages in the lung following inoculation with PBS (white arrows) than did their wildtype counterparts. (a) x20 magnification, (b) x63 magnification. Top left panel: anti-influenza virus + alexafluor 488; bottom left panel: anti-F4/80 + alexafluor 594; right panel: overlaid image.
Representative of n=2

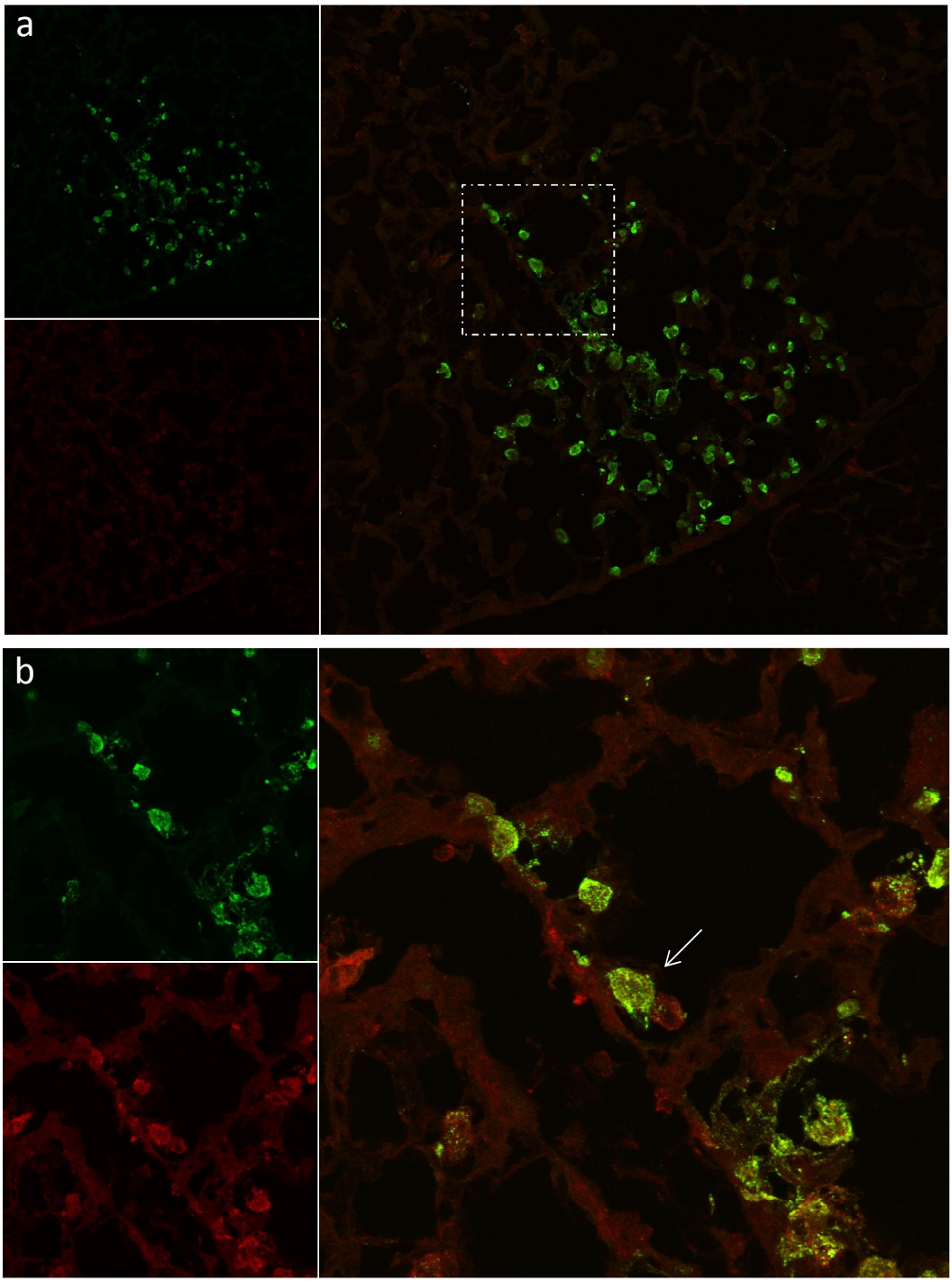

Figure 5.15 Immunofluorescence for virus positive macrophages; IFNγR$^{-/-}$ d2.
At day 2 post infection, IFNγR$^{-/-}$ mice displayed discrete areas of infection with macrophages localising to these regions and becoming positive for viral proteins (white arrows). (a) x20 magnification, (b) x63 magnification. Top left panel: anti-influenza virus + alexafluor 488; bottom left panel: anti-F4/80 + alexafluor 594; right panel: overlaid image.
Representative of n=3

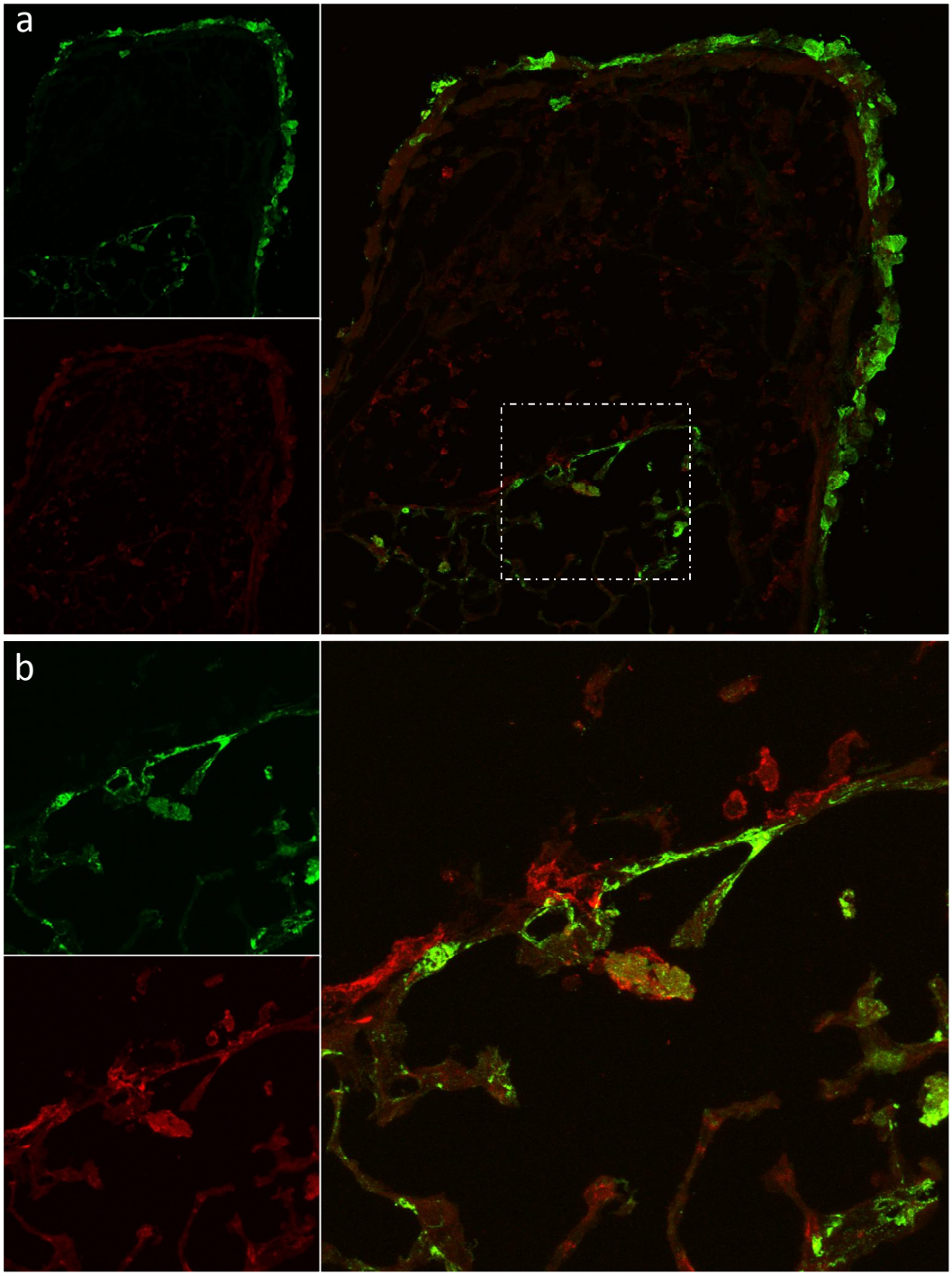

Figure 5.16 Immunofluorescence for virus positive macrophages; IFNγR$^{-/-}$ d4.
At day 4 post infection, IFNγR$^{-/-}$ mice demonstrated large areas of infiltration, localising close to areas of infected epithelium. (a) x20 magnification, (b) x63 magnification. Top left panel: anti-influenza virus + alexafluor 488; bottom left panel: anti-F4/80 + alexafluor 594; right panel: overlaid image.
Representative of n=3

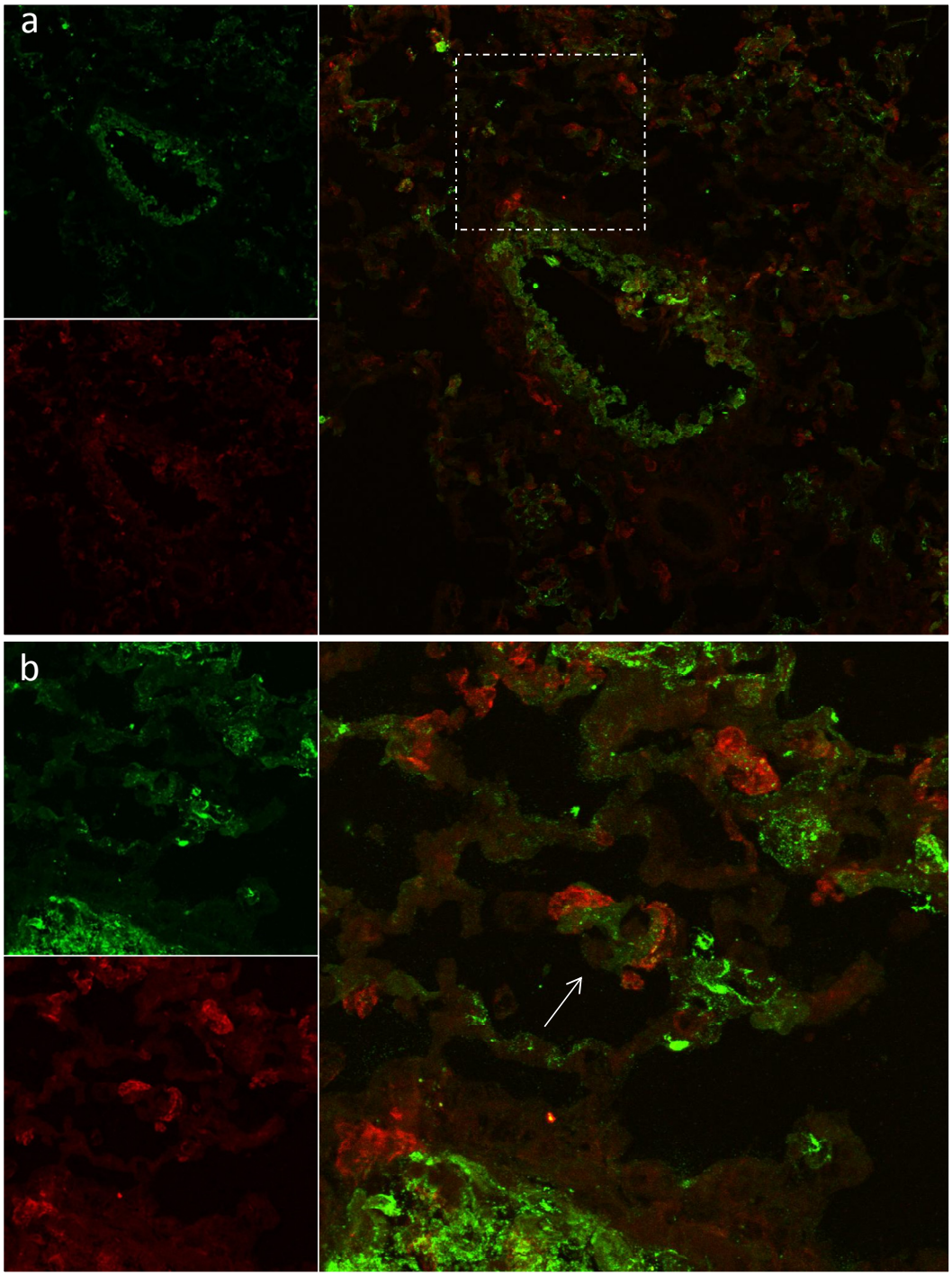

Figure 5.17 Immunofluorescence for virus positive macrophages; IFNγR$^{-/-}$ d6.
At day 6 post infection, macrophages were evident in the thickening alveolar space walls (white arrows) and surrounding the bronchioles. (a) x20 magnification, (b) x63 magnification. Top left panel: anti-influenza virus + alexafluor 488; bottom left panel: anti-F4/80 + alexafluor 594; right panel: overlaid image.
Representative of n=3

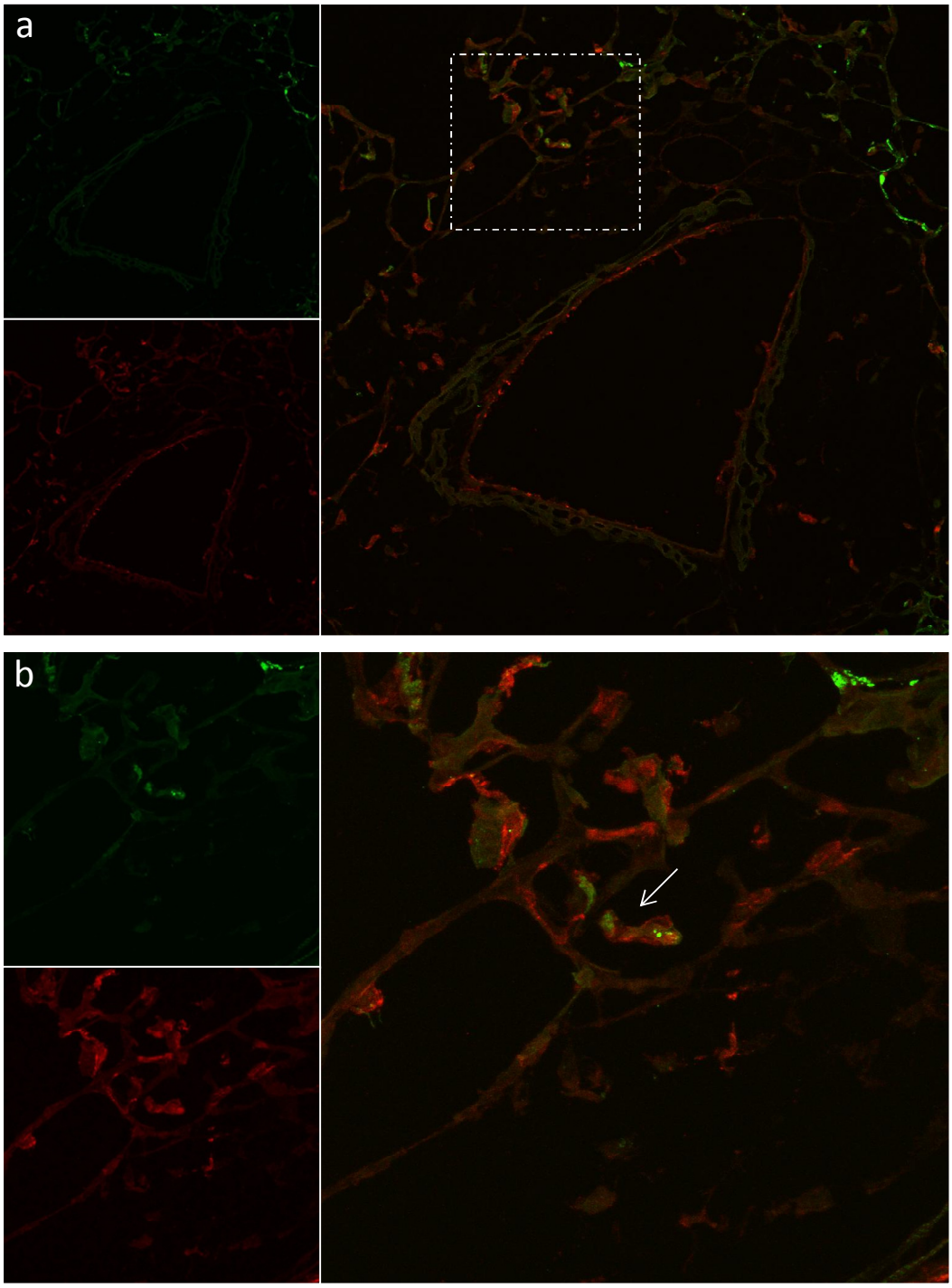

Figure 5.18 Immunofluorescence for virus positive macrophages; IFNγR$^{-/-}$ d8.
Very little virus remained at day 8 post infection, with macrophages mainly localising around blood vessels and in areas where infected epithelium remained (white arrows). (a) x20 magnification, (b) x63 magnification. Top left panel: anti-influenza virus + alexafluor 488; bottom left panel: anti-F4/80 + alexafluor 594; right panel: overlaid image.
Representative of n=3

served in the airspaces, and the alveolar space walls showed less pathology. Macrophages continued to localise with virus positive tissue (Figure 5.18b, white arrow), suggesting ongoing scavenging for any remaining infected cells. In contrast to the Sv129 animals, infection in IFNγR$^{-/-}$ mice appeared to be approaching clearance by day 8, consistent with the NS1 stain (Figure 5.6), and a similar decrease in macrophage numbers was apparent.

In addition to macrophages accounting for a large proportion of infiltrating cells in the lungs of both strains of mice following infection with WSN, other cell types may also be involved in deciding the outcome of infection. Neutrophils are known to be recruited in large numbers to the influenza virus infected lung and contribute to the inflammatory environment following infection. Therefore, sections were stained for Ly6G, a neutrophil specific marker (Daley *et al.*, 2008), to assess differences between Sv129 (Figure 5.19a, c, e) and IFNγR$^{-/-}$ mice (Figure 5.19b, d, f) in their ability to recruit this cell type.

Lungs from both strains of mice showed small numbers of Ly6G positive cells following mock infection with PBS (Figure 5.19a&b). However, challenge with virus led to strong staining for this marker, especially in the wildtype Sv129 animals. At day 4 post infection, much of the Sv129 inflammatory infiltrate within the tissue appeared to be Ly6G positive (Figure 5.19c), although absolute quantification was not performed. IFNγR$^{-/-}$ mice showed very strong staining around the bronchioles (Figure 5.19d) but not the diffuse pattern observed in the wildtypes. By day 8, both strains showed reduced staining compared with day 4 levels. However, neutrophils were still present in large numbers within the lungs of both wildtype and knockout mice at this late timepoint, distributed in focal patches of infiltration and with single cells scattered throughout the tissue. Wildtype animals showed more widespread Ly6G expression throughout the lung than did the IFNγR$^{-/-}$ mice, suggesting that, in addition to higher numbers of macrophages remaining in the Sv129

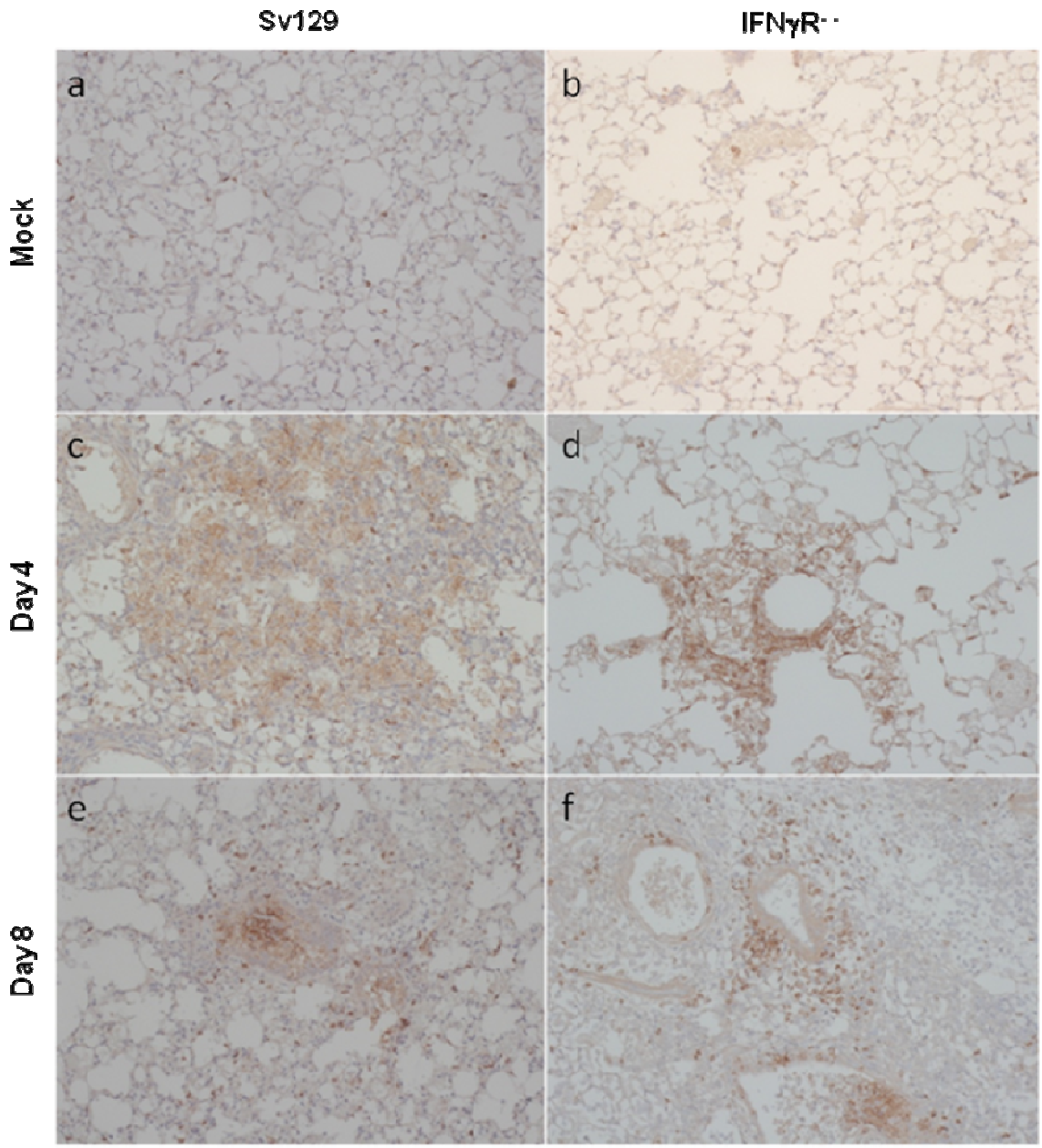

Figure 5.19 Distribution of neutrophils following infection with WSN.
Immunohistochemistry for the neutrophil specific marker Ly6G demonstrated high numbers of neutrophils infiltrating into the Sv129 lung at day 4 (c) and day 8 (e) post infection, along with those elicited by inoculation with PBS (a). Although reduced in comparison to wildtype animals, IFNγR$^{-/-}$ mice also demonstrated low level positivity following mock infection with PBS (b), and infiltration of neutrophils at days 4 (d) and 8 (f) post infection. Representative of n=3

lung late in infection, large numbers of neutrophils are also present. Together, these cells are likely to contribute to immunopathology and excessive cytokine production within the lung, potentially exacerbating infection and accounting for the differences in clinical outcome in the two strains of mice.

5.2.3 Cytokine expression following infection with WSN

It is evident that infection with influenza virus draws many inflammatory cells into the lungs of both Sv129 and IFNγR$^{-/-}$ mice. Many of these are macrophages and neutrophils. However, IFNγR$^{-/-}$ mice demonstrate reduced cellular infiltration and, taken together with the in vitro gene expression data presented in Chapter 4, it is likely that these mice may demonstrate a reduced inflammatory response to virus, resulting in ameliorated disease due to limited immunopathology. As such, mRNA expression of classical and alternative markers was investigated in vivo in order to deduce the extent of the inflammatory response in the lungs of Sv129 and IFNγR$^{-/-}$ mice.

Whole lungs were harvested following euthanasia at days 2, 4, 6 and 8, or upon 30% weight loss in accordance with UK Home Office project licence. A small portion of lung was excised from the same position in each animal and stored in RNAlater for RNA extraction, as described in Chapter 2.9.2. qPCR was then utilised to assess the extent of gene expression following infection with WSN. Samples were normalised against two housekeeping genes, CNX and SDHA as described in Chapter 2.12.3, and fold changes were expressed relative to the average gene expression of the mock infected control group. Log_{10} fold changes were plotted and statistical analyses carried out using the software package R.

Sv129 mice showed a pattern of increasing iNOS mRNA expression throughout the course of infection (Figure 5.20, red boxes), while IFNγR$^{-/-}$ mice demonstrated baseline levels until day 6, at which point iNOS mRNA express-

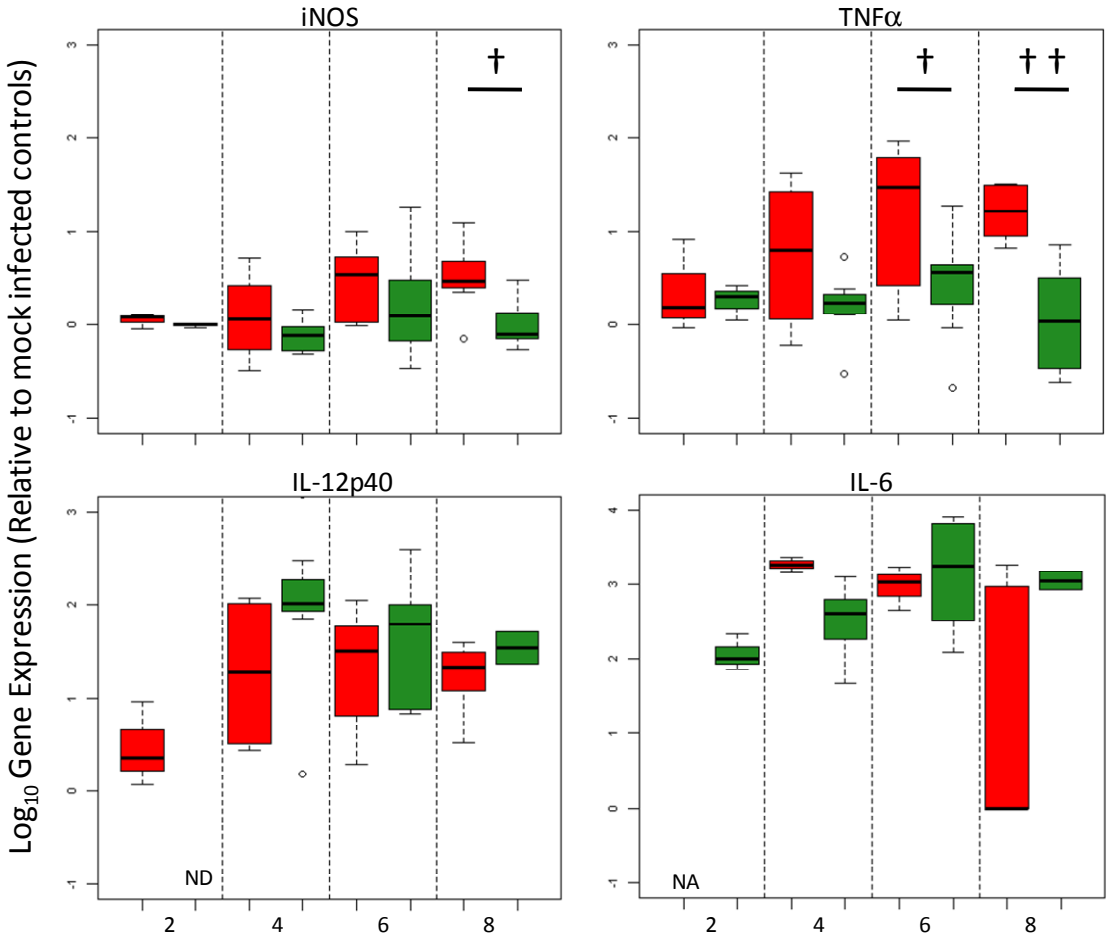

Figure 5.20 'Classical' mRNA expression profile following infection with WSN.
RNA was extracted from lungs following infection with WSN and qPCR used to assess expression levels for inflammatory modulators. Samples were normalised against two housekeeping genes, CNX and SDHA, followed by normalisation against average expression of mock infected controls.
NA = qPCR not performed, ND = not detected
† indicates statistical significance between Sv129 and IFNγR$^{-/-}$ mice
(† $p<0.05$, †† $p<0.005$)
■ Sv129 ■ IFNγR$^{-/-}$
n=7 per timepoint

ion peaked before declining by day 8 (Figure 5.20, green boxes). Despite these differences in trend between Sv129 and IFNγR$^{-/-}$ mice, mRNA expression only reached statistical significance at day 8 post infection (p=<0.05), when wildtype expression of iNOS mRNA was still increasing but levels in the knockout animals were returning to baseline.

TNFα mRNA expression demonstrated a similar trend to iNOS in both strains of mice, with an increasing pattern of expression in Sv129 mice (Figure 5.20, red boxes) but low levels expressed in the IFNγR$^{-/-}$ animals, with a peak at day 6 (Figure 5.20, green boxes). TNFα mRNA expression was significantly lower in the absence of IFNγ signalling at days 6 (p=<0.05) and 8 (p=<0.005) post infection, compared to wildtype Sv129 mice.

IL-12p40 however, showed a different pattern of expression to the two previously discussed genes. Sv129 mice demonstrated elevated IL-12p40 mRNA expression at day 4 followed by a very slight declining trend towards day 8 (Figure 5.20, red boxes). qPCR failed to detect this mRNA at day 2 post infection in IFNγR$^{-/-}$ mice, but expression rapidly increased at day 4, with higher levels of IL-12p40 mRNA being expressed by IFNγR$^{-/-}$ animals at this timepoint than their wildtype counterparts (Figure 5.20, green boxes). This elevated trend continued until termination of the experiment at day 8, but differences in expression between the two strains of mice failed to reach statistical significance.

IL-6 mRNA expression was also examined, although no statistical analysis was carried out due to a limited number of samples being available for this particular PCR. However, the two strains appeared to show differing patterns of expression for this mRNA. Sv129 RNA was not assessed at day 2, but by day 4 showed strong upregulation compared to mock infected controls. Expression then began to decline towards day 8, but was extremely variable in nature (Figure 5.20, red boxes). IFNγR$^{-/-}$ animals, however, demonstrated

increasing expression of IL-6 mRNA, reaching a peak at day 6, similar to TNFα and iNOS mRNA expression, followed by a slight decline at day 8 but remaining strongly upregulated from baseline even at this late timepoint (Figure 5.20, green boxes).

Markers of alternative activation were also assessed to determine whether in the absence of IFNγ signalling, a more T_H2 skewed environment was achieved within the infected lung. Initially at day 2 post infection, Arg-1 mRNA expression was significantly higher in the IFNγR$^{-/-}$ lung than in Sv129 animals (Figure 5.21, first panel, p=<0.005). By day 4, Arg-1 mRNA expression had achieved similar levels in both strains of mice, and despite substantial variation, a relatively constant trend of expression was observed in both wildtype and IFNγR$^{-/-}$ animals.

Conversely, CD206 expression demonstrated significant differences in expression between the two strains of mice. Sv129 mice showed declining mRNA expression throughout the course of infection (Figure 5.21, red boxes), while IFNγR$^{-/-}$ showed significantly higher expression at days 2 (p=<0.05), 6 (p=<0.05) and 8 (p=<0.0005), although a temporary dip was observed at day 4 (Figure 5.21, green boxes). This is consistent with the CD206 mRNA expression data from the in vitro BMDMϕ, which showed IFNγR$^{-/-}$ BMDMϕ to upregulate this mRNA upon infection with WSN (Figure 4.9).

Sv129 IL-10 mRNA expression followed a similar trend to that observed for iNOS and TNFα expression, steadily increasing with time (Figure 5.21, red boxes). IFNγR$^{-/-}$ mice were elevated at day 2 post infection for this mRNA, followed by a temporary decrease in expression at day 4. However, IL-10 mRNA expression increased steadily from this timepoint until termination of the experiment (Figure 5.21, green boxes).

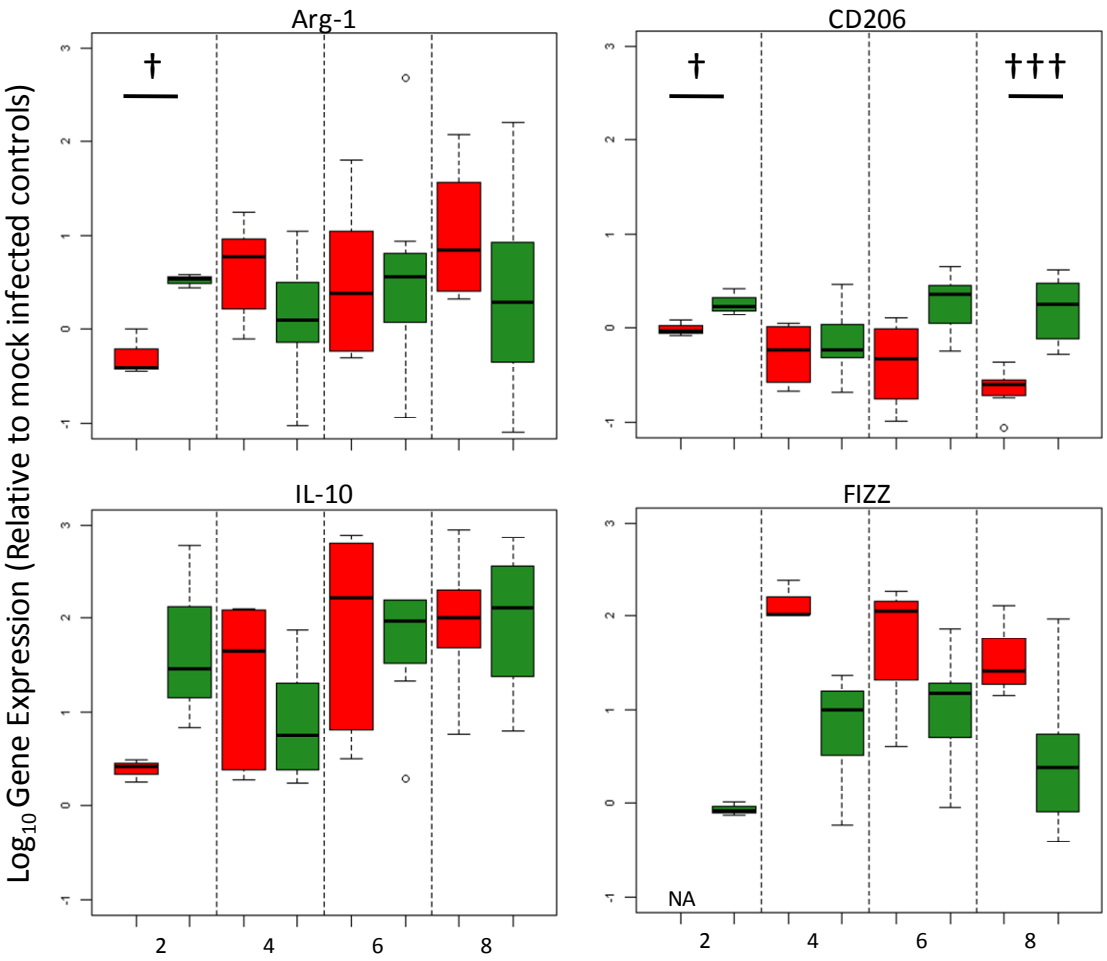

Figure 5.21 'Alternative' mRNA expression profile following infection with WSN.
RNA was extracted from lungs following infection with WSN and qPCR used to assess expression levels for markers of alternative activation. Samples were normalised against two housekeeping genes, CNX and SDHA, followed by normalisation against average expression of mock infected controls.
NA = qPCR not performed, ND = not detected
† indicates statistical significance between Sv129 and IFNγR$^{-/-}$ mice
(† $p<0.05$, †† $p<0.005$)
■ Sv129 ■ IFNγR$^{-/-}$
n= 7 per timepoint

Similar to IL-6, analysis of FIZZ mRNA expression was limited. However, Sv129 mice appeared to show a surprisingly high level of expression (Figure 5.21, red boxes). This was highest at day 4 post infection, the earliest timepoint assessed, and then declined towards day 8. This level of expression was substantially higher than that observed in the IFNγR$^{-/-}$ mice (Figure 5.21, green boxes). Interestingly, the pattern of FIZZ expression was remarkably similar to that of IL-6 mRNA. IL-6 is known to induce IL-4 production from naive T cells (Rincon *et al.*, 1997), and taken together with the elevated IL-10 mRNA expression, it is possible that the observed upregulation in FIZZ and Arg-1 mRNA is due to induction of these immunomodulatory cytokines.

IL-12p40 and TGFβ were also measured by ELISA (Figure 5.22). Wildtype Sv129 mice demonstrated a steady increase in IL-12p40 concentration (Figure 5.22a, red bars), while in contrast to this, IFNγR$^{-/-}$ showed a peak at day 4 post infection, with levels being significantly higher in the knock out than the wildtype animals at days 4 and 6 ($p<0.0005$ & $p<0.05$ respectively). IL-12p40 then declined to significantly lower levels than Sv129 mice (Figure 5.22a, green bars, $p<0.005$). This is in agreement with the mRNA expression data which showed elevated IL-12p40 mRNA at day 4 followed by decreasing levels in the IFNγR$^{-/-}$ animals, and elevated but steady expression in Sv129 mice (Figure 5.20).

TGFβ however, was detectable at low levels in Sv129 mice at day 2 post infection, but subsequently declined to undetectable levels by the end of the experiment. IFNγR$^{-/-}$ animals demonstrated higher concentrations of this cytokine early in infection, but this failed to reach statistical significance due to some animals within both strains failing to express TGFβ. By day 4, TGFβ levels were similar between the two strains. However, in contrast to wildtype animals, the knockout mice retained some TGFβ at day 8 (Figure 5.22b). Despite the role this cytokine plays in wound healing and tissue repair, it appears that neither strain of mice upregulate TGFβ following influenza virus

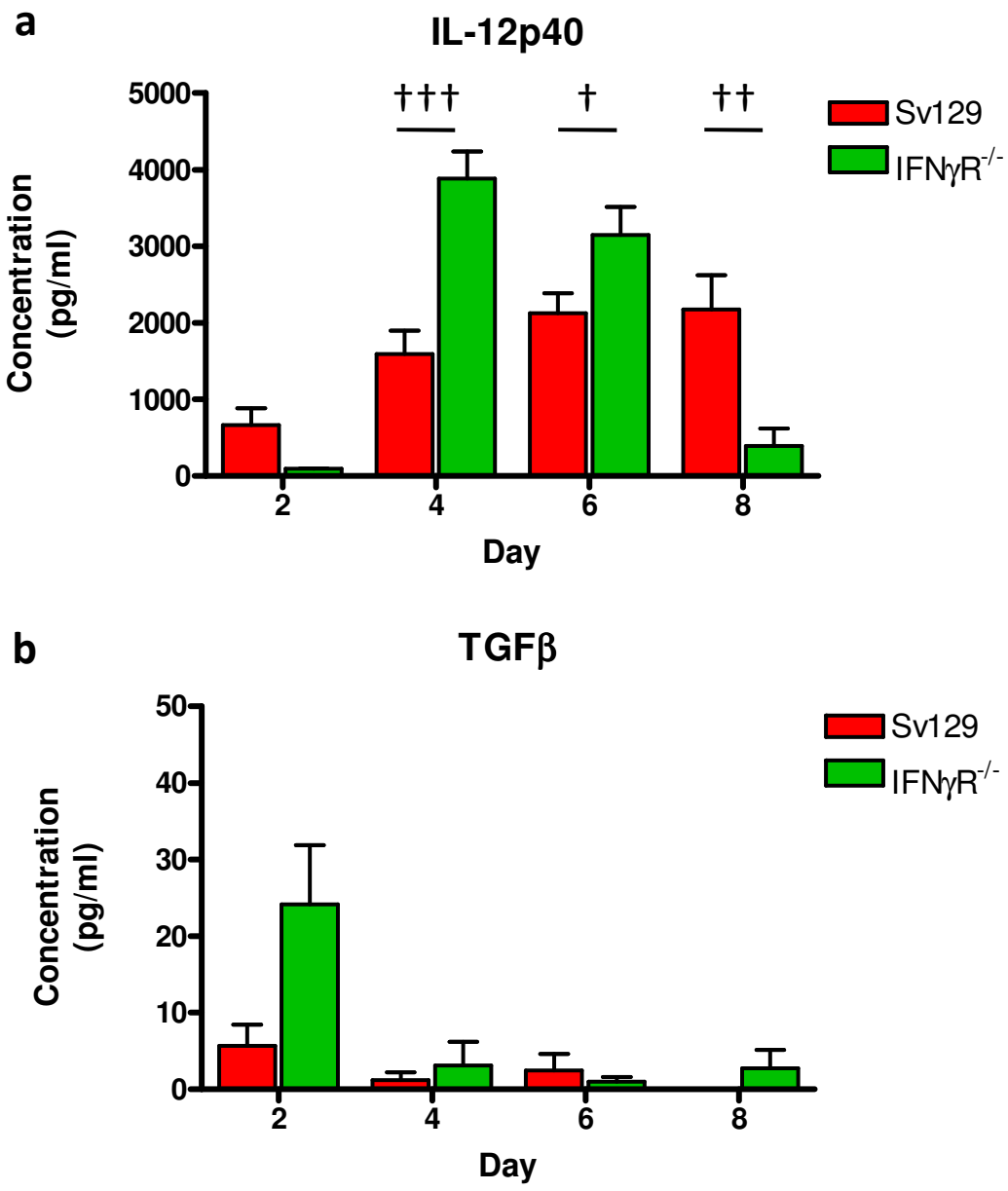

Figure 5.22 ELISA detection of IL-12p40 and TGFβ.
IL-12p40 (a) and TGFβ (b) concentrations in lung homogenates were measured by ELISA. The average concentration of cytokine for mock infected mice was subtracted to determine induction of cytokine in response to virus. The average background concentration of both cytokines was higher in Sv129 mice than IFNγR$^{-/-}$ animals; 226pg/ml vs 126pg/ml for IL-12p40 and 56pg/ml vs 30pg/ml for TGFβ.
† $p<0.05$, †† $p<0.005$, ††† $p<0.0005$
n= 7 per timepoint

infection, regardless of the need to repair damage within the lung and return this fragile environment to homeostasis.

5.3 Summary of results and discussion

The data presented in this chapter demonstrate that inhibition of IFNγ signalling results in ameliorated disease and mild immunopathology in vivo. Sv129 mice suffered from severe disease, rapid weight loss and early onset of symptoms, while IFNγR$^{-/-}$ mice were protected. Further investigation revealed that wildtype Sv129 mice showed intense and diffuse cellular infiltration throughout the lungs, a large proportion of which consisted of macrophages and neutrophils. This in turn led to elevated mRNA expression for proinflammatory genes iNOS, TNFα and IL-6, ultimately resulting in the extreme morbidity observed in this strain of mice, despite a concurrent increase in IL-10 and FIZZ mRNA expression.

Conversely, IFNγR$^{-/-}$ mice demonstrated mild clinical symptoms with limited weight loss. Although largely composed of macrophages and neutrophils, cellular infiltration into the lung appeared less extreme than that observed in wildtype mice, and consistent with this, lower levels of mRNA for inflammatory modulators were detected. However, inflammatory infiltration was qualitatively assessed by examination of histological sections only. Quantitative analysis is required to confirm differences between the two strains under investigation.

Viral titres also differed between the two strains of mice, with Sv129 mice showing titres of around one log higher than IFNγR$^{-/-}$ animals. This was corroborated by immunohistochemical analysis of lung sections which showed more widespread and intense staining for viral proteins in the wildtype animals. Sv129 animals also appeared to show more severe damage to the bronchiolar epithelium compared to IFNγR$^{-/-}$ mice. As previously discussed, it is possible that IFNγR$^{-/-}$ cells are less permissive to either viral entry or

replication and therefore this may limit the amount of replicating virus and consequent pathology and cytokine production observed in the lungs of these mice compared to their wildtype counterparts. Macrophages from both strains of mice stained positive for viral proteins to a similar extent in vitro, indicating that the differing pathology observed is likely due to finite numbers of infiltrating cells, recruited by cytokine production in the epithelium and resident macrophages, rather than differing infectivity or efficiency of macrophage function within the lung, although absolute quantification of cellular influx is required to confirm this. This suggests that differences in viral permissiveness between Sv129 and IFNγR$^{-/-}$ epithelial cells have an important effect on the overall pathology and clinical outcome of the disease.

Interestingly, IFNγR$^{-/-}$ mice demonstrated most weight loss at day 6 post infection. This timepoint coincides with highest expression of iNOS, TNFα and IL-6 mRNA expression, as well as that of the viral mRNA M1, despite declining viral titres at this timepoint. This strongly suggests that the severity of symptoms observed is closely linked to the levels of proinflammatory cytokines induced by the virus. Sv129 mice demonstrated increasing expression of mRNA for proinflammatory modulators throughout the course of infection, indicating that excessive production and accumulation of cytokines within the lungs exacerbates disease. This is in agreement with previous studies which have shown peak titres of PR8 virus and maximal cytokine expression to be temporally distinct (Hennet *et al.*, 1992), resulting in a cytokine storm-like illness as the virus is cleared. Infection with highly pathogenic influenza viruses H5N1 and the 1918 H1N1 virus have similarly shown dramatically elevated cytokine expression, resulting in severe disease and organ failure (Cheung *et al.*, 2002; Kobasa *et al.*, 2007; Perrone *et al.*, 2008), and so the pattern observed during WSN infection is characteristic of a highly pathogenic virus.

Two potential hypotheses may explain the lack of a cytokine storm in the IFNγR$^{-/-}$ mice. Firstly, it is possible that reduced replication in these animals limits pathology and induction of proinflammatory cytokines. This hypothesis implies that the substantial and rapid replication observed in wildtype animals is responsible for induction of the uncontrolled cytokine response rather than immune dysregulation per se. Alternatively, the lack of IFNγ signalling may impair the inflammatory response sufficiently that no cytokine cascade occurs. However, this second hypothesis does not explain the lower viral titres observed and necessitates further investigation of potential mechanisms of viral clearance and control in the absence of a strong cytokine response.

Infection with highly pathogenic influenza viruses of both avian and human origin have been shown to increase infiltration of neutrophils and macrophages to the respiratory tract (Perrone *et al.*, 2008; Sakai *et al.*, 2000). Immunostaining for F4/80 and Ly6G positive cells strongly suggests that increased numbers of macrophages and neutrophils found in the wildtype Sv129 lung contribute to the inflammatory cytokine environment, and this high expression of inflammatory mediators may result in further influx of these cells, ultimately resulting in a cytokine storm and severe morbidity.

Neutrophils play a vital role during influenza virus infection and are responsible, along with macrophages, for clearance of infected cells. This phagocytic process results in activation of macrophages, further enhancing clearance of the infection (Hashimoto *et al.*, 2007). Targeted depletion of neutrophils using a monoclonal antibody against Ly6G resulted in infection with the low pathogenic HKx31 influenza virus becoming systemic and lethal (Tate *et al.*, 2009). However, despite this crucial role in clearance, neutrophils also contribute to the proinflammatory cytokine environment in the lung, adding to excess tissue damage and organ failure. Inhibiting recruitment of neutrophils to the infected lung reduced immunopathology, and although mice ultimately succumbed to infection, survival was prolonged in comparison to

infected controls (Sakai *et al.*, 2000). IFNγR$^{-/-}$ mice appeared to demonstrate fewer infiltrating neutrophils compared with Sv129 animals, although absolute quantification is required to confirm this observation. However, taken together with the findings of previous studies, this suggests that infiltration of reduced numbers of neutrophils may be beneficial to the host, as this limits the production of damaging proinflammatory cytokines while still facilitating clearance of infected material.

A functional CTL response is known to be protective against influenza virus infection. However, infection may result in dysregulation of this response, leading to enhanced viral replication and immunopathology. Upon infection, macrophages upregulate expression of TNFα and TRAIL (Herold *et al.*, 2008), which has been implicated in induction of apoptosis of human T cells during highly pathogenic influenza virus infection in vitro (Zhou *et al.*, 2006). It is possible that during in vivo infection, CTL numbers are reduced by TRAIL mediated apoptosis, resulting in a poor CTL response and prolonged viral replication. Additionally, nitric oxide production by mϕ has been shown to suppress T cell activation (Hamilton *et al.*, 2010). WSN infected IFNγR$^{-/-}$ mice express reduced iNOS and TNFα and it is tempting to speculate that a reduction in TRAIL expression may also occur compared with Sv129 counterparts. It may, therefore, be possible that by impairing the inflammatory response to virus, the CTL response is protected from TRAIL and nitric oxide mediated dysregulation and may function efficiently to clear the infection. However, neither expression of TRAIL, nor CTL numbers or responses were assessed during this project. Investigation of these parameters on the IFNγR$^{-/-}$ background may help to elucidate the role that dysregulated cytokine production plays in functional immune responses to virus.

Further to this, the speed of viral replication has been implicated in generation of an efficient CTL response. Rapidly replicating virus induces a poor CTL response, due to increased FasL expression in the lymph nodes. This results

in apoptosis of circulating CTLs and reduction of the overall magnitude of the anti-influenza response. However, delayed replication fails to upregulate FasL, allowing an efficient CTL response to proceed (Legge & Braciale, 2005). IFNγR$^{-/-}$ animals demonstrate delayed replication in comparison to Sv129 mice, evidenced by limited NS1 staining at early timepoints. However, FasL induced apoptosis of circulating CTLs was found to be IL-12p40 dependent. IFNγR$^{-/-}$ mice demonstrate delayed onset of IL-12p40 expression, being detectable at day 4 rather than day 2 as in Sv129 mice, but expression of this mRNA was higher in the IFNγR$^{-/-}$ animals than their wildtype counterparts, so protection of these mice is unlikely to be due to subversion of this interaction.

Inhibition of IFNγ signalling leads to lower cytokine production and fewer inflammatory cells, but whether this is due to cells within the IFNγR$^{-/-}$ lung being less permissive to viral replication and therefore recruiting fewer inflammatory cells to the lung, or whether the lack of IFNγ signalling merely limits the inflammatory potential of infiltrating cells remains to be elucidated. TRAIL expression on infiltrating macrophages induces apoptosis in alveolar epithelial cells (AEC) (Herold *et al.*, 2008), which aside from causing immunopathology in itself, also reduces the number of epithelial cells available to interact with macrophages. AEC express inhibitory molecules such as CD200, which are involved in maintaining macrophage quiescence during homeostasis and preventing inappropriate inflammatory responses. However, disruption of the CD200:CD200R interaction results in macrophage activation, and during influenza virus infection, apoptosis and sloughing of AEC leads to a loss of CD200 expression and further activation of macrophages in the lung (Snelgrove *et al.*, 2008). The reduced level of infection, as observed using anti-NS1 staining, concurrent with the inhibition of proinflammatory mediators in IFNγR$^{-/-}$ mice may ultimately result in enhanced survival of AEC and maintenance of suppressive interactions with macrophages, further reducing the inflammatory environment within the lung.

Infection was established in a delayed manner in IFNγR$^{-/-}$ mice compared to Sv129 animals, similar to the kinetics observed following in vitro infection of BMDMϕ. As previously discussed, it is possible that absence of the sialylated IFNγ receptor on the surface of both AEC and macrophages alike substantially impedes viral entry to the cell, leading to delayed and limited infection. Consistent with this hypothesis, IFNγR$^{-/-}$ mice show lower viral titres in the lung compared to their wildtype counterparts and reduced staining for viral antigens in the epithelium. This in turn will have a dramatic effect on the cytokine environment, as fewer infected cells results in lower induction of proinflammatory cytokines, further indicating a vital role for viral replication in development of the cytokine storm. It is interesting that IFNγR$^{-/-}$ and wildtype Sv129 mice showed no difference in survival following infection with the H3N2 virus, HKx31 (Price *et al.*, 2000). Despite seemingly being in contrast to the data presented here, this could be explained by the ability of the HKx31 virus to utilise CD206 on the surface of macrophages, facilitating efficient infection of this cell type (Reading *et al.*, 2000) and leading to reduced free virus available to infect epithelial cells and cause disease (Tate *et al.*, 2010c). Infection of macrophages via CD206 and subsequent sequestration of virus strains such as HKx31 may negate the role played by the IFNγ receptor in internalisation of a strain of virus such as WSN, which does not bind to CD206. However, many other sialylated endocytic receptors are present on the surface of both epithelial cells and macrophages in addition to the IFNγ receptor, limiting the likelihood of this receptor playing a major role in the protection of IFNγR$^{-/-}$ cells from infection.

An alternative hypothesis regarding the limited infection observed in IFNγR$^{-/-}$ mice suggests that macrophages play a limiting role in virus dissemination. It has previously been reported that influenza virus more readily infects resident rather than infiltrating macrophages, demonstrated by culturing of resistant "exudate" macrophages for 7 days, by which time they acquire a "resident" phenotype and are susceptible to influenza virus infection (Rodgers & Mims,

1981). It is possible that potential differences in the numbers of resident alveolar macrophages between wildtype Sv129 and IFNγR$^{-/-}$ mice may affect the outcome of disease. Following mock infection with PBS, it appeared that IFNγR$^{-/-}$ mice showed higher numbers of macrophages, which may be resident rather than recruited to the lungs. As it has also been shown that efficient infection of macrophages in vivo ameliorates disease (Tate *et al.*, 2010c), it is possible that higher numbers of resident alveolar macrophages may limit the early dissemination of virus and delay establishment of infection by becoming infected themselves in an abortive infection. Enhanced infection of resident alveolar macrophages may result in less free virus coming into contact with the epithelium and therefore limit spread of the virus. Macrophages in the lungs of both Sv129 and IFNγR$^{-/-}$ mice stain positive for viral proteins, but whether this is phagocytosed material or active infection is unknown. Further staining using the polyclonal anti-NS1, or an equivalent antibody to detect newly synthesised proteins would elucidate this, shedding light on whether differences arise in viral replication within macrophages of these strains of mice. Additionally, clarification of the cellular constitution of the naive lung in both strains of mice is necessary to identify any underlying differences, especially in CTL and resident macrophage numbers, which may have an effect on disease outcome.

Interestingly, CD206 was upregulated in IFNγR$^{-/-}$ mice following infection. As discussed in Chapter 4, WSN is unlikely to interact with this receptor due to a lack of glycosylation sites on its HA and NA proteins. However, CD206 can exist as a truncated, soluble form of the receptor (sCD206) which is secreted and may act as an opsonin for pathogens displaying mannosylated moieties (Martinez-Pomares *et al.*, 1998). sCD206 has subsequently been reported to bind macrophages and dendritic cells via sialoadhesin (Martinez-Pomares *et al.*, 1999) and simultaneously bind mannosylated antigens, transporting them to the subcapsular sinus and presenting them to circulating B cells (Carrasco & Batista, 2007; Junt *et al.*, 2007; Martinez-Pomares & Gordon, 1999). In the

absence of IFNγ mediated suppression, CD206 mRNA is upregulated following infection with influenza virus, further implicating this receptor in host defence against infection.

Surprisingly, FIZZ, a known marker of alternative activation in macrophages, was upregulated in a manner similar to IL-6, following infection of both Sv129 and IFNγR$^{-/-}$ animals. FIZZ was initially identified during allergic inflammation of the lung, where it is produced by epithelial cells, type II pneumocytes and macrophages (Holcomb *et al.*, 2000). It has been demonstrated to play a role in wound healing and fibrosis and is abundantly found in injured lungs where it induces expression of type I collagen (Liu *et al.*, 2004). Interestingly, it has recently been shown that FIZZ may also play a role in immune modulation, as FIZZ deficient mice demonstrated exacerbated T_H2 inflammation following implantation of *S. masoni* eggs (Nair *et al.*, 2009). This study showed FIZZ to inhibit expression of IL-4, while having no effect on expression of T_H1 cytokines. This role is in apparent contradiction of its expression in alternatively activated macrophages, which are generally thought of as T_H2 type cells. However, FIZZ appears to limit excessive T_H2 responses induced by alternatively activated macrophages while promoting repair of damaged tissue. In the present study, the concurrent expression of IL-6 and alternative markers FIZZ and Arg-1 is intriguing, as the latter are induced by IL-4, while IL-6 induces early IL-4 expression from naive T cells (Rincon *et al.*, 1997), yet T_H1 cytokines TNFα and IL-12 dominate the response to influenza virus. It may be possible that elevated IL-6 induces IL-4 expression from T cells present in the bronchus associated lymphoid tissue which, in addition to priming these T cells for a T_H2 response, may be released within the lung resulting in alternative activation of macrophages and upregulation of wound healing molecules FIZZ and Arg-1. FIZZ may then function to inhibit this T_H2 response, ultimately allowing progression of the inflammatory response to virus. No evidence of fibrosis is detectable within the lungs during the 8 day observation period. Further timepoints may indicate development of fibrosis,

but as IFNγR$^{-/-}$ mice display lower FIZZ expression consistent with milder infection, it is likely that high expression of this gene is a result of severe disease, and as such the mice would not survive a longer course of infection.

The Sv129 background has been identified as $T_H1$biased, as determined by failure of splenocytes to produce IL-4 in response to concavalin A, even in the presence of exogenous IL-4 (Schijns *et al.*, 1994). This strain of mouse also demonstrates resistance to infection with *L. major* in an IL-12 dependent manner (Mattner *et al.*, 1996), while the prototype T_H2 BALB/c mouse is susceptible. Interestingly, disruption of either subunit of IL-12 on the Sv129 background results in strong IL-4 expression following *L. major* infection (Mattner *et al.*, 1996), while IFNγR$^{-/-}$ animals demonstrate a predominantly T_H1 cytokine profile with expression of IL-2 and IFNγ, but reduced IL-10 in response to psuedorabies virus (Schijns *et al.*, 1994). This suggests that IL-12 controls development of a functional T_H1 response on this background. The detection of IL-12 mRNA and functional protein in the present study indicates that IFNγR$^{-/-}$ mice may develop a T_H1-like response in CD4$^+$ T cells, and that limited viral replication detected may play a greater role in the decreased proinflammatory cytokine mRNA expression observed than an overt skewing of the immune response. However, to truly understand the extent to which a T_H2 response develops in the mutant mice versus their wildtype counterparts, it would be vital to measure expression of IL-4, especially in light of the intriguing FIZZ and Arg-1 expression observed.

In summary, disruption of the IFNγ receptor results in reduced immunopathology and ameliorated disease following infection with influenza virus, but whether this is due to impaired inflammation, limited viral replication or altered viral clearance remains to be elucidated.

6 Discussion and Future Directions

6.1 Discussion

Infection with the mouse adapted influenza A virus, WSN, resulted in release of pro-inflammatory cytokines in Sv129 BMDMϕ in vitro and within the lung following in vivo infection. Infection resulted in severe weight loss, clinical symptoms and decreased survival. Symptoms were largely attributed to the excessive inflammatory response and cellular infiltration into the lung, ultimately resulting in severe pneumonia and organ failure. This thesis aimed to investigate the hypothesis that alteration of the inflammatory response may be beneficial to the host and limit the tissue damage suffered as a result of the classical immune response to influenza virus.

BMDMϕ can be alternatively activated by incubation with IL-4 (Stein *et al.*, 1992), resulting in a broadly anti-inflammatory phenotype. It was hypothesised that inhibition of the classical, inflammatory macrophage response to influenza, by infecting alternatively activated macrophages or mice unable to respond to IFNγ, may lead to ameliorated disease.

Both classical and alternatively activated BMDMϕ were successfully infected with the WSN strain of influenza virus, but the alternatively activated group demonstrated enhanced positivity for virus concurrent with reduced survival. The same was true of IFNγR$^{-/-}$ BMDMϕ, although establishment of infection on this background was somewhat delayed. However, by 48 hours post infection, BMDMϕ of both backgrounds demonstrated similar levels of staining for viral proteins, although those on the IFNγR$^{-/-}$ background were markedly reduced in their ability to survive infection, especially in the alternatively activated group.

Delayed infection was also evident in vivo following infection of IFNγR$^{-/-}$ mice. Wildtype Sv129 mice displayed strong and widespread positivity for the viral protein NS1 as early as day 2, which remained evident until termination of the experiment at day 8. IFNγR$^{-/-}$ mice, however, showed substantially less NS1 positivity at day 2, and following the peak of NS1 production at day 4, declined to almost undetectable levels by day 8.

Both the in vitro and in vivo infection data suggest that a block is imposed by IFNγR$^{-/-}$ cells during the infection process, most likely either at the attachment and entry stage or during early replication. BMDMϕ from both strains of mice can become alternatively activated in the presence of IL-4, and both display similar levels of viral positivity by 48 hours post infection, suggesting that induction of an anti-inflammatory environment within the cell does not provide a substantial block to replication. However, cells on the IFNγR$^{-/-}$ background are unable to respond to IFNγ, either given exogenously in vitro, or locally produced in vivo, and therefore no IFNγ-induced inflammatory burst occurs early in infection. It is possible that the virus hijacks this rapid burst of metabolic activity to synthesis its own early proteins such as NS1, and in the absence of this activity, establishment of infection is delayed. However, the cellular microenvironment may ultimately be more permissive for viral replication due to reduced iNOS expression, allowing the virus to replicate to similar levels as seen in Sv129 cells, but with delayed kinetics.

Influenza virus binds to SA, which is ubiquitously expressed on the cell surface. However, avian and mammalian influenza viruses differ in their specificity for SA linkages, with avian viruses preferentially binding α2,3 linked SA and mammalian viruses binding α2,6 (Connor *et al.*, 1994). This preference dictates the host species restriction of influenza viruses. Despite binding of SA being a prerequisite for infection, it does not necessarily lead to efficient internalisation of the virus. Reading and colleagues have recently proposed a model whereby influenza interacts with SA on the surface of the cell to bring

the virion into close contact with endocytic receptors, which then facilitate entry and uncoating of the virus in acidified vesicles (Tate *et al.*, 2010a; Upham *et al.*, 2010). This could explain the differences in infection kinetics between Sv129 and IFNγR$^{-/-}$ animals both in vitro and in vivo. The IFNγ receptor is internalised following binding of its ligand, whereby it enters the endosomal pathway. It is possible to speculate that sialic acid mediated binding of influenza virus to the IFNγ receptor may facilitate entry and infection via binding of SA followed by internalisation through the normal IFNγ receptor pathway. IFNγ receptors are highly expressed on the surface of many cell types, including macrophages and epithelial cells (Valente *et al.*, 1992) and therefore disruption of this receptor may result in a net loss of suitable SA and receptors to mediate internalisation in both in vitro generated BMDMϕ and during in vivo infection of IFNγR$^{-/-}$ mice.

Upon establishment of infection, it is evident that inhibition of IFNγ signalling leads to an impaired inflammatory response both in vitro and in vivo. IFNγR$^{-/-}$ BMDMϕ generated a transient upregulation of iNOS and TNFα mRNA at 16 hours, which was not sustained in the absence of IFNγ signalling. These proinflammatory mediators were markedly reduced compared to Sv129 BMDMϕ by 48 hours post infection.

Following infection of alternatively activated macrophages, BMDMϕ from both genetic backgrounds demonstrated a reduced inflammatory response. This was intriguing as infection with WSN was evidently sufficiently proinflammatory to induce a subset of alternatively activated macrophages into classical activation. However, complete infection of the BMDMϕ population was not achieved, suggesting that the subset that remained uninfected may be capable of sustaining their alternative activation profile. Furthermore, alternatively activated BMDMϕ from both Sv129 and IFNγR$^{-/-}$ mice demonstrated enhanced positivity for viral proteins and reduced survival in vitro following infection. This may result in efficient elimination of virus as it

has recently been demonstrated that the efficiency with which macrophages become infected by influenza virus is inversely correlated with disease severity (Tate *et al.*, 2010c). This, along with the subdued inflammatory response to virus in alternatively activated BMDMϕ and the impaired response observed from IFNγR$^{-/-}$ BMDMϕ suggested that the inflammatory response may be subverted in vivo using either genetically modified mice or alternatively activating stimuli.

Indeed, infection of IFNγR$^{-/-}$ mice did result in ameliorated disease and improved clinical score, associated with a reduction in immunopathology and cytokine expression. As seen in vitro, IFNγR$^{-/-}$ mice displayed significantly lower iNOS and TNFα mRNA, although IL-12p40 mRNA expression was slightly higher in the IFNγR$^{-/-}$ animals than their wildtype counterparts.

High concentrations of inflammatory mediators TNFα and iNOS have often been associated with highly pathogenic influenza viruses and severe pathology (Cheung *et al.*, 2002). These mediators were elevated in Sv129 animals and BMDMϕ compared to those on the IFNγR$^{-/-}$ background, which achieved a greatly reduced peak expression at day 6 post infection. This timepoint correlated with maximum weight loss in these animals, while virus titres were declining. Although it has also been shown that elevated TNFα does not necessarily preclude immunopathology (Monteerarat *et al.*, 2010), it certainly appears to be involved in this model. Furthermore, several studies have demonstrated the contribution made by this cytokine to the damaging immunopathology observed. TNFαR$^{-/-}$ mice showed delayed morbidity with a highly pathogenic strain of H5N1 (Szretter *et al.*, 2007), while blocking TNFα with monoclonal antibodies resulted in maintenance of body weight and improved clinical score following infection (Hussell *et al.*, 2001). Anti-TNFα therapy has proved successful in treating inflammatory diseases such as rheumatoid arthritis (Maini *et al.*, 1995), while pharmacological inhibition of NFκB signalling using Sulfasalazine has been of benefit in treating the

inflammatory arthritis resulting from macrophage derived TNFα during Ross River Virus infection (Lidbury *et al.*, 2008). Inhibition of iNOS and TNFα using the drug Pioglitazone ameliorated PR8-induced inflammation and immunopathology (Aldridge *et al.*, 2009), demonstrating an important role of these proinflammatory molecules in disease progression. Consistent with this, inhibition of IFNγ signalling ultimately results in ameliorated disease due to reduced recruitment of inflammatory cells and subsequently, reduced expression of inflammatory mediators.

Other mechanisms of protection are also of interest, for example, maintaining the structural integrity of the lung in order to prevent induction of inflammatory responses. CD200 is an inhibitory molecule expressed on the surface of epithelial cells and interacts with CD200R on macrophages within the lung. Loss of this interaction leads to activation of macrophages and inflammatory responses (Snelgrove *et al.*, 2008). During influenza virus infection, epithelial cells become infected and apoptotic, sloughing off in the process, therefore decreasing the available CD200 to inactivate macrophages, ultimately leading to higher cytokine expression, failure to resolve inflammation and severe disease. Treatment with an agonising anti-CD200R antibody resulted in decreased macrophage activation and improved clinical score (Copland *et al.*, 2007; Snelgrove *et al.*, 2008).

Interestingly, IFNγR$^{-/-}$ BMDMϕ demonstrated higher baseline levels of TGFβ than wildtype Sv129 counterparts. Expression of this cytokine is also higher early in infection in vivo in IFNγR$^{-/-}$ mice. TGFβ and IL-10 upregulate the expression of CD200R on macrophages (Snelgrove *et al.*, 2008), suggesting that in addition to an impaired inflammatory response resulting from inhibition of IFNγ signalling, macrophages in this strain of mice may be more responsive to CD200-mediated inactivation, further preventing development of inflammatory responses in the lung following infection with WSN.

TGFβ, along with IL-6, is required for development of T_H17 cells. IL-6 expression increased with time during infection of IFNγR$^{-/-}$ mice, a pattern of expression which corresponds temporally to development of the T cell response. It has been suggested that T_H17 responses may be protective during influenza virus infection as IL-17 induces proliferation of airway epithelial cells (Inoue *et al.*, 2006), thereby reducing influenza mediated immunopathology and additionally, may enhance CD200, CD200R interactions by replenishing the epithelial cell layer. This is, however, controversial as while some groups demonstrate protection following adoptive transfer of ex vivo activated T_H17 cells (McKinstry *et al.*, 2009), others show disruption of IL-17 signalling to be beneficial in reducing TNFα and IL-6 levels (Crowe *et al.*, 2009). However, it may be of interest to investigate whether in the absence of IFNγ signalling, a T_H17-like environment develops.

IFNγR$^{-/-}$ mice demonstrated increased expression of CD206 mRNA both in vivo and following in vitro activation of BMDMϕ compared with wildtype Sv129 animals. Wildtype Sv129 BMDMϕ displayed efficient upregulation of this receptor following IL-4 stimulation as expected, but strongly downregulated expression in vivo. This receptor has been implicated not only in facilitating influenza virus attachment and entry (Reading *et al.*, 2000), but also as a soluble opsonin capable of displaying antigen to B cells in its native form in the subcapsular sinus (Junt *et al.*, 2007; Martinez-Pomares & Gordon, 1999). The upregulation of this receptor on the IFNγR$^{-/-}$ background is intriguing. It may be possible that upregulation of this receptor, especially in its soluble form, may be a non specific defence against infection, upregulated in the absence of IFNγ signalling. Given the T_H1 skewed phenotype of Sv129 and the elevated expression of CD206 observed in the BALB/c BMDMϕ following infection (Figure 4.9), it would be interesting to investigate the expression and potential role of this receptor in vivo on the T_H2 oriented BALB/c background.

Inhibition of respiratory virus associated immunopathology has been the subject of investigation by many studies, and subversion of this response appears to efficiently enhance clinical outcome. However, each of the many studies has investigated a different mediator in the inflammatory response, often using genetically modified animals. NOS2$^{-/-}$ (Karupiah *et al.*, 1998), TNFαR$^{-/-}$ (Szretter *et al.*, 2007), platelet activating factor R$^{-/-}$ (Garcia *et al.*, 2010) and TLR3$^{-/-}$ mice (Le Goffic *et al.*, 2006), along with depletion of TNFα and iNOS using monoclonal antibodies (Hussell *et al.*, 2001) or drugs (Aldridge *et al.*, 2009) have all demonstrated protection from influenza induced immunopathology to varying degrees. Conversely, disruption of TLR4 (Hashimoto *et al.*, 2007), CD200 (Snelgrove *et al.*, 2008) and CCL5 (Tyner *et al.*, 2005) genes exacerbated disease severity and inflammatory responses following respiratory virus infection. While individually significant, taken together as a whole, these studies serve to emphasise the complexity of the inflammatory response to viral infection, with a high degree of redundancy between mediators further complicating dissection of this response. The results presented herein provide further evidence as to the validity of subverting the inflammatory response as a means to ameliorate influenza virus induced immunopathology.

6.2 Future directions

Although ablation of the INFγ receptor ameliorated disease following influenza virus infection, this raises further questions with regards to the wildtype mouse. For example, does inhibition of IFNγ signalling using monoclonal antibodies result in the same degree of amelioration in Sv129 mice as observed in IFNγR$^{-/-}$ animals? This may also help to investigate the role of the IFNγ receptor in viral entry versus impairment of the inflammatory response on disease severity.

Likewise, is it possible to alter the course of disease in the wildtype mouse by intra-tracheal transfer of ex vivo activated macrophages? Given the enhanced capacity of alternatively activated BMDMϕ to take up virus and undergo apoptosis, it is possible that free virus may be more efficiently captured by these macrophages either due to enhanced infection or phagocytosis, ultimately resulting in abortive infection and protection of epithelial cells from infection.

If this indeed proves to be possible, then investigating means of inducing alternative activation of in vivo macrophages may be important. For example, helminth worms and their products are known to induce this activation state in vivo and so would co-infection of mice with a parasitic worm, or treatment with worm products eg implantation of schistosome eggs, provide protection from influenza virus induced pathology? This approach is of course, complicated by the presence of a second pathogen and the possibility of pathology induced by the parasite or its derived products, for example fibrosis due to enhanced FIZZ and Arg-1 expression.

On a more fundamental level, there appears to be some discrepancy between Sv129 and IFNγR$^{-/-}$ animals in their baseline expression of several cytokines and cellular composition in the lung. It is possible that due to these

differences, and to the altered cytokine environment following infection, cells such as CTLs may become differentially activated in IFNγR$^{-/-}$ animals. It may be of interest to further characterise the IFNγR$^{-/-}$ mouse on the Sv129 background with regards to cytokine expression and cell distribution during homeostasis, especially cells of the innate immunity which have thus far been overlooked by previous studies. The downstream effects of differences in cytokine expression and cell proportions may have important consequences for the immune response to viral infection.

Although further study is clearly warranted, the data presented in this thesis show that subversion of the host inflammatory response by inhibiting IFNγ signalling results in ameliorated disease and improved prognosis following influenza virus infection and furthermore, implicate the IFNγ receptor as a facilitator of efficient influenza virus infection.

References

Aderem, A. & Underhill, D. M. (1999). Mechanisms of phagocytosis in macrophages. *Annu Rev Immunol* **17**, 593-623.

Akaike, T., Noguchi, Y., Ijiri, S., Setoguchi, K., Suga, M., Zheng, Y. M., Dietzschold, B. & Maeda, H. (1996). Pathogenesis of influenza virus-induced pneumonia: involvement of both nitric oxide and oxygen radicals. *Proc Natl Acad Sci U S A* **93**, 2448-2453.

Aldridge, J. R., Jr., Moseley, C. E., Boltz, D. A., Negovetich, N. J., Reynolds, C., Franks, J., Brown, S. A., Doherty, P. C., Webster, R. G. & Thomas, P. G. (2009). TNF/iNOS-producing dendritic cells are the necessary evil of lethal influenza virus infection. *Proc Natl Acad Sci U S A* **106**, 5306-5311.

Ali, A., Avalos, R. T., Ponimaskin, E. & Nayak, D. P. (2000). Influenza virus assembly: effect of influenza virus glycoproteins on the membrane association of M1 protein. *J Virol* **74**, 8709-8719.

Allen, I. C., Scull, M. A., Moore, C. B., Holl, E. K., McElvania-TeKippe, E., Taxman, D. J., Guthrie, E. H., Pickles, R. J. & Ting, J. P. (2009). The NLRP3 inflammasome mediates in vivo innate immunity to influenza A virus through recognition of viral RNA. *Immunity* **30**, 556-565.

Anderson, C. F. & Mosser, D. M. (2002). Cutting edge: biasing immune responses by directing antigen to macrophage Fc gamma receptors. *J Immunol* **168**, 3697-3701.

Anthony, R. M., Urban, J. F., Jr., Alem, F., Hamed, H. A., Rozo, C. T., Boucher, J. L., Van Rooijen, N. & Gause, W. C. (2006). Memory T(H)2 cells induce alternatively activated macrophages to mediate protection against nematode parasites. *Nat Med* **12**, 955-960.

Aragon, T., de la Luna, S., Novoa, I., Carrasco, L., Ortin, J. & Nieto, A. (2000). Eukaryotic translation initiation factor 4GI is a cellular target for NS1 protein, a translational activator of influenza virus. *Mol Cell Biol* **20**, 6259-6268.

Avalos, R. T., Yu, Z. & Nayak, D. P. (1997). Association of influenza virus NP and M1 proteins with cellular cytoskeletal elements in influenza virus-infected cells. *J Virol* **71**, 2947-2958.

Bach, E. A., Szabo, S. J., Dighe, A. S., Ashkenazi, A., Aguet, M., Murphy, K. M. & Schreiber, R. D. (1995). Ligand-induced autoregulation of IFN-gamma receptor beta chain expression in T helper cell subsets. *Science* **270**, 1215-1218.

Basso, A. S., Cheroutre, H. & Mucida, D. (2009). More stories on Th17 cells. *Cell Res* **19**, 399-411.

Belser, J. A., Wadford, D. A., Pappas, C., Gustin, K. M., Maines, T. R., Pearce, M. B., Zeng, H., Swayne, D. E., Pantin-Jackwood, M., Katz, J. M. & Tumpey, T. M. (2010). Pathogenesis of pandemic influenza A (H1N1) and triple-reassortant swine influenza A (H1) viruses in mice. *J Virol* **84**, 4194-4203.

Bergmann, M., Garcia-Sastre, A., Carnero, E., Pehamberger, H., Wolff, K., Palese, P. & Muster, T. (2000). Influenza virus NS1 protein counteracts PKR-mediated inhibition of replication. *J Virol* **74**, 6203-6206.

Bernabei, P., Coccia, E. M., Rigamonti, L., Bosticardo, M., Forni, G., Pestka, S., Krause, C. D., Battistini, A. & Novelli, F. (2001). Interferon-gamma receptor 2 expression as the deciding factor in human T, B, and myeloid cell proliferation or death. *J Leukoc Biol* **70**, 950-960.

Blaas, D., Patzelt, E. & Kuechler, E. (1982). Identification of the cap binding protein of influenza virus. *Nucleic Acids Res* **10**, 4803-4812.

Bluyssen, H. A., Muzaffar, R., Vlieststra, R. J., van der Made, A. C., Leung, S., Stark, G. R., Kerr, I. M., Trapman, J. & Levy, D. E. (1995). Combinatorial association and abundance of components of interferon-stimulated gene factor 3 dictate the selectivity of interferon responses. *Proc Natl Acad Sci U S A* **92**, 5645-5649.

Boehm, U., Klamp, T., Groot, M. & Howard, J. C. (1997). Cellular responses to interferon-gamma. *Annu Rev Immunol* **15**, 749-795.

Bot, A., Bot, S. & Bona, C. A. (1998). Protective Role of Gamma Interferon during the Recall Response to Influenza Virus. *Journal of Viology* **72**, 6637-6645.

Broug-Holub, E., Toews, G. B., van Iwaarden, J. F., Strieter, R. M., Kunkel, S. L., Paine, R., 3rd & Standiford, T. J. (1997). Alveolar macrophages are required for protective pulmonary defenses in murine Klebsiella pneumonia: elimination of alveolar macrophages increases neutrophil recruitment but decreases bacterial clearance and survival. *Infect Immun* **65**, 1139-1146.

Buchmuller-Rouiller, Y. & Mauel, J. (1986). Correlation between enhanced oxidative metabolism and leishmanicidal activity in activated macrophages from healer and nonhealer mouse strains. *The Journal of Immunology* **136**, 3884-3890.

Burgui, I., Aragon, T., Ortin, J. & Nieto, A. (2003). PABP1 and eIF4GI associate with influenza virus NS1 protein in viral mRNA translation initiation complexes. *J Gen Virol* **84**, 3263-3274.

Butt, K. M., Smith, G. J., Chen, H., Zhang, L. J., Leung, Y. H., Xu, K. M., Lim, W., Webster, R. G., Yuen, K. Y., Peiris, J. S. & Guan, Y. (2005). Human infection with an avian H9N2 influenza A virus in Hong Kong in 2003. *J Clin Microbiol* **43**, 5760-5767.

Calore, E. E., Uip, D. E. & Perez, N. M. (2011). Pathology of the swine-origin influenza A (H1N1) flu. *Pathol Res Pract* **207**, 86-90.

Carrasco, Y. R. & Batista, F. D. (2007). B cells acquire particulate antigen in a macrophage-rich area at the boundary between the follicle and the subcapsular sinus of the lymph node. *Immunity* **27**, 160-171.

Castrucci, M. R. & Kawaoka, Y. (1993). Biologic importance of neuraminidase stalk length in influenza A virus. *J Virol* **67**, 759-764.

CDC, Centres for Disease Control and Prevention. (1997). Isolation of avian influenza A(H5N1) viruses from humans--Hong Kong, May-December 1997. *MMWR Morb Mortal Wkly Rep* **46**, 1204-1207.

Celada, A. & Schreiber, R. D. (1987). Internalization and degradation of receptor-bound interferon-gamma by murine macrophages. Demonstration of receptor recycling. *J Immunol* **139**, 147-153.

Chakkalath, H. R. & Titus, R. G. (1994). Leishmania major-parasitized macrophages augment Th2-type T cell activation. *J Immunol* **153**, 4378-4387.

Chan, M. C. W., Cheung, C. Y., Chui, W. H., Tsao, S. W., Nicholls, J. M., Chan, Y. O., Chan, R. W. Y., Long, H. T., Poon, L. L. M., Guan, Y. & Peiris, J. S. M. (2005). Proinflammatory Cytokine Responses Induced by Influenza A (H5N1) Viruses in Primary Human Alveolar and Bronchial Epithelial Cells. *Respiratory Research* **6**, 135-146.

Chang, E. Y., Guo, B., Doyle, S. E. & Cheng, G. (2007). Cutting edge: involvement of the type I IFN production and signaling pathway in lipopolysaccharide-induced IL-10 production. *J Immunol* **178**, 6705-6709.

Chen, B. J., Leser, G. P., Morita, E. & Lamb, R. A. (2007). Influenza virus hemagglutinin and neuraminidase, but not the matrix protein, are required for assembly and budding of plasmid-derived virus-like particles. *J Virol* **81**, 7111-7123.

Chen, W., Calvo, P. A., Malide, D., Gibbs, J., Schubert, U., Bacik, I., Basta, S., O'Neill, R., Schickli, J., Palese, P., Henklein, P., Bennink, J. R. & Yewdell, J. W. (2001). A novel influenza A virus mitochondrial protein that induces cell death. *Nat Med* **7**, 1306-1312.

Cheung, C. Y., Poon, L. L. M., Lau, A. S. Y., Shortridge, K. F., Gordon, S., Guan, Y. & Peiris, M. (2002). Induction of Proinflammatory Cytokines in Human Macrophages by Influenza A (H5N1) Viruses: A Mechanism for Unusual Severity of Human Disease? *Lancet* **360**, 1831-1837.

Coccia, E. M., Marziali, G., Stellacci, E., Perrotti, E., Ilari, R., Orsatti, R. & Battistini, A. (1995). Cells resistant to interferon-beta respond to interferon-gamma via the Stat1-IRF-1 pathway. *Virology* **211**, 113-122.

Conenello, G. M., Tisoncik, J. R., Rosenzweig, E., Varga, Z. T., Palese, P. & Katze, M. G. (2011). A single N66S mutation in the PB1-F2 protein of influenza A virus increases virulence by inhibiting the early interferon response in vivo. *J Virol* **85**, 652-662.

Connor, R. J., Kawaoka, Y., Webster, R. G. & Paulson, J. C. (1994). Receptor specificity in human, avian, and equine H2 and H3 influenza virus isolates. *Virology* **205**, 17-23.

Copland, D., Calder, C., Raveney, B., Nicholson, L., Phillips, J., Cherwinski, H., Jenmalm, M., Sedgwick, J. & Dick, A. (2007). Monoclonal antibody-mediated CD200 receptor signaling suppresses macrophage activation and tissue damage in experimental uveoretinitis. *American Journal of Pathology* **171**, 580-588.

Corry, D. B., Folkesson, H. G., Warnock, M. L., Erle, D. J., Matthay, M. A., Wiener-Kronish, J. P. & Locksley, R. M. (1996). Interleukin 4, but not interleukin 5 or eosinophils, is required in a murine model of acute airway hyperreactivity. *J Exp Med* **183**, 109-117.

Coyle, A. J., Tsuyuki, S., Bertrand, C., Huang, S., Aguet, M., Alkan, S. S. & Anderson, G. P. (1996). Mice lacking the IFN-gamma receptor have impaired ability to resolve a lung eosinophilic inflammatory response associated with a prolonged capacity of T cells to exhibit a Th2 cytokine profile. *J Immunol* **156**, 2680-2685.

Crawley, M. J. (2007). Mixed-Effects Models. In *The R Book*, pp. 627-628: John Wiley & Sons, Ltd.

Croen, K. D. (1993). Evidence for antiviral effect of nitric oxide. Inhibition of herpes simplex virus type 1 replication. *J Clin Invest* **91**, 2446-2452.

Cros, J. F., Garcia-Sastre, A. & Palese, P. (2005). An unconventional NLS is critical for the nuclear import of the influenza A virus nucleoprotein and ribonucleoprotein. *Traffic* **6**, 205-213.

Crowe, C. R., Chen, K., Pociask, D. A., Alcorn, J. F., Krivich, C., Enelow, R. I., Ross, T. M., Witztum, J. L. & Kolls, J. K. (2009). Critical role of IL-17RA in immunopathology of influenza infection. *J Immunol* **183**, 5301-5310.

Daley, J. M., Thomay, A. A., Connolly, M. D., Reichner, J. S. & Albina, J. E. (2008). Use of Ly6G-specific monoclonal antibody to deplete neutrophils in mice. *J Leukoc Biol* **83**, 64-70.

Davies, E. G., Isaacs, D. & Levinsky, R. J. (1982). Defective immune interferon production and natural killer activity associated with poor neutrophil mobility and delayed umbilical cord separation. *Clin Exp Immunol* **50**, 454-460.

de Jong, M. D., Simmons, C. P., Thanh, T. T., Hien, V. M., Smith, G. J., Chau, T. N., Hoang, D. M., Chau, N. V., Khanh, T. H., Dong, V. C., Qui, P. T., Cam, B. V., Ha do, Q., Guan, Y., Peiris, J. S., Chinh, N. T., Hien, T. T. & Farrar, J. (2006). Fatal outcome of human influenza A (H5N1) is associated with high viral load and hypercytokinemia. *Nat Med* **12**, 1203-1207.

Desmedt, M., Rottiers, P., Dooms, H., Fiers, W. & Grooten, J. (1998). Macrophages induce cellular immunity by activating Th1 cell responses and suppressing Th2 cell responses. *J Immunol* **160**, 5300-5308.

Devitt, A., Moffatt, O. D., Raykundalia, C., Capra, J. D., Simmons, D. L. & Gregory, C. D. (1998). Human CD14 mediates recognition and phagocytosis of apoptotic cells. *Nature* **392**, 505-509.

Di Marzio, P., Puddu, P., Conti, L., Belardelli, F. & Gessani, S. (1994). Interferon gamma upregulates its own gene expression in mouse peritoneal macrophages. *J Exp Med* **179**, 1731-1736.

Diebold, S. S., Kaisho, T., Hemmi, H., Akira, S. & Reis e Sousa, C. (2004). Innate antiviral responses by means of TLR7-mediated recognition of single-stranded RNA. *Science* **303**, 1529-1531.

Dittmann, J., Stertz, S., Grimm, D., Steel, J., Garcia-Sastre, A., Haller, O. & Kochs, G. (2008). Influenza A virus strains differ in sensitivity to the antiviral action of Mx-GTPase. *J Virol* **82**, 3624-3631.

Dorman, S. E., Uzel, G., Roesler, J., Bradley, J. S., Bastian, J., Billman, G., King, S., Filie, A., Schermerhorn, J. & Holland, S. M. (1999). Viral infections in interferon-gamma receptor deficiency. *J Pediatr* **135**, 640-643.

Drapier, J. C., Wietzerbin, J. & Hibbs, J. B., Jr. (1988). Interferon-gamma and tumor necrosis factor induce the L-arginine-dependent cytotoxic effector mechanism in murine macrophages. *Eur J Immunol* **18**, 1587-1592.

Dustin, M. L., Rothlein, R., Bhan, A. K., Dinarello, C. A. & Springer, T. A. (1986). Induction by IL 1 and interferon-gamma: tissue distribution, biochemistry, and function of a natural adherence molecule (ICAM-1). *J Immunol* **137**, 245-254.

Edwards, J. P., Zhang, X., Frauwirth, K. A. & Mosser, D. M. (2006). Biochemical and functional characterization of three activated macrophage populations. *J Leukoc Biol* **80**, 1298-1307.

Egorov, A., Brandt, S., Sereinig, S., Romanova, J., Ferko, B., Katinger, D., Grassauer, A., Alexandrova, G., Katinger, H. & Muster, T. (1998). Transfectant influenza A viruses with long deletions in the NS1 protein grow efficiently in Vero cells. *J Virol* **72**, 6437-6441.

Eichelberger, M., Allan, W., Zijlstra, M., Jaenisch, R. & Doherty, P. C. (1991). Clearance of influenza virus respiratory infection in mice lacking class I major histocompatibility complex-restricted CD8+ T cells. *J Exp Med* **174**, 875-880.

Else, K. J., Finkelman, F. D., Maliszewski, C. R. & Grencis, R. K. (1994). Cytokine-mediated regulation of chronic intestinal helminth infection. *J Exp Med* **179**, 347-351.

Elton, D., Simpson-Holley, M., Archer, K., Medcalf, L., Hallam, R., McCauley, J. & Digard, P. (2001). Interaction of the influenza virus nucleoprotein with the cellular CRM1-mediated nuclear export pathway. *J Virol* **75**, 408-419.

Enami, M., Sharma, G., Benham, C. & Palese, P. (1991). An influenza virus containing nine different RNA segments. *Virology* **185**, 291-298.

Engelhardt, O. G., Smith, M. & Fodor, E. (2005). Association of the influenza A virus RNA-dependent RNA polymerase with cellular RNA polymerase II. *J Virol* **79**, 5812-5818.

Fadok, V. A., Bratton, D. L., Konowal, A., Freed, P. W., Westcott, J. Y. & Henson, P. M. (1998). Macrophages that have ingested apoptotic cells in vitro inhibit proinflammatory cytokine production through autocrine/paracrine mechanisms involving TGF-beta, PGE2, and PAF. *J Clin Invest* **101**, 890-898.

Falcon, A. M., Fortes, P., Marion, R. M., Beloso, A. & Ortin, J. (1999). Interaction of influenza virus NS1 protein and the human homologue of Staufen in vivo and in vitro. *Nucleic Acids Res* **27**, 2241-2247.

Farrar, M. A. & Schreiber, R. D. (1993). The molecular cell biology of interferon-gamma and its receptor. *Annu Rev Immunol* **11**, 571-611.

Fischer, T., Thoma, B., Scheurich, P. & Pfizenmaier, K. (1990). Glycosylation of the human interferon-gamma receptor. N-linked carbohydrates contribute to structural heterogeneity and are required for ligand binding. *J Biol Chem* **265**, 1710-1717.

Fleetwood, A. J., Lawrence, T., Hamilton, J. A. & Cook, A. D. (2007). Granulocyte-macrophage colony-stimulating factor (CSF) and macrophage CSF-dependent macrophage phenotypes display differences in cytokine profiles and transcription

factor activities: implications for CSF blockade in inflammation. *J Immunol* **178**, 5245-5252.

Fouchier, R. A., Schneeberger, P. M., Rozendaal, F. W., Broekman, J. M., Kemink, S. A., Munster, V., Kuiken, T., Rimmelzwaan, G. F., Schutten, M., Van Doornum, G. J., Koch, G., Bosman, A., Koopmans, M. & Osterhaus, A. D. (2004). Avian influenza A virus (H7N7) associated with human conjunctivitis and a fatal case of acute respiratory distress syndrome. *Proc Natl Acad Sci U S A* **101**, 1356-1361.

Francis, T., Jr. (1934). Transmission of Influenza by a Filterable Virus. *Science* **80**, 457-459.

Francis, T., Jr. & Magill, T. P. (1935). Cultivation of Human Influenza Virus in an Artificial Medium. *Science* **82**, 353-354.

Francis, T. & Moore, A. E. (1940). A Study of the Neurotropic Tendency in Strains of the Virus of Epidemic Influenza. *J Exp Med* **72**, 717-728.

Frucht, D. M., Fukao, T., Bogdan, C., Schindler, H., O'Shea, J. J. & Koyasu, S. (2001). IFN-gamma production by antigen-presenting cells: mechanisms emerge. *Trends Immunol* **22**, 556-560.

Fujii, S., Akaike, T. & Maeda, H. (1999). Role of nitric oxide in pathogenesis of herpes simplex virus encephalitis in rats. *Virology* **256**, 203-212.

Fujii, Y., Goto, H., Watanabe, T., Yoshida, T. & Kawaoka, Y. (2003). Selective incorporation of influenza virus RNA segments into virions. *Proc Natl Acad Sci U S A* **100**, 2002-2007.

Fultz, M. J., Barber, S. A., Dieffenbach, C. W. & Vogel, S. N. (1993). Induction of IFN-gamma in macrophages by lipopolysaccharide. *Int Immunol* **5**, 1383-1392.

Gajewski, T. F. & Fitch, F. W. (1988). Anti-proliferative effect of IFN-gamma in immune regulation. I. IFN-gamma inhibits the proliferation of Th2 but not Th1 murine helper T lymphocyte clones. *J Immunol* **140**, 4245-4252.

Gangadharan, B., Hoeve, M. A., Allen, J. E., Ebrahimi, B., Rhind, S. M., Dutia, B. M. & Nash, A. A. (2008). Murine gammaherpesvirus-induced fibrosis is associated with the development of alternatively activated macrophages. *J Leukoc Biol* **84**, 50-58.

Gao, P., Wantanabe, S., Ito, T., Goto, H., Wells, K., McGregor, M., Cooley, A. J. & Kawaoka, Y. (1999). Biological Heterogeneity, Including Systemic Replication in Mice, of H5N1 Influenza A Virus Isolates from Humans in Hong Kong. *Journal of Virology* **73**, 3184-3189.

Garceau, V., Smith, J., Paton, I. R., Davey, M., Fares, M. A., Sester, D. P., Burt, D. W. & Hume, D. A. (2010). Pivotal Advance: Avian colony-stimulating factor 1 (CSF-1), interleukin-34 (IL-34), and CSF-1 receptor genes and gene products. *J Leukoc Biol* **87**, 753-764.

Garcia-Sastre, A., Egorov, A., Matassov, D., Brandt, S., Levy, D. E., Durbin, J. E., Palese, P. & Muster, T. (1998). Influenza A virus lacking the NS1 gene replicates in interferon-deficient systems. *Virology* **252**, 324-330.

Garcia, C. C., Russo, R. C., Guabiraba, R., Fagundes, C. T., Polidoro, R. B., Tavares, L. P., Salgado, A. P., Cassali, G. D., Sousa, L. P., Machado, A. V. &

Teixeira, M. M. (2010). Platelet-activating factor receptor plays a role in lung injury and death caused by Influenza A in mice. *PLoS Pathog* **6**, e1001171.

Garner, R. E., Rubanowice, K., Sawyer, R. T. & Hudson, J. A. (1994). Secretion of TNF-alpha by alveolar macrophages in response to Candida albicans mannan. *J Leukoc Biol* **55**, 161-168.

Geiss, G. K., Salvatore, M., Tumpey, T. M., Carter, V. S., Wang, X., Basler, C. F., Taubenberger, J. K., Bumgarner, R. E., Palese, P., Katze, M. G. & Garcia-Sastre, A. (2002). Cellular transcriptional profiling in influenza A virus-infected lung epithelial cells: the role of the nonstructural NS1 protein in the evasion of the host innate defense and its potential contribution to pandemic influenza. *Proc Natl Acad Sci U S A* **99**, 10736-10741.

Gerber, J. S. & Mosser, D. M. (2001). Reversing lipopolysaccharide toxicity by ligating the macrophage Fc gamma receptors. *J Immunol* **166**, 6861-6868.

Glaser, L., Stevens, J., Zamarin, D., Wilson, I. A., Garcia-Sastre, A., Tumpey, T. M., Basler, C. F., Taubenberger, J. K. & Palese, P. (2005). A single amino acid substitution in 1918 influenza virus hemagglutinin changes receptor binding specificity. *J Virol* **79**, 11533-11536.

Gobert, A. P., Cheng, Y., Akhtar, M., Mersey, B. D., Blumberg, D. R., Cross, R. K., Chaturvedi, R., Drachenberg, C. B., Boucher, J. L., Hacker, A., Casero, R. A., Jr. & Wilson, K. T. (2004). Protective role of arginase in a mouse model of colitis. *J Immunol* **173**, 2109-2117.

Gomez-Puertas, P., Albo, C., Perez-Pastrana, E., Vivo, A. & Portela, A. (2000). Influenza virus matrix protein is the major driving force in virus budding. *J Virol* **74**, 11538-11547.

Gonzalez, S. & Ortin, J. (1999a). Characterization of influenza virus PB1 protein binding to viral RNA: two separate regions of the protein contribute to the interaction domain. *J Virol* **73**, 631-637.

Gonzalez, S. & Ortin, J. (1999b). Distinct regions of influenza virus PB1 polymerase subunit recognize vRNA and cRNA templates. *Embo J* **18**, 3767-3775.

Gordon, S. (2003). Alternative activation of macrophages. *Nat Rev Immunol* **3**, 23-35.

Goto, H. & Kawaoka, Y. (1998). A novel mechanism for the acquisition of virulence by a human influenza A virus. *Proc Natl Acad Sci U S A* **95**, 10224-10228.

Goto, H., Wells, K., Takada, A. & Kawaoka, Y. (2001). Plasminogen-binding activity of neuraminidase determines the pathogenicity of influenza A virus. *J Virol* **75**, 9297-9301.

Graham, M. B., Braciale, V. L. & Braciale, T. J. (1994). Influenza virus-specific CD4+ T helper type 2 T lymphocytes do not promote recovery from experimental virus infection. *J Exp Med* **180**, 1273-1282.

Graham, M. B., Dalton, D. K., Giltinan, D., Braciale, V. L., Stewart, T. A. & Braciale, T. J. (1993). Response to influenza infection in mice with a targeted disruption in the interferon gamma gene. *J Exp Med* **178**, 1725-1732.

Grattendick, K., Stuart, R., Roberts, E., Lincoln, J., Lefkowitz, S. S., Bollen, A., Moguilevsky, N., Friedman, H. & Lefkowitz, D. L. (2002). Alveolar

macrophage activation by myeloperoxidase: a model for exacerbation of lung inflammation. *Am J Respir Cell Mol Biol* **26**, 716-722.

Green, S. J., Meltzer, M. S., Hibbs, J. B. & Nacy, C. A. (1990). Activated macrophages destroy intracellular Leishmania major amastigotes by an L-arginine-dependent killing mechanism. *The Journal of Immunology* **144**, 278-283.

Hai, R., Schmolke, M., Varga, Z. T., Manicassamy, B., Wang, T. T., Belser, J. A., Pearce, M. B., Garcia-Sastre, A., Tumpey, T. M. & Palese, P. (2010). PB1-F2 expression by the 2009 pandemic H1N1 influenza virus has minimal impact on virulence in animal models. *J Virol* **84**, 4442-4450.

Hale, B. G., Jackson, D., Chen, Y. H., Lamb, R. A. & Randall, R. E. (2006). Influenza A Virus NS1 Protein Binds p85b and Activates Phosphatidylinositol-3-Kinase Signalling. *Proc Natl Acad Sci U S A* **103**, 14194-14199.

Haller, O., Stertz, S. & Kochs, G. (2007). The Mx GTPase family of interferon-induced antiviral proteins. *Microbes Infect* **9**, 1636-1643.

Hamilton, M. J., Antignano, F., von Rossum, A., Boucher, J. L., Bennewith, K. L. & Krystal, G. (2010). TLR Agonists That Induce IFN-{beta} Abrogate Resident Macrophage Suppression of T Cells. *J Immunol* **185**, 4545-4553.

Hancock, A., Armstrong, L., Gama, R. & Millar, A. (1998). Production of interleukin 13 by alveolar macrophages from normal and fibrotic lung. *Am J Respir Cell Mol Biol* **18**, 60-65.

Hashimoto, Y., Moki, T., Takizawa, T., Shiratsuchi, A. & Nakanishi, Y. (2007). Evidence for Phagocytosis of Influenza Virus-Infected Apoptotic cells by Neutrophils and Macrophages in Mice. *Journal of Immunology* **178**, 2448-2457.

Hatta, M., Gao, P., Halfmann, P. & Kawaoka, Y. (2001). Molecular Basis for High Virulence of Hong Kong H5N1 Influenza Viruses. *Science* **293**, 1840-1842.

Hay, A. J., Lomniczi, B., Bellamy, A. R. & Skehel, J. J. (1977). Transcription of the influenza virus genome. *Virology* **83**, 337-355.

Heinzel, F. P., Sadick, M. D., Holaday, B. J., Coffman, R. L. & Locksley, R. M. (1989). Reciprocal expression of interferon gamma or interleukin 4 during the resolution or progression of murine leishmaniasis. Evidence for expansion of distinct helper T cell subsets. *J Exp Med* **169**, 59-72.

Hennet, T., Ziltener, H. J., Frei, K. & Peterhans, E. (1992). A kinetic study of immune mediators in the lungs of mice infected with influenza A virus. *J Immunol* **149**, 932-939.

Henrichsen, P., Bartholdy, C., Christensen, J. P. & Thomsen, A. R. (2005). Impaired virus control and severe CD8+ T-cell-mediated immunopathology in chimeric mice deficient in gamma interferon receptor expression on both parenchymal and hematopoietic cells. *J Virol* **79**, 10073-10076.

Herbert, D. R., Holscher, C., Mohrs, M., Arendse, B., Schwegmann, A., Radwanska, M., Leeto, M., Kirsch, R., Hall, P., Mossmann, H., Claussen, B., Forster, I. & Brombacher, F. (2004). Alternative macrophage activation is essential for survival during schistosomiasis and downmodulates T helper 1 responses and immunopathology. *Immunity* **20**, 623-635.

Herfst, S., Chutinimitkul, S., Ye, J., de Wit, E., Munster, V. J., Schrauwen, E. J., Bestebroer, T. M., Jonges, M., Meijer, A., Koopmans, M., Rimmelzwaan, G. F., Osterhaus, A. D., Perez, D. R. & Fouchier, R. A. (2010). Introduction of virulence markers in PB2 of pandemic swine-origin influenza virus does not result in enhanced virulence or transmission. *J Virol* **84**, 3752-3758.

Herold, S., Steinmueller, M., von Wulffen, W., Cakarova, L., Pinto, R., Pleschka, S., Mack, M., Kuziel, W. A., Corazza, N., Brunner, T., Seeger, W. & Lohmeyer, J. (2008). Lung epithelial apoptosis in influenza virus pneumonia: the role of macrophage-expressed TNF-related apoptosis-inducing ligand. *J Exp Med* **205**, 3065-3077.

Herold, S., von Wulffen, W., Steinmueller, M., Pleschka, S., Kuziel, W. A., Mack, M., Srivastava, M., Seeger, W., Maus, U. A. & Lohmeyer, J. (2006). Alveolar Epithelial Cells Direct Monocyte Transepithelial Migration upon Influenza Virus Infection: Impact of Chemokines and Adhesion Molecules. *Journal of Immunology* **177**, 1817-1824.

Hesse, M., Modolell, M., La Flamme, A. C., Schito, M., Fuentes, J. M., Cheever, A. W., Pearce, E. J. & Wynn, T. A. (2001). Differential regulation of nitric oxide synthase-2 and arginase-1 by type 1/type 2 cytokines in vivo: granulomatous pathology is shaped by the pattern of L-arginine metabolism. *J Immunol* **167**, 6533-6544.

Hilton, D. J., Zhang, J. G., Metcalf, D., Alexander, W. S., Nicola, N. A. & Willson, T. A. (1996). Cloning and characterization of a binding subunit of the interleukin 13 receptor that is also a component of the interleukin 4 receptor. *Proc Natl Acad Sci U S A* **93**, 497-501.

Hoffmann, K. F., Cheever, A. W. & Wynn, T. A. (2000). IL-10 and the Dangers of Immune Polarization: Excessive Type 1 and Type 2 Cytokine Responses Induce Distinct Forms of Lethal Immunopathology in Murine Schistosomiasis. *The Journal of Immunology* **164**, 6406-6416.

Holcomb, I. N., Kabakoff, R. C., Chan, B., Baker, T. W., Gurney, A., Henzel, W., Nelson, C., Lowman, H. B., Wright, B. D., Skelton, N. J., Frantz, G. D., Tumas, D. B., Peale, F. V., Jr., Shelton, D. L. & Hebert, C. C. (2000). FIZZ1, a novel cysteine-rich secreted protein associated with pulmonary inflammation, defines a new gene family. *EMBO J* **19**, 4046-4055.

Hsu, M. T., Parvin, J. D., Gupta, S., Krystal, M. & Palese, P. (1987). Genomic RNAs of influenza viruses are held in a circular conformation in virions and in infected cells by a terminal panhandle. *Proc Natl Acad Sci U S A* **84**, 8140-8144.

Huang, S., Hendriks, W., Althage, A., Hemmi, S., Bluethmann, H., Kamijo, R., Vilcek, J., Zinkernagel, R. M. & Aguet, M. (1993). Immune response in mice that lack the interferon-gamma receptor. *Science* **259**, 1742-1745.

Hume, D. A. (2008). Macrophages as APC and the dendritic cell myth. *J Immunol* **181**, 5829-5835.

Hussell, T., Pennycook, A. & Openshaw, P. J. (2001). Inhibition of tumor necrosis factor reduces the severity of virus-specific lung immunopathology. *Eur J Immunol* **31**, 2566-2573.

Ichinohe, T., Lee, H. K., Ogura, Y., Flavell, R. & Iwasaki, A. (2009). Inflammasome recognition of influenza virus is essential for adaptive immune responses. *J Exp Med* **206**, 79-87.

Ilyushina, N. A., Ducatez, M. F., Rehg, J. E., Marathe, B. M., Marjuki, H., Bovin, N. V., Webster, R. G. & Webby, R. J. (2010). Does Pandemic A/H1N1 Virus Have the Potential To Become More Pathogenic? *MBio* **1**, e00249-00210.

Inoue, D., Numasaki, M., Watanabe, M., Kubo, H., Sasaki, T., Yasuda, H., Yamaya, M. & Sasaki, H. (2006). IL-17A promotes the growth of airway epithelial cells through ERK-dependent signaling pathway. *Biochem Biophys Res Commun* **347**, 852-858.

Jackson, D., Hossain, M. J., Hickman, D., Perez, D. R. & Lamb, R. A. (2008). A new influenza virus virulence determinant: the NS1 protein four C-terminal residues modulate pathogenicity. *Proc Natl Acad Sci U S A* **105**, 4381-4386.

Jackson, D., Killip, M. J., Galloway, C. S., Russell, R. J. & Randall, R. E. (2010). Loss of function of the influenza A virus NS1 protein promotes apoptosis but this is not due to a failure to activate phosphatidylinositol 3-kinase (PI3K). *Virology* **396**, 94-105.

Jia, D., Rahbar, R., Chan, R. W., Lee, S. M., Chan, M. C., Wang, B. X., Baker, D. P., Sun, B., Peiris, J. S., Nicholls, J. M. & Fish, E. N. (2010). Influenza virus non-structural protein 1 (NS1) disrupts interferon signaling. *PLoS One* **5**, e13927.

Job, E. R., Deng, Y. M., Tate, M. D., Bottazzi, B., Crouch, E. C., Dean, M. M., Mantovani, A., Brooks, A. G. & Reading, P. C. (2010). Pandemic H1N1 influenza A viruses are resistant to the antiviral activities of innate immune proteins of the collectin and pentraxin superfamilies. *J Immunol* **185**, 4284-4291.

Johann, A. M., Barra, V., Kuhn, A. M., Weigert, A., von Knethen, A. & Brune, B. (2007). Apoptotic cells induce arginase II in macrophages, thereby attenuating NO production. *FASEB J* **21**, 2704-2712.

Junt, T., Moseman, E. A., Iannacone, M., Massberg, S., Lang, P. A., Boes, M., Fink, K., Henrickson, S. E., Shayakhmetov, D. M., Di Paolo, N. C., van Rooijen, N., Mempel, T. R., Whelan, S. P. & von Andrian, U. H. (2007). Subcapsular sinus macrophages in lymph nodes clear lymph-borne viruses and present them to antiviral B cells. *Nature* **450**, 110-114.

Kamijo, R., Harada, H., Matsuyama, T., Bosland, M., Gerecitano, J., Shapiro, D., Le, J., Koh, S. I., Kimura, T., Green, S. J. & et al. (1994). Requirement for transcription factor IRF-1 in NO synthase induction in macrophages. *Science* **263**, 1612-1615.

Kamijo, R., Shapiro, D., Le, J., Huang, S., Aguet, M. & Vilcek, J. (1993). Generation of nitric oxide and induction of major histocompatibility complex class II antigen in macrophages from mice lacking the interferon gamma receptor. *Proc Natl Acad Sci U S A* **90**, 6626-6630.

Karupiah, G., Chen, J. H., Mahalingam, S., Nathan, C. F. & MacMicking, J. D. (1998). Rapid interferon gamma-dependent clearance of influenza A virus and

protection from consolidating pneumonitis in nitric oxide synthase 2-deficient mice. *J Exp Med* **188**, 1541-1546.

Karupiah, G., Xie, Q. W., Buller, R. M., Nathan, C., Duarte, C. & MacMicking, J. D. (1993). Inhibition of viral replication by interferon-gamma-induced nitric oxide synthase. *Science* **261**, 1445-1448.

Kato, H., Takeuchi, O., Sato, S., Yoneyama, M., Yamamoto, M., Matsui, K., Uematsu, S., Jung, A., Kawai, T., Ishii, K. J., Yamaguchi, O., Otsu, K., Tsujimura, T., Koh, C. S., Reis e Sousa, C., Matsuura, Y., Fujita, T. & Akira, S. (2006). Differential roles of MDA5 and RIG-I helicases in the recognition of RNA viruses. *Nature* **441**, 101-105.

Kawai, T. & Akira, S. (2010). The role of pattern-recognition receptors in innate immunity: update on Toll-like receptors. *Nat Immunol* **11**, 373-384.

Kearley, J., Buckland, K. F., Mathie, S. A. & Lloyd, C. M. (2009). Resolution of allergic inflammation and airway hyperreactivity is dependent upon disruption of the T1/ST2-IL-33 pathway. *Am J Respir Crit Care Med* **179**, 772-781.

Kilbourne, E. D., Schulman, J. L., Schild, G. C., Schloer, G., Swanson, J. & Bucher, D. (1971). Related studies of a recombinant influenza-virus vaccine. I. Derivation and characterization of virus and vaccine. *J Infect Dis* **124**, 449-462.

Kim, E. Y., Battaile, J. T., Patel, A. C., You, Y., Agapov, E., Grayson, M. H., Benoit, L. A., Byers, D. E., Alevy, Y., Tucker, J., Swanson, S., Tidwell, R., Tyner, J. W., Morton, J. D., Castro, M., Polineni, D., Patterson, G. A., Schwendener, R. A., Allard, J. D., Peltz, G. & Holtzman, M. J. (2008). Persistent activation of an innate immune response translates respiratory viral infection into chronic lung disease. *Nat Med* **14**, 633-640.

Kitamura, T., Sato, N., Arai, K. & Miyajima, A. (1991). Expression cloning of the human IL-3 receptor cDNA reveals a shared beta subunit for the human IL-3 and GM-CSF receptors. *Cell* **66**, 1165-1174.

Klenk, H. D., Rott, R., Orlich, M. & Blodorn, J. (1975). Activation of influenza A viruses by trypsin treatment. *Virology* **68**, 426-439.

Kobasa, D., Jones, S. M., Shinya, K., Kash, J. C., Copps, J., Ebihara, H., Hatta, Y., Kim, J. H., Halfmann, P., Hatta, M., Feldmann, F., Alimonti, J. B., Fernando, L., Li, Y., Katze, M. G., Feldmann, H. & Kawaoka, Y. (2007). Aberrant Innate Immune Response in Lethal Infection of Macaques with the 1918 Influenza Virus. *Nature* **445**, 319-323.

Kobasa, D., Takada, A., Shinya, K., Hatta, M., Halfmann, P., Theriault, S., Suzuki, H., Nishimura, H., Mitamura, K., Sugaya, N., Usui, T., Murata, T., Maeda, Y., Watanabe, S., Suresh, M., Suzuki, T., Suzuki, Y., Feldmann, H. & Kawaoka, Y. (2004). Enhanced virulence of influenza A viruses with the haemagglutinin of the 1918 pandemic virus. *Nature* **431**, 703-707.

Koch, M., Witzenrath, M., Reuter, C., Herma, M., Schutte, H., Suttorp, N., Collins, H. & Kaufmann, S. H. (2006). Role of local pulmonary IFN-gamma expression in murine allergic airway inflammation. *Am J Respir Cell Mol Biol* **35**, 211-219.

Kong, W. P., Hood, C., Yang, Z. Y., Wei, C. J., Xu, L., Garcia-Sastre, A., Tumpey, T. M. & Nabel, G. J. (2006). Protective Immunity to Lethal Challenge of the

1918 Pandemic Influenza Virus by Vaccination. *Proc Natl Acad Sci U S A* **103**, 15987-15991.

Koopmans, M., Wilbrink, B., Conyn, M., Natrop, G., van der Nat, H., Vennema, H., Meijer, A., van Steenbergen, J., Fouchier, R., Osterhaus, A. & Bosman, A. (2004). Transmission of H7N7 avian influenza A virus to human beings during a large outbreak in commercial poultry farms in the Netherlands. *Lancet* **363**, 587-593.

Koprowski, H., Zheng, Y. M., Heber-Katz, E., Fraser, N., Rorke, L., Fu, Z. F., Hanlon, C. & Dietzschold, B. (1993). In vivo expression of inducible nitric oxide synthase in experimentally induced neurologic diseases. *Proc Natl Acad Sci U S A* **90**, 3024-3027.

Kovacsovics-Bankowski, M., Clark, K., Benacerraf, B. & Rock, K. L. (1993). Efficient major histocompatibility complex class I presentation of exogenous antigen upon phagocytosis by macrophages. *Proc Natl Acad Sci U S A* **90**, 4942-4946.

Kovacsovics-Bankowski, M. & Rock, K. L. (1994). Presentation of exogenous antigens by macrophages: analysis of major histocompatibility complex class I and II presentation and regulation by cytokines. *Eur J Immunol* **24**, 2421-2428.

Kumar, H., Koyama, S., Ishii, K. J., Kawai, T. & Akira, S. (2008). Cutting edge: cooperation of IPS-1- and TRIF-dependent pathways in poly IC-enhanced antibody production and cytotoxic T cell responses. *J Immunol* **180**, 683-687.

Kurowska-Stolarska, M., Kewin, P., Murphy, G., Russo, R. C., Stolarski, B., Garcia, C. C., Komai-Koma, M., Pitman, N., Li, Y., Niedbala, W., McKenzie, A. N., Teixeira, M. M., Liew, F. Y. & Xu, D. (2008). IL-33 induces antigen-specific IL-5+ T cells and promotes allergic-induced airway inflammation independent of IL-4. *J Immunol* **181**, 4780-4790.

Kurowska-Stolarska, M., Stolarski, B., Kewin, P., Murphy, G., Corrigan, C. J., Ying, S., Pitman, N., Mirchandani, A., Rana, B., van Rooijen, N., Shepherd, M., McSharry, C., McInnes, I. B., Xu, D. & Liew, F. Y. (2009). IL-33 amplifies the polarization of alternatively activated macrophages that contribute to airway inflammation. *J Immunol* **183**, 6469-6477.

La Gruta, N. L., Kedzierska, K., Stambas, J. & Doherty, P. C. (2007). A question of self-preservation: immunopathology in influenza virus infection. *Immunology and Cell Biology* **85**, 85-92.

Ladner, M. B., Martin, G. A., Noble, J. A., Wittman, V. P., Warren, M. K., McGrogan, M. & Stanley, E. R. (1988). cDNA cloning and expression of murine macrophage colony-stimulating factor from L929 cells. *Proc Natl Acad Sci U S A* **85**, 6706-6710.

Lamb, R. A., Choppin, P. W., Chanock, R. M. & Lai, C. J. (1980). Mapping of the two overlapping genes for polypeptides NS1 and NS2 on RNA segment 8 of influenza virus genome. *Proc Natl Acad Sci U S A* **77**, 1857-1861.

Lamb, R. A., Lai, C. J. & Choppin, P. W. (1981). Sequences of mRNAs derived from genome RNA segment 7 of influenza virus: colinear and interrupted mRNAs code for overlapping proteins. *Proc Natl Acad Sci U S A* **78**, 4170-4174.

Larkin, J., 3rd, Johnson, H. M. & Subramaniam, P. S. (2000). Differential nuclear localization of the IFNGR-1 and IFNGR-2 subunits of the IFN-gamma receptor complex following activation by IFN-gamma. *J Interferon Cytokine Res* **20**, 565-576.

Lazarowitz, S. G. & Choppin, P. W. (1975). Enhancement of the infectivity of influenza A and B viruses by proteolytic cleavage of the hemagglutinin polypeptide. *Virology* **68**, 440-454.

Le Goffic, R., Balloy, V., Lagranderie, M., Alexopoulou, L., Escriou, N., Flavell, R., Chignard, M. & Si-Tahar, M. (2006). Detrimental contribution of the Toll-like receptor (TLR)3 to influenza A virus-induced acute pneumonia. *PLoS Pathog* **2**, e53.

Legge, K. L. & Braciale, T. J. (2005). Lymph node dendritic cells control CD8+ T cell responses through regulated FasL expression. *Immunity* **23**, 649-659.

Lentsch, A. B., Shanley, T. P., Sarma, V. & Ward, P. A. (1997). In vivo suppression of NF-kappa B and preservation of I kappa B alpha by interleukin-10 and interleukin-13. *J Clin Invest* **100**, 2443-2448.

Li, S., Min, J. Y., Krug, R. M. & Sen, G. C. (2006). Binding of the influenza A virus NS1 protein to PKR mediates the inhibition of its activation by either PACT or double-stranded RNA. *Virology* **349**, 13-21.

Li, S., Schulman, J., Itamura, S. & Palese, P. (1993). Glycosylation of neuraminidase determines the neurovirulence of influenza A/WSN/33 virus. *J Virol* **67**, 6667-6673.

Li, Z., Chen, H., Jiao, P., Deng, G., Tian, G., Li, Y., Hoffmann, E., Webster, R. G., Matsuoka, Y. & Yu, K. (2005). Molecular Basis of Replication of Duck H5N1 Influenza Viruses in a Mammalian Mouse Model. *Journal of Virology* **79**, 12058-12064.

Lidbury, B. A., Rulli, N. E., Suhrbier, A., Smith, P. N., McColl, S. R., Cunningham, A. L., Tarkowski, A., van Rooijen, N., Fraser, R. J. & Mahalingam, S. (2008). Macrophage-derived proinflammatory factors contribute to the development of arthritis and myositis after infection with an arthrogenic alphavirus. *J Infect Dis* **197**, 1585-1593.

Liew, F. Y., Millott, S., Parkinson, C., Palmer, R. M. & Moncada, S. (1990). Macrophage killing of Leishmania parasite in vivo is mediated by nitric oxide from L-arginine. *The Journal of Immunology* **144**, 4794-4797.

Lin, H., Lee, E., Hestir, K., Leo, C., Huang, M., Bosch, E., Halenbeck, R., Wu, G., Zhou, A., Behrens, D., Hollenbaugh, D., Linnemann, T., Qin, M., Wong, J., Chu, K., Doberstein, S. K. & Williams, L. T. (2008). Discovery of a cytokine and its receptor by functional screening of the extracellular proteome. *Science* **320**, 807-811.

Lin, K. L., Sweeney, S., Kang, B. D., Ramsburg, E. & Gunn, M. D. (2011). CCR2-antagonist prophylaxis reduces pulmonary immune pathology and markedly improves survival during influenza infection. *J Immunol* **186**, 508-515.

Lio, D., Scola, L., Crivello, A., Bonafe, M., Franceschi, C., Olivieri, F., Colonna-Romano, G., Candore, G. & Caruso, C. (2002). Allele frequencies of +874T--

>A single nucleotide polymorphism at the first intron of interferon-gamma gene in a group of Italian centenarians. *Exp Gerontol* **37**, 315-319.

Lipatov, A. S., Andreansky, S., Webby, R. J., Hulse, D. J., Rehg, J. E., Krauss, S., Perez, D. R., Doherty, P. C., Webster, R. G. & Sangster, M. Y. (2005). Pathogenesis of Hong Kong H5N1 Influenza Virus NS Gene Reassortants in Mice: The Role of Cytokines and B- and T-cell Responses. *Journal of General Virology* **86**, 1121-1130.

Liu, T., Dhanasekaran, S. M., Jin, H., Hu, B., Tomlins, S. A., Chinnaiyan, A. M. & Phan, S. H. (2004). FIZZ1 stimulation of myofibroblast differentiation. *Am J Pathol* **164**, 1315-1326.

Loke, P., Gallagher, I., Nair, M. G., Zang, X., Brombacher, F., Mohrs, M., Allison, J. P. & Allen, J. E. (2007). Alternative activation is an innate response to injury that requires CD4+ T cells to be sustained during chronic infection. *J Immunol* **179**, 3926-3936.

Loke, P., Nair, M. G., Parkinson, J., Guiliano, D., Blaxter, M. & Allen, J. E. (2002). IL-4 dependent alternatively-activated macrophages have a distinctive in vivo gene expression phenotype. *BMC Immunol* **3**, 7.

Lorsbach, R. B., Murphy, W. J., Lowenstein, C. J., Snyder, S. H. & Russell, S. W. (1993). Expression of the nitric oxide synthase gene in mouse macrophages activated for tumor cell killing. Molecular basis for the synergy between interferon-gamma and lipopolysaccharide. *J Biol Chem* **268**, 1908-1913.

Louie, J. K., Acosta, M., Winter, K., Jean, C., Gavali, S., Schechter, R., Vugia, D., Harriman, K., Matyas, B., Glaser, C. A., Samuel, M. C., Rosenberg, J., Talarico, J. & Hatch, D. (2009). Factors associated with death or hospitalization due to pandemic 2009 influenza A(H1N1) infection in California. *JAMA* **302**, 1896-1902.

Lu, X., Tumpey, T. M., Morken, T., Zaki, S. R., Cox, N. J. & Katz, J. M. (1999). A Mouse Model for the Evaluation of Pathogenesis and Immunity to Influenza A (H5N1) Viruses Isolated from Humans. *Journal of Virology* **73**, 5903-5911.

Lund, J. M., Alexopoulou, L., Sato, A., Karow, M., Adams, N. C., Gale, N. W., Iwasaki, A. & Flavell, R. A. (2004). Recognition of single-stranded RNA viruses by Toll-like receptor 7. *Proc Natl Acad Sci U S A* **101**, 5598-5603.

Luo, G. X., Luytjes, W., Enami, M. & Palese, P. (1991). The polyadenylation signal of influenza virus RNA involves a stretch of uridines followed by the RNA duplex of the panhandle structure. *J Virol* **65**, 2861-2867.

MacMicking, J., Xie, Q. W. & Nathan, C. (1997). Nitric oxide and macrophage function. *Annu Rev Immunol* **15**, 323-350.

Maines, T. R., Jayaraman, A., Belser, J. A., Wadford, D. A., Pappas, C., Zeng, H., Gustin, K. M., Pearce, M. B., Viswanathan, K., Shriver, Z. H., Raman, R., Cox, N. J., Sasisekharan, R., Katz, J. M. & Tumpey, T. M. (2009). Transmission and pathogenesis of swine-origin 2009 A(H1N1) influenza viruses in ferrets and mice. *Science* **325**, 484-487.

Maini, R. N., Elliott, M. J., Brennan, F. M. & Feldmann, M. (1995). Beneficial effects of tumour necrosis factor-alpha (TNF-alpha) blockade in rheumatoid arthritis (RA). *Clin Exp Immunol* **101**, 207-212.

Mantovani, A., Sica, A., Sozzani, S., Allavena, P., Vecchi, A. & Locati, M. (2004). The chemokine system in diverse forms of macrophage activation and polarization. *Trends Immunol* **25**, 677-686.

Martin, K. & Helenius, A. (1991). Nuclear transport of influenza virus ribonucleoproteins: the viral matrix protein (M1) promotes export and inhibits import. *Cell* **67**, 117-130.

Martinez-Pomares, L., Crocker, P. R., Da Silva, R., Holmes, N., Colominas, C., Rudd, P., Dwek, R. & Gordon, S. (1999). Cell-specific glycoforms of sialoadhesin and CD45 are counter-receptors for the cysteine-rich domain of the mannose receptor. *J Biol Chem* **274**, 35211-35218.

Martinez-Pomares, L. & Gordon, S. (1999). Potential role of the mannose receptor in antigen transport. *Immunol Lett* **65**, 9-13.

Martinez-Pomares, L. & Gordon, S. (2007). Antigen presentation the macrophage way. *Cell* **131**, 641-643.

Martinez-Pomares, L., Mahoney, J. A., Kaposzta, R., Linehan, S. A., Stahl, P. D. & Gordon, S. (1998). A functional soluble form of the murine mannose receptor is produced by macrophages in vitro and is present in mouse serum. *J Biol Chem* **273**, 23376-23380.

Mattner, F., Magram, J., Ferrante, J., Launois, P., Di Padova, K., Behin, R., Gately, M. K., Louis, J. A. & Alber, G. (1996). Genetically resistant mice lacking interleukin-12 are susceptible to infection with Leishmania major and mount a polarized Th2 cell response. *Eur J Immunol* **26**, 1553-1559.

Mazur, I., Anhlan, D., Mitzner, D., Wixler, L., Schubert, U. & Ludwig, S. (2008). The proapoptotic influenza A virus protein PB1-F2 regulates viral polymerase activity by interaction with the PB1 protein. *Cell Microbiol* **10**, 1140-1152.

McAuley, J. L., Chipuk, J. E., Boyd, K. L., Van De Velde, N., Green, D. R. & McCullers, J. A. (2010a). PB1-F2 proteins from H5N1 and 20 century pandemic influenza viruses cause immunopathology. *PLoS Pathog* **6**, e1001014.

McAuley, J. L., Zhang, K. & McCullers, J. A. (2010b). The effects of influenza A virus PB1-F2 protein on polymerase activity are strain specific and do not impact pathogenesis. *J Virol* **84**, 558-564.

McKinstry, K. K., Strutt, T. M., Buck, A., Curtis, J. D., Dibble, J. P., Huston, G., Tighe, M., Hamada, H., Sell, S., Dutton, R. W. & Swain, S. L. (2009). IL-10 deficiency unleashes an influenza-specific Th17 response and enhances survival against high-dose challenge. *J Immunol* **182**, 7353-7363.

Meagher, L. C., Savill, J. S., Baker, A., Fuller, R. W. & Haslett, C. (1992). Phagocytosis of apoptotic neutrophils does not induce macrophage release of thromboxane B2. *J Leukoc Biol* **52**, 269-273.

Metcalf, D. (1986). The molecular biology and functions of the granulocyte-macrophage colony-stimulating factors. *Blood* **67**, 257-267.

Mibayashi, M., Martinez-Sobrido, L., Loo, Y. M., Cardenas, W. B., Gale, M., Jr. & Garcia-Sastre, A. (2007). Inhibition of retinoic acid-inducible gene I-mediated induction of beta interferon by the NS1 protein of influenza A virus. *J Virol* **81**, 514-524.

Mills, C. D., Kincaid, K., Alt, J. M., Heilman, M. J. & Hill, A. M. (2000). M-1/M-2 macrophages and the Th1/Th2 paradigm. *J Immunol* **164**, 6166-6173.

Min, J. Y. & Krug, R. M. (2006). The primary function of RNA binding by the influenza A virus NS1 protein in infected cells: Inhibiting the 2'-5' oligo (A) synthetase/RNase L pathway. *Proc Natl Acad Sci U S A* **103**, 7100-7105.

Min, J. Y., Li, S., Sen, G. C. & Krug, R. M. (2007). A site on the influenza A virus NS1 protein mediates both inhibition of PKR activation and temporal regulation of viral RNA synthesis. *Virology* **363**, 236-243.

Modolell, M., Corraliza, I. M., Link, F., Soler, G. & Eichmann, K. (1995). Reciprocal regulation of the nitric oxide synthase/arginase balance in mouse bone marrow-derived macrophages by TH1 and TH2 cytokines. *Eur J Immunol* **25**, 1101-1104.

Mok, C. K. P., Lee, D. C. W., Cheung, C. Y., Peiris, M. & Lau, A. S. Y. (2007). Differential Onset of Apoptosis in Influenza A Virus H5N1- and H1N1- Infected Human Blood Macrophages. *Journal of General Virology* **88**, 1275-1280.

Moltedo, B., Lopez, C. B., Pazos, M., Becker, M. I., Hermesh, T. & Moran, T. M. (2009). Cutting edge: stealth influenza virus replication precedes the initiation of adaptive immunity. *J Immunol* **183**, 3569-3573.

Monteerarat, Y., Sakabe, S., Ngamurulert, S., Srichatraphimuk, S., Jiamtom, W., Chaichuen, K., Thitithanyanont, A., Permpikul, P., Songserm, T., Puthavathana, P., Nidom, C. A., Mai le, Q., Iwatsuki-Horimoto, K., Kawaoka, Y. & Auewarakul, P. (2010). Induction of TNF-alpha in human macrophages by avian and human influenza viruses. *Arch Virol* **155**, 1273-1279.

Moran, T. M., Park, H., Fernandez-Sesma, A. & Schulman, J. L. (1999). Th2 responses to inactivated influenza virus can Be converted to Th1 responses and facilitate recovery from heterosubtypic virus infection. *J Infect Dis* **180**, 579-585.

Moskophidis, D. & Kioussis, D. (1998). Contribution of virus-specific CD8+ cytotoxic T cells to virus clearance or pathologic manifestations of influenza virus infection in a T cell receptor transgenic mouse model. *J Exp Med* **188**, 223-232.

Mosmann, T. R., Cherwinski, H., Bond, M. W., Giedlin, M. A. & Coffman, R. L. (1986). Two types of murine helper T cell clone. I. Definition according to profiles of lymphokine activities and secreted proteins. *J Immunol* **136**, 2348-2357.

Mosser, D. M. & Edwards, J. P. (2008). Exploring the full spectrum of macrophage activation. *Nat Rev Immunol* **8**, 958-969.

Muller, U., Steinhoff, U., Reis, L. F., Hemmi, S., Pavlovic, J., Zinkernagel, R. M. & Aguet, M. (1994). Functional role of type I and type II interferons in antiviral defense. *Science* **264**, 1918-1921.

Muramoto, Y., Takada, A., Fujii, K., Noda, T., Iwatsuki-Horimoto, K., Watanabe, S., Horimoto, T., Kida, H. & Kawaoka, Y. (2006). Hierarchy among viral

RNA (vRNA) segments in their role in vRNA incorporation into influenza A virions. *J Virol* **80**, 2318-2325.

Murphy, K., Travers, P. & Walport, M. (2008). *Janeway's Immunobiology*. New York: Garland Science.

Nair, M. G., Du, Y., Perrigoue, J. G., Zaph, C., Taylor, J. J., Goldschmidt, M., Swain, G. P., Yancopoulos, G. D., Valenzuela, D. M., Murphy, A., Karow, M., Stevens, S., Pearce, E. J. & Artis, D. (2009). Alternatively activated macrophage-derived RELM-{alpha} is a negative regulator of type 2 inflammation in the lung. *J Exp Med* **206**, 937-952.

Nathan, C. F., Murray, H. W., Wiebe, M. E. & Rubin, B. Y. (1983). Identification of interferon-gamma as the lymphokine that activates human macrophage oxidative metabolism and antimicrobial activity. *The Journal of Experimental Medicine* **158**, 670-689.

Nemeroff, M. E., Qian, X. Y. & Krug, R. M. (1995). The influenza virus NS1 protein forms multimers in vitro and in vivo. *Virology* **212**, 422-428.

Noben-Trauth, N., Shultz, L. D., Brombacher, F., Urban, J. F., Jr., Gu, H. & Paul, W. E. (1997). An interleukin 4 (IL-4)-independent pathway for CD4+ T cell IL-4 production is revealed in IL-4 receptor-deficient mice. *Proc Natl Acad Sci U S A* **94**, 10838-10843.

O'Neill, R. E., Jaskunas, R., Blobel, G., Palese, P. & Moroianu, J. (1995). Nuclear import of influenza virus RNA can be mediated by viral nucleoprotein and transport factors required for protein import. *J Biol Chem* **270**, 22701-22704.

O'Neill, R. E., Talon, J. & Palese, P. (1998). The influenza virus NEP (NS2 protein) mediates the nuclear export of viral ribonucleoproteins. *Embo J* **17**, 288-296.

O'Shea, J. J. & Murray, P. J. (2008). Cytokine signaling modules in inflammatory responses. *Immunity* **28**, 477-487.

Osterlund, P., Pirhonen, J., Ikonen, N., Ronkko, E., Strengell, M., Makela, S. M., Broman, M., Hamming, O. J., Hartmann, R., Ziegler, T. & Julkunen, I. (2010). Pandemic H1N1 2009 influenza A virus induces weak cytokine responses in human macrophages and dendritic cells and is highly sensitive to the antiviral actions of interferons. *J Virol* **84**, 1414-1422.

Ozawa, M., Basnet, S., Burley, L. M., Neumann, G., Hatta, M. & Kawaoka, Y. (2011). Impact of Amino Acid Mutations in PB2, PB1-F2, and NS1 on the Replication and Pathogenicity of Pandemic (H1N1) 2009 Influenza Viruses. *J Virol* **85**, 4596-4601.

Paine, R., 3rd, Morris, S. B., Jin, H., Wilcoxen, S. E., Phare, S. M., Moore, B. B., Coffey, M. J. & Toews, G. B. (2001). Impaired functional activity of alveolar macrophages from GM-CSF-deficient mice. *Am J Physiol Lung Cell Mol Physiol* **281**, L1210-1218.

Palese, P. & Shaw, M. L. (2006). Orthomyxoviridae: The Viruses and their Replication. In *Fields' Virology*, 5th edn, pp. 1648-1689. Edited by D. M. Knipe & P. M. Howley. Philadelphia: Lippencott Williams and Wilkins.

Palese, P., Tobita, K., Ueda, M. & Compans, R. W. (1974). Characterization of temperature sensitive influenza virus mutants defective in neuraminidase. *Virology* **61**, 397-410.

Palladino, G., Mozdzanowska, K., Washko, G. & Gerhard, W. (1995). Virus-neutralizing antibodies of immunoglobulin G (IgG) but not of IgM or IgA isotypes can cure influenza virus pneumonia in SCID mice. *J Virol* **69**, 2075-2081.

Pang, I. K. & Iwasaki, A. (2011). Inflammasomes as mediators of immunity against influenza virus. *Trends Immunol* **32**, 34-41.

Peiris, J. S., Yu, W. C., Leung, C. W., Cheung, C. Y., Ng, W. F., Nicholls, J. M., Ng, T. K., Chan, K. H., Lai, S. T., Lim, W. L., Yuen, K. Y. & Guan, Y. (2004). Re-emergence of fatal human influenza A subtype H5N1 disease. *Lancet* **363**, 617-619.

Perez, J. T., Varble, A., Sachidanandam, R., Zlatev, I., Manoharan, M., Garcia-Sastre, A. & tenOever, B. R. (2010). Influenza A virus-generated small RNAs regulate the switch from transcription to replication. *Proc Natl Acad Sci U S A* **107**, 11525-11530.

Perrone, L. A., Plowden, J. K., Garcia-Sastre, A., Katz, J. M. & Tumpey, T. M. (2008). H5N1 and 1918 pandemic influenza virus infection results in early and excessive infiltration of macrophages and neutrophils in the lungs of mice. *PLoS Pathog* **4**, e1000115.

Pesce, J., Kaviratne, M., Ramalingam, T. R., Thompson, R. W., Urban, J. F., Jr., Cheever, A. W., Young, D. A., Collins, M., Grusby, M. J. & Wynn, T. A. (2006). The IL-21 receptor augments Th2 effector function and alternative macrophage activation. *J Clin Invest* **116**, 2044-2055.

Pichlmair, A., Schulz, O., Tan, C. P., Naslund, T. I., Liljestrom, P., Weber, F. & Reis e Sousa, C. (2006). RIG-I-mediated antiviral responses to single-stranded RNA bearing 5'-phosphates. *Science* **314**, 997-1001.

Pine, R. (1992). Constitutive expression of an ISGF2/IRF1 transgene leads to interferon-independent activation of interferon-inducible genes and resistance to virus infection. *J Virol* **66**, 4470-4478.

Pinto, L. H., Holsinger, L. J. & Lamb, R. A. (1992). Influenza virus M2 protein has ion channel activity. *Cell* **69**, 517-528.

Pozzi, L. A., Maciaszek, J. W. & Rock, K. L. (2005). Both dendritic cells and macrophages can stimulate naive CD8 T cells in vivo to proliferate, develop effector function, and differentiate into memory cells. *J Immunol* **175**, 2071-2081.

Pradel, L. C., Mitchell, A. J., Zarubica, A., Dufort, L., Chasson, L., Naquet, P., Broccardo, C. & Chimini, G. (2009). ATP-binding cassette transporter hallmarks tissue macrophages and modulates cytokine-triggered polarization programs. *Eur J Immunol* **39**, 2270-2280.

Prasse, A., Germann, M., Pechkovsky, D. V., Markert, A., Verres, T., Stahl, M., Melchers, I., Luttmann, W., Muller-Quernheim, J. & Zissel, G. (2007). IL-

10-producing monocytes differentiate to alternatively activated macrophages and are increased in atopic patients. *J Allergy Clin Immunol* **119**, 464-471.

Pribul, P. K., Harker, J., Wang, B., Wang, H., Tregoning, J. S., Schwarze, J. & Openshaw, P. J. (2008). Alveolar macrophages are a major determinant of early responses to viral lung infection but do not influence subsequent disease development. *J Virol* **82**, 4441-4448.

Price, G. E., Gaszewska-Mastarlarz, A. & Moskophidis, D. (2000). The role of alpha/beta and gamma interferons in development of immunity to influenza A virus in mice. *J Virol* **74**, 3996-4003.

Qin, H., Roberts, K. L., Niyongere, S. A., Cong, Y., Elson, C. O. & Benveniste, E. N. (2007). Molecular mechanism of lipopolysaccharide-induced SOCS-3 gene expression in macrophages and microglia. *J Immunol* **179**, 5966-5976.

Reading, P. C., Miller, J. L. & Anders, E. M. (2000). Involvement of the mannose receptor in infection of macrophages by influenza virus. *J Virol* **74**, 5190-5197.

Reading, P. C., Morey, L. S., Crouch, E. C. & Anders, E. M. (1997). Collectin-mediated antiviral host defense of the lung: evidence from influenza virus infection of mice. *J Virol* **71**, 8204-8212.

Reading, P. C., Whitney, P. G., Pickett, D. L., Tate, M. D. & Brooks, A. G. (2010). Influenza viruses differ in ability to infect macrophages and to induce a local inflammatory response following intraperitoneal injection of mice. *Immunol Cell Biol* **88**, 641-650.

Rehwinkel, J., Tan, C. P., Goubau, D., Schulz, O., Pichlmair, A., Bier, K., Robb, N., Vreede, F., Barclay, W., Fodor, E. & Reis e Sousa, C. (2010). RIG-I detects viral genomic RNA during negative-strand RNA virus infection. *Cell* **140**, 397-408.

Renegar, K. B., Small, P. A., Jr., Boykins, L. G. & Wright, P. F. (2004). Role of IgA versus IgG in the control of influenza viral infection in the murine respiratory tract. *J Immunol* **173**, 1978-1986.

Rincon, M., Anguita, J., Nakamura, T., Fikrig, E. & Flavell, R. A. (1997). Interleukin (IL)-6 directs the differentiation of IL-4-producing CD4+ T cells. *J Exp Med* **185**, 461-469.

Robb, N. C., Smith, M., Vreede, F. T. & Fodor, E. (2009). NS2/NEP protein regulates transcription and replication of the influenza virus RNA genome. *J Gen Virol* **90**, 1398-1407.

Robertson, J. S., Nicolson, C., Newman, R., Major, D., Dunleavy, U. & Wood, J. M. (1992). High growth reassortant influenza vaccine viruses: new approaches to their control. *Biologicals* **20**, 213-220.

Rodgers, B. & Mims, C. A. (1981). Interaction of influenza virus with mouse macrophages. *Infect Immun* **31**, 751-757.

Rossman, J. S., Jing, X., Leser, G. P. & Lamb, R. A. (2010). Influenza virus M2 protein mediates ESCRT-independent membrane scission. *Cell* **142**, 902-913.

Rothlein, R., Dustin, M. L., Marlin, S. D. & Springer, T. A. (1986). A human intercellular adhesion molecule (ICAM-1) distinct from LFA-1. *J Immunol* **137**, 1270-1274.

Sakai, S., Kawamata, H., Mantani, N., Kogure, T., Shimada, Y., Terasawa, K., Sakai, T., Imanishi, N. & Ochiai, H. (2000). Therapeutic effect of anti-macrophage inflammatory protein 2 antibody on influenza virus-induced pneumonia in mice. *J Virol* **74**, 2472-2476.

Salvatore, M., Basler, C. F., Parisien, J. P., Horvath, C. M., Bourmakina, S., Zheng, H., Muster, T., Palese, P. & Garcia-Sastre, A. (2002). Effects of influenza A virus NS1 protein on protein expression: the NS1 protein enhances translation and is not required for shutoff of host protein synthesis. *J Virol* **76**, 1206-1212.

Scheiffele, P., Rietveld, A., Wilk, T. & Simons, K. (1999). Influenza viruses select ordered lipid domains during budding from the plasma membrane. *J Biol Chem* **274**, 2038-2044.

Scherle, P. A., Palladino, G. & Gerhard, W. (1992). Mice can recover from pulmonary influenza virus infection in the absence of class I-restricted cytotoxic T cells. *J Immunol* **148**, 212-217.

Schijns, V. E., Haagmans, B. L. & Horzinek, M. C. (1995). IL-12 stimulates an antiviral type 1 cytokine response but lacks adjuvant activity in IFN-gamma-receptor-deficient mice. *J Immunol* **155**, 2525-2532.

Schijns, V. E., Haagmans, B. L., Rijke, E. O., Huang, S., Aguet, M. & Horzinek, M. C. (1994). IFN-gamma receptor-deficient mice generate antiviral Th1-characteristic cytokine profiles but altered antibody responses. *J Immunol* **153**, 2029-2037.

Schroder, K., Hertzog, P. J., Ravasi, T. & Hume, D. A. (2004). Interferon-gamma: an overview of signals, mechanisms and functions. *J Leukoc Biol* **75**, 163-189.

Schultz-Cherry, S., Dybdahl-Sissoko, N., Neumann, G., Kawaoka, Y. & Hinshaw, V. S. (2001). Influenza virus ns1 protein induces apoptosis in cultured cells. *J Virol* **75**, 7875-7881.

Seo, S. H., Hoffmann, E. & Webster, R. G. (2002). Lethal H5N1 Influenza Viruses Escape Host Anti-viral Cytokine Responses. *Nature Medicine* **8**, 950-954.

Shibata, Y., Metzger, W. J. & Myrvik, Q. N. (1997). Chitin particle-induced cell-mediated immunity is inhibited by soluble mannan: mannose receptor-mediated phagocytosis initiates IL-12 production. *J Immunol* **159**, 2462-2467.

Simmons, C. P., Bernasconi, N. L., Suguitan Jr., A. L., Mills, K., Ward, J. M., Chau, N. V. V., Hien, T. T., Sallusto, F., Ha, D. Q., Farrar, J., de Jong, M. D., Lanzavecchia, A. & Subbarao, K. (2007). Prophylactic and Therapeutic Efficacy of Human Monoclonal Antibodies Against H5N1 Influenza. *PLoS Medicine* **4**, 928-936.

Smith, G. J., Vijaykrishna, D., Bahl, J., Lycett, S. J., Worobey, M., Pybus, O. G., Ma, S. K., Cheung, C. L., Raghwani, J., Bhatt, S., Peiris, J. S., Guan, Y. & Rambaut, A. (2009). Origins and evolutionary genomics of the 2009 swine-origin H1N1 influenza A epidemic. *Nature* **459**, 1122-1125.

Snelgrove, R. J., Goulding, J., Didierlaurent, A. M., Lyonga, D., Vekaria, S., Edwards, L., Gwyer, E., Sedgwick, J. D., Barclay, A. N. & Hussell, T. (2008). A critical function for CD200 in lung immune homeostasis and the severity of influenza infection. *Nature Immunology* **9**, 1074-1083.

Song, C., Luo, L., Lei, Z., Li, B., Liang, Z., Liu, G., Li, D., Zhang, G., Huang, B. & Feng, Z. H. (2008). IL-17-producing alveolar macrophages mediate allergic lung inflammation related to asthma. *J Immunol* **181**, 6117-6124.

Song, M. M. & Shuai, K. (1998). The suppressor of cytokine signaling (SOCS) 1 and SOCS3 but not SOCS2 proteins inhibit interferon-mediated antiviral and antiproliferative activities. *J Biol Chem* **273**, 35056-35062.

Staeheli, P., Haller, O., Boll, W., Lindenmann, J. & Weissmann, C. (1986). Mx protein: constitutive expression in 3T3 cells transformed with cloned Mx cDNA confers selective resistance to influenza virus. *Cell* **44**, 147-158.

Stanley, E. R., Chen, D. M. & Lin, H. S. (1978). Induction of macrophage production and proliferation by a purified colony stimulating factor. *Nature* **274**, 168-170.

Stasakova, J., Ferko, B., Kittel, C., Sereinig, S., Romanova, J., Katinger, H. & Egorov, A. (2005). Influenza A mutant viruses with altered NS1 protein function provoke caspase-1 activation in primary human macrophages, resulting in fast apoptosis and release of high levels of interleukins 1beta and 18. *J Gen Virol* **86**, 185-195.

Stein, M. & Gordon, S. (1991). Regulation of tumor necrosis factor (TNF) release by murine peritoneal macrophages: role of cell stimulation and specific phagocytic plasma membrane receptors. *Eur J Immunol* **21**, 431-437.

Stein, M., Keshav, S., Harris, N. & Gordon, S. (1992). Interleukin 4 potently enhances murine macrophage mannose receptor activity: a marker of alternative immunologic macrophage activation. *J Exp Med* **176**, 287-292.

Stenger, S., Donhauser, N., Thuring, H., Rollinghoff, M. & Bogdan, C. (1996). Reactivation of latent leishmaniasis by inhibition of inducible nitric oxide synthase. *J Exp Med* **183**, 1501-1514.

Stout, R. D., Jiang, C., Matta, B., Tietzel, I., Watkins, S. K. & Suttles, J. (2005). Macrophages sequentially change their functional phenotype in response to changes in microenvironmental influences. *J Immunol* **175**, 342-349.

Strassmann, G., Patil-Koota, V., Finkelman, F., Fong, M. & Kambayashi, T. (1994). Evidence for the involvement of interleukin 10 in the differential deactivation of murine peritoneal macrophages by prostaglandin E2. *J Exp Med* **180**, 2365-2370.

Stuart-Harris, C. H. (1939). A Neurotropic Strain of Influenza Virus. *The Lancet* **233**, 497-499.

Stumpo, R., Kauer, M., Martin, S. & Kolb, H. (2003). IL-10 induces gene expression in macrophages: partial overlap with IL-5 but not with IL-4 induced genes. *Cytokine* **24**, 46-56.

Sun, J., Madan, R., Karp, C. L. & Braciale, T. J. (2009). Effector T cells control lung inflammation during acute influenza virus infection by producing IL-10. *Nat Med* **15**, 277-284.

Sweet, M. J., Campbell, C. C., Sester, D. P., Xu, D., McDonald, R. C., Stacey, K. J., Hume, D. A. & Liew, F. Y. (2002). Colony-stimulating factor-1 suppresses responses to CpG DNA and expression of toll-like receptor 9 but enhances responses to lipopolysaccharide in murine macrophages. *J Immunol* **168**, 392-399.

Swihart, K., Fruth, U., Messmer, N., Hug, K., Behin, R., Huang, S., Del Giudice, G., Aguet, M. & Louis, J. A. (1995). Mice from a genetically resistant background lacking the interferon gamma receptor are susceptible to infection with Leishmania major but mount a polarized T helper cell 1-type CD4+ T cell response. *J Exp Med* **181**, 961-971.

Szalay, G., Ladel, C. H., Blum, C. & Kaufmann, S. H. (1996). IL-4 neutralization or TNF-alpha treatment ameliorate disease by an intracellular pathogen in IFN-gamma receptor-deficient mice. *J Immunol* **157**, 4746-4750.

Szretter, K. J., Gangappa, S., Lu, X., Smith, C., Shieh, W. J., Zaki, S. R., Sambhara, S., Tumpey, T. M. & Katz, J. M. (2007). Role of host cytokine responses in the pathogenesis of avian H5N1 influenza viruses in mice. *J Virol* **81**, 2736-2744.

Takeda, M., Leser, G. P., Russell, C. J. & Lamb, R. A. (2003). Influenza virus hemagglutinin concentrates in lipid raft microdomains for efficient viral fusion. *Proc Natl Acad Sci U S A* **100**, 14610-14617.

Talon, J., Horvath, C. M., Polley, R., Basler, C. F., Muster, T., Palese, P. & Garcia-Sastre, A. (2000). Activation of interferon regulatory factor 3 is inhibited by the influenza A virus NS1 protein. *J Virol* **74**, 7989-7996.

Tanaka, H. & Samuel, C. E. (1994). Mechanism of interferon action: structure of the mouse PKR gene encoding the interferon-inducible RNA-dependent protein kinase. *Proc Natl Acad Sci U S A* **91**, 7995-7999.

Tang, C., Inman, M. D., van Rooijen, N., Yang, P., Shen, H., Matsumoto, K. & O'Byrne, P. M. (2001). Th type 1-stimulating activity of lung macrophages inhibits Th2-mediated allergic airway inflammation by an IFN-gamma-dependent mechanism. *J Immunol* **166**, 1471-1481.

Tate, M. D., Brooks, A. G. & Reading, P. C. (2010a). Correlation between sialic acid expression and infection of murine macrophages by different strains of influenza virus. *Microbes Infect* **13**, 202-207.

Tate, M. D., Brooks, A. G. & Reading, P. C. (2010b). Inhibition of lectin-mediated innate host defences in vivo modulates disease severity during influenza virus infection. *Immunol Cell Biol* **89**, 482-491.

Tate, M. D., Deng, Y. M., Jones, J. E., Anderson, G. P., Brooks, A. G. & Reading, P. C. (2009). Neutrophils Ameliorate Lung Injury and the Development of Severe Disease during Influenza Infection. *J Immunol*.**183,** 7441-7450

Tate, M. D., Pickett, D. L., van Rooijen, N., Brooks, A. G. & Reading, P. C. (2010c). Critical role of airway macrophages in modulating disease severity during influenza virus infection of mice. *J Virol* **84**, 7569-7580.

Tate, M. D., Schilter, H. C., Brooks, A. G. & Reading, P. C. (2011). Responses of mouse airway epithelial cells and alveolar macrophages to virulent and avirulent strains of influenza A virus. *Viral Immunol* **24**, 77-88.

Thepen, T., Van Rooijen, N. & Kraal, G. (1989). Alveolar macrophage elimination in vivo is associated with an increase in pulmonary immune response in mice. *J Exp Med* **170**, 499-509.

Thomas, P. G., Dash, P., Aldridge, J. R., Jr., Ellebedy, A. H., Reynolds, C., Funk, A. J., Martin, W. J., Lamkanfi, M., Webby, R. J., Boyd, K. L., Doherty, P. C. & Kanneganti, T. D. (2009). The intracellular sensor NLRP3 mediates key innate and healing responses to influenza A virus via the regulation of caspase-1. *Immunity* **30**, 566-575.

Tiemessen, M. M., Jagger, A. L., Evans, H. G., van Herwijnen, M. J., John, S. & Taams, L. S. (2007). CD4+CD25+Foxp3+ regulatory T cells induce alternative activation of human monocytes/macrophages. *Proc Natl Acad Sci U S A* **104**, 19446-19451.

To, K. F., Chan, P. K., Chan, K. F., Lee, W. K., Lam, W. Y., Wong, K. F., Tang, N. L., Tsang, D. N., Sung, R. Y., Buckley, T. A., Tam, J. S. & Cheng, A. F. (2001). Pathology of fatal human infection associated with avian influenza A H5N1 virus. *Journal of Medical Virology* **63**, 242-246.

Tumpey, T. M., Basler, C. F., Aguilar, P. V., Zeng, H., Solorzano, A., Swayne, D. E., Cox, N. J., Katz, J. M., Taubenberger, J. K., Palese, P. & Garcia-Sastre, A. (2005). Characterization of the reconstructed 1918 Spanish influenza pandemic virus. *Science* **310**, 77-80.

Tumpey, T. M., Lu, X., Morken, T., Zaki, S. R. & Katz, J. M. (2000). Depletion of Lymphoctyes and Diminished Cytokine Production in Mice Infected with Highly Virulent Influenza A (H5N1) Virus Isolated from Humans. *Journal of Viology* **74**, 6105-6116.

Turnbull, I. R., Gilfillan, S., Cella, M., Aoshi, T., Miller, M., Piccio, L., Hernandez, M. & Colonna, M. (2006). Cutting edge: TREM-2 attenuates macrophage activation. *J Immunol* **177**, 3520-3524.

Tushinski, R. J., Oliver, I. T., Guilbert, L. J., Tynan, P. W., Warner, J. R. & Stanley, E. R. (1982). Survival of mononuclear phagocytes depends on a lineage-specific growth factor that the differentiated cells selectively destroy. *Cell* **28**, 71-81.

Tyner, J. W., Uchida, O., Kajiwara, N., Kim, E. Y., Patel, A. C., O'Sullivan, M. P., Walker, M. J., Schwendener, R. A., Cook, D. N., Danoff, T. M. & Holtzman, M. J. (2005). CCL5-CCR5 Interaction Provides Antiapoptotic Signals for Macrophage Survival During Viral Infection. *Nature Medicine* **11**, 1180-1187.

Upham, J. P., Pickett, D., Irimura, T., Anders, E. M. & Reading, P. C. (2010). Macrophage receptors for influenza A virus: role of the macrophage galactose-type lectin and mannose receptor in viral entry. *J Virol* **84**, 3730-3737.

Valente, G., Ozmen, L., Novelli, F., Geuna, M., Palestro, G., Forni, G. & Garotta, G. (1992). Distribution of interferon-gamma receptor in human tissues. *Eur J Immunol* **22**, 2403-2412.

van Furth, R. & Cohn, Z. A. (1968). The origin and kinetics of mononuclear phagocytes. *J Exp Med* **128**, 415-435.

Varga, Z. T., Ramos, I., Hai, R., Schmolke, M., Garcia-Sastre, A., Fernandez-Sesma, A. & Palese, P. (2011). The influenza virus protein PB1-F2 inhibits the induction of type i interferon at the level of the MAVS adaptor protein. *PLoS Pathog* **7**, e1002067.

Vissers, J. L., van Esch, B. C., Hofman, G. A. & van Oosterhout, A. J. (2005). Macrophages induce an allergen-specific and long-term suppression in a mouse asthma model. *Eur Respir J* **26**, 1040-1046.

Vodovotz, Y., Bogdan, C., Paik, J., Xie, Q. W. & Nathan, C. (1993). Mechanisms of suppression of macrophage nitric oxide release by transforming growth factor beta. *J Exp Med* **178**, 605-613.

Vreede, F. T. & Brownlee, G. G. (2007). Influenza virion-derived viral ribonucleoproteins synthesize both mRNA and cRNA in vitro. *J Virol* **81**, 2196-2204.

Vreede, F. T., Jung, T. E. & Brownlee, G. G. (2004). Model suggesting that replication of influenza virus is regulated by stabilization of replicative intermediates. *J Virol* **78**, 9568-9572.

Wang, D., Harmon, A., Jin, J., Francis, D. H., Christopher-Hennings, J., Nelson, E., Montelaro, R. C. & Li, F. (2010). The lack of an inherent membrane targeting signal is responsible for the failure of the matrix (M1) protein of influenza A virus to bud into virus-like particles. *J Virol* **84**, 4673-4681.

Wang, X., Li, M., Zheng, H., Muster, T., Palese, P., Beg, A. A. & Garcia-Sastre, A. (2000). Influenza A virus NS1 protein prevents activation of NF-kappaB and induction of alpha/beta interferon. *J Virol* **74**, 11566-11573.

Wanidworanun, C. & Strober, W. (1993). Predominant role of tumor necrosis factor-alpha in human monocyte IL-10 synthesis. *J Immunol* **151**, 6853-6861.

Watanabe, H., Numata, K., Ito, T., Takagi, K. & Matsukawa, A. (2004). Innate immune response in Th1- and Th2-dominant mouse strains. *Shock* **22**, 460-466.

Wei, X. Q., Charles, I. G., Smith, A., Ure, J., Feng, G. J., Huang, F. P., Xu, D., Muller, W., Moncada, S. & Liew, F. Y. (1995). Altered immune responses in mice lacking inducible nitric oxide synthase. *Nature* **375**, 408-411.

Wells, M. A., Albrecht, P., Daniel, S. & Ennis, F. A. (1978). Host defense mechanisms against influenza virus: interaction of influenza virus with murine macrophages in vitro. *Infect Immun* **22**, 758-762.

WHO (2011). Cumulative Number of Confirmed Human Cases of Avian Influenza A/(H5N1) Reported to WHO. www.who.int/csr/disease/avian_influenza/country/cases_table_2011_05_13/en/.

Wise, H. M., Foeglein, A., Sun, J., Dalton, R. M., Patel, S., Howard, W., Anderson, E. C., Barclay, W. S. & Digard, P. (2009). A complicated message: Identification of a novel PB1-related protein translated from influenza A virus segment 2 mRNA. *J Virol* **83**, 8021-8031.

Wright, P. F., Neumann, G. & Kawaoka, Y. (2006). Orthomyxoviruses. In *Fields' Virology*, 5th edn, pp. 1693-1740. Edited by D. M. Knipe & P. M. Howley. Philadelphia: Lippencott Williams and Wilkins.

Wright, S. D. & Silverstein, S. C. (1983). Receptors for C3b and C3bi promote phagocytosis but not the release of toxic oxygen from human phagocytes. *J Exp Med* **158**, 2016-2023.

Yamamoto, Y., Klein, T. W. & Friedman, H. (1997). Involvement of mannose receptor in cytokine interleukin-1beta (IL-1beta), IL-6, and granulocyte-

macrophage colony-stimulating factor responses, but not in chemokine macrophage inflammatory protein 1beta (MIP-1beta), MIP-2, and KC responses, caused by attachment of Candida albicans to macrophages. *Infect Immun* **65**, 1077-1082.

Yoshida, M., Leigh, R., Matsumoto, K., Wattie, J., Ellis, R., O'Byrne, P. M. & Inman, M. D. (2002). Effect of interferon-gamma on allergic airway responses in interferon-gamma-deficient mice. *Am J Respir Crit Care Med* **166**, 451-456.

Zamarin, D., Garcia-Sastre, A., Xiao, X., Wang, R. & Palese, P. (2005). Influenza virus PB1-F2 protein induces cell death through mitochondrial ANT3 and VDAC1. *PLoS Pathog* **1**, e4.

Zamarin, D., Ortigoza, M. B. & Palese, P. (2006). Influenza A virus PB1-F2 protein contributes to viral pathogenesis in mice. *J Virol* **80**, 7976-7983.

Zaragoza, C., Ocampo, C. J., Saura, M., McMillan, A. & Lowenstein, C. J. (1997). Nitric oxide inhibition of coxsackievirus replication in vitro. *J Clin Invest* **100**, 1760-1767.

Zeng, H., Pappas, C., Katz, J. M. & Tumpey, T. M. (2011). The 2009 pandemic H1N1 and triple-reassortant swine H1N1 influenza viruses replicate efficiently but elicit an attenuated inflammatory response in polarized human bronchial epithelial cells. *J Virol* **85**, 686-696.

Zheng, Y. M., Schafer, M. K., Weihe, E., Sheng, H., Corisdeo, S., Fu, Z. F., Koprowski, H. & Dietzschold, B. (1993). Severity of neurological signs and degree of inflammatory lesions in the brains of rats with Borna disease correlate with the induction of nitric oxide synthase. *J Virol* **67**, 5786-5791.

Zhirnov, O. P., Konakova, T. E., Wolff, T. & Klenk, H. D. (2002). NS1 protein of influenza A virus down-regulates apoptosis. *J Virol* **76**, 1617-1625.

Zhou, J., Law, H. K. W., Cheung, C. Y., Ng, I. H. Y., Peiris, J. S. M. & Lau, Y. L. (2006). Funtional Tumour Necrosis Factor-Related Apotosis-Inducing Ligand Production by Avian Influenza Virus-Infected Macrophages. *Journal of Infectious Diseases* **193**, 945-953.